DEVELOPMENT OF MULTI AND DOUBLE WALLED CARBON NANOTUBES (CNTs)/ VINYLESTER NANOCOMPOSITES

A Thesis Submitted to
the Graduate School of Engineering and Sciences of
İzmir Institute of Technology
in Partial Fulfillment of the Requirements for the Degree of

DOCTOR OF PHILOSOPHY

in Mechanical Engineering

by
Abdullah Tuğrul SEYHAN

August 2008
İZMİR

We approve the thesis of **Abdullah Tuğrul SEYHAN**

_____

Assoc. Prof. Dr. Metin TANOĞLU
Supervisor

_____

Prof. Dr. Sevgi ULUTAN
Committee Member

_____

Assoc. Prof. Dr. Lütfi ÖZYÜZER
Committee Member

_____

Assoc. Prof. Dr. Sedat Akkurt
Committee Member

_____

Assoc. Prof. Dr. Funda TIHMINLIOĞLU
Committee Member

07 August 2008

_____

Assoc. Prof. Dr. Metin TANOĞLU
Head of the Mechanical Engineering Department

_____

Prof. Dr. Hasan BÖKE
Dean of the Graduate School of Engineering and Science

ACKNOWLEDGEMENT

This thesis was achieved between October 2003 and August 2008 as a collaborative work between Mechanical Engineering Department, Izmir Institute of Technology and Polymers and Polymer Composite Section, Technische Universitaet Hamburg Harburg (TUHH). We acknowledge the financial support of TUBITAK, Turkey and JULICH, Germany research centers under joint project number JULICH 5-103M048.

I would like to express my gratefulness to my Advisor, Associate Prof. Dr. Metin Tanoğlu, for his friendship, support, motivation and guidance through this dissertation. I am also indebted to him to give me sufficient freedom to pursue my own ideas and develop myself as an independent researcher. I would also like to show my great appreciation to Prof. Dr.-Ing. Karl Schulte for his patience and scientific independence he provided me when performing my scheduled experiments at TUHH. It was absolutely a priceless experience for me to meet him. Particularly, I would like to acknowledge his beyond belief headship. In common, not only professionally, but also at the personal level, they both have been extremely considerate towards me during this thesis.

I would like to acknowledge Dr. Florian H.Gojny for his appreciable contribution at the very beginning of this thesis. I also wish to thank to Dr. Luis Prado for his fruitful discussions about the polymer chemistry work in this thesis. I would like to express my gratitude to Associate Prof. Dr. Lütfi Özyüzer and Yılmaz Şimsek for their assistance in measurements of electrical conductivity and in evaluation of the corresponding results obtained. I am also thankful to Josef Kovacs for assisting me in performing electrical conductivity measurements at TUHH. I would like to also thank to Malte Wichmann for his help and patience in use of rheometry, dynamic mechanical analyzer and TEM at TUHH. I would like to appreciate De la Vega Alejandra for her help in use of Raman Spectroscopy. I would like to thank to Özlem Çağlar for his help in FTIR measurements. I wish to thank to Hella Wilde and Ingrid Hoffmann for their concerted efforts to make me speak German in precise manner. Poliya Polyester Corp., Istanbul is also acknowledged for the supply of the resins used in this study. Graduate studies have not only helped me grow academically, but also offered me a chance to meet many new people.

I have been fortunate to have friends like Eduard Illnich, Andreas Gagel, Stephan Hinz, Leif-Ole Meyer, Florian Gehrig, Dr. Bodo Fiedler, Kirsten Prehn, Dr. Georg Broza, Peter Guhrs, Wilfried Maker, Matthias Nolte, Jan Sumfleth and Hans Wittich.

Special thanks go to the polymer composite group in IYTE and the workers of IZTECH Materials Research Center. I would like to appreciate deeply my room-mates Uğur Türkan and Emre Yalamaç for the moments that we shared together.

I would like to express my special thanks to my family, Şükran and Ömer Seyhan for providing me with inspiration and constant encouragement during my graduate work. Without them, this dissertation would not have been materialized.

Finally, although she has not been able to be with me for every so often during this thesis, I would like to acknowledge my sweetheart, *Aylin* for her incredible patience, selfless love and emotional support during this thesis. She lends a purpose to all my endeavors.

ABSTRACT

DEVELOPMENT OF MULTI AND DOUBLE WALLED CARBON NANOTUBES (CNTs)/ VINYLESTER NANOCOMPOSITES

This study focuses on development and characterization of thermosetting resin based nanocomposites containing multi and double walled carbon nanotubes with and without amine functional groups (MWCNT, DWCNTs, MWCNT-NH_2 and DWCNT-NH_2). A novel 3-roll milling technique was conducted to prepare the resin suspensions with carbon nanotubes (CNTs). Rheological measurements performed on the resin suspensions showed that addition of very low contents (0.05, 0.1 and 0.3 wt. %) of MWCNTs and MWCNT-NH_2 affected the flow characteristic of the resin, significantly. Further, the curing behavior of a vinylester-polyester hybrid resin suspensions containing 0.3 wt % of MWCNTs and MWCNT-NH_2 was intensively studied. It was found that regardless of amine groups, presence of CNTs affected the polymerization of the hybrid matrix resin. Final individual fractional conversion rates of styrene and vinylester monomers were found to be vastly dependent on the type of CNTs. Glass transition temperature (T_g) values of the nanocomposites with MWCNTs and MWCNT-NH_2 were found to increase with filler content. Moreover, nanocomposites containing MWCNTs and MWCNT-NH_2 were found to possess higher tensile strength, elastic modulus as well as fracture toughness and fracture energy as compared to the neat hybrid resin. On the other hand, electrical properties of the nanocomposites were also investigated and it was found that nanocomposites with MWCNTs exhibited the lowest percolation threshold value. In addition, nanocomposites with amino functionalized CNTs were found to exhibit lower electrical conductivity as compared to those with untreated CNTs. Nanocomposites with AC electric field induced aligned CNTs were also prepared. Finally, based on the findings obtained for CNT/ resin suspensions, as a case study, electrically conductive glass fiber reinforced composite laminates were successfully produced, using the CNT modified resin suspensions as matrix material, via Vacuum Assisted Resin Transfer Molding (VARTM) and Resin Transfer Molding (RTM) methods.

ÖZET

ÇOK VE İKİ TABAKALI KARBON NANOTÜP / VİNİLESTER NANOKOMPOZİTLERİN GELİŞTİRİLMESİ

Bu çalışma, amin gruplu ve grupsuz iki ve çok tabakalı nanotüpleri (MWCNTs, DWCNTs, MWCNT-NH_2 ve DWCNT-NH_2) içeren vinilester ve poliester hibrid esaslı reçinelerin geliştirilmesi ve karakterizasyonu üzerine odaklanmıştır. Üç silindirli değirmen tekniği, karbon nanotüp ihtiva eden reçine süspansiyonlarını hazırlamak için kullanılmıştır. Reçine süspansiyonları üzerinde gerçekleştirilen reolojik ölçümler, çok düşük konsantrasyonda (% ağ. 0.05, 0.1 ve 0.3) ilave edilen MWCNTs ve MWCNT-NH_2 nin hibrid reçinenin akış özelliklerini belirgin bir biçimde etkilediğini göstermiştir. Ağ. % 0.3 MWCNTs ve MWCNT-NH_2 içeren hibrid reçinelerin kürlenme davranışı oldukça kapsamlı çalışılmıştır. Sonuçta, amin fonksiyonel grupları olsun ya da olmasın, nanotüplerin hibrid reçinenin polimerizasyonunu etkilediği bulunmuştur. Ayrıca, sitiren ve vinilester monomerlerinin son dönüşüm oranlarının, karbon nanotüp çeşidine göre değiştiği bulunmuştur. Nanokompozitlerin camsı geçiş sıcaklıklarının nanotüp oranı ile arttığı gözlemlenmiştir. MWCNTs ve MWCNT-NH_2 içeren nanokompozitler, katkısız hibrid reçineye göre daha yüksek çekme mukavemeti, elastik modulus, kırılma tokluğu ve enerjisi değerleri göstermişlerdir. Diğer taraftan, nanokompozitlerin elektriksel özellikleri de incelenmiştir. Sonuçta, MWCNTs ihtiva eden nanokompozitlerin en düşük elektriksel iletkenlik eşik (percolation threshold) değerine sahip olduğu bulunmuştur. AC elektrik alanı altında yönlendirilmiş nanotüp içeren nanokompozitler de ayrıca üretilmiştir. Son olarak, CNT/ reçine süspansiyonlarından elde edilen sonuçlara dayalı olarak, bir durum çalışması olarak, CNT modifiye edilmiş reçine süspansiyonları kullanılarak elektriksel iletkenliğe sahip cam elyaf takviyeli kompozit laminalar vakum destekli reçine kalıplama metodu (VARTM) ve reçine kalıplama metodu (RTM) kullanılarak başarı ile üretilmiştir.

TABLE OF CONTENTS

LIST OF FIGURES

LIST OF TABLES

Table **Page**

CHAPTER 1

INTRODUCTION

1.1. Background

Polymers and polymer based composites have been study of interest over the last two decades due to their relatively low costs and ease of processing. However, polymers exhibit poor damage tolerance, low mechanical strength and stiffness relative to other engineering materials such as metals (Tanoglu and Seyhan 2003). Therefore, their utilization as construction materials in industrial applications has been restricted to some extent. For that reason, various different methods including use of relevant chemical stabilizers and reinforcement constituents or blending of different types of polymers have been conducted to tailor mechanical and physical properties of polymers (Gojny 2006, Mccrum, et al. 1997). Of all, the most commonly utilized method to improve the performance of polymers is to turn them into composite structures, using reinforcing materials with high strength and modulus such as glass fibers. However, due to continuing innovations in the industrial applications, the sustainable evolutions expected from polymer based composite structures have been amended continuously.

At this stage, nanotechnology opens up a new perspective to shape new generations of composite structures. Nanoparticles possess unique mechanical and physical properties which make them one of the most promising fillers to develop the future composite materials (Harris 2000). Further, nanotechnology intends to reveal the size-related effects of nano particles to design innovative products with novel properties and functions (Ajayan, et al. 1999). Therefore, nanocomposites, which are encompassed under nanotechnology, have aroused great scientific and industrial attention during the last years. As very recent example, carbon nanotubes (CNTs) with extraordinary mechanical, thermal and electrical properties have been applied for various types of polymers to manufacture electrically conductive nanocomposites with at least retained or improved mechanical properties (Gojny, et al. 2006, Schandler, et al. 1998, Gojny, et al. 2004). Unlike micro-sized filler particles that usually compromise mechanical properties of polymers, for instance, resulting in a high strength but low toughness,

CNTs are anticipated to stimulate a synchronized increase in mechanical strength, stiffness, ductility and toughness of polymers in which they are embedded.

However, despite the fact that there are many published studies on CNT reinforced polymer composites, realization of the expected enhancement in the overall response of the resultant composites has not clearly been demonstrated so far (Ajayan and Schandler 2000, Gong, et al. 2000, Fidelus, et al. 2005). At this point, two major issues need to be solved to accomplish the so-pronounced improved properties in the resulting CNT filled nanocomposites (Gojny and Schulte 2004, Aizawa and Schaffer 2003). These are;

- Weak interfacial bonding between the carbon nanotubes and the matrix resin due to very inert surfaces of CNTs
- Strong tendency of CNTs to form agglomerates because of their huge surface area and aspect ratio

A good bonding of CNTs to the matrix polymer is essential to benefit the potential of CNTs as structural reinforcement. Some chemical functional groups such as amino and carboxyl groups have been applied over the surfaces of CNTs in order to promote the compatibility at the interface between CNTs and the surrounding polymer matrix (Hiura, et al. 1995, Duesberg, et al. 1998, Gojny, et al. 2003). However, in general, the length of the CNTs is ruptured and their perfect structure is partially distorted during any chemical treatment (Hiura, et al. 1995, Dillon, et al. 1999). In other words, aspect ratio of CNTs is reduced. This leads to CNT modified composites to exhibit mechanical strength values very far below the theoretical expectations. It is for this reason that proper functionalization of CNTs is highly critical to the ultimate performance of their resulting nanocomposites.

The huge surface area of carbon nanotubes leads to strong attractive forces to occur between the CNTs themselves (Ge, et al. 1994, Harris 2000). Therefore, accomplishment of homogeneous dispersion of carbon nanotubes within the polymer matrix has also been big challenge. In general, CNTs have a huge surface area, several orders of magnitude larger than the surface of their micro-sized counterpart particles such as carbon black (CB) (Treacy, et al. 1996, Fiedler, et al. 2006). This provokes CNTs to form relatively large agglomerates. Extent of agglomeration is highly critical to mechanical properties of CNT modified composites. A number of different techniques including high speed mechanical stirring, direct mixing and sonication have been used for proper dispersion of CNTs within polymers. In general, these methods are incapable

to break up the agglomerates into individual nanotubes. Of all, sonication has been the most widely utilized technique to process CNT/ thermosetting resins such as epoxy, polyester and vinylester (Gong, et al., Gojny. et al. 2003). In this technique, a pulsed ultrasound with certain amplitude is intended for uniform dispersion of CNTs by dividing their agglomerates into smaller ones or individuals. However, the magnitude of vibration energy applied is limited to distance from the sonicator tip. Therefore, it is not scalable from laboratory to industrial manufacturing settings and not cost effective any more. Sonication technique may also diminish the length of nanotubes, applying a local energy input nearby the sonicator tip. Remaining the high aspect ratio of CNTs unchanged during blending processing is expected to make it possible to achieve enhanced properties in their resulting nanocomposites.

On the other hand, mechanical and physical properties of the CNTs are highly dependent on the production techniques such as chemical vapor deposition (CVD), electric arc discharge method and laser ablation (Ajayan, et al. 1999, Journet and Bernier 1998, Che, et al. 1998). This means that production techniques affect the physical properties of CNTs such as the defect density, degree of graphitization, the aspect ratio (in other words, the length and diameter distribution) and the density. All these properties are vastly critical to the ultimate properties of the polymers in which they are embedded (Biercuk, et al. 2002, Gojny 2006).

In summary, regardless of production method, proper dispersion of CNTs within polymers and enhanced interface between CNTs and the surrounding polymer matrix resin are required to accomplish the so-pronounced superior properties in the resulting nanocomposites.

1.2. Objectives

This study focuses on establishing a fundamental science base to improve the properties of a cost effective matrix resins by the addition of nano particles. More specifically, this study aims to obtain electrically conductive thermosetting resins with enhanced or at least retained mechanical and thermal properties. For this purpose, vinylester and unsaturated polyester resins that are commonly used as matrix resins in composite industry were studied to prepare polymer nanocomposites containing very low amounts of CNTs with and without chemical functional groups.

The specific objectives of this work are as follows;

- Develop CNT / polymer nanocomposites via 3-roll milling technique.
- Enhance dispersion of CNTs within the vinylester and polyester resin blends with the help of amine (NH_2) surface functional groups over the surfaces of CNTs.
- Reveal the effects of CNTs with and without amine functional groups on the cure behavior of the hybrid resin systems.
- Examine the applicability of CNTs as structural reinforcement in polymers, evaluating rheological, thermal and mechanical properties of their resulting nanocomposites.
- Establish a structure property relationship by associating the microstructure of the nanocomposites with their final properties
- Investigate potential of CNTs as conductive filler, performing electrical conductivity measurements on the composite samples, beginning from room temperature to 77 K.
- As an application of the prepared CNT/polymer suspensions, manufacture CNT modified glass fiber reinforced composites using Vacuum Assisted Resin Transfer Molding (VARTM) and Resin Transfer Molding (RTM) techniques.
- Relate the measured mechanical properties of the matrix resin to the response of CNT modified glass fiber composites under various mechanical loading configurations.

1.3 Dissertation Outline

The foregoing discussions establish the significance of formation of the interphase region between CNTs and polymer matrices. The background information given in this present chapter implies the effects of interfacial interactions between CNTs and the surrounding polymer matrix on the ultimate performance of their resulting nanocomposites. Importance of homogenous dispersion of CNTs within polymers was also emphasized, considering briefly common dispersion methods in comparative manner.

Relevant literature regarding structure and properties of CNTs as well as their manufacturing techniques are presented in Chapter 2 in order to better interpret the

structure property relationship in their related nanocomposites. Moreover, some recent studies focused on mechanical, thermal and electrical properties of CNT modified nanocomposites are also summarized in this chapter.

The materials systems used in this work, experimental techniques conducted to disperse CNTs within polymer systems to produce nanocomposites were highlighted in Chapter 3. Principles of 3-roll milling technique and its advantages over other common techniques including mechanical stirring, direct mixing and sonication are discussed in details. Rheological and mechanical properties of the several types of hybrid resin systems containing different types of CNTs with and without amine functional groups are also given in the same chapter. Dispersion state of different types of CNTs with and without amine functional groups within the matrix resins revealed by Transmission Electron Microscopy (TEM) are given in this chapter as well.

In Chapter 4, the rheological behavior of vinylester/polyester hybrid resin suspensions containing MWCNTs, MWCNT-NH_2, DWCNTs and DWCNT-NH_2 is reported. Dynamic viscoelastic and steady shear measurements via parallel plate oscillatory rheometer were performed for this purpose. In this respect, liquid samples without curing agents were taken from 3-roll milling processed resin suspensions containing different content of CNTs with and without amine functional groups. Rheological behavior of the suspensions was evaluated based on the content and type of CNTs, besides amine functional groups over their surfaces.

In Chapter 5, a number of analytical techniques including Dynamic Scanning Calorimetry (DSC), Fourier Infrared Spectroscopy (FTIR), Raman Spectroscopy (RS) and Thermal Gravimetric Analyzer (TGA) were conducted to demonstrate the effects of MWCNTs and MWCNT-NH_2 on the curing behavior of the hybrid resin, with particular emphasis on amine functional groups over the surfaces of CNTs. For DSC and FTIR measurements, catalyzed liquid resin samples were used to follow the reactions that take place within the resin system. DSC results showed the overall response of the resin system with the presence of CNTs with and without amine functional groups. An autocatalytic model was also used to fit the experimental data obtained from DSC measurements. FTIR investigation was carried out to reveal the effects of non-functionalized and amino-functionalized CNTs on the individual conversions of styrene and vinylester resin monomers in the system. Moreover, RS measurements were further done on the cured hybrid polymer and its nanocomposites to follow the conversion of double carbon bonds of hybrid resin in the presence of CNTs with and without amine

functional groups. TGA measurements were executed on the cured samples to interpret the effects of CNTs on thermal degradation mechanism of the hybrid polymer matrix resin.

In Chapter 6, thermo-mechanical properties of the nanocomposites obtained via polymerization of the suspensions containing various amounts of MWCNTs, MWCNT-NH_2, DWCNTs and DWCNT-NH_2 were investigated, using Dynamic Mechanical Analyzer (DMA). The findings were evaluated in conjunction with rheogical behavior of their corresponding suspensions, as discussed in details in Chapter 4. TEM was also used to highlight the dispersion state of CNTs within the polymer matrix resin.

In Chapter 7, tensile mechanical properties and fracture toughness of the nanocomposites were presented. Modified Halpin-Tsai model was also applied to correlate the predicted elastic moduli of the nanocomposites containing various types of CNTs with the experimentally measured values. Scanning Electron Microscopy (SEM) was employed to relate the failure modes that occurred in fracture surfaces of the specimens to the measured tensile strength and fracture toughness values of the nanocomposites.

In Chapter 8, temperature dependence of electrical conductivity of CNT modified nanocomposites was investigated from room temperature to 77 K, by using four-point probe test method. Room temperature conductivity of the same nanocomposites was also measured using impedance spectroscopy technique. Further experiments aimed to align the CNTs within the hybrid resin were also performed, using AC electrical field at various concentrations below the percolation threshold. DSC measurements were then performed on the nanocomposites containing randomly oriented and AC field induced aligned CNTs to interpret the effect of alignment on the thermal properties of the resulting nanocomposites.

In Chapter 9, composite laminates with and without CNT modification were manufactured using VARTM and RTM methods. The matrix dominated mechanical properties including interlaminar fracture toughness (mode I and mode II) and interlaminar shear strength of the VARTM processed composites were investigated to relate the properties of CNT modified matrix resin to the mechanical response of their fabric reinforced structures. Moreover, mechanical tensile properties of RTM processed laminates with and without CNT modification were also evaluated in comparative manner.

Finally in Chapter 10, conclusions of these studies and overall outlook are given.

1.4 Unique Contributions

This dissertation aims to establish a fundamental science base to produce nanocomposites based on a very cost effective polymer resin with very low filler content of CNTs.

To our knowledge, this study is the first in the literature on the preparation of electrically conductive thermosetting polyester and vinylester resins based nanocomposites with retained mechanical properties. A novel dispersion technique called 3-roll milling was used to disperse CNTs within polymers without rupturing their lengths, or distorting their physical properties. This study also developed a new methodology to make it possible to work on commercial styrene containing thermosetting resins via 3-roll milling. For this purpose, a specially formulized styrene free polyester resin with an appropriate viscosity was used to disperse CNTs under intensive shear by the help of 3-roll milling. The resin stuff achieved was then blended with vinylester resin.

Temperature dependency of electrical conductivities of the nanocomposites was also revealed, using four point probe test. It was shown that electrical conductivity of the nanocomposites is a function of temperature. Further, nanocomposites with anisotropic electrical properties were achieved with application of alternating current (AC) field during curing.

This work also shows that RTM and VARTM techniques are highly applicable to manufacture CNT modified fabric reinforced composites. The findings showed that CNTs could be used as distributed sensors to detect onset, propagation and evolution of damages that occur in the composite parts during their service life.

CHAPTER 2

RELEVANT LITERATURE

2.1 Nanotechnology

A broad and interdisciplinary research area called nanotechnology has come into view as a consequence of the recent explosive developments in materials science. Nanotechnology involves the production and application of structures, devices and systems, controlling shape and size at the nanometer scale (Calvert 1999). A nanometer is one millionth of a millimeter. Therefore, the use of nanotechnology is believed to make it possible to realize new materials with novel properties and functionality (Ajayan, et al. 1999). On behalf of these expectations, significant resources are being allocated worldwide for research and development in nanostructure science and technology. These efforts have been devoted to various different aims, including controlling the nanoscale size and synthesis, characterizing electrical, optical, magnetic, and chemical properties of the materials obtained, and establishing the relationship between the nanostructure and final properties of the materials (Smalley 1997). The applications to which nanotechnologies can be applied covers materials manufacturing, nano-electronics and computer technology, medicine and health, aeronautics and space exploration, environment and energy, biotechnology and agriculture, and security (Biercuk, et al. 2002, Lau and Hui 2002). Therefore, the range of materials that are encompassed under the nanotechnology definition is widespread. Nanoparticles, nanocrystals, nanodots, self-assembly monolayers, and more importantly nanotubes have been the recent examples due in this definition.

The potential uses and benefits of nano-materials and nano-devices are expected to lead to breakthroughs of many frontiers. The recent discovery of some nanostructures including carbon nanotubes, molecular motors, DNA-based assemblies, quantum dots, and molecular switches offers an unprecedented opportunity to further accomplish the sophisticated design of the new functional materials (Ebbesen 1997, Smalley 1997). For example, since variations at the nanometer scale affect electronic and atomic interactions, the nanoscale material design should enable one to control the material properties such as magnetization, and catalytic activity without inducing any change to

the chemical composition. Moreover, in the medical field, nanoscience and technology could allow one to place artificial components and assemblies inside the cells and to pattern new materials by imitating the self-assembly rules of nature (Lau and Hui 2002). Finally, nanoscale structures display a high surface-to-volume ratio, which is ideal for applications that involve composite materials, chemical reactions, drug delivery, and energy storage.

2.2. Carbon Nanotubes (CNTs)

Carbon nanotubes (CNTs) are long cylinders of covalently bonded carbon atoms. They are composed of thin tubes with diameters of only a few nanometers, but thousands of times of this dimension in length (Ebbesen and Ajaian 1992). There are two basic types of CNTs. These are single walled carbon nanotubes (SWCNTs) and multi walled carbon nanotubes (MWCNTs). SWCNTs are generally regarded as a single graphene sheet that is monolayer of sp^2-bonded carbon atoms rolled into a seamless cylinder (Iijima 1991). Figure 2.1 show the illustration of a single walled carbon nanotube structure, as an example.

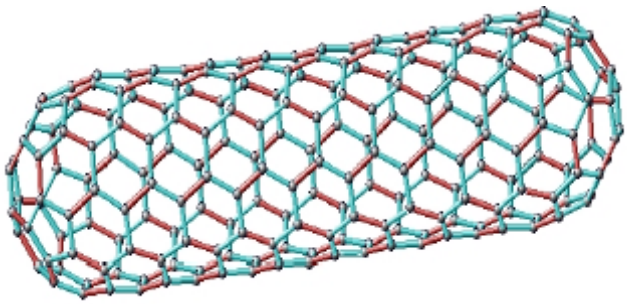

Figure 2.1. Illustration of a single walled carbon nanotube structure

(Source: Gojny 2006)

The carbon atoms in the cylinder have partial sp^3 character that increases as the radius of curvature of the cylinder decreases. MWCNTs are made of nested graphene cylinders coaxially arranged around a central hollow core with interlayer separations of 0.34 nm. A particular sort of MWCNTs is double walled carbon nanotubes (DWCNTs) that consist of two concentric graphene cylinders. DWCNTs are hypothetically supposed to have higher flexural modulus than SWCNTs and higher toughness than

MWCNTs due to the two walls and their relatively small size. In particular, CNTs exhibit an extremely desirable combination of unique mechanical, thermal and electrical properties based upon its hexagonal lattice arrangement and chiral vector. Theoretical and experimental studies showed that they have tensile elastic modulus specifically greater than 1 TPa, which is comparable to that of diamond 1.2 TPa. Moreover, they are at least 100 times stronger than steel, but only one-sixth heavy with a tensile strength of 11-200 GPa (Lu 1997). As well, they conduct heat and electricity along their length with very little resistance acting like tiny electrical wires or paths for rapid diffusion of heat. They are supposed to have an electric-current carrying capacity of 1000 times higher than copper wires. As conductive filler, they are more effective than traditional micro carbon black particles (Lau and Hui 2002). In addition to these superior properties, carbon nanotubes have an enormous surface area per gram of 500 times more than a regular carbon fiber does. Actually, specific surface area of carbon nanotubes depends on their diameter and the number of sidewalls. SWCNTs possess the largest surface area. Peigney et al. (2001) theoretically found that the larger the diameter of the CNTs and the higher the numbers of graphitic layers, the lower the surface area is. Surface area is vastly critical to the modification of the mechanical and physical properties of polymers. These subjects of interest will be also discussed in details in the next sections.

2.2.1. Atomic Structure of CNTs

There are two possible high symmetry structures for nanotubes known as zig-zag and armchair. Nanotubes do not have symmetric forms, but have structures in which the hexagons are arranged helically around the tube axis (Moniruzzaman and Winey 2006). These structures are generally known as chiral, because they can exist in two mirror-related forms. Figure 2.2 depicts the diagram of a sheet of graphite to be rolled to form a carbon nanotube with different symmetry. The material properties of carbon nanotubes strongly depend on the arrangement of the carbon atoms in the lattice. In particular, the electronic properties are influenced by the tube chirality significantly. The cylinder is produced by rolling up the sheet such that the two end points of the vector are superimposed. So, the chiral vector, often known as the roll up vector can be described by the following equation.

$$C_h = na_1 + ma_2 \quad (2.1)$$

Where the integers (n, m) are the number of steps along the zig-zag carbon bonds of the hexagonal lattice a_1 and a_2 are the unit cell base vectors of the grapheme sheet.

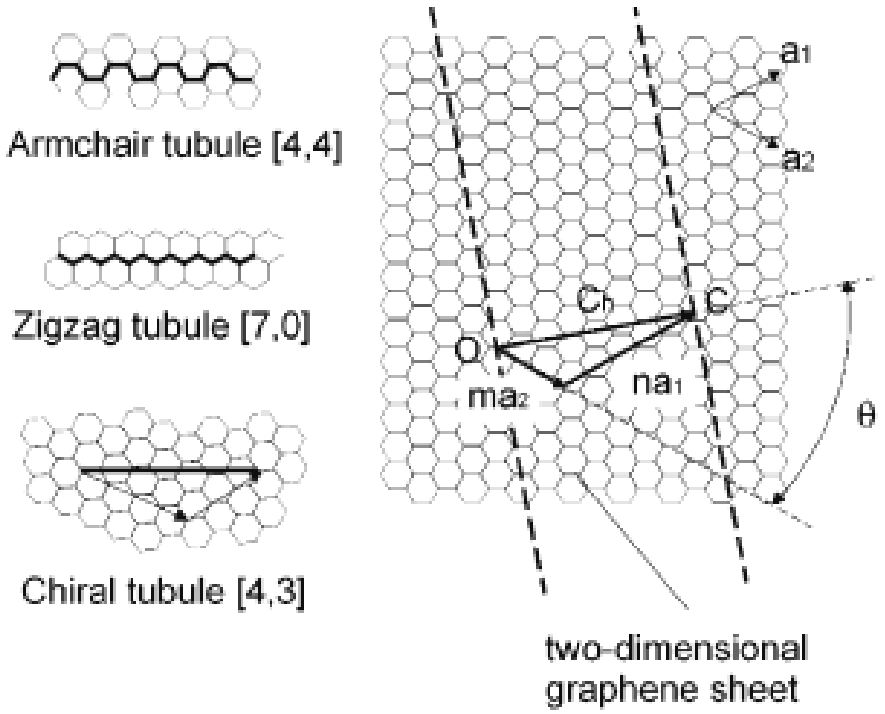

Figure 2.2. Diagram of a sheet of graphite to be rolled to form a carbon nanotube

(Source: Lau and Hui 2002)

The chiral angle (Θ) teta is measured an angle between the chiral vector Ch with respect to zigzag direction (n, 0) where (Θ) = 0 and the unit vectors of a_1, a_2. The armchair nanotube is defined as the (Θ) =30 and the translation indices is (n, n). All other types of nanotubes could be defined as a pair of indices (n, m), where n is not equaled to m (Lau and Hui 2002). The chirality of the carbon nanotubes affects the material properties. Especially, the electronic conductivity is highly sensitive to a slight change of these parameters (Thostenson, et al. 2001).

2.2.2. Mechanical Properties of CNTs

CNTs with extraordinary mechanical properties have been study of interest in materials science to produce functional polymer based nanocomposites with enhanced mechanical properties. In this manner, theoretical calculations were first carried out to predict the mechanical properties of carbon nanotubes. Different theoretical results regarding elastic modulus and its dependence on the nanotube diameter and helicity were reported in comparative manner. The predictions were found to vary with the types of calculation method to describe the interatomic bonding. It was found that elastic modulus of the CNTs ranges from 1 to 5 TPa, depending on theoretical methods used. Lu (1997) calculated the elastic properties of MWCNTs, using the empirical lattice dynamic models. He found that elastic properties are independent of chirality, tube radius, and number of layers and elastic properties are the same for all nanotubes with a radius larger than 1nm. Ru (2000) used the elastic shell model to study the effect of van der Waals forces on the axial buckling of DWCNTs. The analysis showed that the van der Waals forces do not increase the critical axial buckling strain of the nanotubes. Based on the multiple column representation that considers interlayer radial displacements along with van der Waals forces, he indicated that the effect of interlayer displacements can not be neglected unless the van der Waals forces are extremely strong.

In fact, experimental observations are beyond the theoretical expectations. In general, elastic modulus of any material can be measured using an extensiometer, provided that there is a large quantity of the material and possibility to shape it into a rod prior to experiment. However, it is a challenging issue to determine experimentally mechanical properties of the CNTs due to their nanometer size that causes difficulties with precision of the experiments. The first measurement of the elastic modulus of MWCNTs came from Treacy et al. (1996). They used TEM to measure the mean square vibration amplitudes of arc grown MWCNTs over a temperature range from room temperature to 800°C. The average value of the modulus obtained from this technique was reported to be about 1.8 TPa. In consequence, they concluded that the higher moduli were obtained from nanotubes with smaller tube diameters.

On the other hand, AFM is also useful tool to measure the elastic modulus of the carbon nanotubes with respect to their deflection. In general, once a suspended nanotube

is located with AFM, their diameter, suspended length, and deflection along the suspended length was determined based on a series of images taken at different loads. Salvetat et al. (1999) used this technique to measure the modulus of arc grown nanotubes. They found that the average modulus value of eleven individual nanotubes was 810 GPa. Similarly, the properties of carbon nanotubes were investigated via AFM (Yu, et al. 2000a, Yu, et al. 2000b). In general, it was generally observed that elastic modulus of SWCNTs and MWCNTs vary from 0.32 to 1.47 and 0.27 to 0.95 TPa, respectively.

It must be recalled that the strength of a material is not defined as the elastic modulus. It depends on actually type of material and process history covering different temperature and pressure cycles. Like all covalent materials, CNTs are brittle at low temperature regardless of their diameter and helicity (Thostenson, et al. 2001, Thostenson, et al. 2005). The flexibility of CNTs at room temperature is not because of any plastic deformation but to their high strength and the unique capability of the hexagonal network to distort for relaxing stress. Nardelli et al. (1998) showed that the behavior of CNTs under tensile strain at elevated temperatures depends on their symmetry and diameter. The bending strength of large diameter MWCNTs was measured by Wong et al. (1997) and an average value of 14.2 GPa was reported. The similar experiments were conducted using the lateral force of an AFM tip to compare qualitatively the bending strength of arc grown and catalytic grown carbon nanotubes. The bending strength of arc grown nanotubes was found to be lower than that of catalytic grown nanotubes, which contain relatively much defects. The presence of local defects causes a local distortion of the graphite lattice structure. Mechanical properties of CNTs are highly associated with the sum of local defects in their structure. On the other hand, electrical conductivity of the carbon nanotubes is also reduced when any kind of structural change in the lattice structure due to process induced defects or chemical treatment of CNTs.

2.3. Manufacturing of CNTs

The production of the nanotubes with a high order of purity and uniformity has been still interesting subject of interest for the researchers. Nanotubes come in different types, and vary significantly depending on the syntheses procedures. The manufacturing

of the carbon nanotubes mainly include arc discharge, laser ablation, thermal and plasma enhanced chemical vapour deposition (CVD and PECVD).

2.3.1. Arc Discharge Process

In arc discharge method, two high purity graphite electrodes as anode and cathode are held a short distance apart under a helium atmosphere as seen in Figure 2.3. Under these conditions, some of the carbon evaporated from the anode re-condensed as a hard cylindrical deposit on the cathodic rod. The key point in the arc–evaporation method is the current applied. Higher current application will result in a hard, sintered material with few free nanotubes (Thostenson, et al. 2001). Therefore, the current should be kept as low as possible. Using arc-discharge method, individual carbon nanotubes could be achieved in generally several hundred microns long.

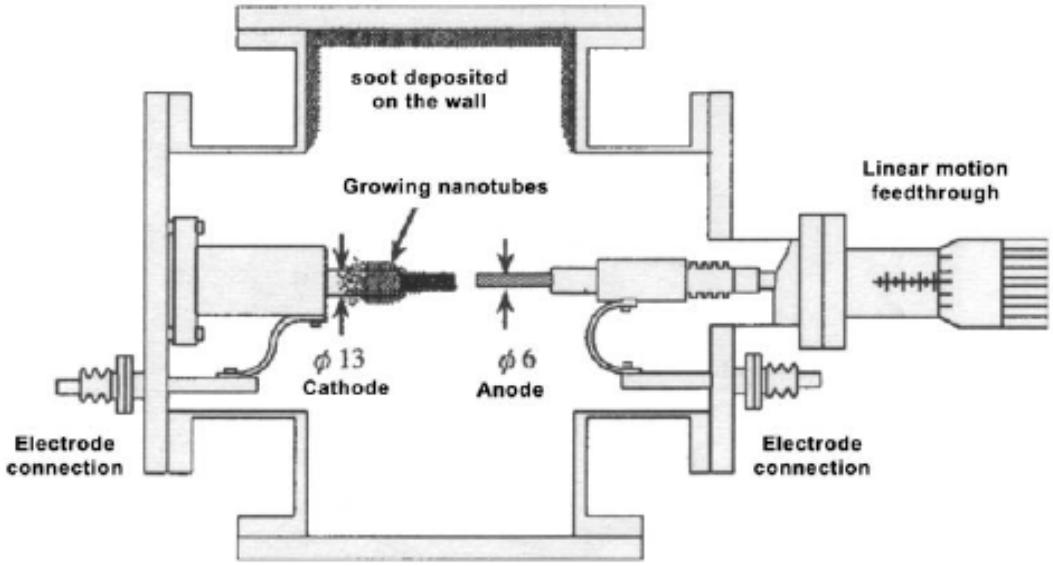

Figure 2.3. Schematic of arc-discharge method for carbon nanotubes
(Source: Saito, et al. 1996)

Arc discharge process has scale up limitations and also sometimes requires the addition of a small amount of metal catalysts, which increases the yield of nanotubes (Zhang, et al. 1999). So the resulting products contain some catalyst particles, amorphous carbons, and non-tubular fullerenes (Journet and Bernier 1998). Therefore, subsequent purification steps are to be required. High temperatures are also necessary

for this technique. Arc discharge technique needs 5000-20000°C and 4.000-5.000°C, respectively. So, the differences in lattice arrangements could exist in the tubes and also there may be a difficulty in the control of chirality and diameter of the nanotubes (Harris 2000).

2.3.2. Laser Ablation Process

Laser ablation has been known as tool for mass production of single wall nanotubes (SWNTs). Schematic of laser ablation is given in Figure 2.4. In laser ablation, a laser is employed to vaporize a graphite target held in a controlled-environment oven (Zhang and Iijima 1999). The carrier gas used can be argon or helium, and the oven temperature was approximately 1200°C (Thostenson, et al. 2001). The condensed material is collected on a cool target (water cooled Cu collector). The condensed material is found to have a significant amount of nanotubes and nanoparticles. In improved laser ablation method, cobalt and nickel catalyst were used either to dope the graphite targets or to coat the silica plate in order to align the growth of the carbon nanotubes (Qin and Iijima 1997).

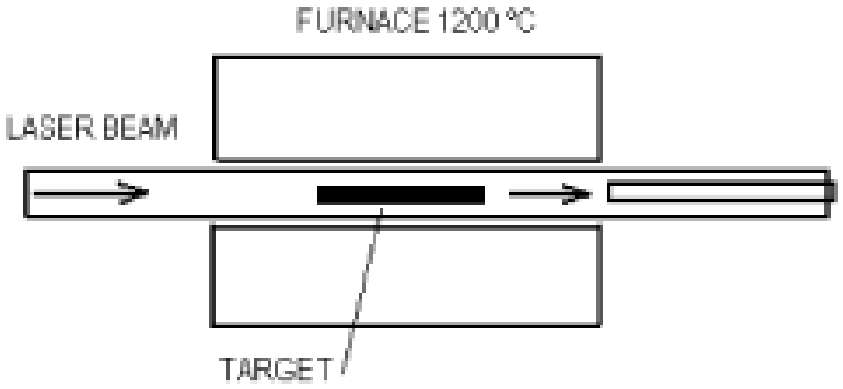

Figure 2.4. Configuration of laser ablation method
(Source: Collins and Avouris 2000)

2.3.3. Chemical Vapor Deposition Process

In arc-discharge and laser ablation processes, the volume of the sample produced is highly dependent on the size of the carbon source (the anode in arc-discharge and the

target in laser ablation) (Thostenson, et al. 2001). Moreover, as explained earlier, intensive purification steps are required to take apart the tubes from the undesired by-products. These drawbacks led to gas phase techniques to be developed. Of all, the chemical vapor deposition (CVD) has been regarded as the best method to produce high purity carbon nanotubes. Generally, the CVD process includes catalyst-assisted decomposition of hydrocarbons, usually ethylene or acetylene, in a tube reactor at 550–750°C and growth of carbon nanotubes over the catalyst upon cooling the system (Nikolaev, et al. 1999). Fe, Ni or Co nanoparticles are usually employed as catalyst (Ge and Sattler 1994). This is a continuous process since the carbon source is always refreshing by flowing gas of interest. Another important aspect related to CVD techniques is its ability to synthesize aligned arrays of carbon nanotubes with controlled diameter and length. CVD can fabricate aligned CNT on a selected area on the substrate. Large-scale synthesis of aligned carbon nanotubes can be achieved by the CVD technique. On the other hand, aligned CNT would be able to be produced with higher yield at lower substrate temperature by using plasma enhanced (PECVD) technique (Bower, et al. 2000).

2.4. Chemical Functionalization of CNTs

Local strain in carbon nanotubes that mainly come from misalignment of the Л orbitals of sp^2 hybridized carbon atoms allows CNTs to be more reactive than a flat graphene sheet (Moniruzzaman and Winey 2006). This means that chemical species can be easier covalently attached to surfaces of CNTs. This covalent functionalization can improve dispersion of nanotubes in solvents and polymers. For example, SWCNTs functionalized with pyrrolidine show the solubility of 50 mg/ml. in chloform even without sonication (Dillon, et al. 1999, Moniruzzaman and Winey 2006). However, untreated SWCNTs were entirely insoluble in this solvent. In this manner, chemical functionalization can offer also the potential to engineer the interface between polymer and the nanotube to optimize composite properties. To improve the mechanical properties, for example, the interfacial adhesion can be modified through covalent or non-covalent interactions between functional groups grafted onto CNTs and the polymer matrix resin. Amino, carboxyl and glycidyl – groups are, for instance, highly compatible with epoxy resins. Amino groups are also believed to be very compatible

with vinylester epoxy resins. The common route, namely the open end functionalization method followed to functionalize CNTs is schematically shown in Figure 2.5.

In particular, the open end functionalization process involves refluxing of CNTs in pure nitric acid or in a mixture of sulphiric and nitric acid to generate carboxylic groups over the surfaces of CNTs (Hiura, et al. 1995). The generated reactive carboxylic groups are modified with relevant multi functional groups such as amines via condensation reactions. The amines are bonded via an amide bond to the CNT, while the other amino groups are accessible to a reaction with the matrix resin such as epoxy or vinylester resin (Gojny, et al. 2003). A remarkable disadvantage of covalent functionalization is the disruption of the extended Л conjugation in nanotubes.

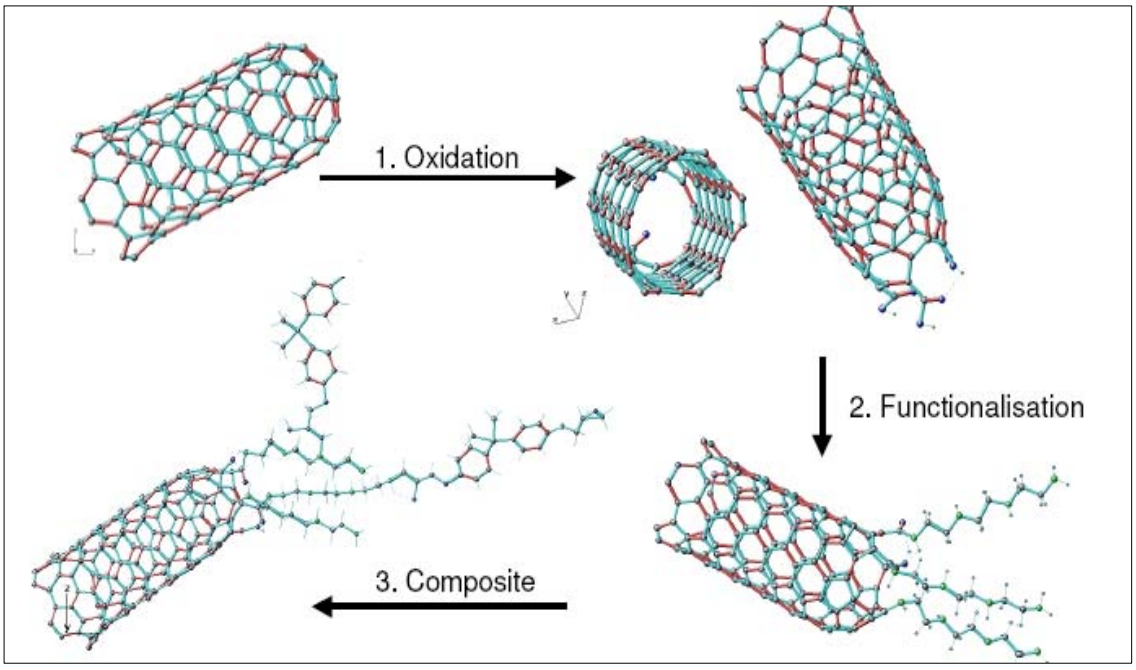

Figure 2.5. Schematic of chemical functionalization of carbon nanotubes
(Source: Gojny, et al. 2003, Gojny 2006)

Although the disrupted Л conjugation is supposed to encompass an impact on the mechanical and probably thermal properties of the nanotubes, so their effect on electrical properties is expected to be more reflective because each covalent functionalization site scatters electrons (Moniruzzaman and Winey 2006, Duesberg, et al. 1998). Non-covalent functionalization is an alternative method for tuning the interfacial interactions of CNTs with polymers. Such functionalizations can be achieved by adsorbing different polymers onto surfaces of CNTs.

The CNTs used in this study are amino-functionalized in ammonia solution via ball-milling process, during which their lengths are reduced and diminished to some extent. In consequence, the break of the CNTs creates highly reactive open ends ready to react with the chains of the surrounding matrix resin. Moreover, the balling process results in CNTs with reduced aspect ratio, which has some significant influences on the performance of their resulting nanocomposites. These effects will be discussed in details in the following chapters.

2.5. CNTs/ Polymer Nanocomposites

Scientific and industrial efforts have been recently focused on nanotechnology and nanomaterials for the future engineering applications. As elucidated earlier, nanomaterials are exhibiting some superior properties, as compared to their micro or macro size counterparts. Polymer nanocomposites have recently emerged as a revolutionary new class of materials that have demonstrated vastly enhanced properties. In this perspective, CNTs with large aspect ratio have recently gained great interest in materials science due to their extraordinary mechanical, thermal and electrical properties (Schandler, et al. 1998, Kolmorov and Crespi 2000). Therefore, substantial effort has been committed to evaluating experimental and theoretical examination of their physical, electrical, and mechanical properties. Due to their so-pronounced astonishing properties, the most common commercial application of carbon nanotubes is based on their use as filler constituents in polymer matrices. This is because carbon nanotubes may have characteristics that can be very beneficial to polymers. They are expected to improve structural properties of polymers.

On the other hand, the use of carbon nanotubes as reinforcing filler for polymer matrix would offer various advantages over the conventional reinforcements, including continuous and short fibers such as glass and carbon (Tibbets and Mchough 1999). It is established that the fiber aspect ratio is the critical factor affecting the resulting structural properties of short-fiber reinforced composites. As the aspect ratio increases, the composite stiffness and strength increase. However, the packing of short fibers in a polymer matrix is highly associated with a percolation phenomenon such that the maximum packing decreases with increasing aspect ratio and may not be sufficient to manufacture a very strong material (Coleman, et al. 1998, Lau and Hui 2002, Shaffer

and Windle 1999a). Carbon nanotubes could overcome these problems by combining their higher aspect ratio, smaller size, and greater strength and stiffness than the corresponding macroscopic forms. In addition, they can not be damaged as easily as carbon fibers during processing due to their inborn ability to withstand large strains (Lordi and Yao 2000). As a result, they are superior over other fillers in composite processing and manufacturing. The incorporation of carbon nanotubes into polymers could enhance not only the mechanical properties, but also the thermal stability and the electrical conductivity of the resulting composites. Moreover, the addition of the carbon nanotubes into insulating polymer systems makes them electrically conductive, enabling other applications in aeronautical such as vertical stabilizers of the aircraft, automotive such as antistatic coating of exterior parts, and consumer goods such as computer housings (Jia, et al. 1999). Therefore, carbon nanotubes with high aspect ratio and the small size are excellent alternatives to the common conductive fillers, such as carbon black. However, it must be considered that, even if the conductive filler is useful to provide a conductive path through an insulating component, its content has to be minimized due to the possible reduction of the mechanical properties of the matrix and the increase in the viscosity, which affects the ease of processing (Gojny, et al. 2003).

The effective use of the carbon nanotubes in polymer composite applications depends strongly on uniform dispersion and orientation of the nanotubes as well as on good interfacial bonding between nanotubes and the surrounding polymer matrix. In fact, the achievement of homogeneous dispersions is vastly critical to the final properties of the composite materials, affecting the fiber–matrix stress transfer ability and, as a consequence, the efficiency and the quality of the composite interface. To attain stable nanotube modified resin dispersions prior to composite processing, since the as-received carbon nanotubes are composed of many entanglements, high shear mechanical stirring or ultrasonic treatments are generally performed. Different solvents (ethanol, toluene, chloroform) and times are employed during sonication. Qian et al. (2000) produced multiwalled carbon nanotube polystyrene composites by a solution evaporation method assisted by high-energy sonication. The process covers separate dispersion and high-energy sonication of the polymer and the nanotubes in toluene (from half a minute to 120 min), followed by mixing, casting into a culture dish, and solvent evaporation. They eventually found that, with addition of 1% of CNTs by weight, elastic modulus and tensile strength of the resulting nanocomposites were improved by 36 and 25 %, respectively. Similarly, Loruie et al. (1999) produced single-

wall nanotube epoxy composites by ethanol sonication of the nanotubes for 2 h, followed by mechanical mixing with the polymer resin, solvent evaporation in a vacuum oven at 50°C, and curing at 72°C for 3 h. They observed that tensile mechanical properties of the epoxy resin were altered in the presence of nanotubes.

The homogeneity of the nanotube dispersion is often investigated by using scanning electron microscopy (Ajayan and Schandler 2000, Sandler, et al. 1999, Schaffer and Windle 1999) and transmission electron microscopy (Ajayan, et al. 1994, Loruie, et al. 1999). Uniform distributions of carbon nanotubes into the polymer matrices are usually accomplished at low loading rates (below 1 wt %) of the nanotube concentrations. This effect is more pronounced in thermoplastics. Geng et al. (2002) obtained 145 % increase in tensile modulus and 300 % increase in yield strength with addition of 1 wt. % fluorinated SWCNTs to polyethylene oxide matrix. Gao et al. (2005) found that composite fibers based on nylon and carboxylated SWCNTs exhibited 153 % higher elastic modulus and 103 % larger tensile strength as compared to neat nylon. On the other hand, nanotube addition has not demonstrated the same improved properties in thermosetting resins. For instance, the epoxy matrices did not seem to be compatible with the pristine carbon nanotubes, forming a weak interfacial bond between the two phases (Ajayan and Sandler 2000, Sandler, et al. 1999). Despite the ultrasonic treatment and long mechanical stirring, many entangled nanotubes were observed in the resulting nanocomposites. Recently, to improve the nanotube dispersion in an epoxy matrix and modify the interfacial bonding, a surfactant was used (Gong, et al. 2000).The surfactant addition was found to influence both the composite thermo mechanical properties and the interfacial adhesion. As a result, improved dispersion and good interfacial bonding of the nanotubes in the epoxy matrix led to a 30 % increase in elastic modulus with only addition of 1 wt. % nanotubes. In addition, when a good dispersion is achieved with the use of a surfactant, the addition of 1 wt% nanotubes could increase the glass transition temperature by a substantial amount (from 63 to 88°C). These results suggest that the nanotubes could find applications both as reinforcing systems and as polymer modifiers for high-temperature uses .In particular, the authors hypothesize that the surfactant can introduce a steric repulsive force between the distributed carbon nanotubes and those aligned along one direction. In another study, Schaffer and Windle (1999), multiwalled carbon nanotubes at different loading rates ranging from 10 to 50 wt% were added to the matrix of poly (vinyl alcohol). As a result, the nanotube addition was found to moderately increase the glass transition temperature (T_g).

On the other hand, increasing attention is paid for the modification of CNT surface, namely the interface between the CNT and the surrounding polymer matrix. If the surface of a CNT, essentially an exposed graphene sheet, is considered, it is seen that it is the weak inter-planar of graphite that provides its solid lubricant quality and resistance to polymer matrix adhesion. This mechanism is enhanced by the chemically inert nature of graphene structure. Numerous researchers ascribed lower than predicted properties of CNT modified nanocomposites to a lack of interfacial bonding (Lourie, et al. 1999, Ajayan and Schandler 2000, Qian, et al. 2000). They agreed that the effective reinforcement of the polymer matrix and the improvement in the composite mechanical properties was a function of the interfacial shear stress between the two phases. As an example, based upon the estimated values of nanotube axial normal stress and elastic modulus, Wagner et al. (1998) concluded that the nanotube/polymer interfacial stress is on the order of 500 MPa and higher, which is an order of magnitude higher than the stress transfer ability of current advanced composites. In their another study (Barber, et al. 2003), they found that the average stress required to remove a single MWCNT from polyethylene butane matrix is 47 MPa, which is about 10 times larger than the adhesion level between the same type of polymer and carbon fibers. These studies demonstrated also the importance of filler size to the interfacial strength. Lordi and Yoa (2000) calculated theoretically the molecular mechanics of binding in-nanotube based polymer composites. They found that the binding energies and frictional forces played only a minor role in determining the strength of the interface, and that the key to forming a strong bond at the interface is having a helical conformation of the polymer around the nanotube. They claimed that the strength of the interface results from entanglement of polymer and nanotubes with each other at molecular level. In brief, it is the shear stress that determines the load transfer efficiency from the matrix to the carbon nanotubes.

Stress transfer between polymers and nanotubes can be also determined using Raman spectroscopy (Frogley, et al. 2002). Raman spectroscopy is a common technique used to characterize carbon materials. It gives information about the amount of ordering, the degree of sp^2-to-sp^3 bonding, and the size of the graphitic crystallites in the material (Dresselhaus, et al. 2005). In particular, when a strain is applied to the material, a Raman peak shift is observed due to the changing of the inter-atomic distances and the vibration frequencies of the normal modes. Cooper et al. (2001) prepared composite specimens by applying an epoxy resin/nanotube mixture to the surface of an epoxy beam. Following the curing of the specimens, stress transfer between nanotubes and

polymer was detected, observing a shift in G Raman band to a lower wave number (Gupta et al., 2004, Frogley, et al. 2002). This shift implies that there is a stress transfer by nanotubes. Ajayan et al. (2000) investigated single walled carbon nanotubes (SWCNTs) modified epoxy resin. They suggested that almost unchanged Raman peak of the nanocomposites in tension mode is due to tube sliding within the nanotube bundles, indicating poor interfacial load transfer between the bundles. Schadler et al. (1998) found the similar results on MWCNTs/ epoxy nanocomposites tested in both tension and compression such that the compressive modulus was higher than tensile modulus of the nanocomposites and the Raman peak shifted only in compression. In principle, observation of a larger shift in compression than in tension showed that the nanotubes carry less strain in tension than in compression due to the poor load transfer between the outer and inner layers. However, in compression, the load was transferred to the inner layers through nanotube bent sections and the slipping was prevented due to the tube structure and geometrical constraint (Zhao and Wagner 2004).

The addition of the carbon nanotubes to a polymer matrix also strongly affects the electrical properties of the composites. This effect can be used for several applications, including optoelectronic, electromagnetic induction shielding, and membrane technologies. These types of systems typically show a percolation behavior. The percolation phenomenon is characterized by the presence of a conductive path through the matrix due to the formation of a three-dimensional network of conductive fillers (Celzard, et al. 1996). A sharp drop characterizes the percolation threshold in the electrical resistance. A significant increase of the electrical conductivity was also found for the nanotube epoxy composite. The polymer matrix (Araldite LY556), investigated by Sandler et al. (1999) is usually used for aircraft applications where high electrical conductivity is required to avoid electrostatic charging and electromagnetic radio frequency interference. For this type of applications the carbon black is commonly used as the conductive filler and its percolation threshold is accomplished at the concentration of 0.5 vol %. The replacement of carbon black with carbon nanotube reduced the required concentration from 5 to 0.04 % and increased the overall conductivity. Finally, it was observed that no negative influence existed on processing and on the finished surface of samples.

The subjects of interest mentioned so far will be discussed later separately in details in the introduction part of each corresponding chapter.

On the other hand, the dispersion of carbon nanotubes in polymer systems attracted research interests not only to reinforce the polymer, but also to improve the electronic properties based on the morphological interactions between the two constituents. Although this subject of interest is beyond the scope of this dissertation, it is worth having an idea about the current applications. In particular, combining the nanotubes and the conjugate polymers, active materials have been obtained for light-emitting diodes, field effect transistors, and photovoltaic devices (Ago, et al. 1999). Curran et al. (1998) investigated the optical properties of a nanotube/PMPV composite that was then used as an emissive layer to fabricate an organic light-emitting diode. The addition of the nanotube to the PMPV polymer caused a gradual decrease of the luminescence intensity due to absorbing, quenching, and scattering phenomena from the nanotubes. Further, the nanotubes acted as a heat sink, avoiding the polymer degradation that can occur at high laser intensities. The LED device showed a better stability in air than that of the polymer. Since, the polymer was chemically undoped; the big advantage of using the nanotube in conjugated polymers was the resulting unchanged electronic processes, which, on the other hand, led to higher mobility of charge carriers due to the increase of the electrical conductivity (Ago, et al 1999, Curran, et al. 1998, Coleman, et al. 1998)

As outlined above, the improvement of the final properties of the composite material depends on the degree of dispersion and the alignment of the carbon nanotubes into the polymer matrix. In fact, as the orientation is critical to the behavior of carbon nanotube based composites, an important issue is the improvement of the processing techniques to control and optimize the microstructure of these nanocomposites, accurately. In the summarized studies above, carbon nanotube modified composites are commonly produced by blending the polymer matrix with the nanotubes, or by sonication followed by solvent evaporation. The suspensions are then cast into molds and allowed to cure at room temperature or in a vacuum oven in the case of thermosetting matrices (Ajayan and Schandler 2000, Sandler, et al. 1999, Schaffer and Windle 1999, Gojny, et al. 2003). More recently, in order to facilitate the dispersion of the nanotubes, 3-roll milling technique was proposed (Gojny, et al. 2004). The principles of this technique and its advantages over other traditional methods such as direct mechanical mixing and sonication will be evaluated in the following chapter.

In summary, CNTs seem to be ideal carbon fibers that can be stiff, at the same time flexible, combining high modulus with high strength. Therefore, they promise the

potential to accomplish multi-functional polymeric materials with enhanced mechanical properties. However, if the advantages of these tubes are to be fully realized, one must overcome some of the barriers that are precluding their use on a large scale. The one challenge is to obtain high yields from the current preparation methods or to invent new methods to produce them on a large scale with preferred orientation. The second one is to explore purification techniques that are simple, relatively inexpensive, do not damage the structure of the nanotubes. The last one is to develop the ability to disperse them effectively as fillers in a matrix with good adhesion and bonding properties. All these issues will be discussed in the following chapters for the resin system studied in this dissertation.

CHAPTER 3

CRITICAL ASPECTS RELATED TO POLYMER NANOCOMPOSITE PROCESSING

3.1. Introduction

In this chapter, an overall view towards to processing of carbon nanotubes with styrene containing thermosetting resins such as polyester and vinylester was addressed. The challenges encountered during various types of dispersion processes including sonication, direct mechanical mixing and 3-roll milling were discussed in concise manner. Based on some experimental results obtained, the advantages of the 3-roll milling over the other mentioned techniques were highlighted. For this purpose, benefits and drawbacks of three different types of resin systems used to produce CNT modified polymer nanocomposites were compared in details.

3.2. Principles of 3-Roll Milling Processing

Having achieved many promising results on the final properties of epoxy based nanocomposites, (Gojny, et al. 2003, Gojny, et al. 2004) proved that 3-roll milling technique is highly capable of dispersing carbon nanotubes homogeneously within thermoset polymers without leading to a rupture and damage of CNTs by reducing drastically their aspect ratio, unlike the other solvent based techniques or treatments do. Figure 3.1 shows the photo of resin suspension being processed on the rolls at t = 30 seconds after it was fed.

3-roll milling technique differs principally from other types of mills in that it applies almost pure shearing rather than compressive impact. The first (1), the second (2) and the third (3) rolls labeled in Figure 3.1 are commonly called feed, center and apron rolls, respectively. Feed and apron rolls rotate in the same direction, while the center roll does in the opposite one (Thostenson and Chou 2006). Arrows on the figure refer to the corresponding rotating direction for each roll. In order to induce high shear rates, angular velocity of the center roll must be higher than that of feed roll (w2>w1).

As the resin suspension is fed into the narrow gap between fed and center rolls, the liquid stuff flows down, covering the adjacent rolls through its surface tension under intensive shear forces. At the end of each given subsequent dwell time, the processed resin suspension is collected by using a scraper blade in contact with the apron roll.

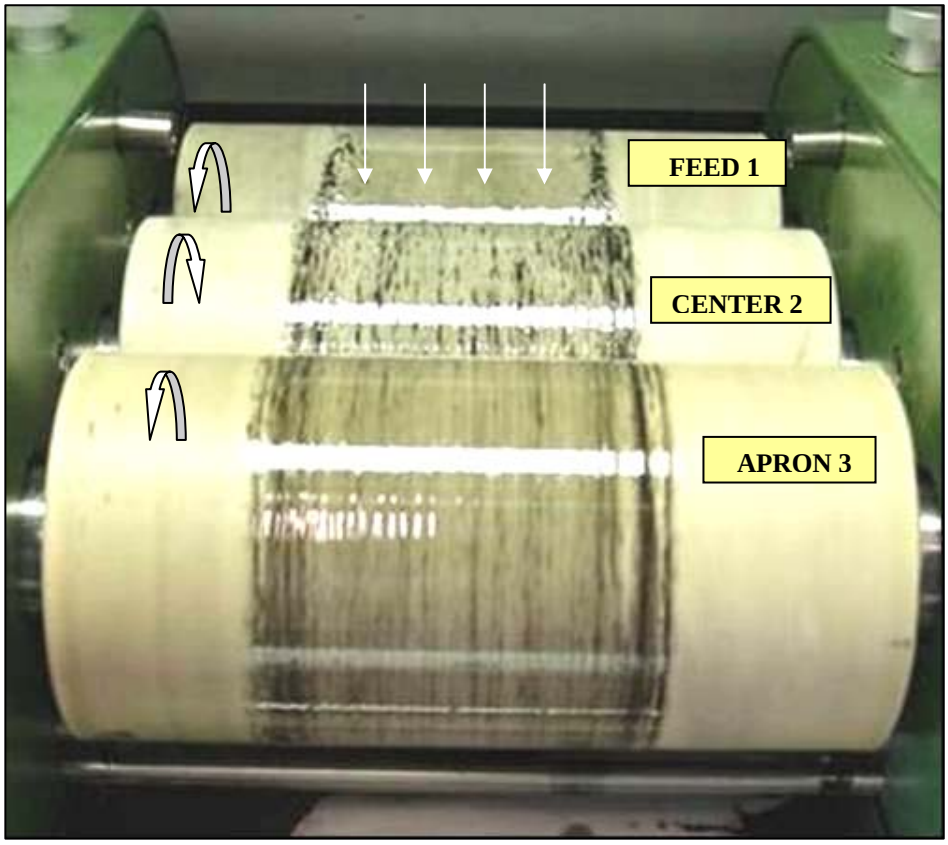

Figure 3.1. Nanotube hybrid resin suspension on the rolls at time t =30 seconds after it was fed.

3.3. Approaches to Processing of CNT/Polymer Systems

An isophthalic commercial unsaturated polyester resin Cam Elyaf 266 with 35 wt. % of styrene was obtained from CAM ELYAF Inc, Turkey. In addition, Poliya 240 an allylic based polyester resin with negligible amount of styrene, Poliya 420 without any styrene and Polivel 701 vinylester resin containing 35wt.% of styrene were obtained from POLİYA POLYESTER Corp, Turkey. Double-wall carbon nanotubes (DWCNTs) and multi-walled carbon nanotubes (MWCNTs) with and without amine functional group (NH_2) produced by chemical vapor deposition (CVD) were obtained from

Nanocyl (Namur Belgium) and used as additives in the involved resin systems. Table 3.1 gives the physical properties of the CNTs used in this thesis. Figure 3.2 depicts the SEM photos of CNTs provided by the producer. CoNAP (Cobalt naphhanate) and MEKP (Methyl Ethyl Ketone Peroxide) were used as an accelerator and initiator, respectively, to polymerize the resin suspensions that contain various amounts of CNTs.

Table 3.1. Physical dimensions and calculated densities of various carbon nanotubes (Source: Gojny, et al. 2006)

NANOTUBE TYPES	L (μm)	d_i (nm)	d_{out} (nm)	ρ_{CNT} (gr/cm^3)
DWCNT	10	2.1	2.8	0.98
DWCNT-NH_2	5	2.1	2.8	0.98
MWCNT	50	4	15	2.09
MWCNT-NH_2	10	4	15	2.09

To prepare CNT/polyester nanocomposites, the first approach was the utilization of the 3-roll milling process using a commercial unsaturated polyester resin. In this manner, 0.1, 0.3 and 0.5 wt. % of CNTs were homogenously dispersed in Cam Elyaf 266 resin under intensive shear force with the dwell time of 2 minutes. The achieved resin suspensions were polymerized with the addition of 0.3 wt. % of CoNAP and 1 wt. % of MEKP into the resin system. During the application of this technique, we encountered some difficulties. The major concern was evaporation of styrene from the polyester resin during the process, which caused a dramatic increase of the viscosity. Styrene evaporation was accelerated due to heat evolved on the rolling mills via viscous dissipation. In fact, viscous dissipation arises from viscous shear stresses and viscous normal stresses. In our case, it accounts for the rate at which mechanical energy induced by the rotating rolls is irreversibly converted to thermal energy due to viscous effects in the resin suspensions. So, the relatively high viscosity polyester resin left on the rolls caused some difficulties with the collection of the resin suspension.

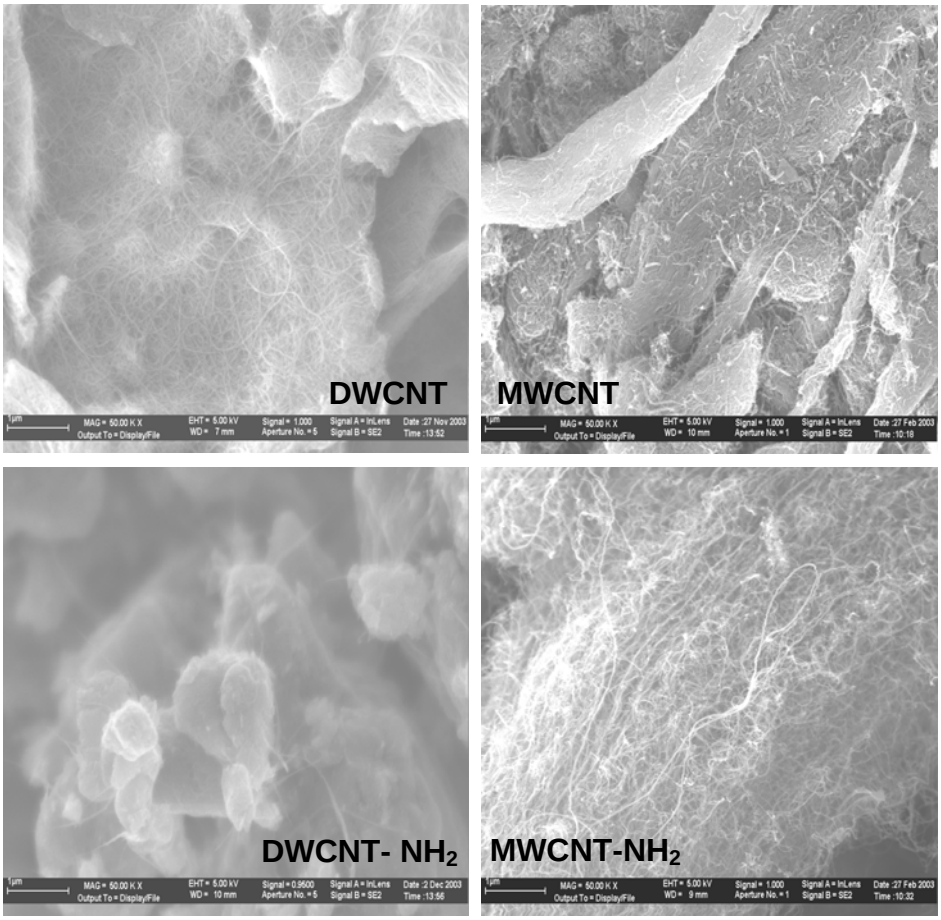

Figure 3.2. SEM photos of the CNTs used in this thesis.

On the other hand, because of the uncontrolled evaporation of styrene, the final styrene compositions within the resin blends were unknown, which makes it very difficult to reproduce the results obtained. Alternatively, the sonication technique was employed with the same CNT/resin systems. The same problems with the sonication technique as in 3-roll milling were again observed (Seyhan, et al. 2007a). Even tough the sonication bath was cooled by water, the local heating due to energy created within the resin system caused styrene to evaporate from the polymer suspension. This leads to a more viscous resin. In addition, it was observed that nanotubes were agglomerated in the volumes closer to the tip of the sonicator. This is because van der Waals attractive forces between the carbon surfaces are sensitive to heat, thus leading to higher agglomeration to occur nearby the sonicator tip. To overcome the difficulty with evaporation of styrene, another resin system was proposed to try.

The second approach to preparation of nanocomposites was to use a blend of polyester resin system with reduced styrene content, appropriate gelation time and viscosity for the 3-roll milling process. In this respect, we employed a special styrene-

free polyester Poliya 420 styrene free and Poliya 240 with very low amount of styrene were utilized as two components for the resin blend. The styrene was later added to the 3-roll milling processed system at a certain amount to promote the degree of cross-linking. After some experimental trials, polyester resin blend was formulated based on 45 wt. % of Poliya 420, 30 wt. % of Poliya 240 and 25 wt. % of styrene with the presence of 0.2 wt. % of CoNAP and 1.5 wt. % of MEKP. The resin blend to be used during 3-roll milling process was prepared by hand-mixing of two types of the polyester resin at a certain ratio (Poliya 420 45 wt. %, Poliya 240 30 wt. %) for 10 minutes. Nanocomposite samples were prepared with dispersion of 0.1, 0.3 and 0.5 wt. % of the carbon nanotubes within the polyester resin blend. After collecting the CNT containing polyester suspension by spatula from the 3-roll milling, 25 wt. % of styrene was further added to the corresponding resin system. The whole system was then subjected to the intensive mixing for half an hour, using magnetic stirrer and finally cast into an aluminum mold and allowed to cure at room temperature followed by a post curing in an oven at 110^{o}C for 2h. Although polyester blend with a lower amount of styrene was introduced to 3-roll milling, the problem with instant evaporation of styrene from the resin system was not entirely overcome. However, difficulties with styrene evaporation and unknown styrene amount in the final product were eliminated by using negligible content of styrene containing resin. In other words, there occurred no resin residues sticking on the surfaces of the rolls, which enables the repeatability of the results obtained. In this manner, the collected resin suspensions were polymerized and the resulting nanocomposites were mechanically characterized.

Considering the relevant experiences in the last two resin systems, the third approach emerged as use of a hybrid resin blend composed of styrene free polyester resin POLİYA 420 and a bisphenol A epoxy based vinylester resin POLİVEL 701 containing 35 % styrene. The point herein is to tailor the interface between amine functionalized CNTs and hybrid matrix resin containing bisphenol A epoxide groups. To prepare the suspensions, various amounts of MWCNTs, MWCNT-NH_2 DWCNTs, DWCNT-NH_2 (0.05, 0.1 and 0.3 wt. %) were first mixed manually with styrene free polyester resin prior to 3-roll milling processing for 10 minutes. A three roll mill (Exakt 120 S Exakt Gmbh) with alumina ceramic rolls was then used to produce the nanocomposites. The gap size between the ceramic rolls was kept constant at 5 μm. The speeds of feed, center and apron rolls were set to 20, 60 and 180 rpm, respectively. The dwell time of polyester/ CNT suspension was about 2 minutes. The collected CNT/

polyester resin suspensions were then blended with vinylester resin at a weight ratio of 1/3 by high speed mechanical stirrer for about 30 min. After the addition of the styrene emission agent (1 wt. %) to the prepared mixture, the CoNAP and MEKP were subsequently introduced into the system at a ratio of 0.2 and 1 wt. %, respectively to polymerize the involved hybrid resin system. Note that emission agent used helps styrene remain the resin system till the end of the reaction. The catalyzed resin suspensions were then allowed to cure at room temperature followed by post curing at 120°C for 2h. Figure 3.3 shows the schematic illustration of nanocomposite processing used throughout the rest of this thesis.

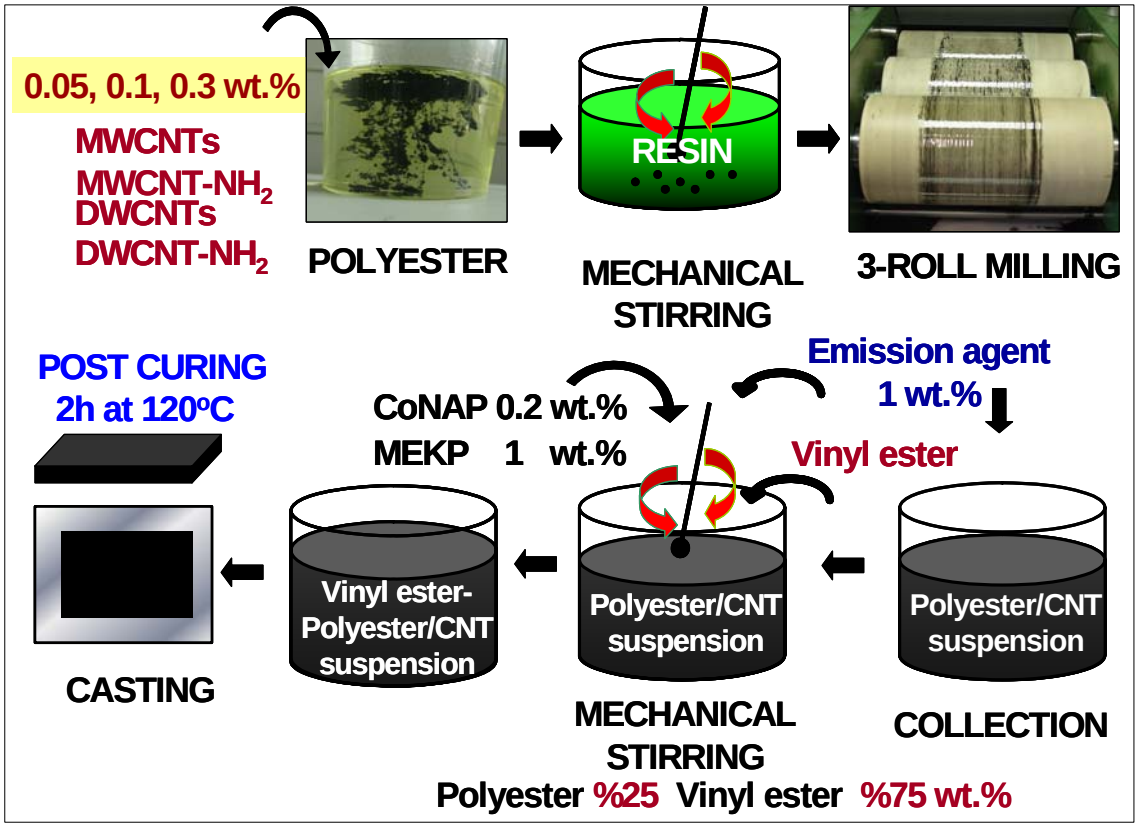

Figure 3.3. The schematic of nanocomposite processing used throughout the rest of this thesis.

With this technique, evaporation of styrene from the resin system was absolutely prevented. In addition, the viscosity of the corresponding styrene-free polyester resin is highly proper to apply higher shear rates within gaps of the rolls to break up the agglomerates and to disentangle nanotube bundles within the intentional dwell time.

3.4. Experimental Characterization of Nanocomposites

In this chapter, the general trend observed for the effects of various types of carbon nanotubes including MWCNTs, DWCNTs, MWCNT-NH_2 and DWCNT-NH_2 on the properties of the matrix resin system used in our second approach was presented in concise manner. This is because the other chapters presented in this thesis cover the studies exploring the chemical and physical interactions of the CNTs with the third matrix resin system in greater details.

The dispersion of the CNTs within the composites obtained were characterized by Transmission electron microscopy (TEM) using a Philips EM 400 at 120 kV acceleration voltages. The ultra thin TEM samples with a thickness of 50 nm were prepared using a microtome cutting at room temperature.

TA Instruments rheometer with parallel plate geometry (500 micrometer gap, and 50 mm plate diameter) was used to analyze the rheological behavior of the polyester suspensions with different loading rates of CNTs. Tests were performed in steady modes at room temperature in order to avoid styrene evaporation during the measurements. For this reason, liquid samples were taken from the collected resin suspension from the 3-roll milling technique without adding any further styrene into it. Steady shear sweeps (SSS) were used to investigate the flow properties of the polyester suspensions by considering the viscosity as a function of increasing shear rates.

Mechanical tensile properties of the composites were determined according to DIN EN ISO 527.1. Dog bone specimens were prepared by countersinking using a mutronic dear drive 2000. The tensile samples were tested using a Zwick servohydrolic machine at a cross head speed of 1 mm/sec. The elongation of the specimen during the test was also measured.

3.5. Results and Discussion

3-roll milling process seems to be more convenient technique than traditional ones such as sonication and direct mixing to disperse carbon nanotubes within a liquid polymer resin. Figure 3.4 are the TEM micrographs showing dispersion state of MWCNTs and DWCNTs with and without functional group in the polyester resin blend at 0.3 wt. % of loading rate. Regardless of amine functional groups, MWCNTs

exhibited better local dispersion in the polyester matrix, as compared to DWCNTs. This is because DWCNTs have relatively high surface area, thus exhibiting higher tendency to form relatively large agglomerates within the matrix resin. In fact, degree of

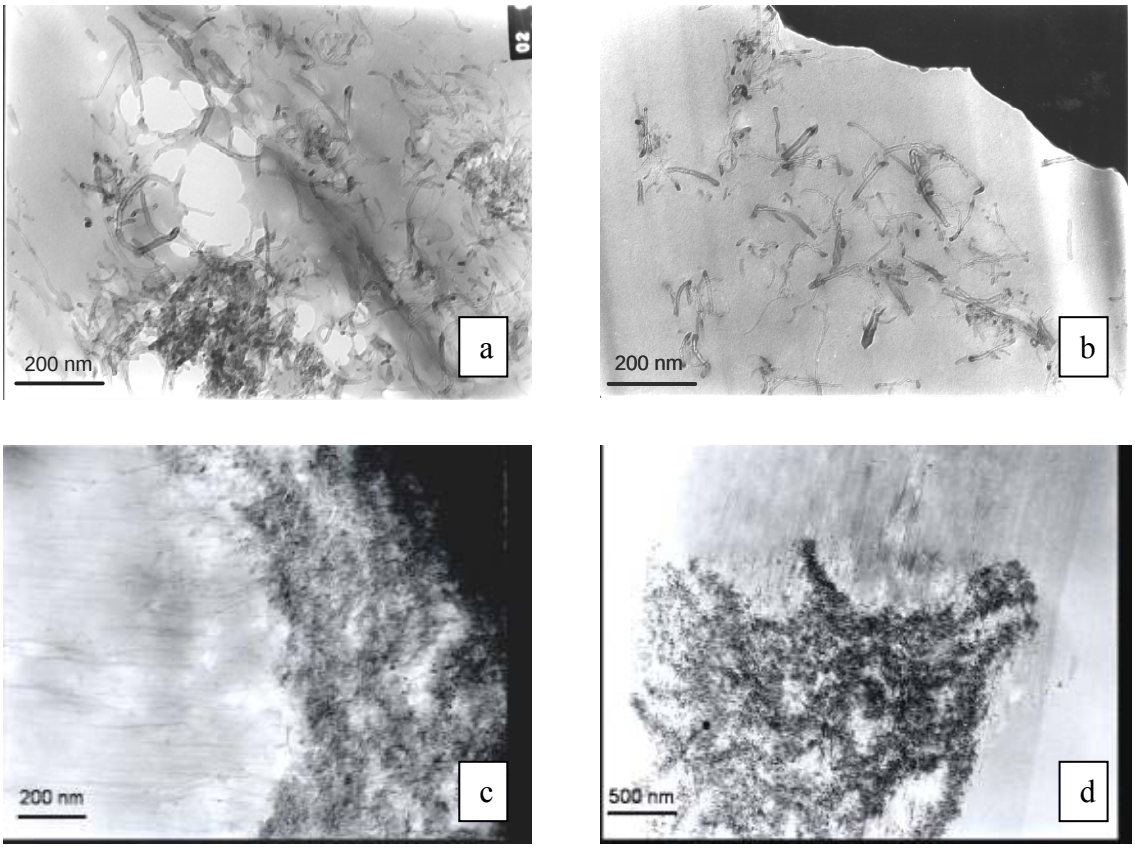

Figure 3.4.TEM micrographs of nanocomposites prepared from POLIYA polyester at 0.3 wt. % loading of (a) MWCNT (b) MWCNT-NH_2 (c) DWCNT (d) DWCNT- NH_2

dispersion of CNTs is vastly critical to the final properties of the nanocomposites. In principle, the better dispersion of CNTs within the surrounding polymer matrix resin, the better final properties in the resulting nanocomposites are observed.

In the literature, rheological behavior of the polymer suspensions was related to dispersion state of carbon nanotubes within the polymer matrix resin. Figures 3.5 and 3.6 give the viscosity as a function of shear rate for the Poliya polyester based suspensions (the second approach) containing MWCNTs and MWCNT-NH_2 at different loading rates, respectively. As it can be seen in the figures, shear thinning behavior was observed for the samples containing either MWCNT or MWCNT-NH_2, such that viscosity is reducing with the increase of shear rates. The viscosity of polyester

suspensions with MWCNT decreases sharply at 0.1 wt. %, but MWCNT-NH_2 does not have the same behavior. This might be due to the fact that nanotubes with amine functional group has better compatibility and thus enhanced chemical interaction with the polyester chains or styrene monomers within the system. In order to investigate the nanofiller effect with and without chemical functional groups on the mechanical properties of the composites, tensile mechanical testing was conducted. In consequence, the tensile properties of Poliya polyester blend polymer were found to be much lower, as compared to those of a common commercial polyester resin in the market. Note that both of the resin components were specially synthesized in collaboration with Poliya. This is the major reason that their individual mechanical properties were low relative to those of a commercial polyester resin.

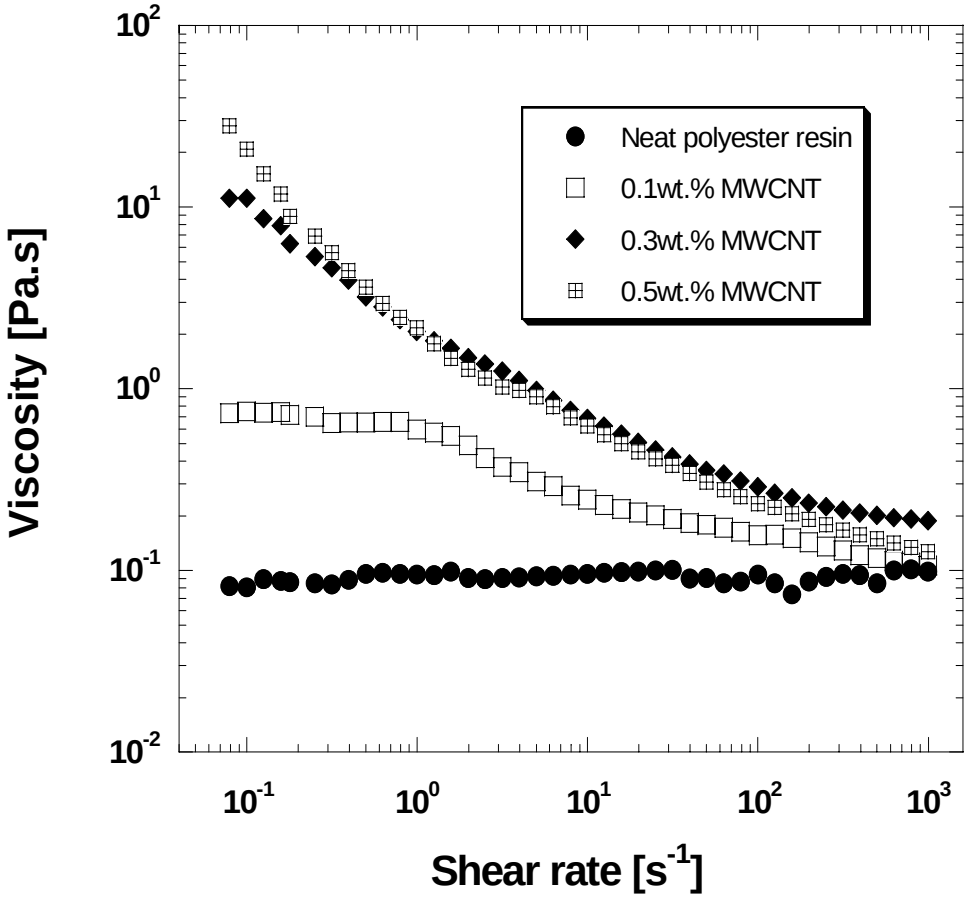

Figure 3.5. Viscosity of the polyester suspension with MWCNTs as a function of shear rate.

Figures 3.7 a and b show the tensile strength of the nanomaterials containing MWCNTs and DWCNTs with and without amine functional groups, respectively. As it can be seen in the figures, MWCNT and DWCNT modified nanocomposites with and

without amine functional group exhibited better mechanical properties as compared to neat polyester resin. Moreover, at each loading rate, composite specimens containing MWCNTs with amine functional group have higher values than those with MWCNTs without any functional group. For instance, the nanocomposites with 0.5 wt. % of MWCNT-NH_2 exhibit about 15 and 6 % higher strength values as compared to the neat polymer and those with similar content of MWCNTs, respectively. This shows the influence of chemical functional group on the interfacial interactions. The same findings were also valid for the composites with DWCNTs and DWCNT-NH_2.

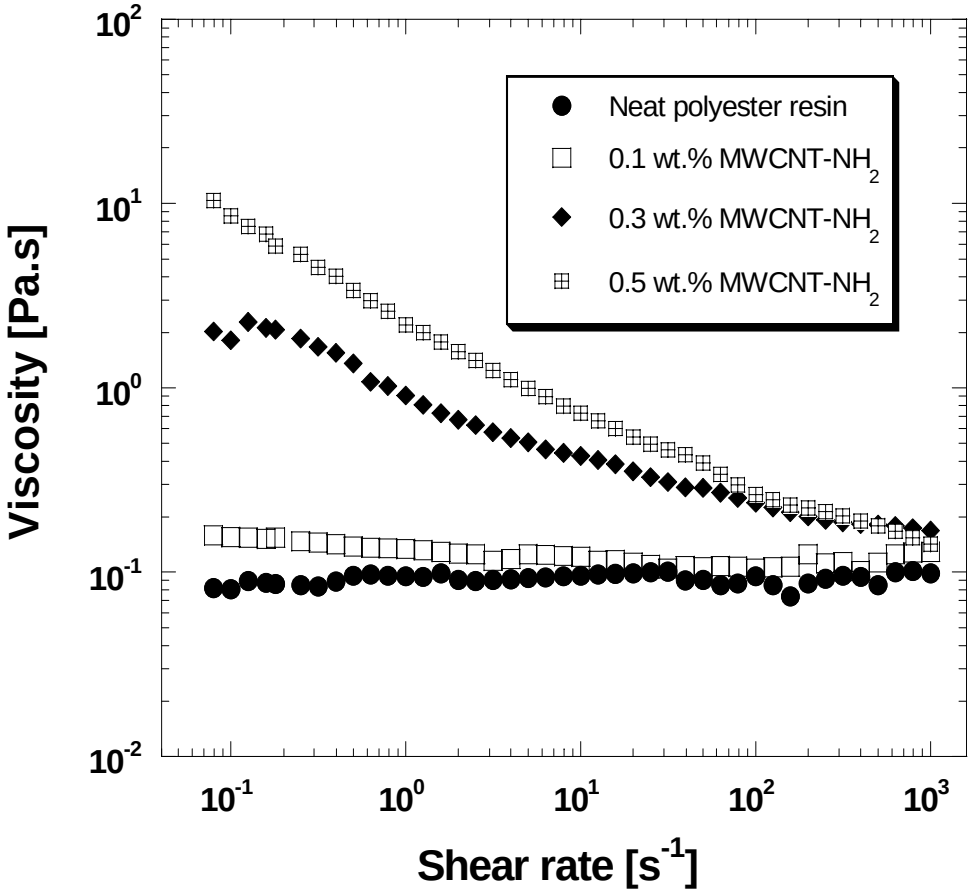

Figure 3.6. Viscosity of the polyester suspension with MWCNT-NH_2 as a function of shear rate.

The nanocomposites containing 0.5 wt. % of DWCNT-NH_2 have about 17 and 5 % higher strength values than the neat polymer and those with DWCNTs, respectively. Note that nanocomposites with DWCNTs with either functional group or not have higher strengths than those with MWCNTs or MWCNT-NH_2 at each loading rate. This can be explained by the higher surface area of the double wall carbon nanotubes, which may result in a better load transfer efficiency at the interface region.

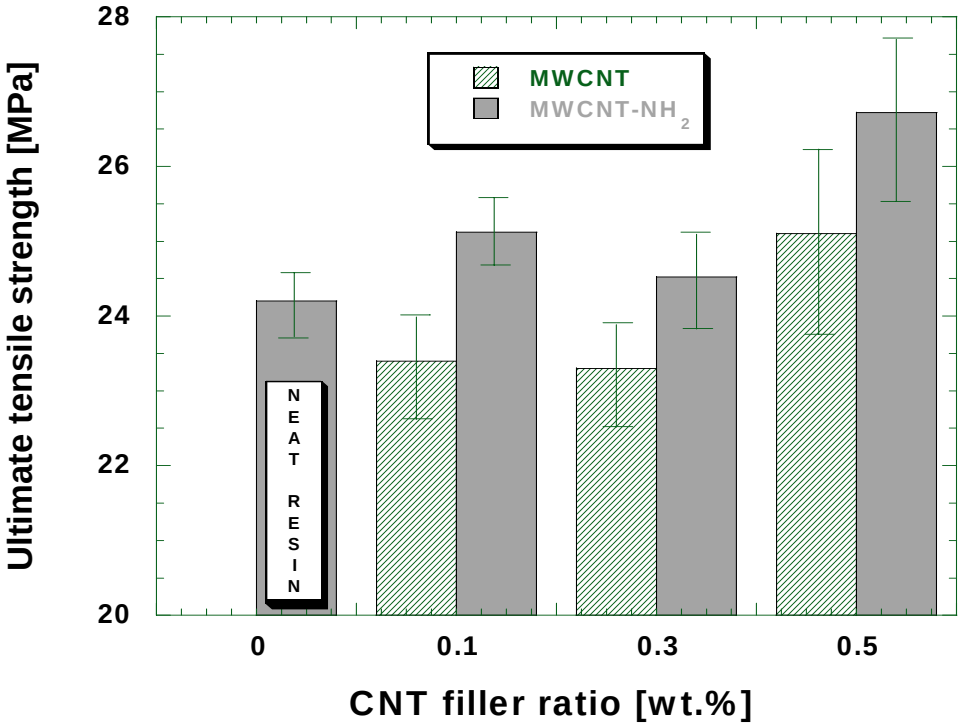

a)

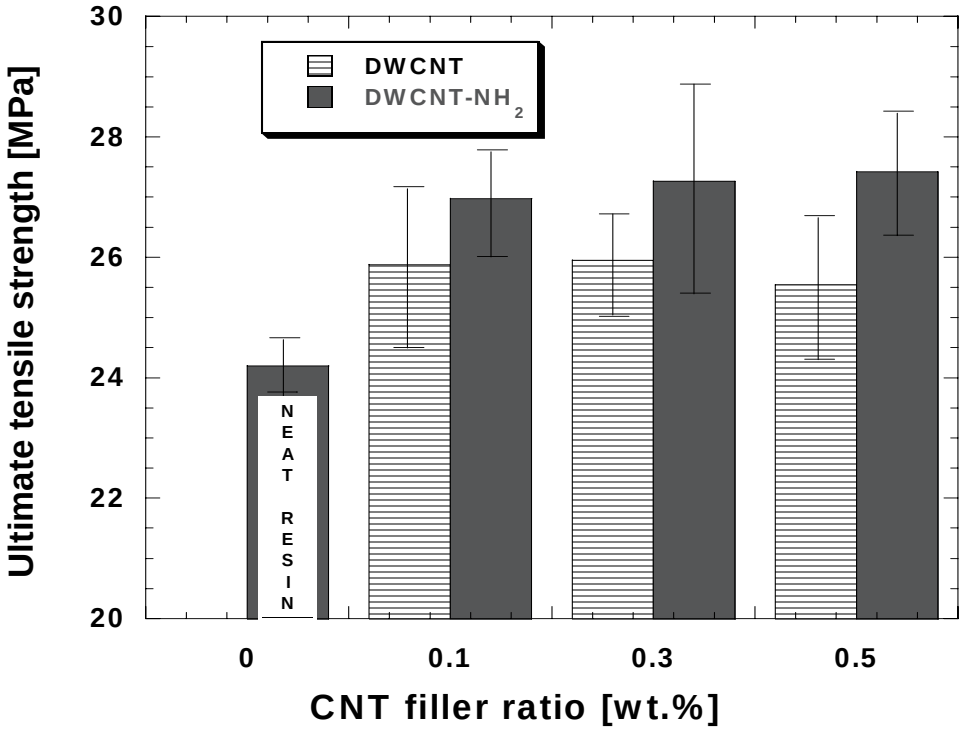

b)

Figure 3.7. Ultimate tensile strength (UTS) of the CNT / polyester nanocomposites as a function of CNT filler ratio a) with MWCNT and MWCNT-NH_2 b) DWCNT and DWCNT-NH_2

However, note that the strength of the neat polyester resin system in principal was not taken as a major concern for comparison in this chapter. Instead, processing of CNT/thermosetting polyester nanocomposites was rather discussed in this chapter with a particular emphasis on three common key issues i) availability of blending of polyester resin with lower amount of carbon nanotubes ii) degree of carbon nanotube dispersion in the corresponding resin and iii) interfacial adhesion / interactions of carbon nanotubes within the resin.

3.6. CONCLUSIONS

In this chapter, the critical aspects and some limitations regarding the processing of thermosetting polyester resins with very low contents of carbon nanotubes were briefly discussed. In this manner, various different techniques including mechanical stirring, sonication and 3-roll milling were conducted to disperse CNTs within thermosetting polyester resins with and without styrene and vinylester resins with styrene.

In consequence, it was revealed that, regardless of dispersion technique, instant evaporation of styrene from the resin systems due to heat evolved via viscous dissipation is the major issue to be considered when blending a thermosetting polyester or vinylester resin with carbon nanotubes. It was also found that 3-roll milling technique is superior over other techniques such as sonication and direct mechanical mixing to disperse CNTs within a thermosetting polyester resin blend. Moreover, it was also found that interaction of functional groups with the surrounding polymer matrix is crucial to final properties of the resulting nanocomposites.

Note that this chapter covers the preliminary results on the processing issues. In the following chapters, interactions of CNTs with matrix resin will be evaluated based on mainly the third approach in details.

CHAPTER 4

RHEOLOGICAL BEHAVIOR OF CNT MODIFIED HYBRID RESIN SUSPENSIONS

4.1 Introduction

Solid-in-liquid suspensions containing non-colloidal particles are characteristically involved in the processing of both thermoplastic and thermosetting polymers (Weg, et al. 2002, Andrews, et al. 2002, Pötschke, et al. 2002). CNTs with high aspect ratio as well as excellent mechanical, thermal and electrical properties are the most promising fillers to fabricate various types of polymer based nanocomposites (Aizawa and Shaffer 2003, Alloui, et al. 2002). Therefore, the understanding of rheological properties of CNT/ polymer suspensions is of primary importance in nanocomposite processing (Rosen, et al. 2002, Song and Youn 2005). However, before all, the study of dispersion state of nanotubes and their relative motion in polymers emerge as the first step to interpret the feasibility of their application as fillers for any type of processing method (Moniruzzaman and Winey 2006). In addition, since the starting material often consists of curved and intertwined carbon nanotubes with different length distribution, the formation of stable polymer dispersions is also a challenge to achieve. Shaffer et al. (1998) and Shaffer and Windle (1999b) oxidized nanotubes, using a mixture of concentrated nitric and sulfuric acid. To characterize dispersion of nanotubes with different length distributions, they also performed bromine pretreatment to achieve a short tube suspension. The two dispersions were characterized in terms of length distribution by TEM image analysis and viscosity measurements by capillary rheometry. The viscosity of both dispersions displayed the same behavior as a function of the tube concentration such that a slight increase occurs at low concentrations up to 0.1 % by volume, followed by a sudden increase above a critical concentration, estimated around 0.5 and 1% by volume for the longer and shorter nanotube suspensions, respectively.

In fact, it is very well known that rheological behavior of particle filled polymer systems is greatly associated with particle-particle interactions, particle polymer

interactions, the dispersion state of particles as well as the shape and orientation of dispersed particles (Yasmin, et al. 2003, Shirono, et al. 2001, Amari, et al. 1997). In this respect, it was stated that the Brownian motion of CNT particles with huge aspect ratio results in more considerable viscoelastic rheological behavior as compared to that of micro-scaled size short fibers or particles such as carbon black (Shaffer, et al. 1998, Shaffer and Windle 1999b, Amari, et al. 1997, Seyhan, et al. 2007b). In particular, it is of primary significance to understand rheological behavior of CNT modified polymer suspensions in order to optimize the manufacturing process of their resulting nanocomposites (Moniruzzaman and Winey 2006). The rheological behavior of concentrated aqueous nanotube dispersions was studied by Kinloch et al. (2002). They disperse the oxidized CNTs within water. They found that the behavior of the dipsersions was found to be similar to that of a reversibly flocculated dispersion, and that, under steady shear, the dispersions rapidly shear thinned. Kim et al. (2005) investigated the rheological behaviour of MWCNTs in polyelectrolyte dispersants based on poly acrylic acid and poly aspartic acid. They concluded that MWCNTs slurries had high intrinsic viscosity and the low maximum solid loading resulting from the high aspect ratio and the strong van der Waals force of MWCNTs. Pötsche et al (2004a) investigated the rheological behavior of the CNT/polycarbonate composites. It was found that viscosity increase of the nanocomposites prepared with CNTs was much higher than those composites prepared with carbon fibers and carbon black (CB) particles. They associate it with the higher aspect ratio of the CNTs. In their later study (Pötsche, et al. 2004b), they performed dynamic measurements on melt mixed polycarbonate MWCNT /polycarbonate nanocomposites and made a comparison between the rheological properties and electrical conductivity of nanocomposites. They found that the electrical threshold (at about 1 wt. %) at room temperature coincided with rheological threshold value. In addition, they concluded that dispersion state of MWCNTs was highly sensitive to the applied strain in the linear viscoelastic region, and that the storage and loss modulus were independent of frequency. Mitchell et al. (2002) investigated the linear viscoelastic properties of polystyrene (PS) nanocomposites containing SWCNTs with and without surface functional groups. They found that the nanotubes with functional groups have better dispersion in PS than those without any functional group. They also revealed that nanocomposites with functionalized nanotubes gave higher storage modulus and complex viscosity values at low frequency. Song and Youn (2005) performed a similar study and stated that poorly dispersed CNTs within

epoxy resin leads to higher storage, loss modulus and complex viscosity values. The rheological behavior of epoxy resin suspensions containing amine, acid and plasma treated carbon nanotubes were also studied by Kim et al. (2006). It was found that the surface modified CNTs/epoxy suspensions exhibited a very strong shear thinning behavior and higher shear viscosity than those with untreated CNTs due to the enhanced interfacial bonding between CNTs and the corresponding epoxy resin in their resulting resin suspensions as compared to homogenously dispersed CNTs.

In this chapter, the rheological behavior of vinylester /polyester hybrid resin suspensions containing various types of fillers including MWCNTs, MWCNT-NH_2, DWCNTs and DWCNT-NH_2 was experimentally determined, performing dynamic viscoelastic and steady shear measurements via parallel plate oscillatory rheometer. All the experimental results obtained were discussed with a particular emphasis on the type of CNTs and amine functional groups over the surfaces of CNTs.

4.2. Experimental

4.2.1 Rheological Measurements

A TA Instruments oscillatory rheometer with parallel plate geometry (500 micrometer gap, and 50 mm plate diameter) was used to analyze the vinylester/polyester resin blend suspensions with different amounts of CNTs with and without amine functional groups. Tests were performed in both dynamic and steady modes at room temperature in order to avoid evaporation of styrene during the measurements. All measurements were taken in Linear Viscoelastic Region (LVR) in which the storage modulus (G') and loss modulus (G") were independent of strain amplitude. Dynamic frequency sweeps (DFS) were then performed in the LVR to investigate the structure of the suspensions. In the DFS, the strain amplitude was remained constant 35 % through whole frequency range. Please note that prior to main experiments, the corresponding value of the strain amplitude was proved to be in the LVR, conducting Dynamic Strain Sweeps (DSS) at a constant frequency. During the DFS, the frequency varied stepwise from 0.1 to 80 rad /sec. Storage modulus (G') and loss modulus (G") values were then measured as a function of frequency. Furthermore, Steady Shear Sweeps (SSS) were

employed to investigate the flow properties of the suspensions by considering the viscosity as a function of increasing shear rates.

4.3. Results and Discussion

4.3.1 Rheological behavior of the resin suspensions with MWCNTs

The storage modulus (G') of the resin suspensions with different loading rates of MWCNTs and MWCNT-NH_2 as a function of oscillatory frequency is shown in Figures 4.1 a and b, respectively. Consequently, G' values were observed to monotonically increase with an increase in the oscillatory frequency. Moreover, the more CNTs incorporated into the corresponding resin blend, the higher G' values were obtained from the resulting resin suspensions. At 0.3 wt. % loading rate, the flow regime of the resin suspensions was significantly altered at low frequencies and a pseudo-solid like behavior becomes more visible. We referred to it as pseudo-solid like because in true-solid like behavior the storage modulus (G') becomes fully independent of frequency (Shaffer, et al. 1998, Shaffer and Windle 1999b, Amari, et al. 1997). In addition, suspensions with 0.1 and 0.3 wt. % of MWCNTs exhibit slightly higher storage modulus values, especially apparent at low frequencies, as compared to those with MWCNT-NH_2. It was reported that carbon nanotubes with very small sizes are very likely to make strong particle-polymer interactions even at very low filling rate because the interfacial area between particles and polymer significantly increases (Moniruzzaman and Winey 2006). So, the high aspect ratio and huge surface area of CNTs may lead to formation of physical network structure, which may give rise to the apparent storage modulus of the corresponding resin suspensions. Similarly, Chan et al. (2002) concluded that, unlike mechanical properties, rheological properties of a sytem are altered substantially, as the size of fillers embedded in the corresponding system decreases. In this respect, the changes in rheological properties of the resin suspensions are highly proportional to the characteristics of physical network structure formed by the strong particle polymer interactions as in the case of CNTs/polymer systems.

Figures 4.2 a and b give the loss modulus values (G") of resin suspensions containing MWCNTs and MWCNT-NH_2, respectively. In fact, the loss modulus is less sensitive to particle morphology and dispersion state of additives than storage modulus.

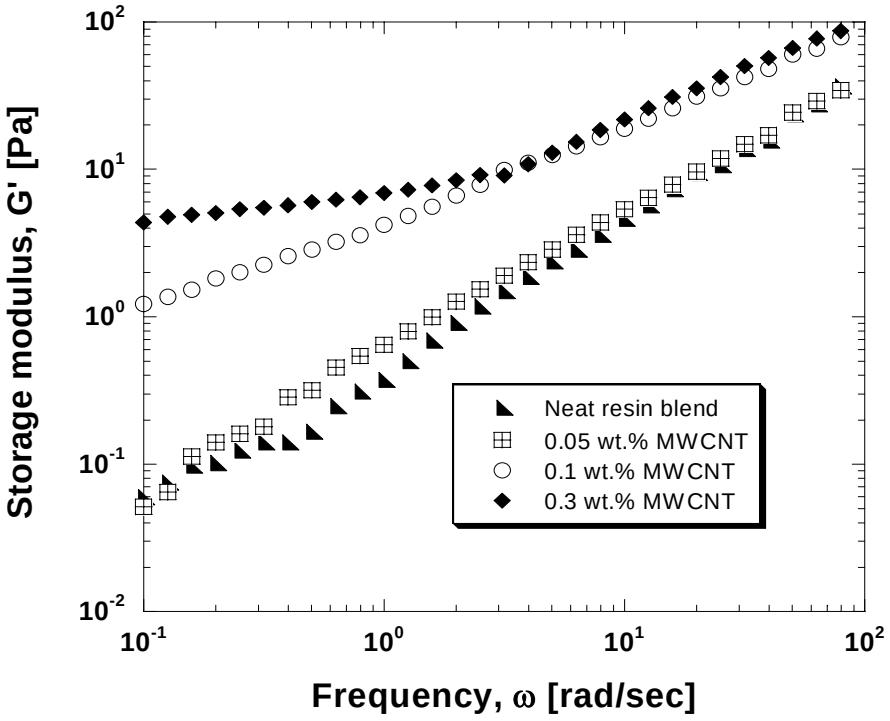

a)

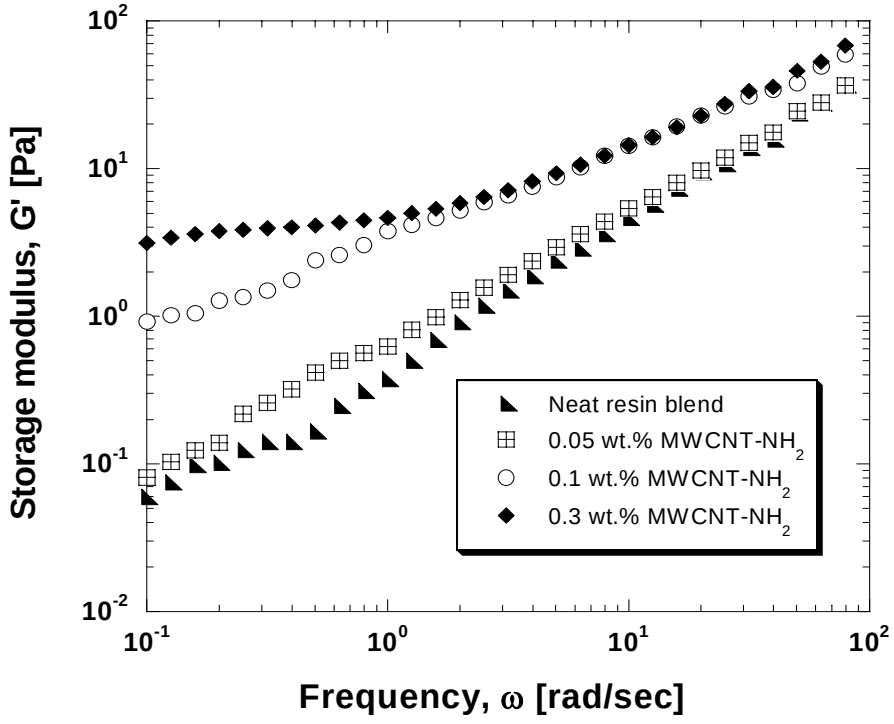

b)

Figure 4.1. The frequency dependence of the storage modulus (G') for the CNT/ resin suspensions with various a) MWCNTs and b) MWCNT-NH_2 contents.

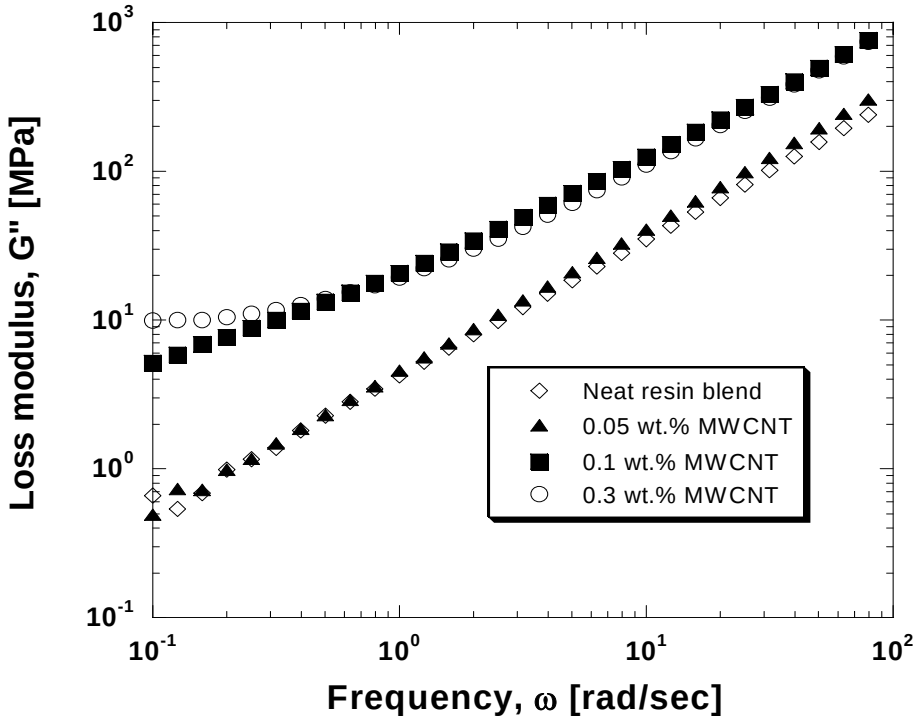

a)

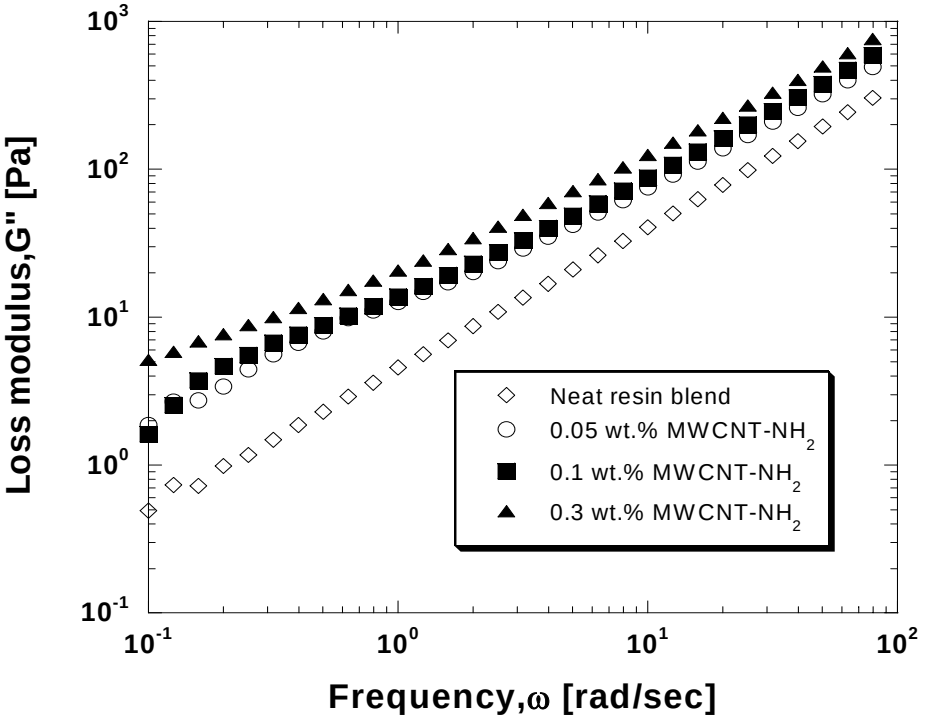

b)

Figure 4.2. The frequency dependence of the loss modulus (G") for the CNT/ resin suspensions with various a) MWCNT b) MWCNT-NH_2 contents.

Loss modulus values as a function of angular frequency increased with respect to content of carbon nanotubes, just in the same manner as storage modulus values. In addition, at 0.3 wt. % loading rate, resin suspension containing untreated carbon nanotubes exhibits viscous behavior (G''>G'), whereas that with amino functionalized carbon nanotubes shows viscoelasticity (G''≈ G'). This verifies that amine functional groups over CNTs surfaces alter the flow characteristic of the resin suspensions.

Figures 4.3 and 4.4 give shear viscosity as a function of shear rate for the neat resin blend and resin suspensions containing MWCNTs and MWCNT-NH_2, respectively. In principle, shear viscosity of pure polymer is divided into two distinct regions including the Newtonian and shear thinning regions (Andrews, et al. 2002, Pötschke, et al. 2002, Seyhan, et al. 2007b). At low shear rate, the Newtonian region with independence of shear rate is observed followed by shear thinning region through which shear viscosity linearly declines with shear rate. As seen in the figures, shear-thinning behavior was observed for each resin suspension with nanotubes such that the viscosity is reducing with an increase in the shear rates. Moreover, the neat resin blend shows almost the Newtonian fluid behavior. In other words, the Newtonian region disappeared when even very low contents of CNTs (0.05 wt. %) was added to the resin blend. This implied that strong particle-particle interactions of CNTs are one major factor leading to an increase in shear viscosity of the corresponding suspensions. On the other hand, at 0.1 wt. % loading rate, the initial shear viscosity of the resin suspension with amino-functionalized nanotubes is slightly lower than that of the suspension with non-functionalized nanotubes. Moreover, resin suspensions containing 0.3 wt. % of MWCNTs and MWCNT-NH_2 exhibited similar initial viscosity values. Based on the experimental findings obtained so far, it seems that amine functional groups do not significantly contribute to the enhancement of dispersion state of CNTs within the corresponding resin blend. Actually, it is not easy to make a single and very precise comment on rheological behavior of polymeric suspensions. This is because it extremely depends on dispersing state of fillers inside, particle-particle interactions, and interaction between particles and disperse medium (polymer resin). In our case, since carbon nanotubes have high aspect ratio, surface area and amine functional groups over their surfaces, both particle-polymer resin blend and particle-particle interactions become more crucial, as elucidated in details during analysis of rheological data above.

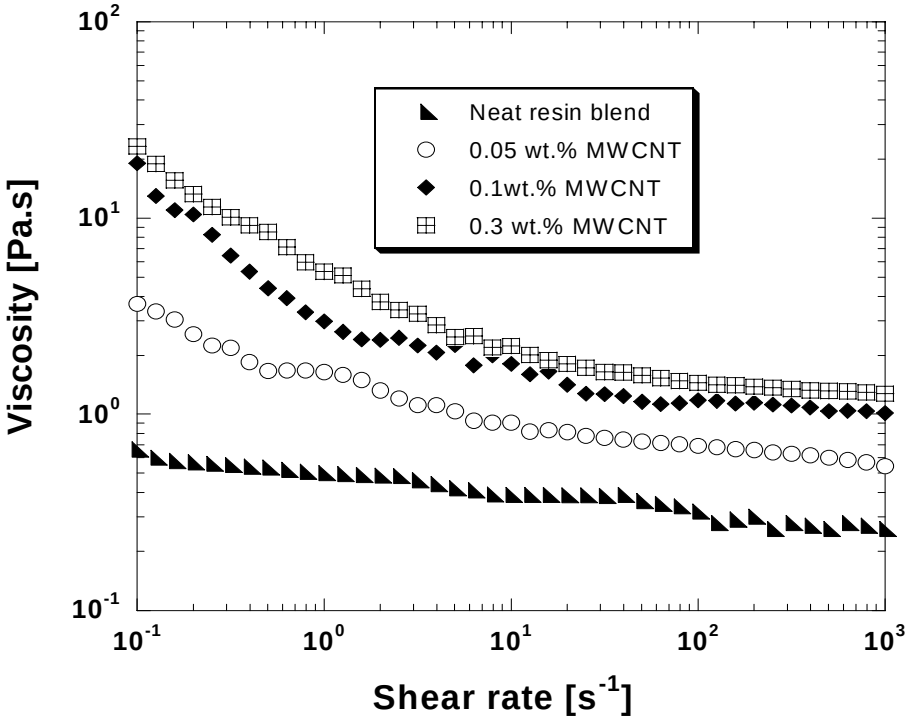

Figure 4.3. Shear rate dependency of viscosity of neat resin blend and CNT/resin suspensions with MWCNTs.

Please note that the amino-functionalized nanotubes used in our experiments were processed in ammonia solution via ball milling process, during which CNTs are broken in length and their aspect ratios are partially diminished. According to information provided by the manufacturer of CNTs (Nanocyl, Belgium), the aspect ratio of multi walled nanotubes with amine functional groups is eventually five times less than that of the nanotubes without any surface treatment. From that point of view, the incorporation of amino functionalized nanotubes (MWCNT- NH_2) with their reduced aspect ratio into the resin system is expected to result in relatively lower storage and loss modulus values as well as much reduced shear viscosity in their corresponding resin suspensions compared to those with MWCNTs. However, in our case, the effect of the surface functionalization on the rheological behavior is relatively insignificant especially at higher loading rate of CNTs embedded into the resin blend. This implies a conceivable occurrence of chemical interactions to some extent between CNTs and disperse medium (resin blend) through the amine functional groups over the surfaces of CNTs.

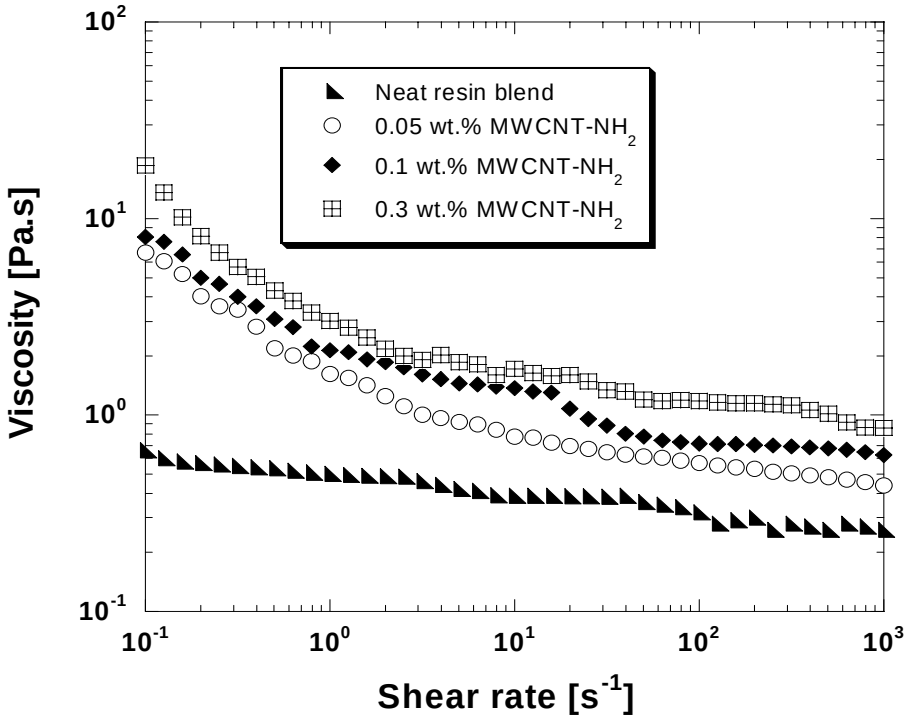

Figure 4.4. Shear rate dependency of viscosity of resin blend and CNT/resin suspensions with MWCNT-NH_2

On the other hand, the transition from liquid like to solid like behavior is highly proportional to the existence of yield stress, which is an expression of the strong particle-particle interactions (Seyhan, et al. 2007b). Note that non-interacting particle filled polymer systems do not show the yield stress. However, in our case, regardless of amine functional groups, at 0.3 wt. % loading rate, a perceptible transition zone occurred, which is ample evidence to the presence of strong polymer particle interactions within the resin matrix.

4.3.2 Rheological behavior of the resin suspensions with DWCNTs

Figures 4.5 and 4.6 give the frequency dependency of the storage modulus (G') values for the hybrid resin suspensions containing various amounts of DWCNTs and DWCNT-NH_2, respectively. At each given concentration, G' values of DWCNT and DWCNT-NH_2 modified resin suspensions were found to increase with increasing frequency. Regardless of filler content, the resin suspensions containing DWCNTs

showed almost the same G' modulus values as those with DWCNT-NH_2, apparent especially at low frequencies. However, the suspensions with DWCNT-NH_2 showed dependency of G' values with respect to CNT content. The highest G' values were obtained from the resin suspensions containing 0.05 wt. % of DWCNT-NH_2. Moreover, at each given concentration, DWCNT-NH_2 modified resin suspensions possessed higher G' values as compared to those with DWCNTs. On the other hand, incorporation of DWCNTs and DWCNT-NH_2 into hybrid resin at the given concentration did not alter significantly the flow regime of their corresponding resin suspensions across the frequency range studied. Some of these findings are contradictory to the results obtained from the suspensions containing MWCNTs or MWCNT-NH_2. It was found that G' values of the resin suspensions with MWCNTs or MWCNT-NH_2, increased with the increment of CNTs content. In addition, regardless of amine functional groups, a noticeable change in G' values was observed when increasing the concentration of CNTs from 0.1 to 0.3 wt. %. Consequently, at 0.3 wt. % loading rate, MWCNTs or MWCNT-NH_2 modified resin suspensions showed a pseudo-solid like behavior, particularly visible at low frequencies. It is very well known that the dependence of storage modulus values on filler concentration is related to geometrical aspect of particles as well as the density of structural networks formed by dispersed particles with polymer chains (Shaffer, et al. 1998, Shaffer and Windle 1999b, Amari, et al. 1997, Seyhan, et al. 2007a). For the present case, orientation of nanotubes with their huge aspect ratio within the hybrid resin is also expected to induce a substantial impact on the characteristic of network structure to be formed. Depending upon the interactions at the interface between CNTs and the chains of the surrounding polymer matrix, this effect is anticipated to be more pronounced when the concentration of CNTs within the system increases, provided that CNTs are uniformly dispersed. Since DWCNTs have larger specific surface area (SSA) and lower density (density of 0.98 gr/cm^3) as compared to MWCNTs (density of 2.09 gr/cm^3), they have higher tendency to form relatively large agglomerates within the resin medium. Therefore, DWCNT modified resin suspensions demonstrate the same rheological behavior as the suspensions containing large micro particles, such as carbon black or glass beads due to inferior particle-particle interactions arising from relatively large condense agglomerates of DWCNTs.

According to the percolation theory, the network structure is formed between the fillers and the dispersed medium, when the fraction of inter-particle bonding exceeds the threshold level (Amari, et al. 1997, Pötsche, et al. 2004a).

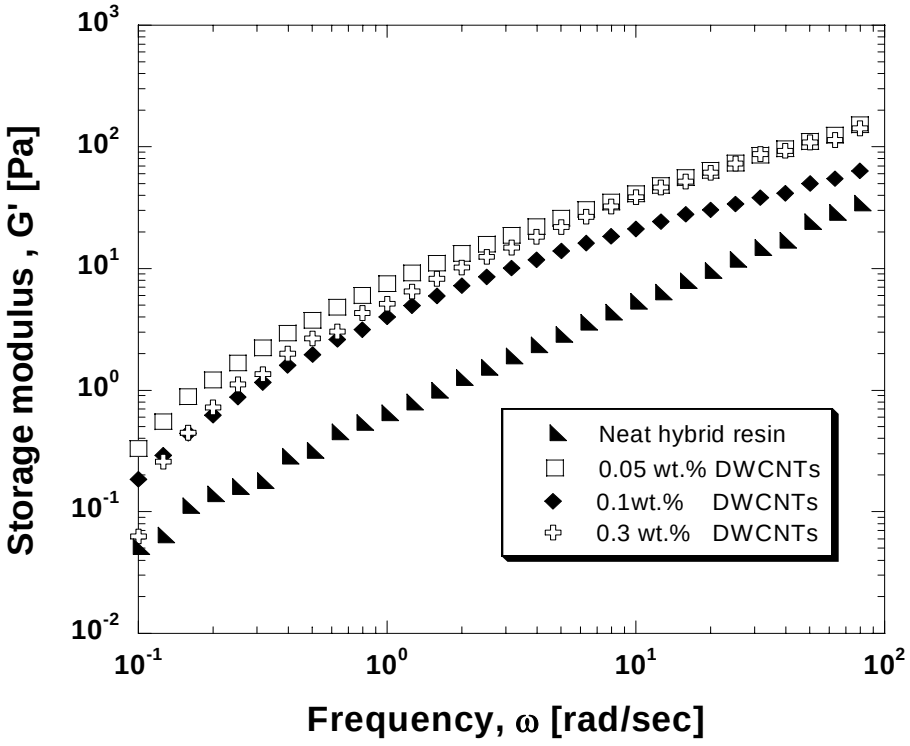

Figure 4.5. The frequency dependence of the storage modulus (G') for the neat resin blend and its suspensions with different content of DWCNTs

From that point of view, presence of relatively large agglomerates of DWCNTs within the matrix resin due to their relatively poor dispersion may shift the rheological threshold value to higher values as compared to MWCNTs. As mentioned earlier, rheological threshold value refers to critical filler loading rate at which the flow regime changes, showing frequency independency at relatively low frequency values. Another reason may be associated with high tendency of DWCNTs to reagglomerate within the resin matrix due to their relatively high particle-particle interactions and attractive forces in between individual particles. As a result, we did not observe a clear frequency independency for resin suspensions with DWCNTs regardless of amine functional groups. Despite lower aspect ratio of DWCNT-NH2 (two times lower than that of the untreated ones) due to functionalization process via ball milling method, DWCNT-NH2 modified resin suspensions exhibited higher G' values than those prepared with DWCNTs.G' values of MWCNTs and MWCNT-NH2 filled resin suspensions were found to be similar, despite the fact that the aspect ratio of MWCNTs is five times larger than that of MWCNT-NH_2. From that point of view, it is reasonable to conclude that amine functional groups over CNTs contribute to the formation of a combined

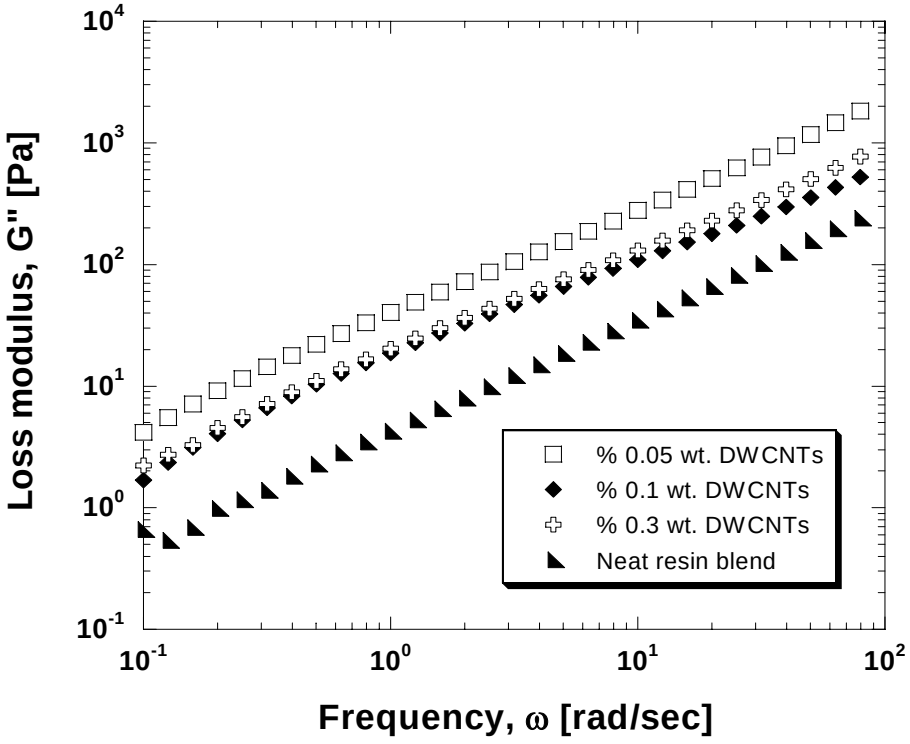

Figure 4.6. The frequency dependence of the storage modulus (G') for the neat resin blend and its suspensions with different content of DWCNT-NH_2

nanotube-polymer network structure based upon geometrical percolation of nanotubes via their huge aspect ratios.

Figures 4.7 and 4.8 show loss modulus (G") values of the hybrid resin suspensions containing different contents of DWCNTs and DWCNT-NH2, respectively. It is known that G" values are less sensitive to the properties and morphology of filler constituents as compared to G' values. As a result, change in the slope of G' (in the terminal zone at low frequencies) is expected to be more remarkable than that in the slope of G". However, comparison of storage and loss modulus values with each other may assist in qualitative determination of the dispersion state of particles within suspension of interest. In consequence, at each given loading rate, resin suspensions containing DWCNTs were found to exhibit viscous behavior (G" > G'), while those with DWCNT-NH_2 showed viscoelasticity (G" ≈ G'). This implies alteration of flow characteristics of resin suspensions to some extent via amine functional groups over surfaces of CNTs. These findings are also very consistent with those for the resin suspensions containing MWCNTs and MWCNT-NH_2.

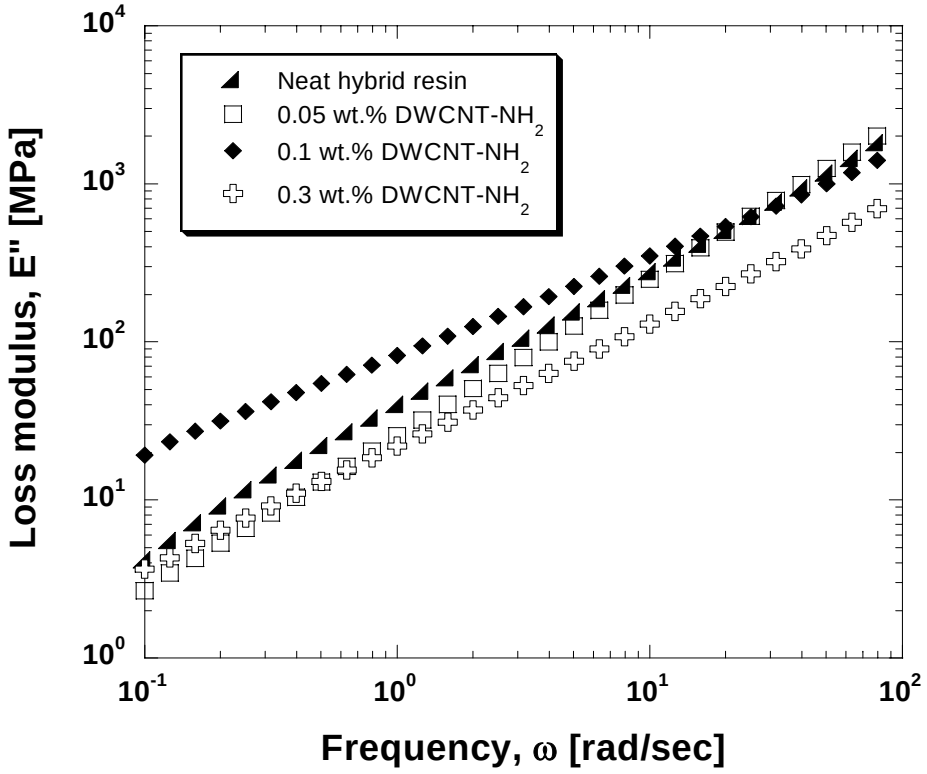

Figure 4.7. The frequency dependence of the loss modulus (G") for the neat resin blend and its suspensions with different content of DWCNTs

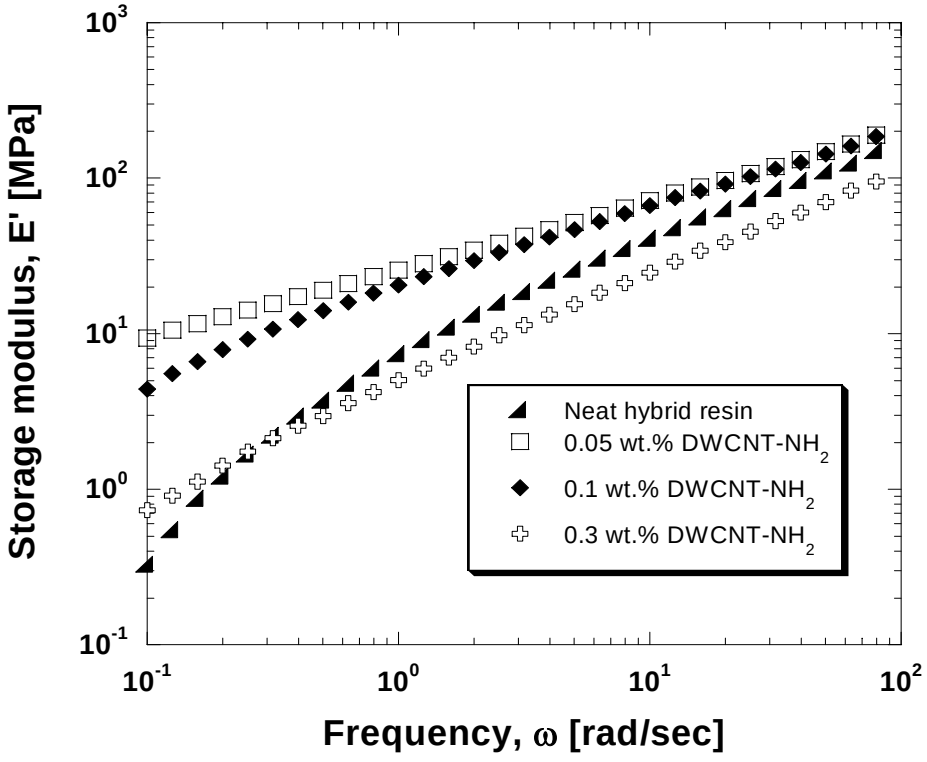

Figure 4.8. The frequency dependence of the loss modulus (G") for the neat resin blend and its suspensions with different content of DWCNT-NH_2

Figures 4.9 and 4.10 give shear viscosity values with respect to shear rate for the neat resin blend and its related suspensions containing different amount of DWCNTs and DWCNT-NH_2, respectively. As seen in the figures, regardless of amine functional groups or content of CNTs, shear thinning behavior was observed for each nanotube modified resin suspension such that viscosity values reduce with increasing shear rate. The neat resin blend is almost the Newtonian fluid behavior. At 0.05 and 0.1 wt. % CNTs content, initial shear viscosity of DWCNT-NH_2 modified resin suspension was found to be higher than that of resin suspension with DWCNTs. This may be attributed to the relatively good dispersibility of amino functionalized nanotubes within the resin medium. Unlike the observed behavior of MWCNTs and MWCNT-NH_2 modified resin suspensions, as the content of DWCNTs or DWCNT-NH_2 increased within the resin blend, shear viscosity of their corresponding resin suspensions decreased at low frequencies with steeper slope. This may be associated with the unstable degree of dispersion and distinct orientation of nanotubes within the resin blend, depending upon their different specific surface area, aspect ratio and distinct particle-particle interactions.

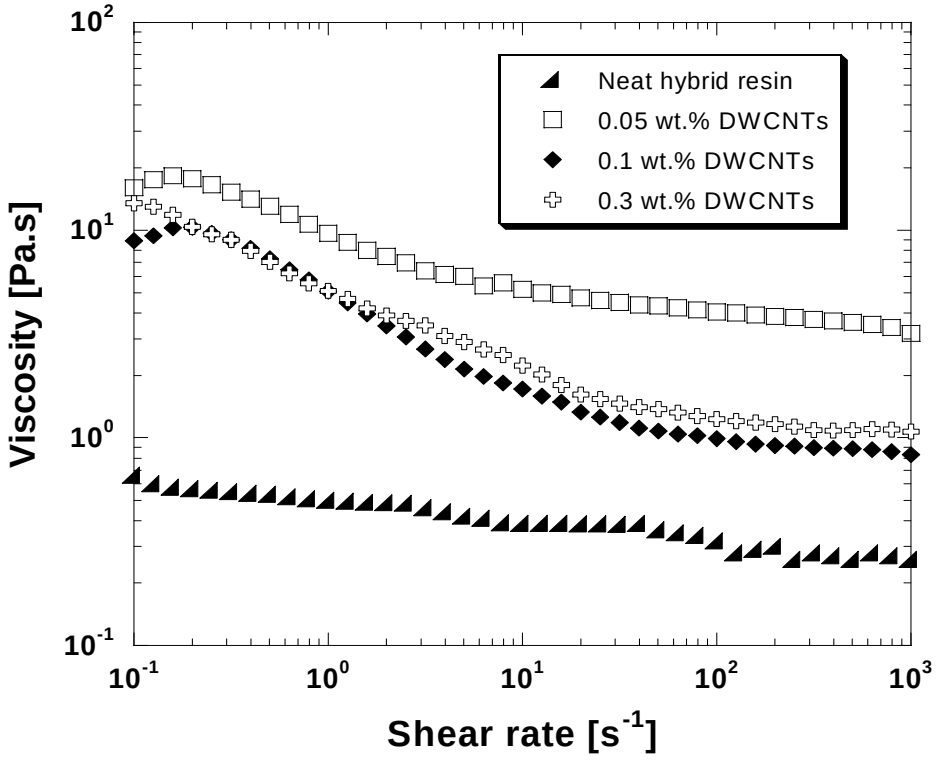

Figure 4.9. Shear rate dependency of viscosity for the neat resin blend and its suspensions with different content of DWCNTs.

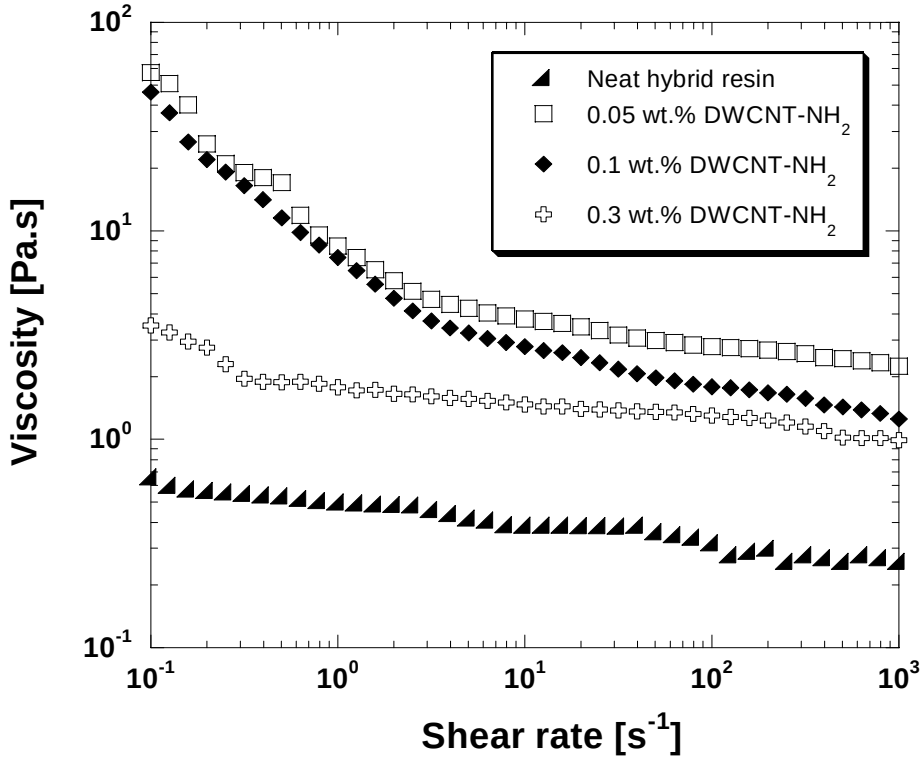

Figure 4.10. Shear rate dependency of viscosity for the neat resin blend and its suspensions with different content of DWCNT-NH_2.

In brief, these findings support the motivations given earlier for the elucidation of frequency dependent storage and loss modulus values of resin suspensions with respect to CNTs.

4.4. Conclusions

Rheological behavior of CNT modified hybrid resin suspensions was characterized by performing linear dynamic viscoelastic measurements and steady shear tests conducting an oscillatory rheometer with parallel plate geometry. Linear dynamic viscoelastic measurements revealed that storage modulus (G') and loss modulus (G'') values of resin suspensions as a function of angular frequency increased with respect to MWCNTs regardless of amine functional groups. In contrary to what is observed for MWCNTs and MWCNT-NH_2, it was found that storage and loss modulus values of DWCNTs and DWCNT-NH_2 modified resin suspensions decreased with increasing filler content. At 0.3 wt. % loading rate, the rheological threshold (pseudo-solid like

behavior) was obtained for MWCNT modified resin suspensions regardless of amine functional groups. This transition zone is highly visible at lower frequencies. However, no transition zone was obtained from the resin suspensions with either DWCNTs or DWCNT-NH_2. Steady shear measurements revealed that, regardless of type of CNTs or amine functional groups, each CNT modified resin suspension exhibited shear thinning behavior with steeper slope, while the hybrid resin was almost the Newtonian fluid. Nevertheless, under steady shear, the response of resin suspensions containing MWCNTs with and without amine functional groups differs contradictorily from that of resin suspensions with DWCNTs or DWCNT-NH_2. Specifically, the shear viscosity values for resin suspensions containing MWCNTs and MWCNT-NH_2 increased with an increase in the content of CNTs, while these values reduced gradually for DWCNTs in a different manner.

CHAPTER 5

CURE KINETICS OF CNT MODIFIED HYBRID RESIN SUSPENSIONS

5.1 Introduction

High performance reinforced composite materials are typically composed of high modulus fibrous reinforcing materials embedded in a thermosetting polymer matrix. The final properties of the resulting composite structures vary, depending on the properties of the reinforcement, interphase and the matrix resin. In this respect, unsaturated polyester (UP) and vinylester (VE) resins are the most common matrix materials utilized for reinforced composite structures (Tanoglu and Seyhan 2003). The both resins possess some superior properties including chemical resistance, low viscosity, relatively high mechanical properties as well as low cost and ability to cure at room temperature (Yang and Lee 2001).

A good understanding of cure kinetics of matrix resins is critical to the understanding of structure and behavior of their resulting reinforced composites. In other words, the cure kinetics provides substantial information regarding the final network structure in matrix resins, which has a significant effect on the properties of the resultant product (Bae, et al. 2000, Jannesari, et al.2005). The information obtained from cure processing is also accessible to composite processing parameters.

CNTs are widely being used as fillers to improve thermal, mechanical and electrical properties of polymers. As compared to their micro sized counterparts such as carbon black (CB) micro particles, CNTs with high aspect ratio and surface area are expected to affect more significantly the curing behavior of the polymer matrix in which they are embedded (Xie, et al. 2004, Puglia, et al. 2003, Roşu, et al. 2004)

Various experimental methods have been conducted by researchers to monitor the progress of cure. Thermal analysis by Differential Scanning Calorimeter (DSC) in both isothermal and dynamic modes is widely applied to study the kinetics of cure reactions (Roşu, et al. 2002, Macan, et al. 2004). Isothermal DSC measurements differ from the non-isothermal ones in that they have complete separation between the

variables of time and temperature. However, a significant development of the cure state can occur before DSC reaches and stabilizes at the desired temperature. As a result, the reaction may not reach the completion at lower temperatures. Alternatively, dynamic DSC measurements could result in a better capture of the cure kinetics at both the on-set and the end of the reaction (Xie, et al. 2004, Puglia, et al. 2003). However, DSC measures in principle only the overall heat release during the reaction, but can not distinguish multiple overlapping reactions which occur in the system (Malek 2000, Lu, et al. 1998). The main emphasis with DSC is on obtaining data to develop empirical models like the autocatalytic kinetic model, which are system specific and thus not representative for all styrene / VE or UP systems (Sanchez, et al. 2000, Caba, et al. 1998). At this stage, researches focused their attention on FTIR spectrometry, which offers the potential to differentiate the rate of isothermal reactions dependent on the spectral changes of different functional groups (Caba, et al. 1998, Li, et al. 1999). In other words, depletion of the reactive species in a sample can be monitored by FTIR in a separate manner, provided that their absorption peaks are noticeable from the product peaks.

Raman spectrometry (RS) is a simple non-destructive technique. Like FTIR spectrometry, it can provide a spectrum of characteristic bandwidths which help identify the chemical species and bond types present in the material of interest (Zhao and Wagner 2004). One advantage of the Raman technique over FTIR is that any shift in characteristic Raman peaks can be attributed to straining of the material, through external and internal stressing (Stevanovic, et al. 2000). In this respect, Raman spectrometry has recently been used to identify CNTs, evaluate their dispersion in polymers, and highlight the interaction between polymer matrix and CNTs in nanocomposites (Zhao and Wagner 2004, Frogley, et al. 2002). In this technique, interaction of CNTs with polymers is reflected by a peak shift or a peak width change.

Understanding of thermal stability of polymer composites is of significance to interpret the effect of filler constituents embedded in polymer matrices on the chemical degradation mechanism of the final product (Ho, et al. 2006, Shih, et al. 2002). Thermo-gravimetric analysis (TGA) is one of the most commonly used thermal analysis techniques to monitor the thermal decomposition of polymeric materials (Ferreira, et al. 2005). In principle, the thermo-analytical curves, like DSC curves, provide only basic information about the process and do not make fine distinction between partial chemical reactions during thermal degradation. However, interpretation of TGA data helps get

also a relevant opinion regarding the curing behavior of polymeric materials in conjunction with the presence of filler constituents.

In summary, the combination of experimental techniques mentioned above helps assess any chemical interaction between reinforcement constituent and the surrounding polymer matrix.

In this chapter, analytical techniques including DSC, FTIR, RS and TGA were employed to explore the effect of MWCNTs and MWCNT-NH_2 on polymerization of the hybrid resin, with particular emphasis on amine functional groups over the surfaces of CNTs. Please note that we ignored to study the curing mechanism of the resin suspensions with DWCNTs and DWCNT-NH_2. This is because they exhibit relatively large dense agglomerates, which may lead to inconsistency and difficulty with reproducibility of the curing data to be obtained. In other words, the more homogenous distribution of CNTs within the polymer matrix, the more accuracy in the experimental results obtained. Therefore, aim herein is to simply monitor what is going during free radical polymerization based on the chemical interactions between monomers and CNTs within the involved suspensions.

5.2 Vinylester and Polyester Resin Systems

Vinylester (VE) monomers are addition products of various epoxide resins and ethylenically unsaturated monocarboxylic acids such as acrylic or methacrylic acids. On the other hand, the term unsaturated polyester (UP) resin is used to describe a class of thermosetting resins consisting of an unsaturated backbone dissolved in a reactive monomer (Kosar and Gomzi 2004). The polyester backbone is synthesized by condensation polymerization. Polyester resins are commonly categorized as ortho and iso resins depending on the nature of the saturated acid portion of the backbone polymer. The difference between them is that ortho and iso resins use orthophthalic acid and isophtalic acid, respectively. Ortho resins are used in contact molding such as marine applications, while iso resins are used in matched die molding, corrosion resistant applications and gel coats (Tanoglu and Seyhan 2003). VE and UP resins are similar to each other in that they both contain styrene as a reactive diluents. Figure 5.1 shows the chemical structure of polyester and vinylester resins.

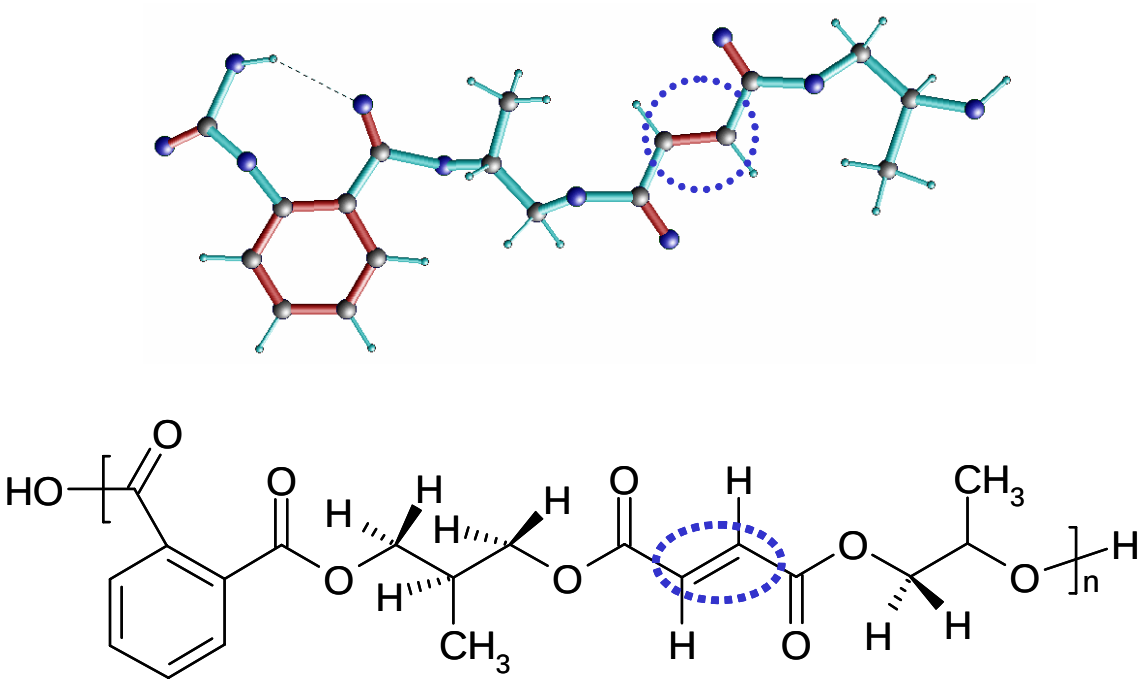

a)

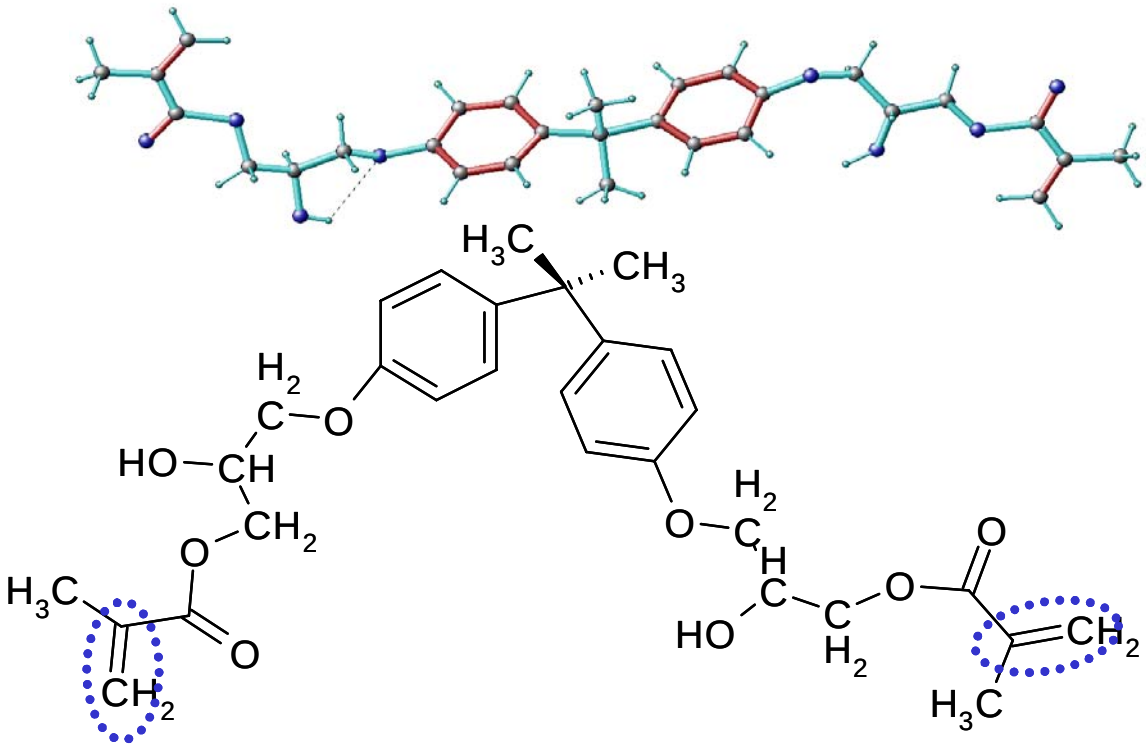

b)

Figure 5.1. The chemical structure of a) thermosetting polyester and b) vinylester resins

As seen in the figure, the UP monomers have usually more than two double bonds per molecule that are located inside the chain, while VE monomers have one double bond at either end of the molecule. In most of the commercial vinylester or polyester resins, the styrene concentration varies from 30 to 55 wt. %. However, the research done on UP can not be directly used for VE resins due to one major difference between the two resins which arises from the number and the location of reactive groups (namely (C=C) bonds in VE and UP monomers (Dua, et al. 1999, Scott, et al. 2002)

VE and UP monomers react via free radical chain growth copolymerization, forming cross-linked polymer networks by the aid of styrene in the system. Note that the term cross-links form between different polymer chains and assist in the formation of a network that tightens as long as the conversion increases. As an example, Figure 5.2 depicts schematically the polyester monomers cross-linked by styrene monomers. As seen in the figure, styrene acts as a bridge between two polyester monomers, just reacting with the opened double carbon bonds of these corresponding monomers.

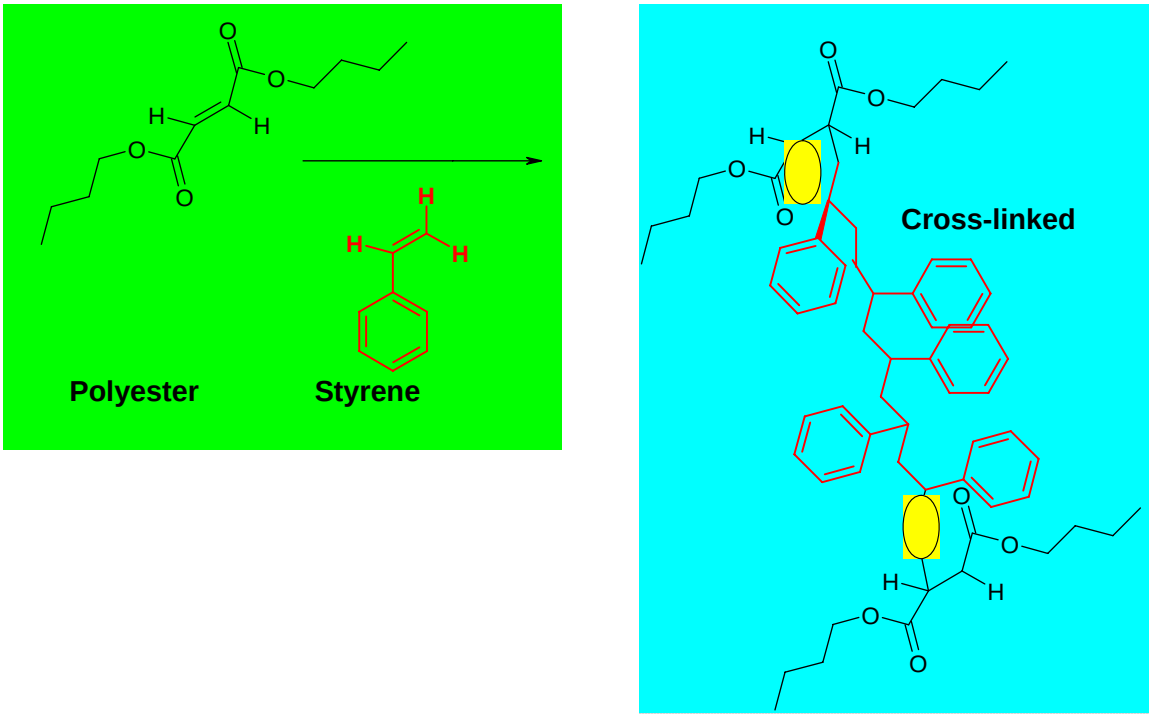

Figure 5.2. Illustration of two polyester monomers cross-linked via styrene

Degree of cross-linking is highly associated with the final properties of the matrix resin. For instance, the glass transition temperature (T_g) of the resin increases with an increase in the degree of cross-linking. In this respect, the term curing can be

described as a combination of chemical and physical processes during which transformation of thermosetting resin systems into a cross-linked network takes place.

Two major features associated with the curing process of VE and or UP includes gelation and vitrification (Batch and Macossa 1992, Tollens and Lee 1993). Gelation of a resin system is characterized by the formation of chemical structures of macroscopic dimensions to which the term infinite network is applied. The infinite network reaches the dimension of the sample itself. The onset of formation of an infinite network is apparent as the asymptotic increase of viscosity and the weight average molecular weight of the resin towards infinity. On the other hand, vitrification occurs when the T_g exceeds the cure temperature. A curing resin system experiences vitrification when the material begins to solidify. Once the material reaches vitrification, the molecular motions of polymer are severely restricted and the reaction is ceased to diffusion limitations on the growing radical species, as well as on the monomers (Dua, et al. 1999, Hsu and Lee 1993).

5.3 Free Radical Chain Growth Copolymerization

The VE or UP cure process is a free radical chain growth copolymerization. For such systems, the polymerization can be divided into three main stages. These are initiation, propagation and termination (Lam and Blauman 1990, Lee and Lee 1994, Dua, et al. 1999, Scott, et al. 2002).

Initiation takes place when the peroxide initiator decomposes into primary free radicals followed by the formation of monomer radicals. With this respect, monomer radicals provide the active sites required to overcome inhibition and to sustain chain reaction. The process of chain initiation is generally considered to involve two steps; the first is the decomposition of the initiator ***I*** to yield a pair of free radicals $R^{\bullet}$

$$I \rightarrow 2R\cdot$$

The second one is the addition of a monomer M to a primary radical R to yield a chain radical as follows

$$R\cdot + M \rightarrow M_1\cdot$$

The most commonly utilized initiators are organic peroxides and hydro peroxides. These initiators decompose into free radicals typically via two methods. The first one is thermal decomposition at elevated temperatures and the second one is the redox decomposition in the presence of metal catalyst such as cobalt naphatane (CoNAP) at low temperatures. In principle, since there are two monomers in either vinly ester or unsaturated polyester resins, two types of monomer radicals are formed. VE is used as a notation for the following formulas.

$$R\cdot + VE \rightarrow VE\cdot$$
$$R\cdot + ST \rightarrow ST\cdot$$

The free radicals have odd number of electrons, and thus they are formed in pairs, either or both of which may initiate polymerization according to the reactions given above. Please note that not all of the radicals in step 1 yield chain radicals, some of them may be lost through side reactions. Radicals generated by initiator decomposition are initially trapped in a solvent cage in which they may either recombine or terminate with another nearby radical to initiate chain polymerization (Dua, et al. 1999, Scott, et al. 2002, Hsu and Lee 1993).

Propagation involves the growth of polymer molecules by successive addition of monomers to the monomer radicals as follows;

$$M_1\cdot + M \rightarrow M_2\cdot$$
$$M_2\cdot + M \rightarrow M_3\cdot$$

In general, it can be defined as follows

$$M_x\cdot + M \rightarrow M_{x+1}\cdot$$

In vinylester resin systems, there are two monomers which can involve in the following types of propagation reactions

$$VE\cdot + VE \rightarrow VE - VE\cdot$$
$$VE\cdot + ST \rightarrow VE - ST\cdot$$
$$ST\cdot + VE \rightarrow ST - VE\cdot$$
$$ST\cdot + ST \rightarrow ST - ST\cdot$$

The first two reactions lead to homo-polymerization of VE and styrene, while the last two reactions refer to the copolymerization of VE and styrene, respectively.

Termination is composed of two mechanisms including bimolecular termination and unimolecular termination. Bimolecular termination can also be divided into two types. The first one; bi molecular termination via coupling as follows

$$M_x\cdot + \cdot M_y \rightarrow M_{x+y}$$

The second one is bimolecular termination via disproportionation through a hydrogen atom. In general, for bimolecular termination, two free radical species have to come close together. In other words, the radical species should have enough translational and segmental diffusivity that the two radicals can react with each other. In cross linking systems, unimolecular termination also plays an important role. This type of termination is mostly caused by entrapment of radicals (Batch and Macossa 1992). Due to extensive cross linking in thermosetting polymers, a large majority of free radicals is trapped within the polymer network and is no longer accessible to monomers or other radicals.

5.4. Interactions of Matrix Resin with CNTs

Interactions of CNTs with the surrounding matrix resin are highly critical to the ultimate properties of the resulting nanocomposites. Figure 5.3 is the illustration of chemical interaction between the amino functionalized CNTs and vinylester resin. As seen in the figure, C-N covalent bonding is supposed to occur between the surfaces of amino functionalized carbon nanotubes as a consequence of opened carbon double bonds of vinylester resin. In addition, weak hydrogen bonds are also supposed to occur as a result of interaction between the hydrogen molecules in vinylester and those

coming from structure of amine groups over the surfaces of CNTs. Please note that the chemical mechanism illustrated in the figure is hypothetical and does not necessarily take place within the resin structure. In fact, there are many factors associated with the complex reactions that occur in the resin system.

Since CNTs exhibit huge surface area and aspect ratio, their interactions with the free radicals generated by the decomposition of the initiator is vastly critical to the characteristics of the network structure formed in the resultant system.

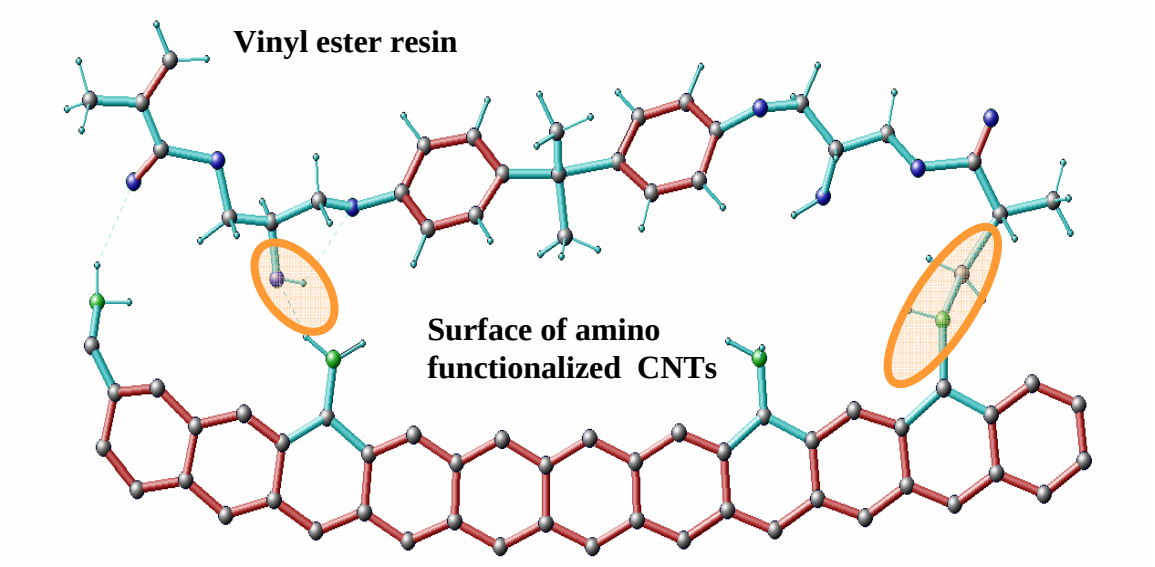

Figure 5.3. Illustration of chemical interaction between the surfaces of amino functionalized CNTs and vinylester polymer chains

In this respect, the probability of amine groups over the surfaces of CNTs to react with the double bonds of the vinylester resin should also be taken into account. Figure 5.4 depicts one of the worst scenarios for the resin system as an example. In this case, amine groups on the surfaces of DWCNTs react with the opened double carbon bonds of polyester resin which are in fact supposed to react with styrene monomers. As a consequence, residual styrene monomers would be most probably polymerized as polystyrene without cross-linking the polyester molecules. This may affect the cross-linking density, just tuning the individual fractional conversion of the monomers in the resin system. Investigation of these interactions encompasses the motivations of this chapter.

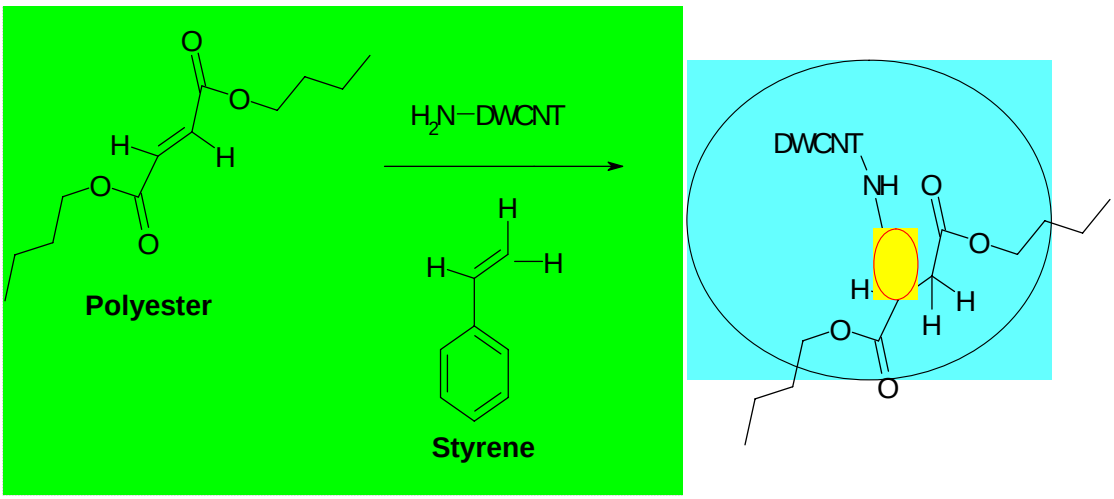

Figure 5.4. An example to the interaction between matrix resin, styrene and CNTs

5.5. Experimental

5.5.1. DSC Measurements

All measurements were performed by a Shimadzu DSC-50 scanning calorimeter. A small quantity of the sample (10-25 mg) was used for the DSC studies in a sealed aluminum pan. Dynamic runs were carried out on the suspensions, using another aluminum empty cell as a reference. The curing thermal data for each sample was obtained from dynamic scans at different heating rates (5, 10, and 20 °C/min) from room temperature up to 200°C in a nitrogen atmosphere. The total heat of the reaction was estimated for each sample from the non-isothermal experiments by integrating the area under peaks of the DSC exotherms obtained.

5.5.1.1. Cure Kinetics Approach via DSC

The basic kinetic approach of thermosetting polymers is that the heat flow measured in DSC is proportional to both overall heat release and the rate of the kinetic process, as given below (Roşu, et al. 2004, Kessler and White 2002, Roşu, et al. 2002)

$$\frac{d\alpha}{dt} = \frac{\phi}{Q} \tag{5.1}$$

where Q is the enthalpy of the curing reaction and ϕ is the measured heat flow, (α) is the extent of the reaction. For the non-isothermal conditions, α is obtained by integrating the equation (5.1) by utilization of constant heating rate (Malek, 2000, Roşu et al. 2002).

$$\alpha = \frac{1}{Q\beta}\int_{T_i}^{T}\phi dT \tag{5.2}$$

where β is the heating rate ($\beta=dT/dt$) and Ti refers to the beginning of the baseline approximation. The rate of kinetic process can be expressed as a function of temperature dependent rate constant. The rate constant $K(T)$ and (α) dependent kinetic model function f (α) is as follows (Roşu, et al. 2002, Roşu, et al. 2004, Puglia, et al. 2003)

$$\frac{d\alpha}{dt} = K(T)f(\alpha) \tag{5.3}$$

$K(T)$ in equation 3 follows Arrhenius form, as given in equation (4) (Xie, et al. 2004)

$$K(T) = A\exp(-\frac{E_a}{RT}) \tag{5.4}$$

Where A is the pre-exponential factor, E_a is the apparent activation energy, R is the gas constant and T is the absolute temperature. In the case of non-isothermal conditions with constant heating rate $\beta=dT/dt$, equation (3) and (4) can be combined and revised into the form, as given below (Roşu, et al. 2002, Roşu, et al. 2004, Jannesari, et al. 2005)

$$\frac{d\alpha}{dT} = \frac{A}{\beta}\exp(-\frac{E_a}{RT})f(\alpha) \tag{5.5}$$

E_a values are determined from the plot of $1/T_i$ *versus* $\ln(\beta_i/T^2_i)$ (Kessler and White 2002). T_i refers to the temperatures which correspond to different degree of cure (α). A very well known autocatalytic equation (Bae, et al. 2002) given below for

thermosetting resin systems was proposed in the present study to model the experimental data.

$$f(\alpha) = \alpha^m (1-\alpha)^n \tag{5.6}$$

In this equation, *m* and *n* are reaction orders. Note that the total order of autocatalytic curing reaction is assumed to be 2 [m+n=2] (Kessler and White 2002, Roşu, et al. 2004). Using the value of *Ea* and the proposed kinetic model, the pre-exponential factor *A* is calculated according to the equation below (Roşu, et al. 2002, Roşu, et al. 2004).

$$A = -\frac{\beta x_p}{Tf'(\alpha_p)} \exp x_p \tag{5.7}$$

where x_p is reduced activation energy (E_a/RT) at the maximum peak, $f'(\alpha_p)$ is the differential form of the kinetic model α_p is the conversion corresponding to the maximum on each DSC curve. After the calculation of the pre exponential factor, using the autocatalytic equation, *m* and *n* values are achieved through non-linear regression at each specific value of degree of conversion (α).

5.5.2. FTIR Measurements

Cure monitoring of vinylester resin containing 0.3 wt. % of MWCNTs and MWCNT-NH_2 were performed by utilizing Schimadzu 8201 FTIR spectrometer in transmission mode. Please note that only neat vinylester resin was used as matrix material to ease the interpretation of data because, in the case of a complex mixture of polymers, it would be hard to differentiate which bands come from which molecules (Dua, et al. 1999, Scott, et al. 2002, Li, et al. 1999). Since vinylester resin contains styrene, CNTs were blended with vinylester resin via high shear mechanical stirring to avoid evaporation of styrene as much as possible. The FTIR spectra of MWCNTs and MWCNT-NH_2 were also taken to correlate the data obtained for their corresponding

nanocomposites. The point herein is to just reflect the effect of individual CNTs or their agglomerates on the free radical polymerization. In this manner, the same specified quantity of CoNAP and MEKP as in the production of the nanocomposites was added to neat liquid vinylester resin and its CNT modified suspensions in order to initiate the polymerization reaction. A drop of this catalyzed mixture was then taken and compressed between two potassium bromide (KBr) transparent crystal plates. This plate of sample was placed into a sealed infrared liquid cell which allows the curing process to be monitored in real time while preventing instant evaporation of styrene. The samples prepared were eventually scanned from 500 cm^{-1} to 4000 cm^{-1} at a resolution of 4 cm^{-1}.

5.5.2.1. Cure Kinetics Approach via FTIR

FTIR spectroscopy was used to monitor the depletion of carbon-carbon double bonds (C=C) for styrene and vinylester systems in separate manner. In this respect, the absorbance at 945 and 910 cm^{-1} were monitored during curing to determine the conversion of both of the monomers. Note that the peaks at 945 and 910 cm^{-1} correspond to out of plane bending of carbon-hydrogen bonds in the vinyl group of the vinylester monomer and wagging of CH_2 in the vinyl group of the styrene monomer, respectively. Aromatic carbon-hydrogen bonds at 830 cm^{-1} in vinylester and 700 cm^{-1} in styrene were used to correct for the changes in the thickness of the samples during reaction. Equations 1 and 2 were then employed to compute normalized fractional conversion of vinylester and styrene double bonds, respectively (Dua, et al 1999, Caba, et al. 1998).

$$\alpha_{VE}(t) = 1 - \left(\frac{At(945cm^{-1})}{Ao(945cm^{-1})} \right) \left(\frac{At(830cm^{-1})}{Ao(830cm^{-1})} \right) \tag{5.8}$$

$$\alpha_{ST}(t) = 1 - \left(\frac{At(910cm^{-1})}{Ao(910cm^{-1})} \right) \left(\frac{At(700cm^{-1})}{Ao(700cm^{-1})} \right) \tag{5.9}$$

In the equation, α is the fractional conversions of double bonds associated with each corresponding monomer at time t, and Ao and At are the normalized absorbance

peaks before the reaction starts and after a certain time *t*. The magnitudes of the relevant absorbance peaks were then measured, considering slight shifts that occurred due to reaction in peak locations and base lines. In this respect, automatic sampling was performed at the specified time intervals and the measurements were terminated once no changes were observed in the absorbance peak area.

5.5.3. Raman Spectroscopy

Raman spectrometry were performed on CNTs, the cured hybrid polymer and its nanocomposites prepared with MWCNTs and MWCNT-NH_2, using Renishaw 2000 Ramanscope, equipped with He-Ne laser, 50 cm^{-1} notch filter, and a 600 groove per mm grating. The wave length and power of laser were set to 633 nm and 20mW, respectively. The spectra collection time was set to 60 seconds in order to achieve a low noise to signal ratio. The spectra were acquired from 100 to 3500 cm^{-1} to detect especially the D and G bands of the CNTs. Please note that Raman spectrometry of CNTs used in this study was already measured by Gojny (Gojny 2006). We used the same spectra for interpretation of the data observed for nanocomposites. For the sake of accurate interpretation, the effect of MWCNTs and MWCNT-NH_2 upon the depletion of C=C of neat hybrid resin was evaluated by subtracting the spectrum of the resultant nanocomposites from the spectrum of each corresponding CNTs. The consequent spectrum and the obtained spectrum of the cured neat hybrid polymer were mutually compared for evaluation. For this approximation, the corresponding peak areas were considered.

5.5.4. Dynamic TGA Runs

A Perkin Elmer, Thermal Gravimetric Analyzer (TGA), was used for investigation of thermal degradation response of the cured hybrid polymer and its resultant nanocomposites containing 0.3 wt. % of MWCNTs and MWCNT-NH_2. A sample of about 10 mg for each batch was placed into alumina crucible. The samples were then heated from ambient temperature up to 700^{o}C in a 50 ml/min nitrogen flow at different heating rates (5, 10, and 20^{o}C/min.). Eventually, sample temperature, sample weight and its first derivative were recorded as a function of time.

5.5.4.1. Kinetic Approach to Thermal Decomposition

It was proved that at a constant degree of conversion, *C*, the activation energy of thermal degradation, E_d for a reaction is related to the heating rate, β, and the temperature, *T*, by the following Arrhenius equation (Shih and Yeng 2002);

$$E_d = -(R/b)\frac{\Delta(\log \beta)}{\Delta(1/T)} \tag{5.10}$$

where b is a constant with a value of 0.475 K^{-1}. The value of E_d can be determined from a plot of logarithm of heating rate versus the reciprocal of the absolute temperature at constant conversion level such that the slope of log β versus 1/T equals to E_d. Note that E_d values considered in this study was calculated based upon 5 wt % of conversion.

5.6. Results and Discussion

5.6.1. DSC Results

Figures 5.5-5.7 show the non-isothermal DSC exotherms observed at various constant heating rates (5, 10 and 20 °C/min.) for the neat resin blend and its suspensions containing MWCNTs and MWCNT-NH_2, respectively. Considering the initial (T_i), the peak (T_p), and the final (T_f) temperatures, and calculating reaction enthalpy (Q) values from each corresponding DSC exotherm, the impact of CNTs on the cure kinetics of the entire resin system was evaluated. The data obtained was given in Table 5.1. As seen in the table, incorporation of CNTs into the polymer blend increases the reaction enthalpy at each given heating rate. The resin suspensions with MWCNTs and MWCNT-NH_2 exhibited 3 and 10 % higher enthalpy values than the neat hybrid resin, respectively. Furthermore, at each heating rate, less curing times were observed for polymer suspensions containing MWCNT-NH_2 than for those with MWCNTs.

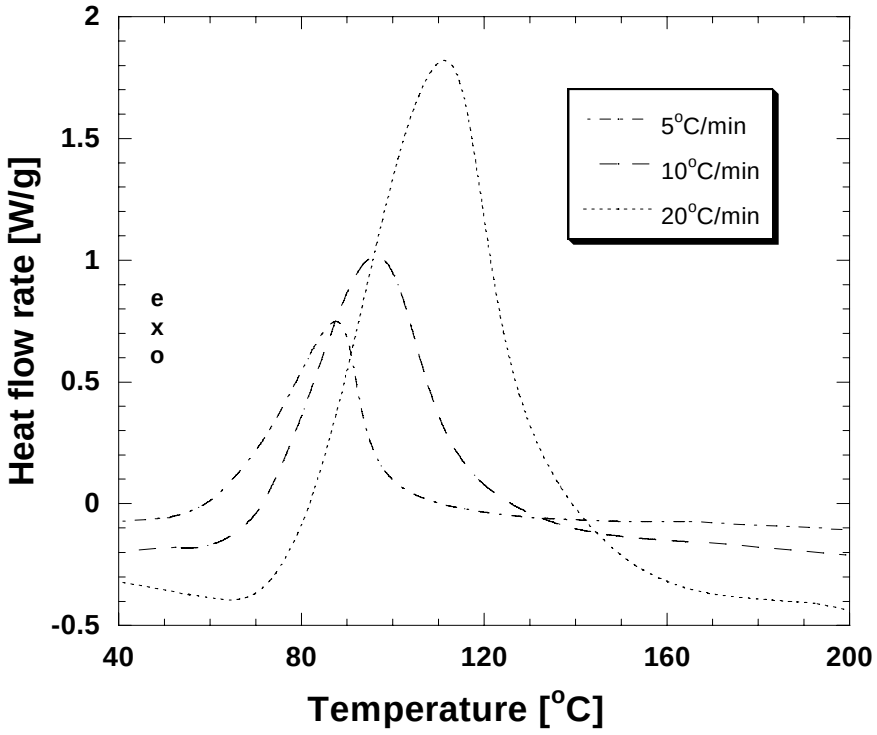

Figure 5.5. Non-isothermal DSC exotherm at different heating rates for the neat vinyl ester/polyester resin blend

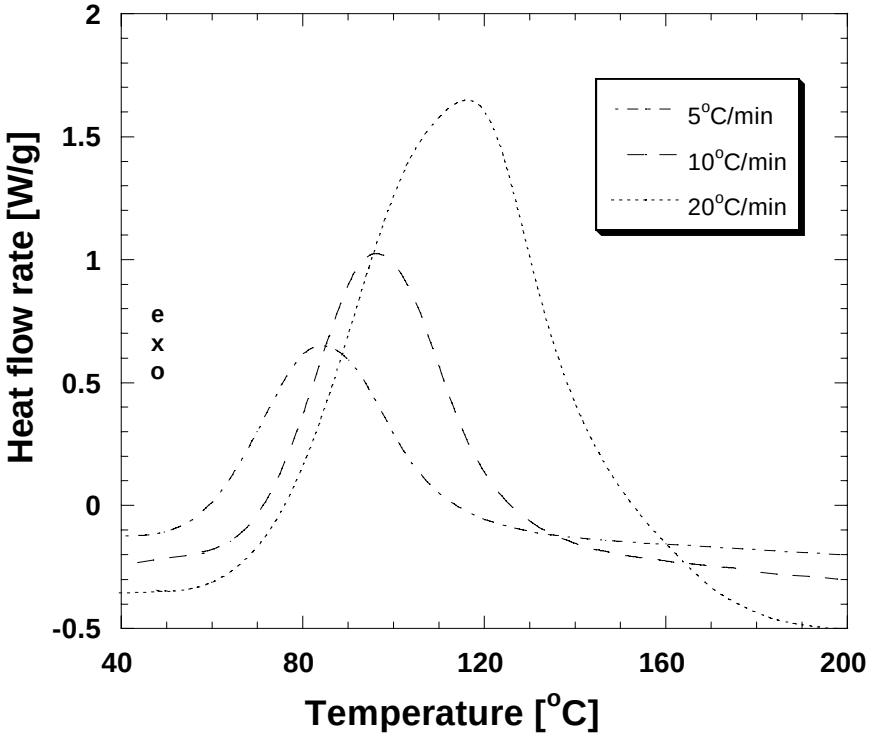

Figure 5.6. Non-isothermal DSC exotherm at different heating rates for CNT/vinylester polyester suspensions containing 0.3 wt. % of MWCNT

Table 5.1. Kinetic data obtained from DSC exotherms for neat polymer and CNT/polymer suspensions.

Sample	Heating Rate (°C/min)	T_i (°C)	T_p (°C)	T_f (°C)	Cure Time (min)	Q (J/g)
Neat resin blend	5	59	88	112	11.0	216
	10	71	96	127	5.6	238
	20	82	110	142	3.0	287
Resin blend MWCNTs	5	58	86	115	11.4	228
	10	69	95	125	5.6	242
	20	76	114	152	3.8	296
Resin blend MWCNT-NH_2	5	52	76	99	9.4	234
	10	60	88	102	4.2	247
	20	72	100	130	2.9	312

On the other hand, T_i value of the neat hybrid resin was lower than that of CNTs modified resin suspensions. This consequence is more pronounced for the suspension with MWCNT- NH_2.

Figure 5.8 gives the variation of E_a for the neat resin blend and CNTs modified suspensions with respect to the degree of cure. Note that E_a values were calculated at 0.05 increments of α values. The results obtained showed that activation energy of each suspension varies with the degree of cure in a different manner from each other. Moreover, it was also found that resin blend with carbon nanotubes featured moderately lower E_a values as compared to neat hybrid resin blend at each stage of cure. This trend is more obvious for the suspensions with MWCNT-NH_2 such that the E_a values decrease at lower degree of cure followed by increase till the end of the curing reaction.

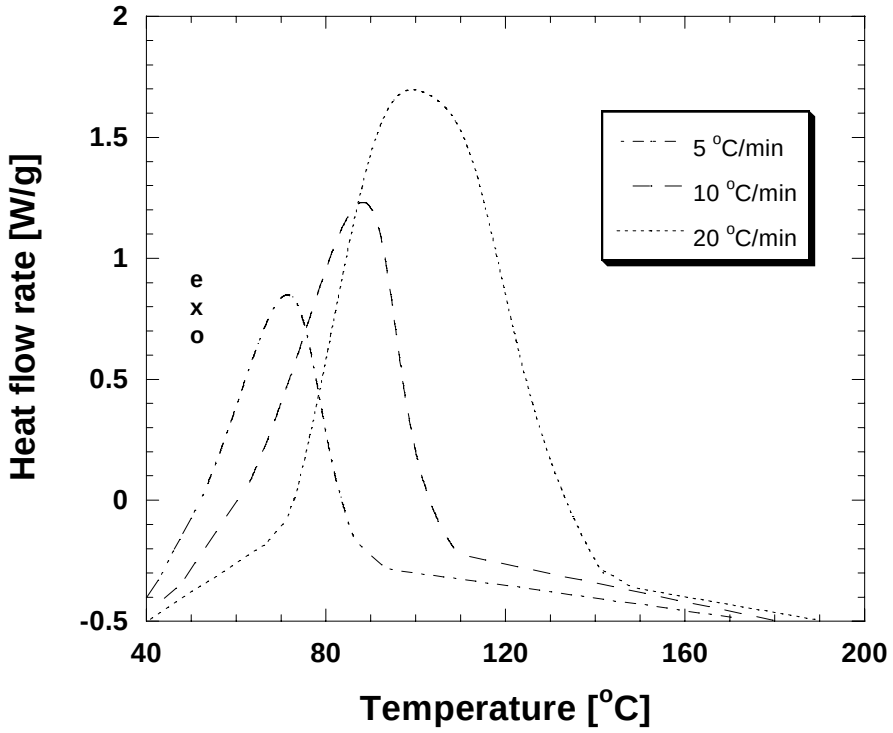

Figure 5.7. Non-isothermal DSC exotherm at different heating rates for CNT/polymer suspensions containing 0.3 wt. % of MWCNT-NH_2

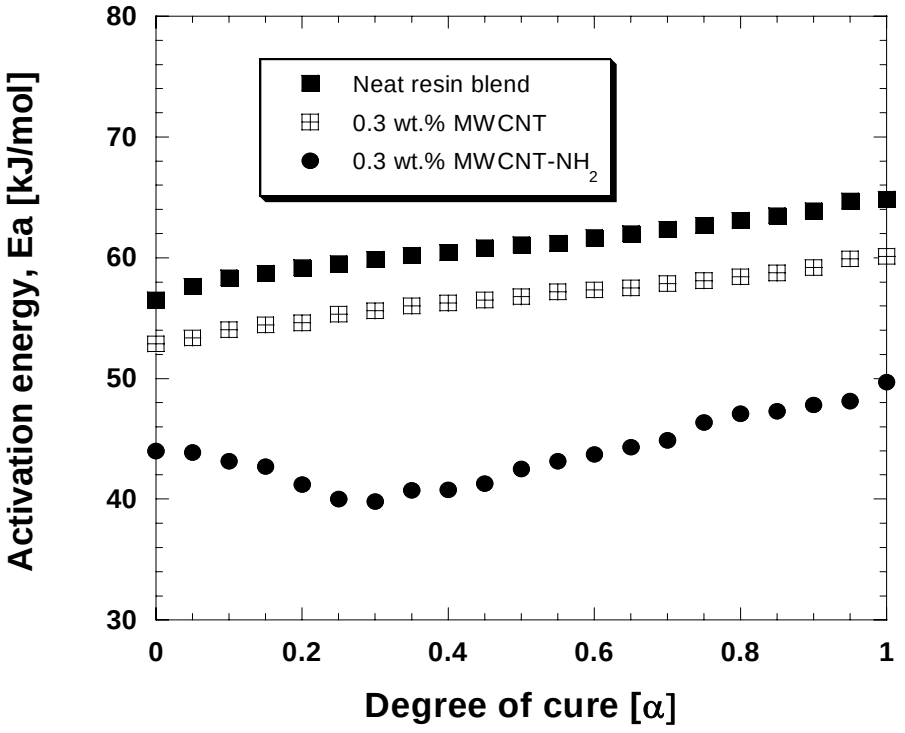

Figure 5.8. The apparent activation energy (Ea) of the samples with and without any filler as a function of degree of conversion

These predictions show the consistency with our main approach that nanotubes alter somewhat the chemical interactions within resin media during curing, and that amine groups alter the curing mechanisms. With the cure kinetic calculations via the proposed autocatalytic reaction model, the mean value of E_a for the neat resin blend and resin suspensions containing MWCNTs and MWCNT-NH_2 were predicted to be 57, 52 and 43 kj/mol, respectively. Table 5.2 gives the related kinetic parameters which account for the curing behavior of the resin suspensions. As seen in the table, no significant differences appear between values for each sample at different heating rates. Figures 5.9-5.11 give the comparison of the experimental and the predicted values for the neat resin blend and its suspensions containing MWCNTs and MWCNT-NH_2, respectively. In consequence, the predicted values were found to be in good agreement with those experimentally obtained. Note that there are some deviations especially at the peak points of the corresponding curves. This may come from the fact that the sum of the kinetic orders (m+n) is not precisely equaled to 2, as presumed, due to some unidentified or sight chemical reactions dependent on interactions of CNTs with the surrounding matrix resin.

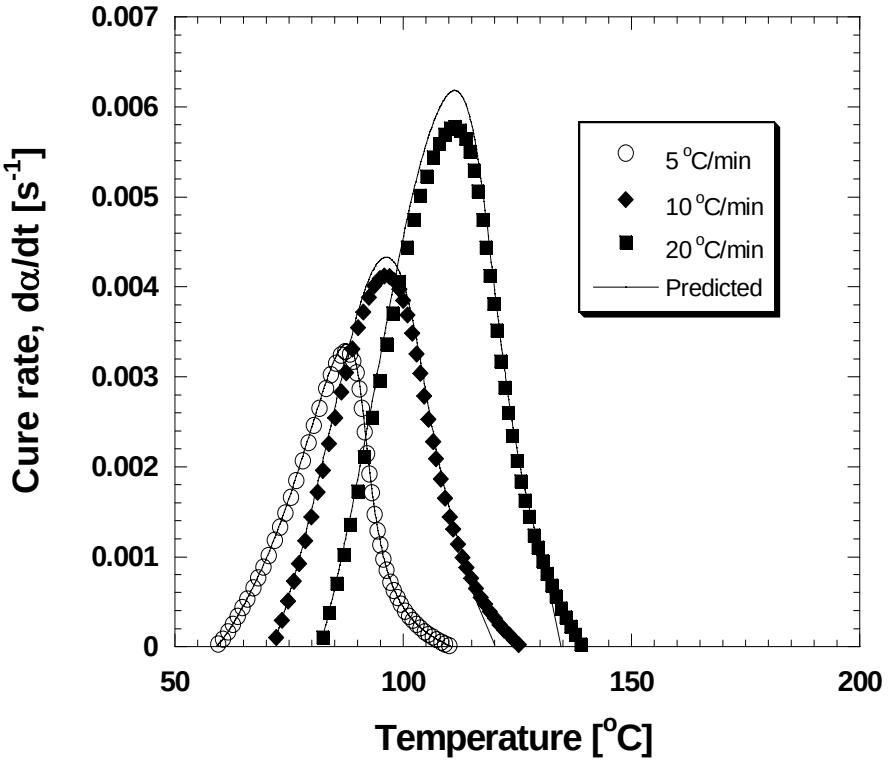

Figure 5.9. Comparison of experimental and predicted values of DSC exotherms for the neat resin blends scanned at different heating rates

Table 5.2. The related kinetic parameters which account for the curing behavior of the resin suspensions.

Sample	Heating rate (°C/min)	E_a (kJ/mol)	ln A	m	n
Neat resin blend	5	57	15.425	0.056	1.944
	10	57	16.142	0.139	1.861
	20	57	15.986	0.088	1.912
Resin blend MWCNT	5	52	14.082	0.134	1.866
	10	52	14.869	0.216	1.784
	20	52	14.293	0.185	1.815
Resin blend MWCNT-NH_2	5	43	12.831	0.0321	1.968
	10	43	13.024	0.0296	1.971
	20	43	12.682	0.0447	1.955

Similar findings were reported in the literature. Puglia et al. (2003) found that, with increasing MWCNTs contents in an epoxy system, the initial reaction rates increased, while the time to the maximum cure rate decreased. The authors ascribed this compromise to the acceleration effect of MWCNTs. Xie et al. (2004) found similar results on the behavior of CNTs in another epoxy resin system. Moreover, Bae et al. (2002) revealed that surface functional groups over the surfaces of CNTs lowered the corresponding activation energy while at the same time reducing the heat of cure, significantly. However, polymerization reaction of epoxy is different from that of vinylester. In our case, primary amine groups over the CNTs are likely to react with the double carbon bonds of the hybrid resin blend and inhibit radical reaction to some extent, thus reducing the cross linking density of the resulting cured polymer.

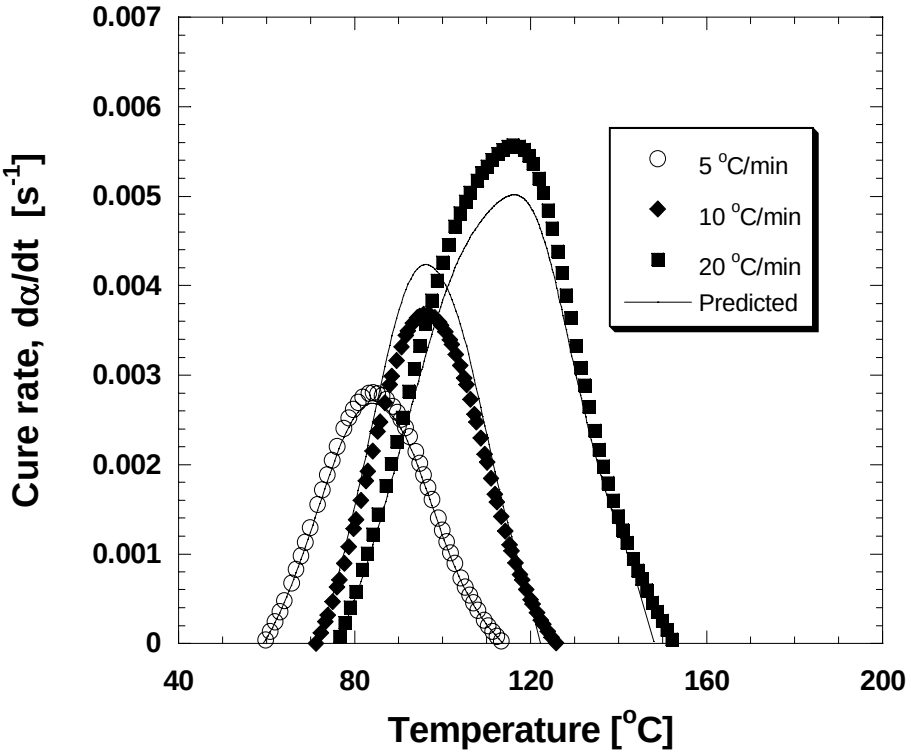

Figure 5.10. Comparison of experimental and predicted values of DSC exotherms for the suspensions with MWCNT scanned at different heating rates

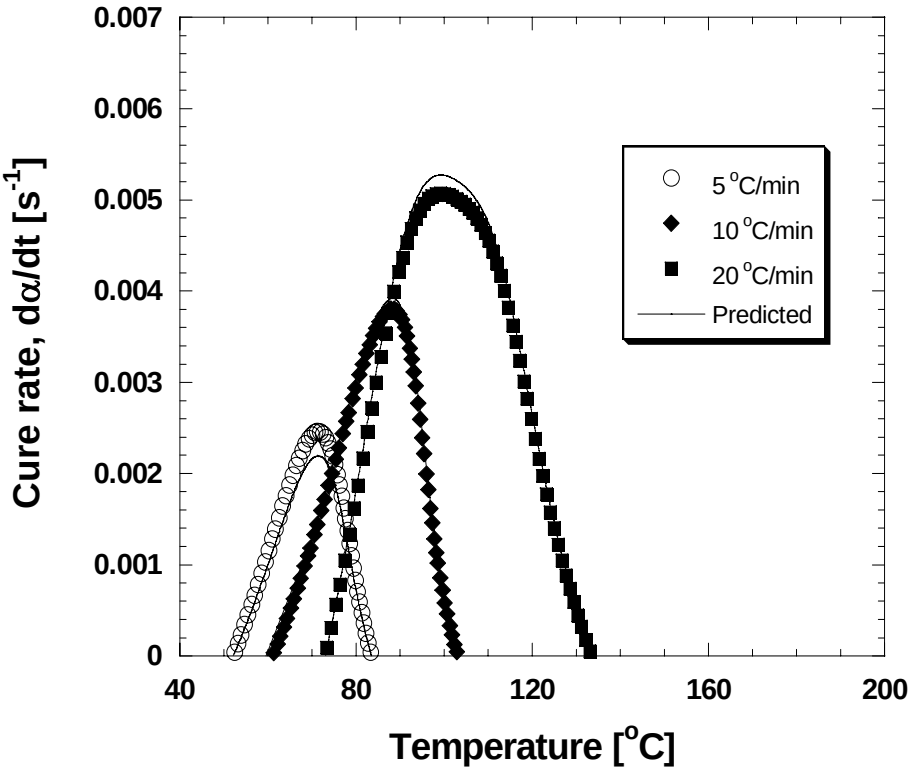

Figure 5.11. Comparison of experimental and predicted values of DSC exothermic for the suspensions with MWCNT-NH_2 scanned at different heating rates

The schematic illustration of this case was already given at the beginning of this chapter. On the other hand, amine groups are grafted onto the surfaces of CNTs by ball milling, during which the lengths of the CNTs are partially diminished. In brief, the length of MWCNT-NH_2 is five times less than that of MWCNTs. In another respect, relatively low aspect ratio of MWCNT-NH_2 due to functionalization process may play a major role in resin cure reactions. Gryschuk, et al (Gryschuk, et al. 2006) stated that aspect ratio and surface area of CNTs are critical to final properties of polymers, and that lower aspect ratio of MWCNTs would probably more beneficial to ultimate properties of highly cross-linked resins like vinylester. Moreover, they also concluded that the amount of MEKP and CoNAP subjected to the entire resin system needs to be optimized dependent upon the type of CNTs.

Although thermal analysis by DSC in both isothermal and dynamic modes is widely used to study the kinetics of cure reactions, DSC does not give information about the individual conversion profiles of VE, UP and styrene. However, in our case, the presence of CNTs in the hybrid resin system that polymerize via decomposition of radicals could change the relative conversion rates of vinylester, polyester and styrene double bonds, which produces significant differences in the network structure to be formed. In fact, it is interesting to know whether the promising results obtained from DSC measurements come mainly from amine functional groups over the surfaces of CNTs or from the reduced aspect ratio of CNTs due to ball milling. Therefore, it is reasonable to further investigate the interaction of untreated and amino functionalized CNTs with the hybrid matrix resin, utilizing more sophisticated analytical tools such as FTIR and Raman spectroscopy.

5.6.2. FTIR Results

As previously elucidated in details, neat vinylester resin was utilized as matrix material for FTIR studies to avoid complexity with polymer blends. The aim herein is to reveal the impact of the presence of CNTs with and without amine functional groups on the chain growth co-polymerization. Figures 5.12 a and b show the transmission spectra for a neat vinylester styrene resin and its suspensions containing 0.3 wt. % of MWCNTs and MWCNT-NH_2 before and after cure, respectively. Please note that the reductions in peak intensity for MWCNT and MWCNT-NH_2 modified suspensions were calculated

after subtraction of the base line corrected spectra of carbon nanotubes. As seen in the figure, CNTs with and without amine functional groups have substantial effects on the peak intensity values of neat vinylester resin. In other words, conversion of individual monomers was altered as expected in the presence of CNTs.

Figures 5.13, 5.14 and 5.15 give experimental plot of fractional double bond conversion of VE and styrene with respect to the reaction time in VE resin and its suspensions with MWCNTs and MWCNT-NH_2, respectively. These graphs were obtained, using the equations given in section 5.4.2.1. Please note that double bond conversions of VE and styrene are based on the initial number of double bonds of VE and styrene, respectively. In this respect, a higher value of conversion obtained for VE bonds does not necessarily mean that more number of VE double bonds would react when compared to styrene double bonds. As given in Figure 5.11, in the very beginning of the reaction, the rate of fractional conversion of VE is more than that of styrene. After a while, the rate of styrene fractional conversion becomes almost equal to that of VE. Almost at the end of the reaction, the rate of conversion of styrene exceeded VE conversion rate. These findings are very consistent with those in other similar studies reported in the literature (Dua, et al. 1999, Scott et al. 2002, Lee and Lee 1994)

However, as depicted in Figures 5.14 and 5.15, it was observed that the individual fractional conversion rates of styrene and vinylester were altered dependent on the amine functional groups over the surfaces of CNTs. The final conversion of styrene exceeded the final conversion of vinylester double bonds in the resin suspensions with MWCNT-NH_2. Nevertheless, final conversion of vinylester double bonds is slightly higher than that of styrene in the resin suspensions with MWCNTs. In this respect, one can conclude that some of amine groups over the surfaces of CNTs react with double bonds of vinylester resin during curing, which are in fact supposed to react with styrene. In this scenario, residual styrene monomers would be polymerized as polystyrene without cross linking the vinylester molecules. In fact, this behavior is very similar to that illustrated in Figure 5.4. Moreover, regardless of amine functional groups, conversions of styrene and vinylester double bonds were found to be slightly lower in the CNT modified resin suspensions than neat vinylester resin. This is astoundingly remarkable because we have obtained better properties from the nanocomposites as compared to neat hybrid polymer. However, degree of dispersion and the distribution of the agglomerates within the resin system are highly capable to change the results obtained.

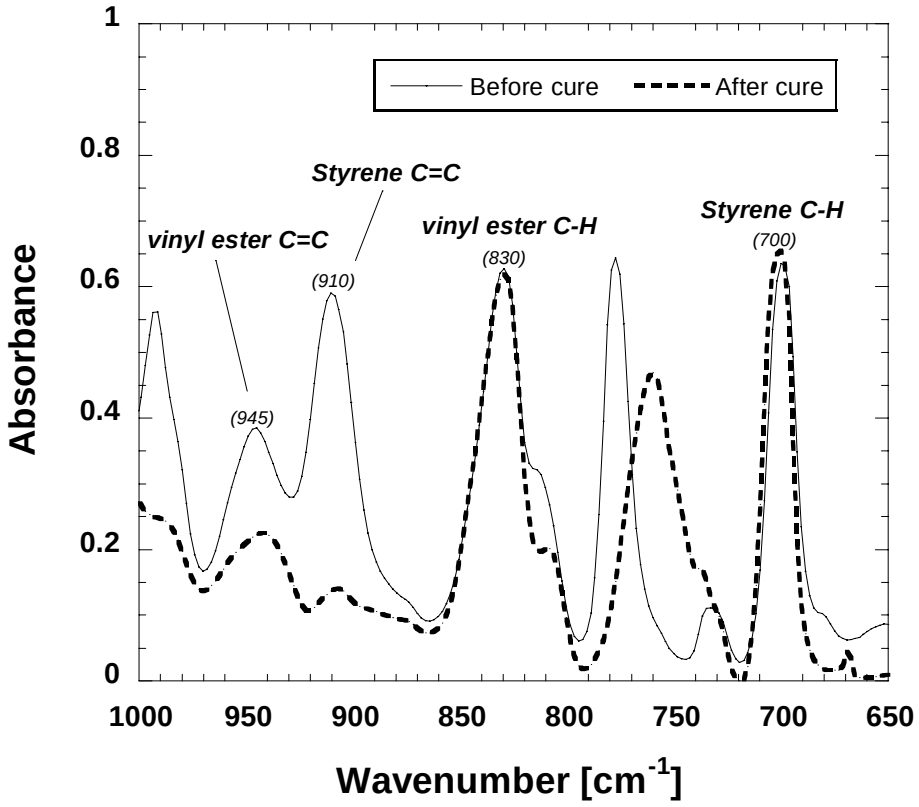

a)

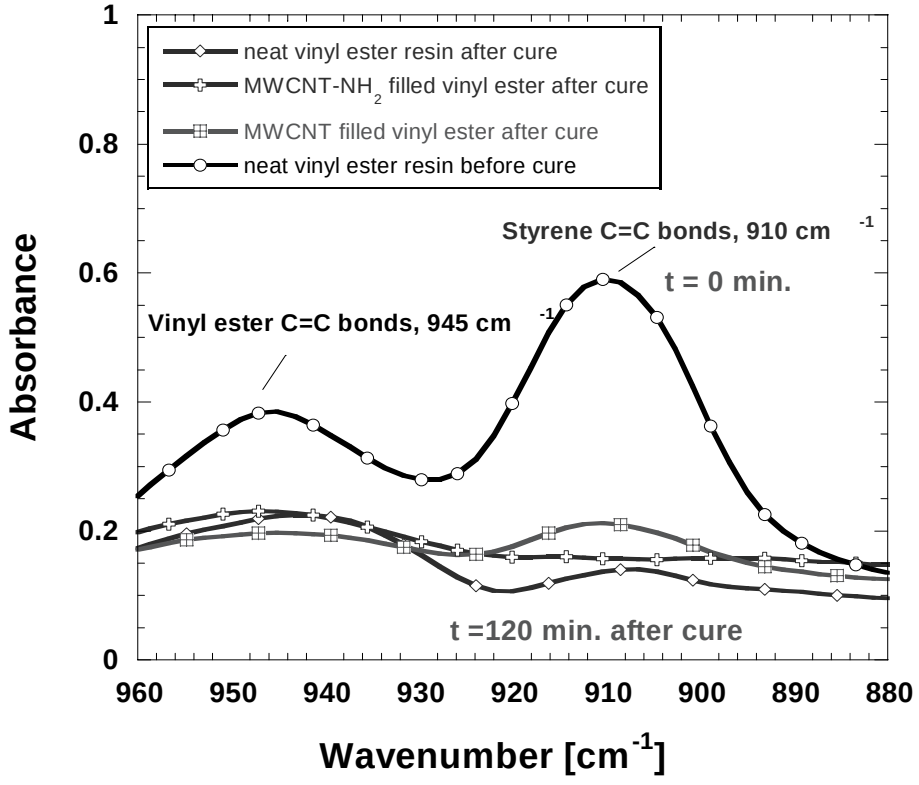

b)

Figure 5.12. FTIR spectra a) neat vinylester resin before and after cure b) suspensions with 0.3 wt. % of MWCNTs and MWCNT-NH_2

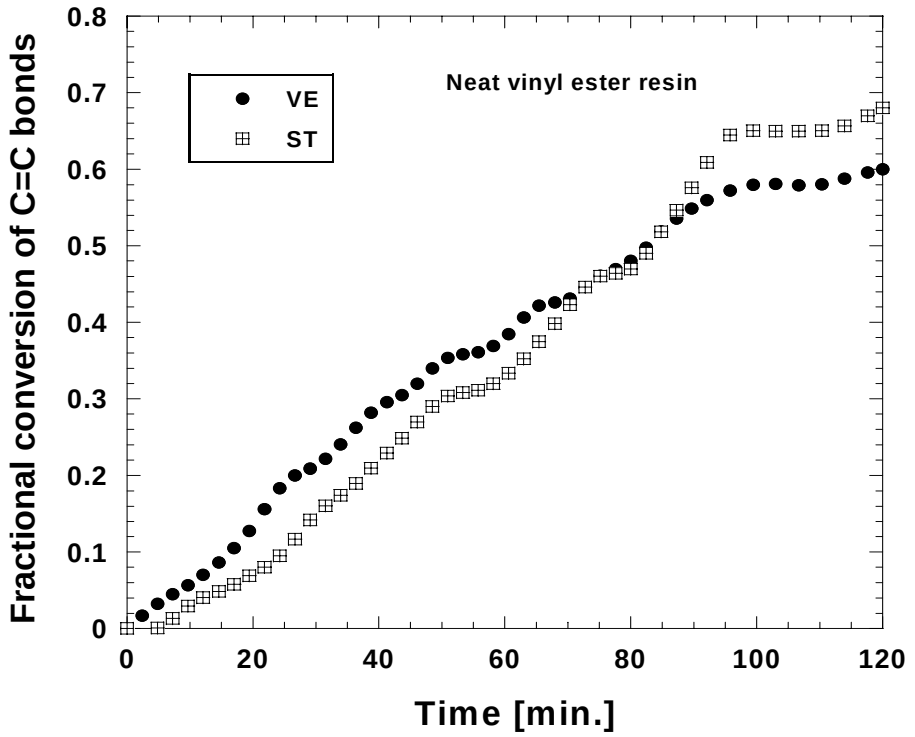

Figure 5.13. Fractional double bond conversions of vinylester and styrene in neat vinyl ester resin as a function of time

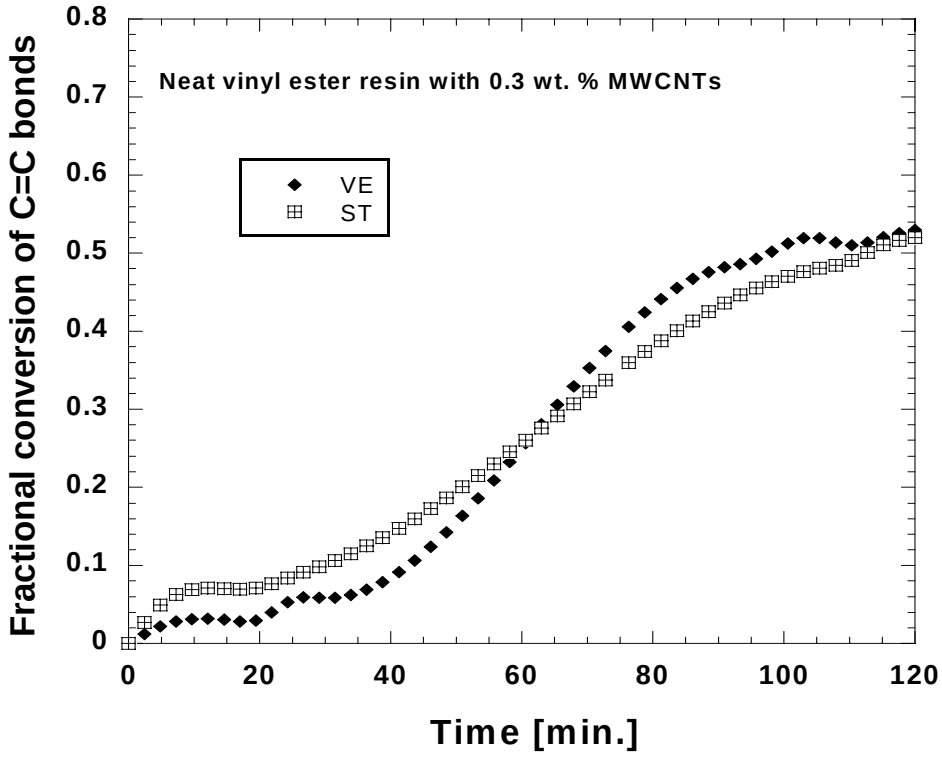

Figure 5.14. Fractional double bond conversions of vinylester and styrene in vinylester resin with 0.3 wt. % of MWCNTs as a function of time

In thermosetting resin systems, diffusion limitation is the major factor that affects polymerization kinetics, changing the mobility of the reacting species (Dua, et al. 1999, Hsu and Lee 1993). Following the gelation of the resin, the decrease in mobility of the growing radical species reduces the bimolecular termination rate (Tollens and Lee 1993). This reduction leads to an increase in the free radical concentration and accelerates the polymerization reaction during the propagation stage. This mechanism is called Trommsdorf effect (Dua, et al. 1999, Scott, et al. 2002, Batch and Macossa 1992). Moreover, this effect is the reason why we observed autocatalytic behavior in the cure reaction of the resins, as already proved via DSC measurements. Please note that diffusion limitation is also critical towards the end of the polymerization reaction. However, in this case, the system starts behaving like a glass because of the vitrification, during which no further reaction takes places due to the lack of ability of monomers and growing species to move (Lam and Plaumann 1990, Dua et al. 1999).

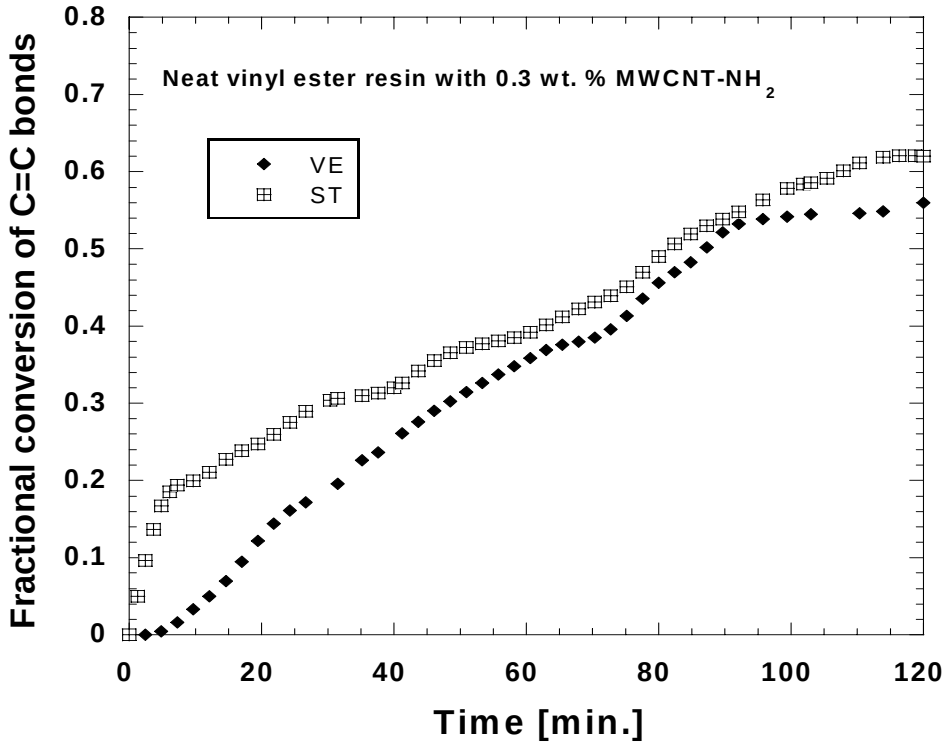

Figure 5.15. Fractional double bond conversions of vinylester and styrene in vinylester resin with 0.3 wt. % of MWCNT-NH_2 as a function of time

When the individual conversions of VE and styrene monomers are compared, it can be seen that, at the very beginning of the reaction, VE monomers have more affinity

to react with the free radicals in neat vinylester resin, however this trend becomes invalid when CNTs with and without amine functional groups are added into the resin system. During propagation stage, conversion of VE monomers exceeds that of the styrene monomers in the suspensions with MWCNTs. However, in the suspensions with MWCNT-NH_2 styrene conversion is always higher than that of VE during propagation stage. In the light of the theoretical issues mentioned in the previous paragraph, it can be said that CNTs substantially influence the diffusion enhanced reaction during propagation stage in the resin system dependent on functional groups on their surfaces. This may be probably due to the fact that presence of CNTs alters the rate of bimolecular termination, beginning from the progression of the reaction till the end of gelation of the resin in a different manner, depending on amine functional groups on their surfaces and thus on their aspect ratios. Moreover, the results obtained from FTIR measurements are highly proportional to those obtained by DSC measurements. In general, we can safely say that amine groups over the surfaces of CNTs promote the dispersion state of CNTs, and that regardless of amine groups, CNTs changed the individual conversion of monomers in the resin system.

5.6.3. Raman Spectroscopy Results

Figures 5.16-5.17 show the Raman spectra of the CNTs used in this study and their nanocomposites, respectively. Note that the data on Figure 5.16 was taken from Gojny (2006). In principle of RS, it is required that area of peaks is compared on the same spectrum, not from one Raman spectrum to another (Gupta, et al. 2004). However, the intensity ratio of one peak to another can be used across the same Raman spectrum in order to monitor chemical reactions involved (Stevanovic, et al. 2000). In this manner, a regular peak unchanged throughout the measurements is taken into account to trace the differences in the areas of the corresponding peaks. As depicted in Figure 5.14, Raman spectrum of CNTs is typically comprised of four different regions (Zhao and Wagner 2004, Dresselhaus, et al. 2005). These are the graphite lattice vibrations, G band (1600 cm^{-1}), structural defects D band (1300 cm^{-1}) the G' band (2600 cm^{-1}) and the low frequency Radial Breathing Modes (RBMs), which corresponds to the collective radial movement of the carbon atoms. RBM is considered to get information regarding diameter and chirality's of the CNTs.

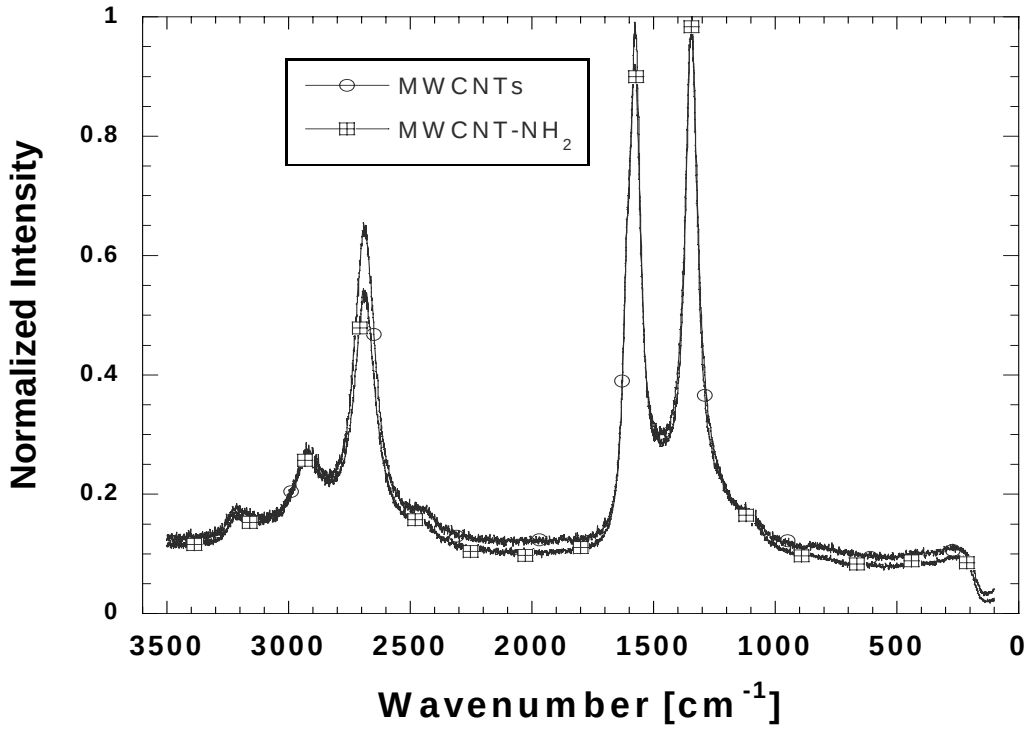

Figure 5.16. Raman spectra of CNTs

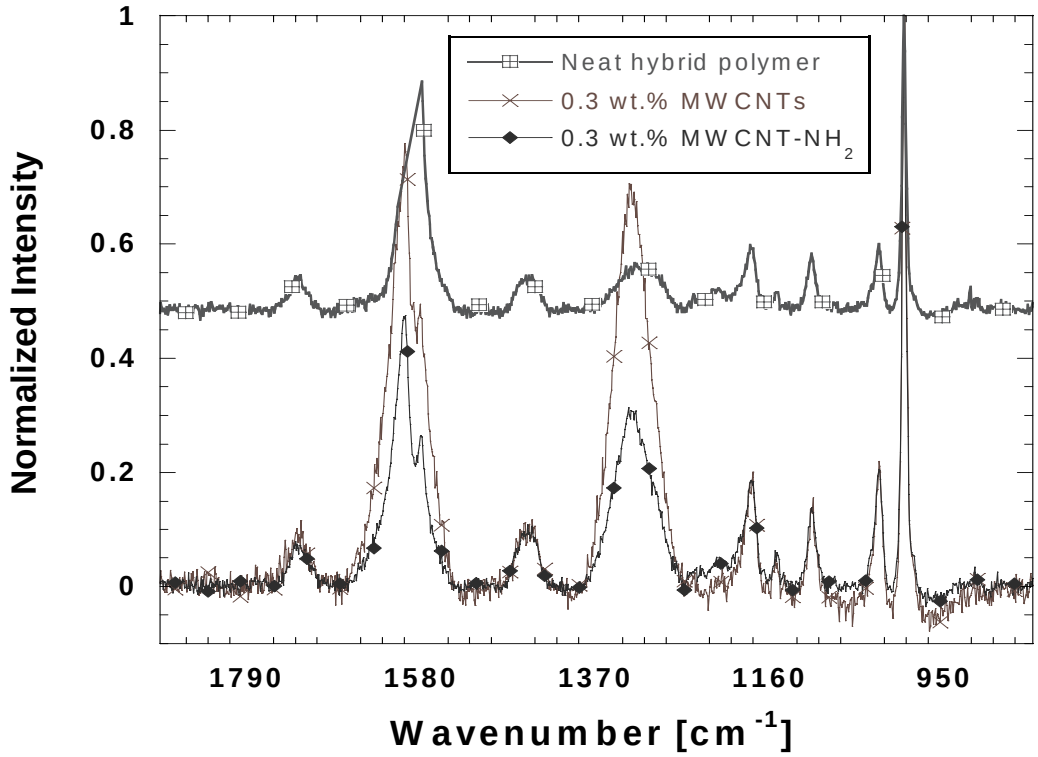

Figure 5.17. Raman spectra of the cured hybrid polymer and its corresponding nanocomposites with 0.3 wt. % MWCNTs and MWCNT-NH_2

Our main emphasis herein is on the G and D bands of the CNTs because they are hypothetically remained constant without being affected by the reaction that takes place in the system. So, the ratio of G and D peak intensities (I_G/I_D) were used to follow the reactions. In Raman spectroscopy, C=C bonds for vinylester resin are visible at 1582 cm^{-1} (aromatic), 1604 cm^{-1} (aromatic), 1667 cm^{-1} (aliphatic) (Stevanovic, et al. 2002). As stated before, these peaks are overlapped with the peaks of G and D bands. Note that the hybrid resin was used for RS measurements, but we followed the shifts in peaks of Vinylester resin, as in the case of FTIR to ease the process of data interpretation. Following the procedure described in section 5.5.2.1., the spectra obtained from the RS measurements were evaluated.

As a result, it was found that CNTs with and without amine functional groups partially interrupted the C=C bonds of hybrid resins, which is principally proportional to the findings obtained from FTIR studies. In greater details, after the subtraction of the peaks from each other, the reduction in the peak areas relative to neat hybrid resin was observed to be 5 % larger for nanocomposites with MWCNTs than those with MWCNT-NH_2. This is ample evidence that amine groups over the surfaces of CNTs changed the individual conversions of the monomers in the hybrid resin system, which is consistent with the findings obtained from FTIR studies. On the other hand, regardless of amine functional groups, the peak intensities at G and D bands in the nanocomposites shifted to the right direction. This shows that carbon nanotubes tuned the interfacial interactions to some extent. Puglia, et al. (Puglia, et al. 2003) followed the same methodology when investigating effect of SWCNTs on the cure kinetics of epoxy resin. They presented a relationship between Raman peak shifting and the curing behavior of SWCNT modified epoxy resin.

5.6.4. TGA Results

Figures 5.18 and 5.19 depict the thermal weight curvatures achieved at constant heating rates (5 and 10 °C/min.) and 20°C/min for the cured neat hybrid polymer and its nanocomposites containing 0.3 wt. % of MWCNTs and MWCNT-NH_2, respectively. There was no significant difference in 5 wt. % degradation temperatures (T_d) of the cured neat hybrid polymer and its nanocomposites with MWCNTs and MWCNT-NH_2, at each constant heating rate.

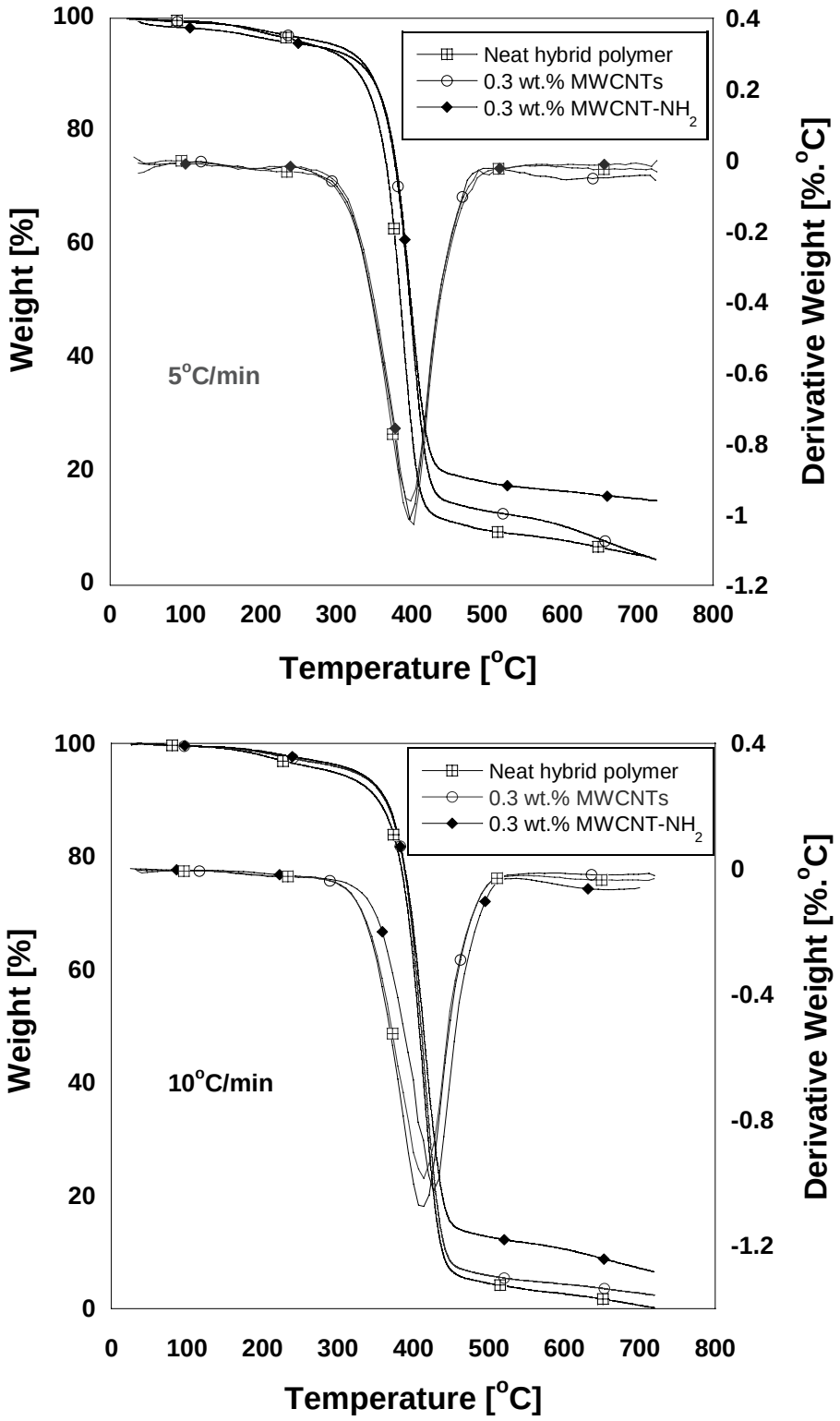

Figure 5.18. TGA thermograms of the cured neat hybrid resin and its corresponding nanocomposites containing 0.3 wt. % of MWCNTs and MWCNT-NH_2 at a constant heating rate of a) 5°C/min. b) 10°C/min

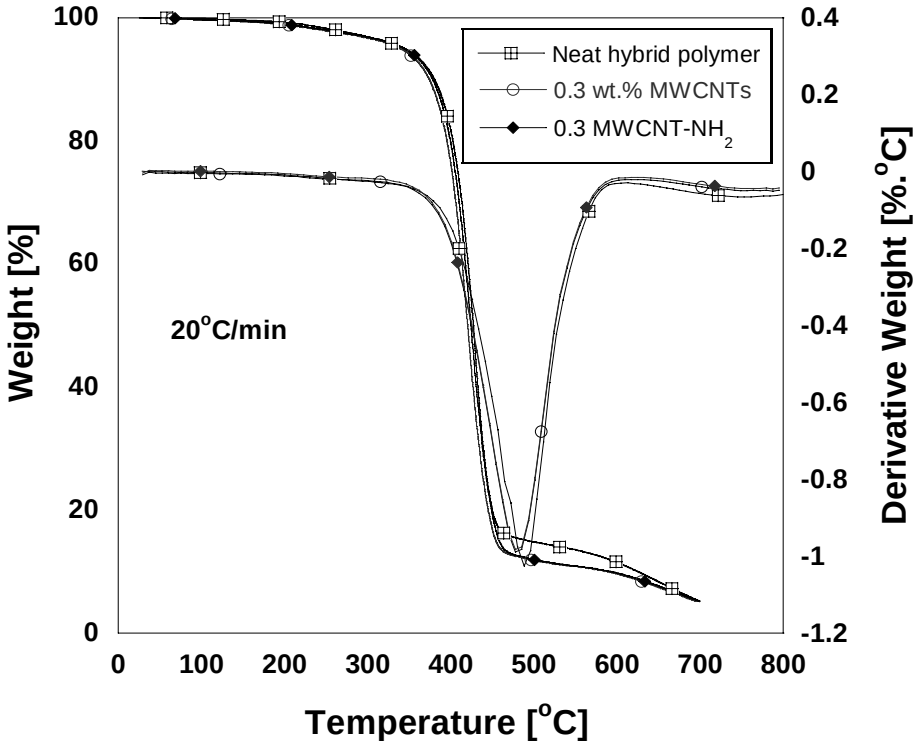

Figure 5.19. TGA thermograms of the cured neat hybrid resin and its corresponding nanocomposites containing 0.3 wt. % of MWCNTs and MWCNT-NH_2 at a constant heating rate of 20°C/min.

However, the char yields at 700°C were always higher for nanocomposites with MWCNT-NH_2 as compared to neat hybrid resin and those with MWCNTs. This implies that relatively high thermal stability was accomplished with incorporation of MWCNT-NH_2. This result shows consistency with the other findings obtained from DSC, FTIR, and RS studies. On the other hand, the first derivative (DTG) of the neat hybrid resin and its nanocomposites showed that just one peak occurs between 250 and 490°C. This implies that degradation of the nanocomposite samples is one-stage process regardless of whether they contain MWCNTs or MWCNT-NH_2. From that point of view, we can conclude that CNTs restrict the entanglement and mobility of polymer chains, thus increasing the T_g and thermal stability of the polymers without disrupting the major steps of free-radical polymerization, significantly. Furthermore, thermal degradation activation energies of the cured hybrid resin and its nanocomposites with MWCNTs and MWCNT-NH_2 were calculated at 5 wt. % conversion level, following the procedure described earlier in this chapter. As a result, degradation activation energies of neat hybrid resin and its nanocomposites containing MWCNTs and MWCNT-NH_2 were

predicted to be 62, 65 and 69 kj/mol, respectively. From that point of view, it can be concluded that MWCNT-NH_2 modified nanocomposites exhibit somewhat higher thermal stability as compared to neat hybrid resin and those with MWCNTs. This is very consistent with earlier findings obtained from DSC, FTIR and RS measurements.

5.7. Conclusions

In this chapter, the cure kinetics of a vinylester/polyester based hybrid resin containing 0.3 wt. % of MWCNTs and MWCNT-NH2 were pinpointed. In this respect, various experimental techniques including DSC, FTIR, RS and TGA were systematically conducted to reveal the effects of CNTs on free radical polymerization. Non-isothermal DSC measurements at different constant heating rates revealed that the presence of CNTs within the resin system alters the polymerization reaction by increasing the heat of cure while decreasing the activation energies (E_a). It was emphasized that relatively low aspect ratio of amino functionalized nanotubes may play a crucial role in alteration of the interfacial chemical interactions during polymerization. Consequently, the suspension with MWCNT-NH_2 exhibits much heat of cure, besides lower activation energies as compared to neat resin blend and the suspension with MWCNTs. The predicted DSC curves via autocatalytic kinetic model were in good agreement with those experimentally obtained. Furthermore, FTIR studies aimed to elucidate the impact of CNTs on the development of the network in a polymer matrix that polymerizes via radicals was performed on neat vinylester resin and its suspensions with the same content of MWCNTs and MWCNT-NH_2 as the hybrid resin. As a result, the final conversion of styrene exceeded the final conversion of vinylester double bonds in the resin suspensions with MWCNT-NH_2, while final conversion of vinylester is higher than that of styrene in the resin suspensions with MWCNTs. RS studies performed on the cured hybrid polymer and its nanocomposites show consistency with FTIR findings such that amine functional groups over the surfaces of CNTs altered the chemical reactions within the resin system. On the other hand, TGA measurements revealed that CNTs increased the thermal stability of the hybrid matrix resin such that E_d values of the nanocomposites prepared with MWCNTs and MWCNT-NH_2 are higher than that of the cured hybrid polymer. Moreover, at each constant heating rate, it was found that nanocomposites with MWCNT-NH_2 exhibited higher char yields as

compared to neat hybrid resin and those prepared with MWCNTs. On behalf of the findings achieved, it was concluded that amine functional groups over the surfaces of CNTs enhanced the dispersibility of CNTs and influenced the relative individual fractional conversions of double bonds in the resin system. In summary, it can be said that presence of CNTs within the resin system alters the conversions of monomers in the system. In other words, amino groups over the surfaces of CNTs induce a compromise such that they enhance the dispersion of CNTs in the resin system while impeding partially the polymerization reaction by disrupting C=C bonds of hybrid resin matrix that are supposed to react with styrene. However, this brings a synergy to the final performance of the nanocomposites. We could safely say that overall improvement of the properties observed for CNT modifed composites results from the competing effects of reinforing efficiency of CNTs and the altered free radical polymerization of the hybrid resin system in the presence of CNTs with and without amine functional groups. The extent of enhancement observed for the ultimate performance of the hybrid polymer with the addition of CNTs will be discussed in the following chapters based on the findings obtained in this chapter.

CHAPTER 6

THERMO-MECHANICAL BEHAVIOR OF CNT MODIFIED NANOCOMPOSITES

6.1 Introduction

Measuring and understanding the temperature dependent material properties is critical to predict the behavior of polymeric components during their service life (Gojny, et al. 2003, Gojny and Schulte 2004, Gojny, et al. 2005a). In Chapter 4, CNTs with huge aspect ratio and surface area were found to alter significantly rheological properties of polymers in which they are embedded, depending on the type of CNTs. It was also shown that dispersion state of CNTs is highly proportional to rheological behavior of the suspensions in which they are embedded. The dispersion state of carbon nanotubes is also expected to be highly related to the dynamic mechanical properties of their resulting nanocomposites. Fidelus et al. (2005) investigated the dynamic mechanical properties of an epoxy based nanocomposites containing MWCNTs and SWCNTs. They found that incorporation of SWCNTs improved the storage modulus of the epoxy resin by 8%. However, addition of MWCNTs into the same epoxy resin did not change the elastic modulus values of the final product in a comparable manner. They also revealed that glass transition temperatures of the nanocomposites containing SWCNTs or MWCNTs increased slightly with respect to nanotube content. Liao et al. (2004) determined thermo mechanical properties of a SWCNT modified epoxy resin. They used relevant solvents and surfactants to ease the dispersion of carbon nanotubes within epoxy resin via sonication. They found that degree of dispersion of CNTs is highly proportional to mechanical properties of their resulting nanocomposites. Moreover, they conclude that solvent assisted preparation of SWCNT modified epoxy nanocomposites shifted the glass transition temperature to lower values. The authors attributed it to the reduced interfacial adhesion due to the use of surfactant and the solvent. Miygawa and Drzal (2004) utilized fluorinated SWCNTs as nano-fillers to improve thermo-mechanical properties of an epoxy resin. However, they observed a

linearly decreasing glass transition temperature with increasing filler content. In this respect, they concluded that not only dispersion state of CNTs but also compatibility of functional groups over surfaces of CNTs with polymer matrix resin is critical to final properties of the nanocomposites.

The effects of interfacial interactions and particle-particle interactions via distinct aspect ratios of CNTs upon the shear viscosity and dynamic rheological properties of the CNT/resin systems were investigated in Chapter 4. It was found that rheological properties of the hybrid resin vary, depending on the type of CNTs and presence of amine groups over their surfaces. From that point of view, it is reasonable to conclude that CNTs affect also the solid state properties of these corresponding liquid suspensions in considerable manner. Therefore, it is interesting to monitor the thermo-mechanical properties of the nanocomposites (solid state) achieved via polymerization of the resin suspensions containing different types of carbon nanotubes (MWCNTs, DWCNTs, MWCNT-NH_2 and DWCNT-NH_2).

In this chapter, CNT/polymer suspensions, rheological properties of which were already presented in Chapter 4 were cross-linked, using peroxide (MEKP) initiator. Dynamic mechanical behaviour of the resulting nanocomposites was determined by Dynamic Mechanical Thermal Analyser (DMTA) to relate the influence of dispersion state of CNTs within the blend to final thermal properties of the corresponding nanocomposites. Transmission electron microscopy (TEM) was also conducted to highlight the achieved dispersion state of CNTs within the matrix resin.

6.2 Experimental

6.2.1. Dynamic Mechanical (DMA) Measurements

Dynamic mechanical properties of the nanocomposites obtained from curing of each sort of resin suspension were investigated by dynamic mechanical thermal analyser, (DMTA) using a GABO EPLOXOR 500 N. For the measurements, rectangular specimens of 50 mm in length, 5 mm in width and 2 mm in thickness were sectioned from larger samples. The tests were performed in tensile mode at a frequency of 10 Hz with a static strain of 0.6 % and dynamic strain of 0.1%, in a

temperature range between –50 and 200^{o} C with a heating rate of 3^{o}C/min. The storage modulus (E'), loss modulus (E") and the loss tangent (tan δ) were determined as a function of temperature.

6.2.2. TEM Investigation

The transmission electron microscopy (TEM) was conducted to investigate the dispersion state of CNTs with and without amine functional groups within the resulting nanocomposites. The TEM images were taken using a Philips EM 400 at 120 kV. Ultra thin films of each type of composites (50 nm) were obtained by ultra microtome cutting.

6.3. Results and Discussion

6.3.1. Thermomechanical Properties of MWCNT Modified Nanocomposites

Figures 6.1 and 6.2 give storage modulus (E') and loss factor (tan δ) values as a function of temperature obtained from dynamic mechanical measurements for the nanocomposites containing MWCNT and MWCNT-NH_2, respectively. The addition of non-functionalized and amino functionalized carbon nanotubes into the polymer system has some considerable effects on the storage modulus in both the glassy and the rubbery states, depending on the nanotube contents within the resin blend. This is due to the stiffening effect of CNTs and interfacial interactions along a huge interfacial area between the CNTs and the polymer matrix. Consequently, CNTs reduced the mobility of the surrounding polymer matrix to some extent leading to an increase in the modulus values. This effect is more pronounced in the glass transition region. As mentioned above, amino functionalized nanotubes have shorter length (lower aspect ratios) compared to that without surface treatment as a result of the functionalization process (ball milling process). So, one can expect relatively lower elastic modulus values from the nanocomposites containing MWCNT- NH_2 compared to those with MWCNTs.

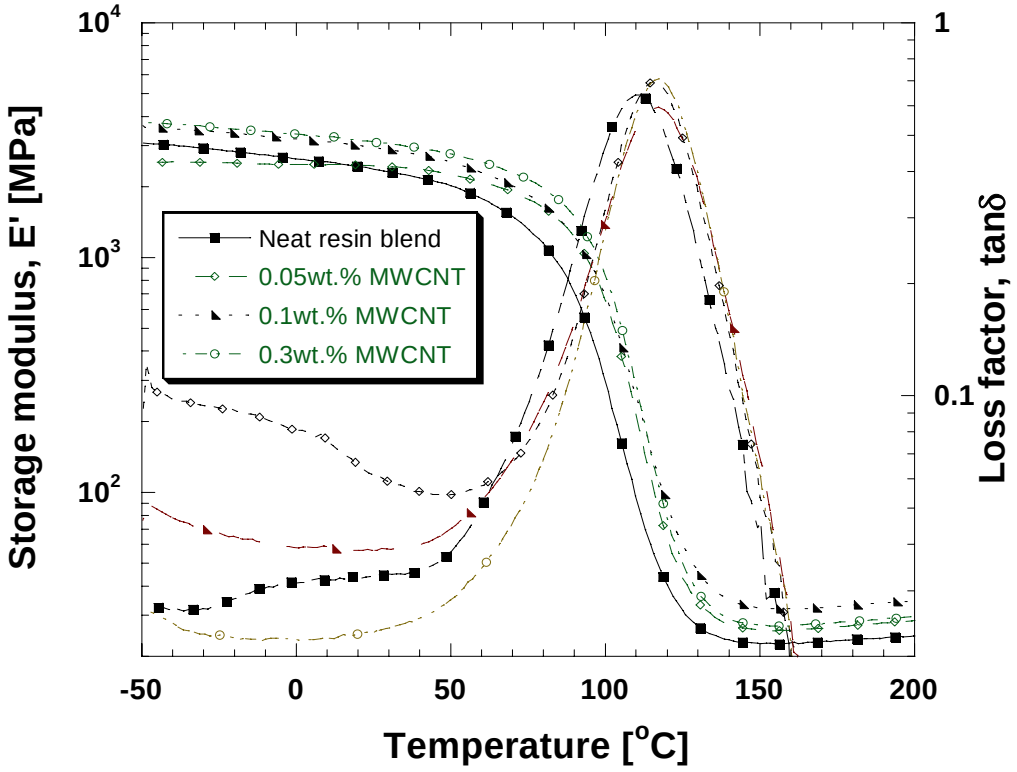

Figure 6.1. Storage modulus and loss factor of nanocomposites containing non-functionalized nanotubes (MWCNT)

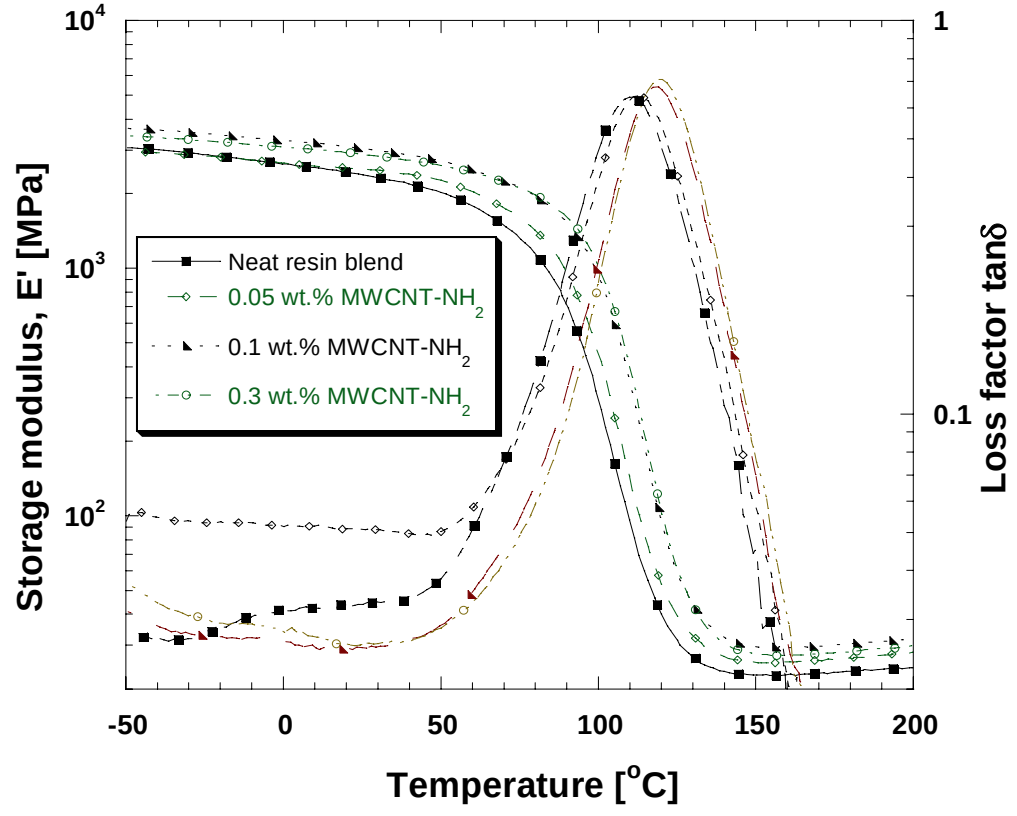

Figure 6.2. Storage modulus and loss factor of nanocomposites containing non-functionalized nanotubes (MWCNT-NH_2)

However, we obtained opposing results in the present case. As an example, the storage modulus values at 20 ^{o}C for the nanocomposites containing 0.3 % wt. of MWCNT-NH_2 and MWCNTs were found to be 3170 and 2930 MPa, respectively, which are also higher than that of the neat resin blend (2430 MPa). These results reveal that relatively enhanced dispersion state of the MWCNT-NH_2 within the matrix compensates the lower aspect ratio of these tubes and provides higher modulus values to their resulting nanocomposites.

In Figures 6.3 and 6.4, the loss modulus (E") values of the nanocomposites containing MWCNTs and MWCNT- NH_2 were given as a function of temperature, respectively. It was found that the loss modulus values at the peak points gets higher, as the nanotube contents increases. In addition, nanocomposites containing amino functionalized nanotubes results in somewhat higher peak values compared to those with non-functionalized nanotubes. In brief, the loss modulus indicates the energy converted into heat and can thus be used as a measurement of viscous component or unrecoverable oscillation energy dissipated per cycle.

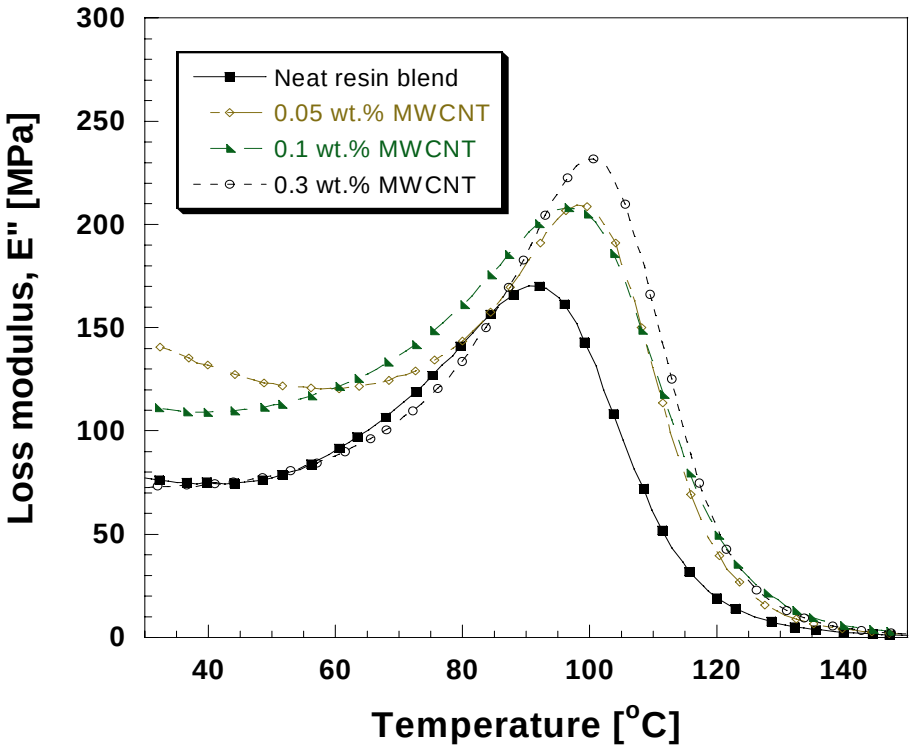

Figure 6.3. Loss modulus values of nanocomposites containing non-functionalized nanotubes (MWCNT)

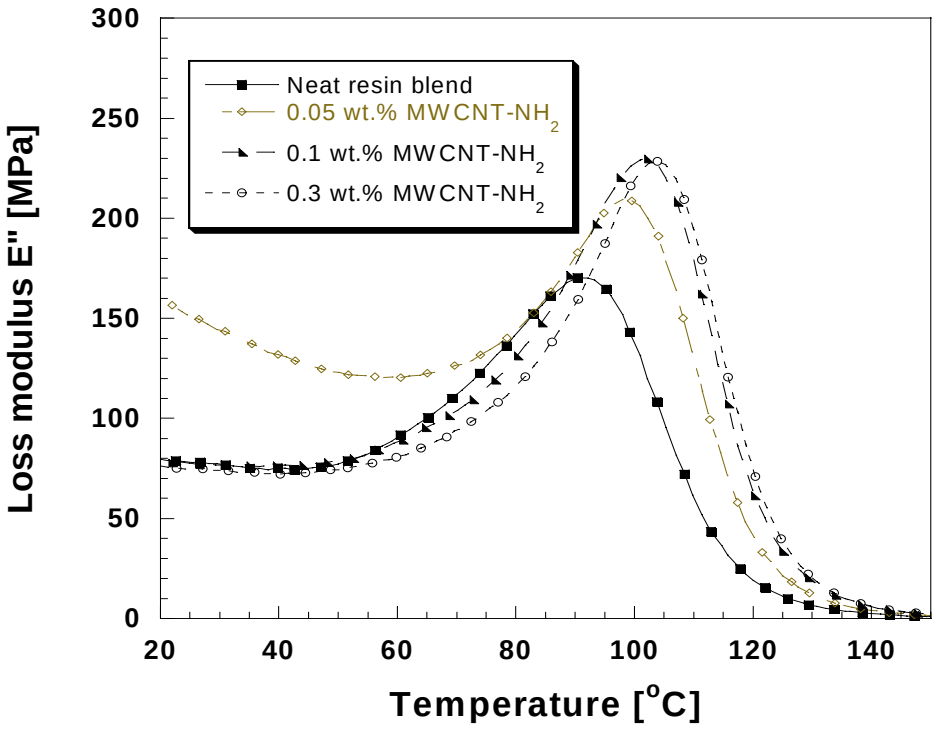

Figure 6.4. Loss modulus values of nanocomposites containing non-functionalized nanotubes (MWCNT-NH_2)

From that point of view, we could furthermore conclude that the satisfactorily dispersed nanotubes with and without treatment would assist in dissipating energy under visco-elastic deformation of the surrounding resin blend matrix. Moreover, higher loss modulus values observed for nanocomposites with MWCNT- NH_2 compared to those with MWCNTs showed that amine functional groups promoted partially the involved chemical interactions at the interface, owing to the same reasons as previously explained above.

Figure 6.5 shows the glass transition temperature (T_g) values of the nanocomposites with MWCNT and MWCNT- NH_2, obtained from the slope of the storage modulus values in the glass transition zone. As seen in the figure, the addition of nanotubes within the resin blends increases the corresponding T_g values significantly. The mobility of the polymer matrix around the nanotubes is reduced due to the presence of the nanotubes. In fact, interfacial covalent bonds are expected to occur between the polymer matrix and the amino functionalized nanotubes, thus resulting in a stronger bonding at the interface with improved T_g. In association with the experimentally determined cure kinetics parameters for the resin suspensions,

we can additionally conclude that incorporation of MWCNTs improved the thermal properties of the hybrid resin system regardless of amino groups over their surfaces, although they affected the fractional conversion of monomers within the resin system.

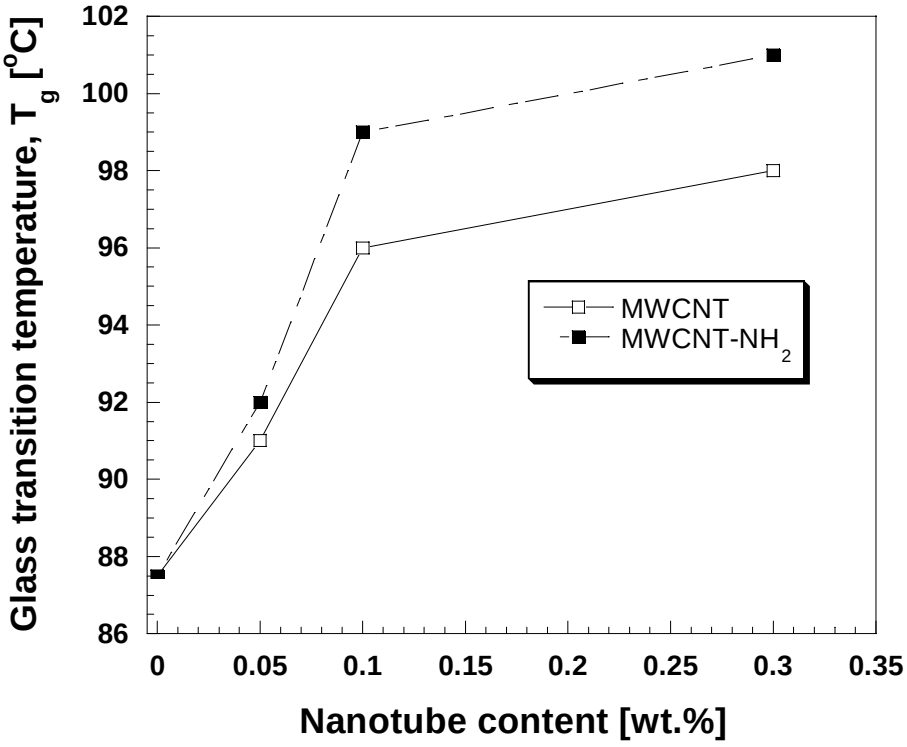

Figure 6.5. Glass transition temperatures of the nanocomposites as a function of nanotube content with and without any functional groups.

In addition, the reduced aspect ratio of amino functionalized nanotubes may have also some effects on the degree of polymerization. Gryschuck et al. (2006) stated that lower aspect ratio of MWCNTs would give better results for highly cross linked thermosetting resins such as vinyl-ester.

Figures 6.6 a and b are the TEM micrographs showing achieved dispersion state of MWCNT and MWCNT-NH_2 at 0.3 wt. % loading within the corresponding resin systems, respectively. Functionalized nanotubes exhibit relatively good dispersion within the matrix resin blend without any significant agglomerates. The TEM characterizations also support our findings that amine functional groups over CNTs improve their dispersion state within the resins enhancing their compatibility with resin blend matrix.

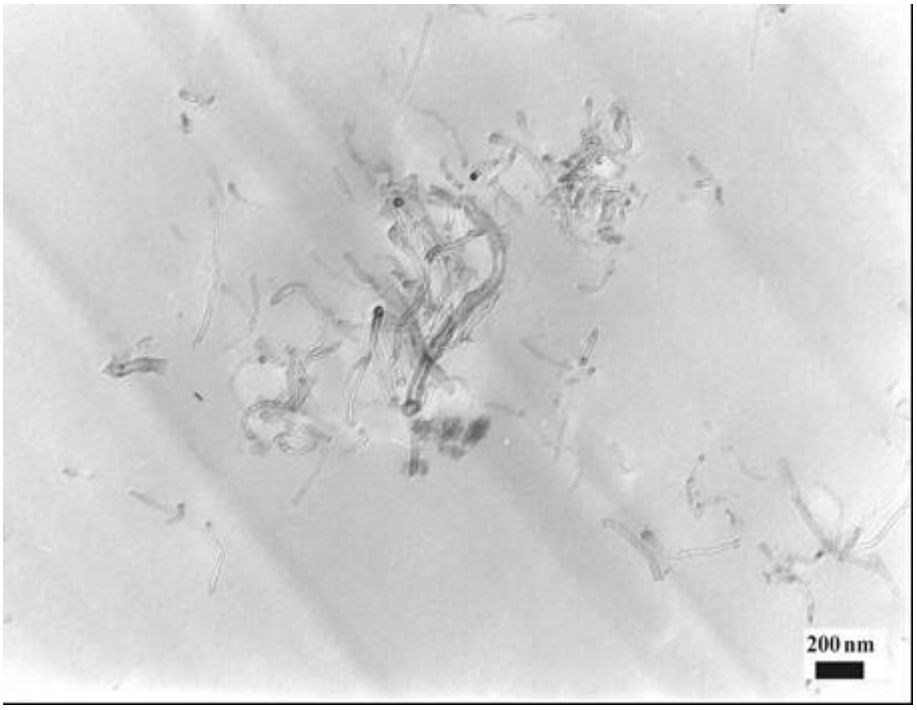

a)

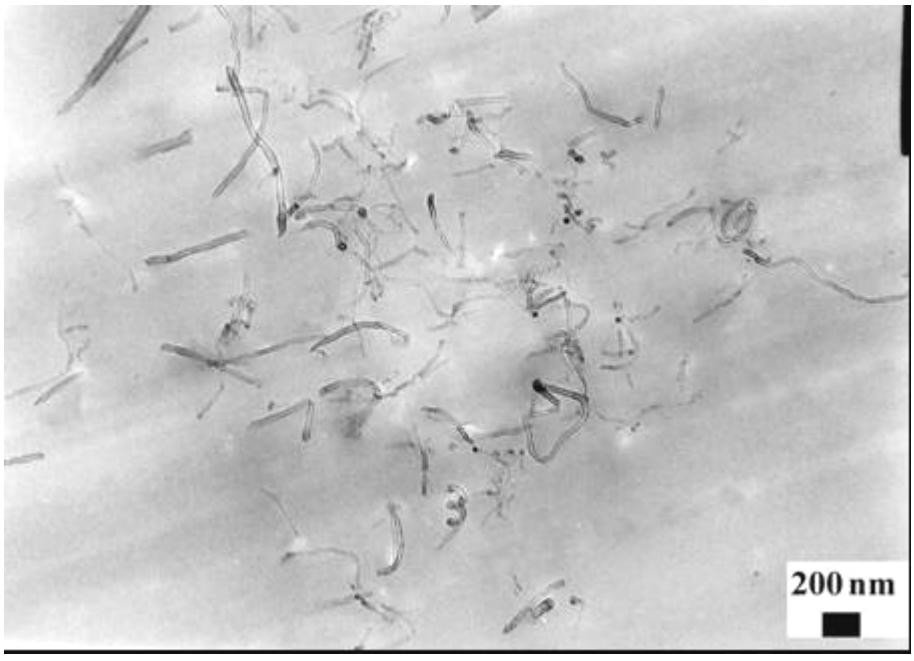

b)

Figure 6.6. TEM micrographs showing achieved (a) dispersion state of MWCNT and (b) MWCNT-NH_2 at 0.3 wt. % loading within the corresponding resin systems.

6.3.2. Thermomechanical Properties of DWCNT Modified Nanocomposites

Figures 6.7 and 6.8 show storage modulus (E') values with respect to temperature obtained from DMA measurements for the nanocomposites containing various amounts of DWCNTs and DWCNT-NH_2, respectively. It is obvious that incorporation of DWCNTs with and without amine functional groups influenced storage modulus values in both the glassy and rubbery states depending upon their content within resin blend. Based upon E' values at 20^oC, nanocomposites containing 0.05 wt. % of DWCNTs was observed to have a modulus value of 2819 MPa, while those containing 0.3 wt. % of DWCNT-NH_2 give a value of 2757 MPa.

It was earlier revealed that despite lower aspect ratio of amino functionalized nanotubes, at each given concentration, MWCNT-NH_2 modified nanocomposites were found to exhibit higher E' values as compared to those with MWCNTs (Seyhan, et al. 2007b). This may be associated with relatively good dispersion of MWCNT-NH_2 within the resin blend. Unlike the nanocomposites with MWCNT-NH_2, lower E' values were obtained from the nanocomposites with 0.3 wt. % of DWCNT-NH_2, as their concentration increases in the resin system. This may be related to the fact that DWCNTs with relatively low density values occupy higher volume within resin blend as compared to MWCNTs. It was already shown that free radicals released by the initiator (MEKP) are too vulnerable to be trapped within the galleries of CNTs (Peng, et al. 2003). Therefore, resin suspensions containing MWCNTs and DWCNTs with and without amine functional groups may have distinct thermal curing properties even at the same given concentration of curing agents due to their different surface area and aspect ratios. T_g values of DWCNTs and DWCNT-NH_2 modified nanocomposites were obtained from the slope of the storage modulus values in the glass transition zone. In conclusion, incorporation of the nanotubes into the resin system shifted the corresponding T_g value of the neat polymer (88^oC) to about 95^oC, regardless of weight content or amine functional groups. However, T_g values of the MWCNTs and MWCNT-NH_2 modified nanocomposites were found to increase with increasing content of nanotubes within the system.

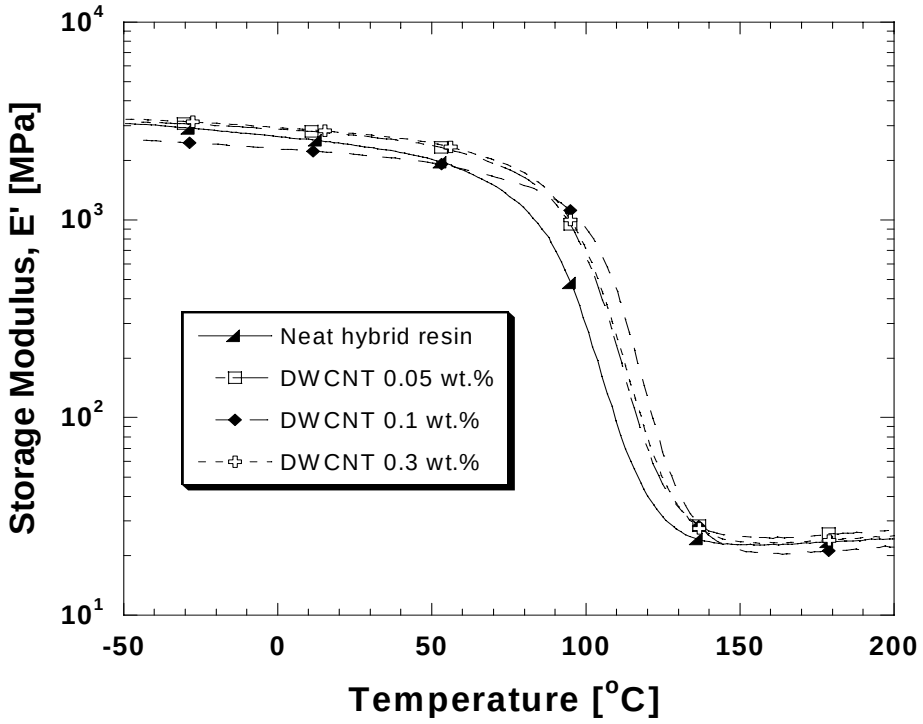

Figure 6.7. Storage modulus of nanocomposites containing non-functionalized nanotubes (DWCNTs).

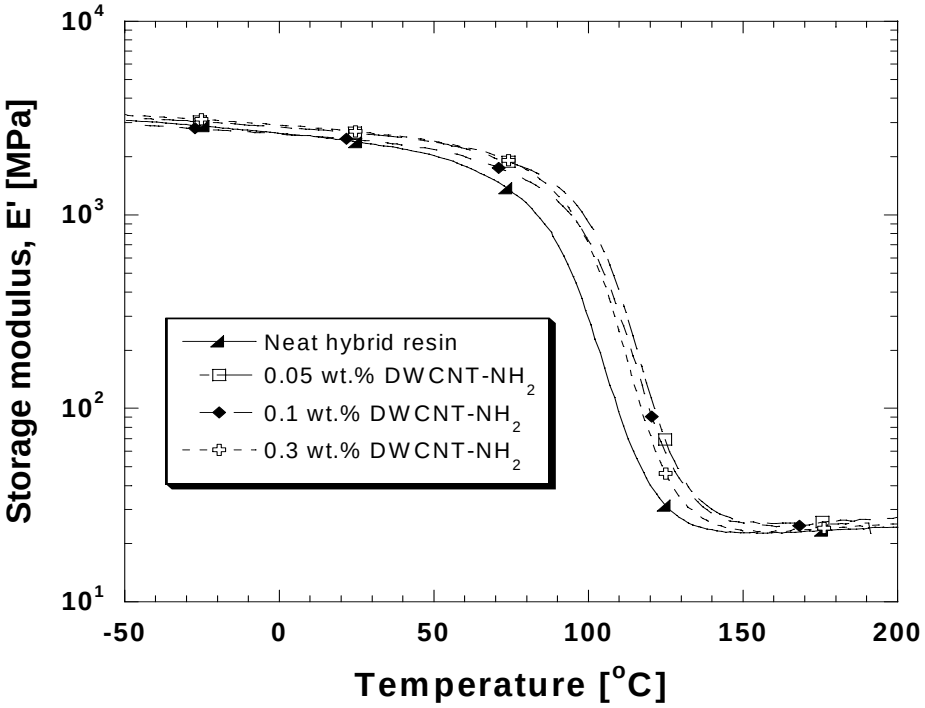

Figure 6.8. Storage modulus of nanocomposites containing amino-functionalized nanotubes (DWCNT-NH_2).

It was also observed that MWCNT and MWCNT-NH_2 modified nanocomposites exhibited larger T_g values than those with DWCNTs and DWCNT-NH_2. In brief, it can be concluded that T_g is highly dependent on the type of CNTs. This is highly consistent with the conclusions regarding the curing behavior of polymer suspensions highlighted in Chapter 5.

Figure 6.9 and 6.10 show the loss modulus values of DWCNTs and DWCNT-NH_2 filled nanocomposites with respect to temperature, respectively. Consequently, for the nanocomposites containing DWCNTs and DWCNT-NH_2 the maximum loss modulus values at the peak points were observed at 0.3 wt. % loading rate. However, at the same concentration, no significant difference in the peak values of the nanocomposites was observed.

Figures 6.11a and b are the TEM micrographs showing the achieved dispersion state of DWCNTs and DWCNT-NH_2 at 0.3 wt. % concentration within the cured hybrid resin, respectively. TEM micrographs reveal that small separate agglomerates of nanotubes within the cured matrix resin blend still exist, regardless of amine functional groups. Since DWCNTs possess great tendency to form dense agglomerates due to their larger surface area than MWCNTs, as expected, there is no significant difference in the dispersion state between DWCNTs and DWCNT-NH_2.

6.4. Conclusions

The thermo-mechanical properties of the nanocomposites containing MWCNTs, MWCNT-NH_2, DWCNTs and DWCNT-NH_2 were investigated in association with rheological behavior of their corresponding resin suspensions. Consequently, the storage (E') and loss modulus (E'') values of the nanocomposites containing MWCNTs, MWCNT-NH_2 were found to increase with an increase in contents of CNTs. In a similar manner, T_g values of the nanocomposites with MWCNTs and MWCNT-NH_2 were found to shift to higher values as compared to that of neat hybrid polymer, as their concentration within the matrix resin was increased. This trend is more obvious for the nanocomposites containing MWCNT-NH_2. TEM studies showed that dispersion of MWCNT-NH_2 is better than that of

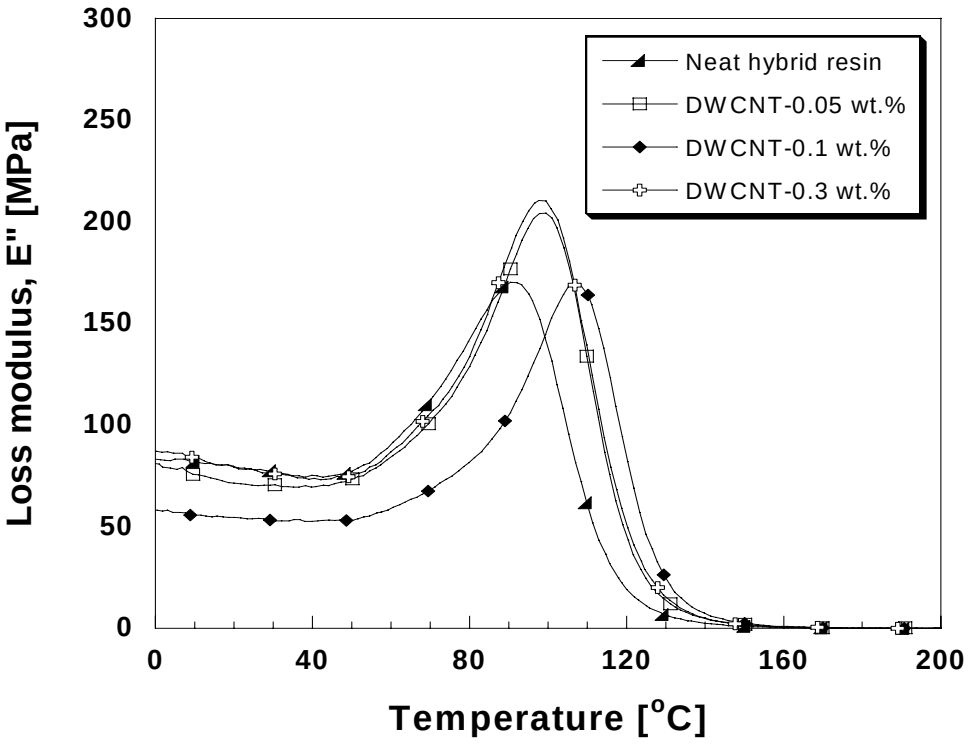

Figure 6.9. Storage modulus of nanocomposites containing amino-functionalized nanotubes (DWCNTs).

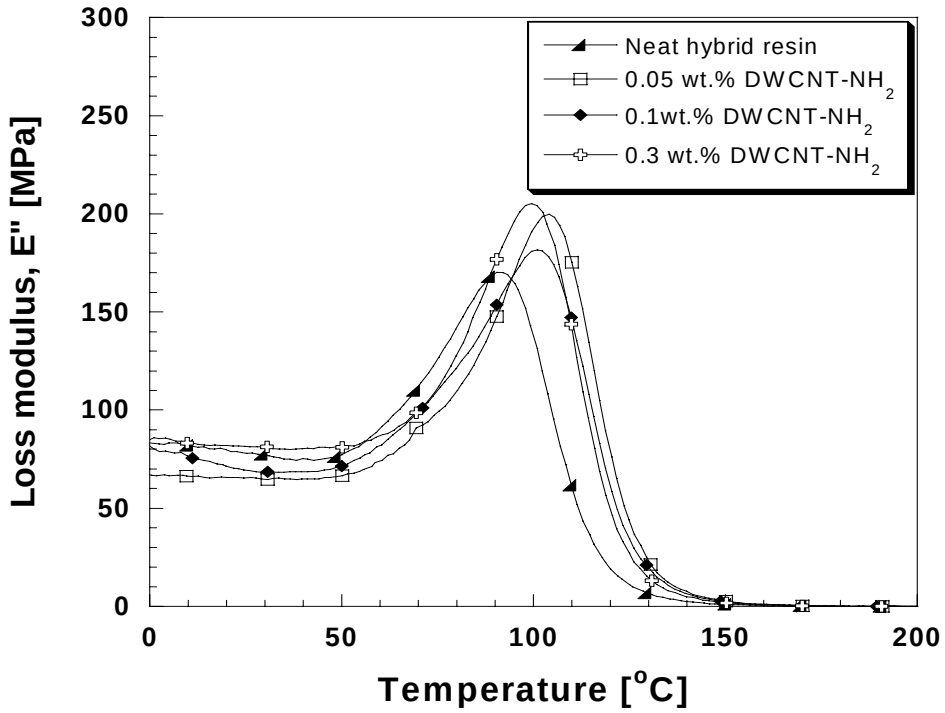

Figure 6.10. Storage modulus of nanocomposites containing amino-functionalized nanotubes (DWCNT-NH_2).

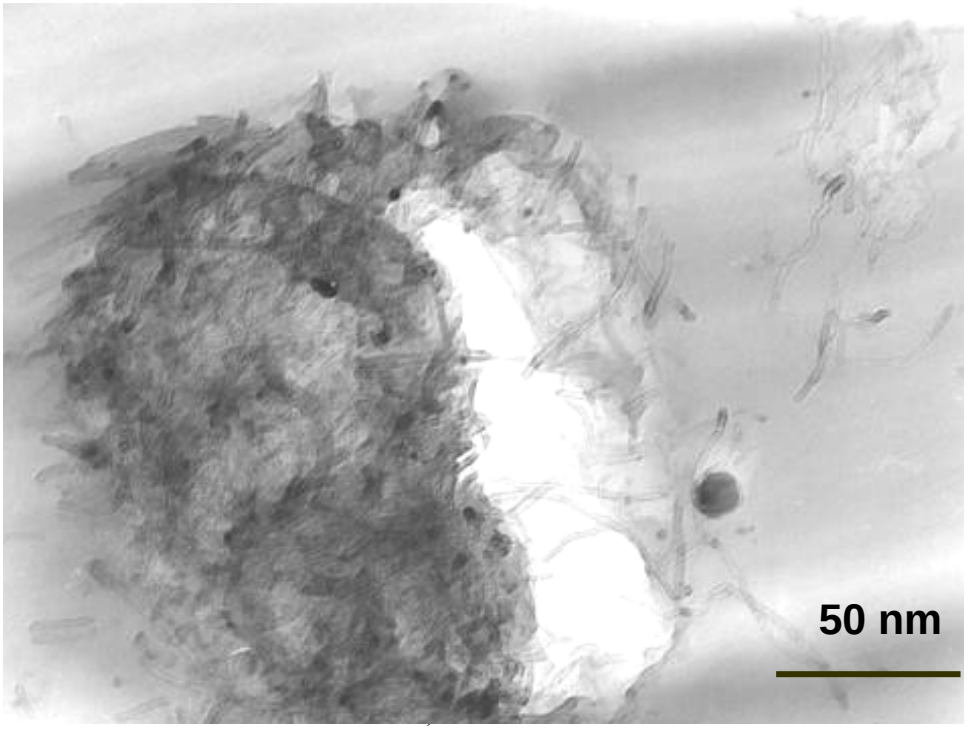

a)

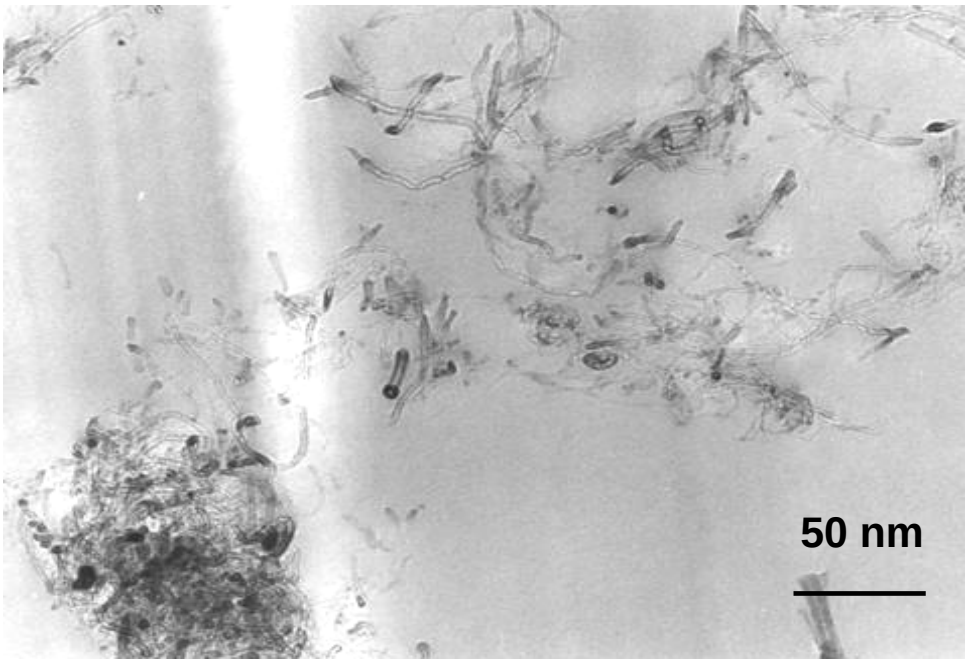

b)

Figure 6.11.TEM micrographs showing the achieved dispersion state of (a) DWCNTs and (b) DWCNT-NH_2 at 0.3 wt. % concentration within the resin blends.

MWCNTs in the hybrid polymer, which shows consistency with the findings obtained.

In contrary to what was observed for MWCNT modified nanocomposites, regardless of amine functional groups, incorporation of DWCNTs was found to decrease the T_g values of the hybrid resin. This trend becomes worse as their concentration increases in the hybrid resin. As a result, it was observed that nanocomposites containing 0.05 wt. % of DWCNT-NH_2 possessed the highest T_g and largest storage and loss modulus values. TEM investigations performed on the cured resin samples demonstrated that the dispersion of DWCNTs within the polymer matrix was poor. As already highlighted in Chapter 5, individual conversions of the monomers in the resin system are dependent on the type of CNTs and amine functional groups over their surfaces. In brief, it may be concluded that higher specific surface area (SSA), lower aspect ratio and inferior dispersion state of DWCNTs within polymer matrix are critical parameters to accomplish the desired properties in the resultant nanocomposites. In other words, they occupy higher volume in the resin system than MWCNTs and thus interact more with radicals released into the resin system. Since amine groups does not adversely affect the final properties of the cure resin system as discussed in Chapter 5, their length less than that of MWCNTs and relatively huge surface area seem to be the major reasons for the reduced thermo mechanical properties observed for DWCNTs in this chapter.

CHAPTER 7

MECHANICAL PROPERTIES OF CNT MODIFIED NANOCOMPOSITES

7.1 Introduction

Nano-particles have recently gained great interest in science and industry owing to their highly considerable promises in enabling the future nano-structured materials with novel properties (Thostenson, et al. 2005). In this manner, CNTs with extraordinary properties offer the potential to improve the mechanical properties of polymers (Park, et al. 2004, Fiedler, et al. 2006). However, amazing large specific surface area (SSA) of the CNTs, several orders of magnitude larger than that of commercial micro-sized reinforcing materials, makes CNTs form relatively larger agglomerates (Peignay, et al. 2001, Gojny and Schulte 2004). This leads to mechanical performance of their resulting nanocomposites to be far below the theoretical predictions. To promote the compatibility at the interface between CNTs and the surrounding polymer matrix, some chemical functional groups are grafted onto the surfaces of CNTs (Gojny, et al. 2003, Seyhan, et al. 2007b). Kim et al. (2006) found that incorporation of untreated, acid and amine treated MWCNTs into an epoxy resin improved tensile strength of the epoxy resin by 61, 69 and 73 %, respectively, without significantly reducing the elastic modulus of the epoxy. Yaping et al. (2006) investigated the effect of MWCNT-NH_2 on the mechanical properties of the epoxy resin. They stated that flexural bending stress and modulus of the nanocomposites were significantly enhanced as compared to those of neat epoxy resin. Moreover, in the same study, impact strength of the corresponding nanocomposites was measured to be two times higher than that of neat epoxy resin. Frankland et al. (2002) theoretically showed that covalent attachment of only one percent of the carbon atoms of the CNT-surface to the matrix polymer improved the interfacial shear strength by over an order of magnitude without decreasing the elastic modulus significantly. In a similar manner, Grujicic et al. (2007) studied the atomic level mechanical properties of three-walled carbon nanotubes (3 WCNT) reinforced vinylester resin with epoxy group, using

molecular mechanics to interpret the effect of covalent functionalization. They revealed that covalent functionalization has a profound impact on the interactions between matrix and nanotubes, as the loads are especially applied in a direction orthogonal to nanotube axis. Allaoui et al. (2003) investigated the effects of MWCNTs on the properties of a rubbery epoxy matrix. They found that tensile strength and modulus were improved with the addition of up to 4 wt. % of MWCNTs into epoxy resin. However, the experimental procedure which they followed to disperse the CNTs homogenously in the matrix resin, using methanol did not make sense. They observed large dense agglomerates via optical microscopy. Bai and Allaoui (2003) addressed the effects of length and aggregate size of MWCNTs on the enhancement in mechanical properties of another epoxy based nanocomposites. They showed that nanocomposites containing up to 4 wt. % of MWCNTs possessed high elastic modulus but low fracture strain relative to neat epoxy resin. The authors attributed this response of the nanocomposites to local defects due to existence of larger agglomerates enhancing early failure. The effects of oxo-fluorinatizied MWCNTs on the fracture toughness of an epoxy based nanocomposites was evaluated, using single edge notch bending (SENB) testing fixture (Park, et al. 2004). They found enhanced bonding of CNTs to the matrix resin via polar interactions, thus leading to better toughness values in the resulting structures. Gojny, et al. (2004) revealed based upon TEM investigations that DWCNTs have moderately fine dispersion in 3-roll milling processed epoxy resin. In the same study, they also showed that blending of very low content (0.1 wt. %) of DWCNTs with epoxy resin via 3-roll milling improved the mechanical properties, such as elastic modulus and fracture toughness of the epoxy resin. Thostenson and Chou (2006) investigated recently the influence of processing parameters on the final dispersion state of carbon nanotubes during 3-roll milling. In this manner, they produced epoxy/nanotube suspensions at various gap settings ranging from subsequently 5 to 50 μm through 3-roll milling by means of Teflon guides which help keep the blend centered on the rollers. They observed that the relatively high fracture toughness values were obtained from the nanocomposites processed at gap settings of 5 and 10 μm.

In this chapter, the influence of CNTs, including MWCNTs, MWCNT-NH_2, DWCNTs and DWCNT-NH_2 upon the tensile mechanical response and fracture toughness of the nanocomposites were evaluated along with the fracture modes on the surfaces of the failed specimens via Scanning Electron Microscopy (SEM) examination.

The dispersion state of the nanotubes in the resulting nanocomposites was also highlighted via Transmission Electron Microscopy (TEM) studies.

7.2. Experimental

7.2.1. Tensile Test

Tensile mechanical properties of the nanocomposites were determined according to DIN EN ISO 527.1. Dog bone shape specimens were prepared by countersinking through Mutronic dear drive 2000. The tensile samples were tested on Zwick Universal testing machine 1445 at a cross head speed of 1 mm/min. The elongation of the specimen during the test was measured by means of distance encoder with a gauge length of 5 mm. Figure 7.1 depicts the tensile test specimen under load.

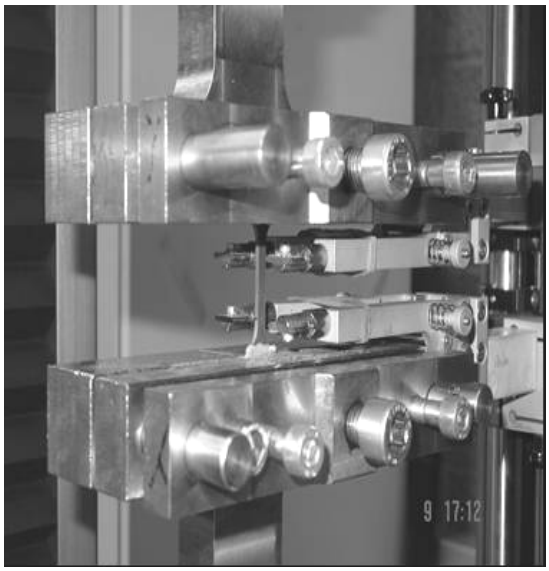

Figure 7.1. A tensile test specimen under load.

7.2.2. Fracture Test

The fracture toughness of the nanocomposites was measured according to ASTM-D 5045-96. Compact tension (CT) specimens were prepared in the same dear drive machine and tested at a crosshead speed of 1.3 mm/min employing the universal testing machine with a 500 N load cell. Figure 7.2 shows a fracture test specimen under

load. The deformation of the specimens was monitored by detecting the crack opening displacement with the encoder. A sharp incipient crack was accomplished watchfully by hammering a razor blade into the corresponding notch. Six specimens of each sample were tested for statistical evaluation. The fracture energy G_{Ic} was calculated based on the equation below.

$$G_{Ic} = \frac{K_{Ic}^2}{E} \tag{7.1}$$

In the above equation, K_{Ic} is fracture toughness and calculated as an average of values for each batch and E is elastic modulus of each corresponding composite.

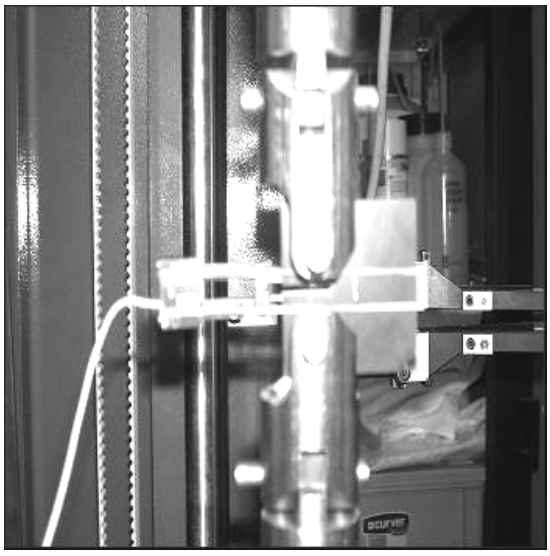

Figure 7.2. A fracture test specimen under load.

7.2.3. Microscopic Investigation

Philips SEM at 3 kV voltages was also used to examine macro-scale fracture failure modes which occurred within each corresponding specimen under tensile mechanical loading. For this purpose, fracture surfaces of tensile and CT specimens failed under loading were examined. The effects of carbon nanotubes with and without amine functional groups on the damage mechanisms of the nanocomposites were then evaluated. Failure modes were also related to the experimentally determined ultimate performance of the nanocomposites.

7.3. Results and Discussion

7.3.1. Dispersion of nanotubes within polymer matrix

Figures 7.3 a, b, c and d are the TEM micrographs showing achieved dispersion of DWCNTs, DWCNT-NH_2, MWCNT and MWCNT-NH_2 at 0.3 wt. % loading rate within the corresponding hybrid polymer resin, respectively. In consequence, MWCNTs and MWCNT-NH_2 were found to exhibit relatively good dispersion within the corresponding hybrid resin system without possessing any significant size agglomerates. However, DWCNTs and DWCNT-NH_2 demonstrated some dense agglomerated zones visible within the hybrid resin. Of all, DWCNTs have the highest tendency to form dense agglomerates within the resin system because of their relatively high surface area. In fact, this is very proportional to rheological properties of the resin suspensions. As the content of DWCNTs increases, lower storage and loss modulus values were obtained form the resin suspensions in which they are embedded, regardless of amine functional groups. This subject of interest was already highlighted in Chapter 4.

7.3.2. Tensile Properties of Nanocomposites

The ultimate tensile strength (UTS) of the nanocomposites containing MWCNTs, MWCNT-NH_2 DWCNTs and DWCNT-NH_2 as a function of filler content is shown in Figure 7.4. In brief, existence of CNTs within the hybrid resin did not improve the UTS of the resultant nanocomposites, significantly. In the literature, a number of studies have expressed that utilization of CNTs with higher surface area and larger aspect ratio resulted in enhanced tensile strength and fracture toughness in epoxy resin based nanocomposites (Allaoui, et al. 2003, Gojny and Schulte 2004, Gojny, et al. 2004). However, the same profound effect of CNTs is not likely to occur in free-radically polymerized resins such as vinylester and polyester. This is because free radicals generated by decomposition of initiator (MEKP) added into the resin system could be too vulnerable to be trapped within the galleries of carbon nanotubes. In this case, use of lower amount of MEKP than the required for the given amount of the resin would lead to heterogeneous polymerization of the resin system, thus decreasing the cross-linking density of the final part. Furthermore, post curing subsequently applied at

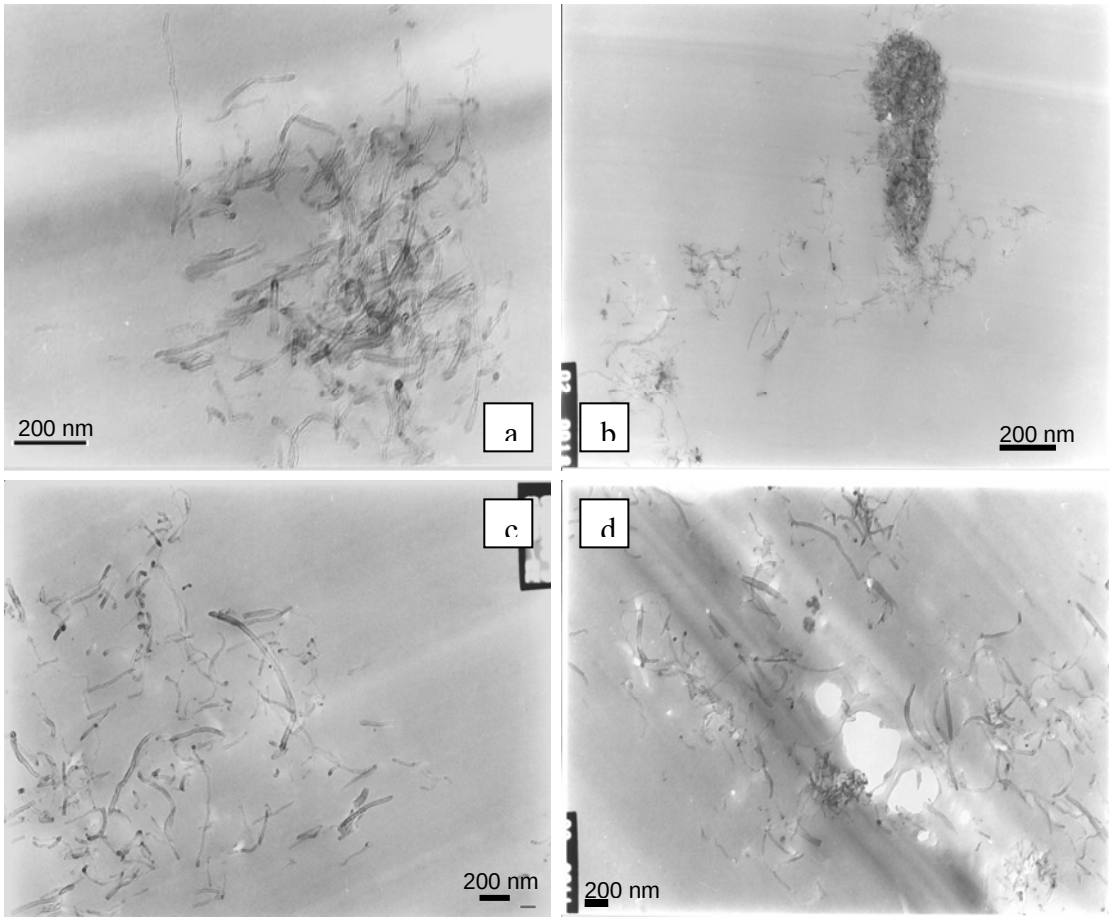

Figure 7.3. TEM micrographs showing achieved dispersion state of nanotubes within hybrid resin at 0.3 wt. % loading rate (a, b, c, d refer to DWCNT, DWCNT-NH_2, MWCNT and MWCNT-NH_2, respectively.)

elevated temperature would further cause the built-in thermal residual stresses to take place, which induces voids and micro-cracks preferably located nearby the zone of agglomerated CNTs within the entire composite part. This may reduce especially the mechanical strength of the resulting nanocomposites. Similarly, Peng et al. (2003) reported that single walled carbon nanotubes are able to effectively trap free radicals released by initiator during room temperature polymerization, thus leading to relatively low cross-linking density across the part. In our case, this is somewhat more relevant for the nanocomposites containing DWCNTs because DWCNTs have relatively high surface area and tendency to form relatively large agglomerates. In other words, when used as fillers, more amounts of free radicals would be possibly entrapped within the galleries of DWCNTs. This is because, at any given weight percentage, DWCNTs occupy higher volume within the resin system than MWCNTs.

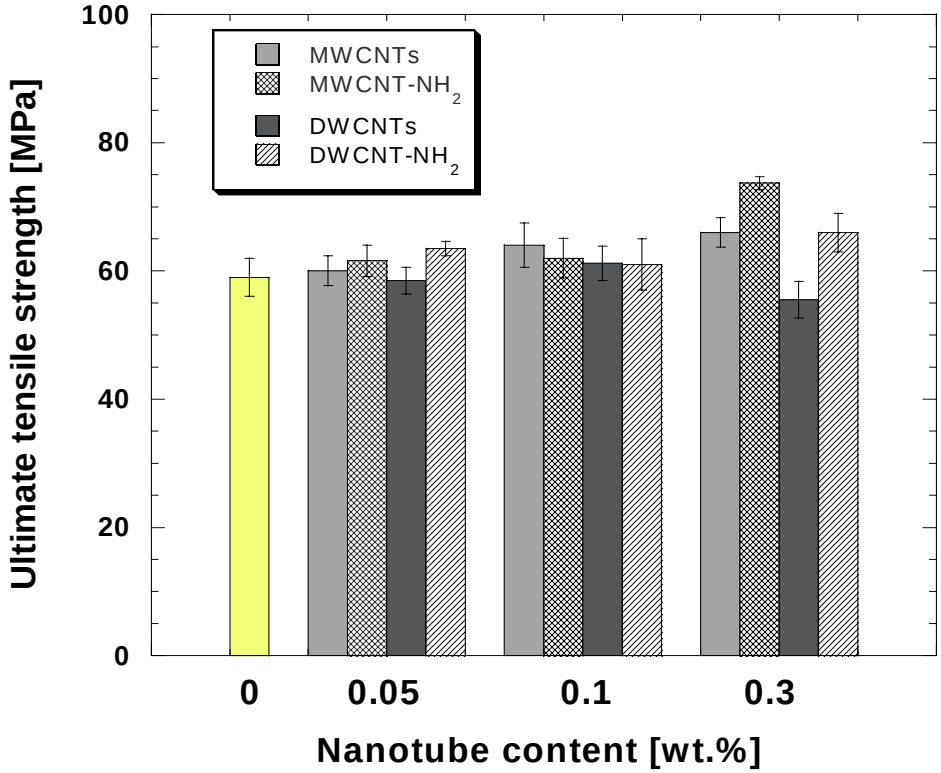

Figure 7.4. Ultimate tensile strength of the nanocomposites containing MWCNT, MWCNT-NH_2, DWCNT and DWCNT-NH_2 with respect to nanotube content.

Amine functional groups over the surfaces of CNTs are expected to improve not the final dispersion state of CNTs within the resin matrix, but the chemical interactions at the interface by increasing the surface polarity of CNTs. In general, regardless of type of CNTs, the nanocomposites containing amino functionalized nanotubes were found to exhibit higher tensile strength compared to those with untreated nanotubes. This is ample evidence that reinforcing efficieny of amine groups is critical to alteration of interfacial interactions between CNTs and the matrix resin. In fact, this expression shows consistency with the results regarding the curing behavior of the resin suspensions, already given in Chapter 5.

Figures 7.5 a and b give the elastic modulus values of the nanocomposites with MWCNTs and MWCNT-NH_2 and those with DWCNTs and DWCNT-NH_2, respectively. It was found that incorporation of MWCNT-NH_2 and MWCNTs into the hybrid resin leads to higher elastic modulus values in the consequent nanocomposites compared to those with DWCNTs and DWCNT-NH_2. At 0.1 wt. % loading rate, elastic modulus of the nanocomposites with MWCNT-NH_2 and MWCNTs is 18 and 15 %

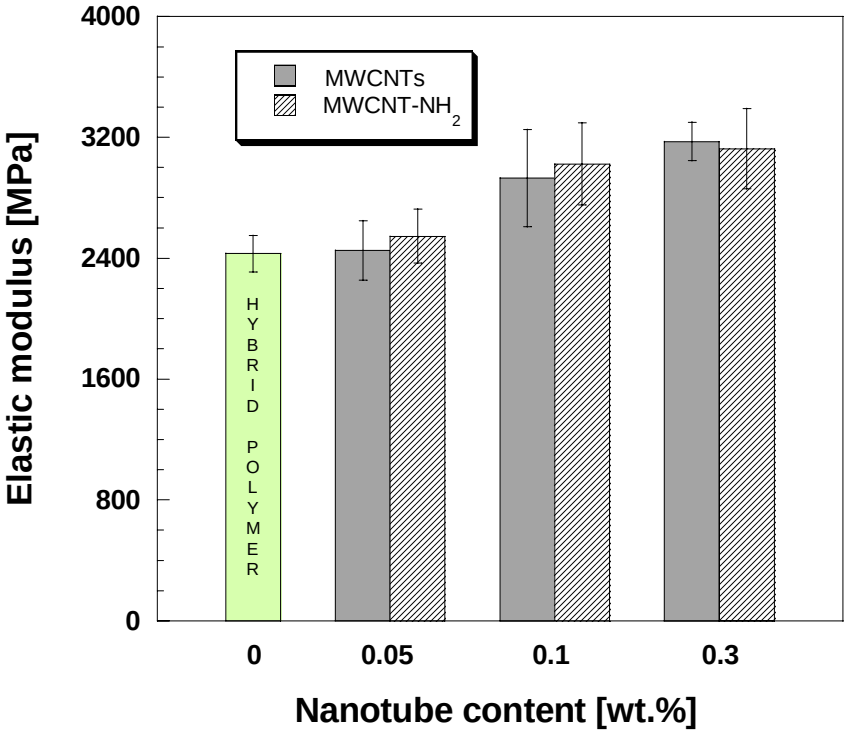

a)

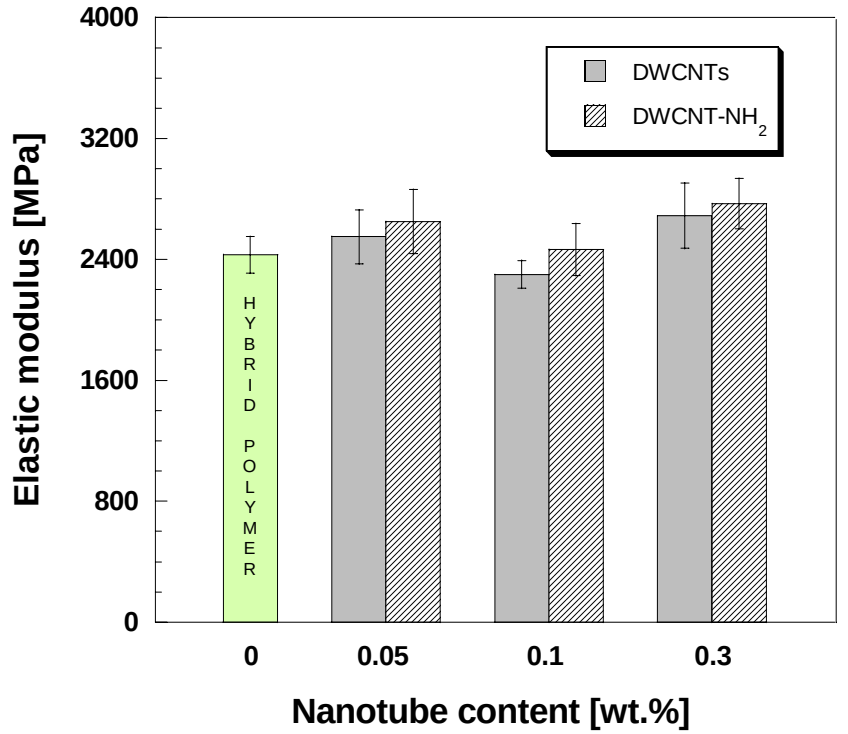

b)

Figure 7.5. Elastic modulus of the nanocomposites with respect to nanotube content a) with MWCNTs and MWCNT-NH_2, b) with DWCNTs and DWCNT-NH_2

higher than that of neat hybrid resin, respectively. However, neither the addition of similar contents of DWCNTs, nor of DWCNT-NH_2 had considerable impact on the modulus values of the hybrid polymer. In a similar manner, the mechanical and thermal properties of vinylester based nanocomposites prepared with untreated MWCNTs were investigated by Gryschuck et al. (2006). The aspect ratio of the CNTs was reported to have substantial effects on the chemical interactions at the interface. In addition, they conclude that cure kinetics of the resin may vary, depending on the volume content of CNTs that the resin contains. Note that the amine treated CNTs used in our study were functionalized using ball milling. During ball milling, CNTs lose their strength partially via their broken carbon-carbon bonds and hence their aspect is reduced. Similarly, Zhu et al. (2007) concluded that the presence of SWCNTs in the vinylester resin retards the radical polymerization rate of vinylester resin during room temperature curing. To promote the local polymerization of vinylester resin, they, therefore, suggested using high temperature initiators that initiate the polymerization at elevated temperature.

At that point, one can expect drastically lower elastic modulus values from the nanocomposites containing MWCNT-NH_2 as compared to those with MWCNTs. However, nanocomposites with MWCNT-NH_2, at each given loading rate, possessed significantly higher elastic modulus than those with MWCNTs, just in the same manner as tensile strength. This is ample evidence that NH_2 functional groups enhance the adhesion at the interface between the CNTs and the polymer matrix and assist in improving dispersion of CNTs within the resin system. We revealed that resin suspensions containing MWCNTs and MWCNT-NH_2 showed similar rheological response, despite five times lower aspect ratio of MWCNT-NH_2 as compared to that of MWCNTs (Seyhan, et al. 2007b). This implies obviously the effectiveness of NH_2 functional groups in dispersion of CNTs. Moreover, the modified Halphin Tsai equation for random orientation of short fibers within nanocomposites was utilized in order to better interpret the reinforcement mechanism of CNTs with and without NH_2 functional groups within corresponding hybrid resin. The final equation employed to calculate the maximum achievable elastic modulus in the resultant nanocomposites is as in the following (Gojny, et al. 2004). Note that this corresponding equation presumes that short fibers posses a perfect distribution and very well impregnation with the surrounding polymer matrix resin. Please note that the predictions obtained via this suggested very well known equation does not necessarily show the CNT induced effects. This is because, at nano level, everything behaves in different manner.

$$E_C = \frac{3}{8}\{1+2\left(\frac{l}{d}\right)\left(\frac{(E_{NT}/E_m)-(d/4t)}{(E_{NT}/E_m)+(l/2t)}\right)V_{NT}\}x$$
$$\{1-\left(\frac{(E_{NT}/E_m)-(d/4t)}{(E_{NT}/E_m)+(l/2t)}\right)V_{NT}\}^{-1}E_m +$$
$$\frac{5}{8}\{1+2\left(\frac{(E_{NT}/E_m)-(d/4t)}{(E_{NT}/E_m)+(d/2t)}\right)V_{NT}\}x \qquad (7.2)$$
$$\left(1-\left(\frac{(E_{NT}/E_m)-(d/4t)}{(E_{NT}/E_m)+(d/2t)}\right)V_{NT}\right)^{-1}E_m$$

Here E_c is the elastic modulus of the composite, l is the length of corresponding nanotube, d is the average outer diameter of nanotubes, E_{NT} is the elastic modulus of the nanotubes (1 TPa for each type of CNTs), E_m is the modulus of the hybrid resin, t is the thickness of graphite layer (0.34 nm.), V_{NT} is the volume content of nanotubes. The volume content of the nanotubes is in fact difficult to calculate because of its dependence on the density, which is related to the diameter distribution and defects as well. In this manner, we employed an approach suggested by Thostenson and Chou (2003) to calculate the density of CNTs (ρ_{CNT}).

$$\rho_{CNT} = \frac{\rho_g\left(d_a{}^2 - d_i^2\right)}{d_a^2} \qquad (7.3)$$

The equation above considers the inner and outer diameters of CNTs *(d_i and d_a)* and the density of graphite (ρ_g). The density of hybrid resin was calculated based on the rule of mixture and taken as 1.13 gr/cm^3 in the calculations. Density of the graphite was considered to be 2.25 gr/cm^3.

Figure 7.6 gives the experimentally obtained elastic modulus of the nanocomposites containing DWCNTs and MWCNTs with and without functional groups in comparison with the predicted ones via Halphin and Tsai equation. Based upon the statistical R^2 values predicted via linear regression of the modulus values of nanocomposites with respect to each given concentration, it can be concluded that the elastic modulus values of nanocomposites with MWCNTs (0.83) and MWCNT-NH_2 (0.60) are in better agreement with the proposed model, as compared to those of the nanocomposites with DWCNTs (0.36) and DWCNT-NH_2 (0.44).

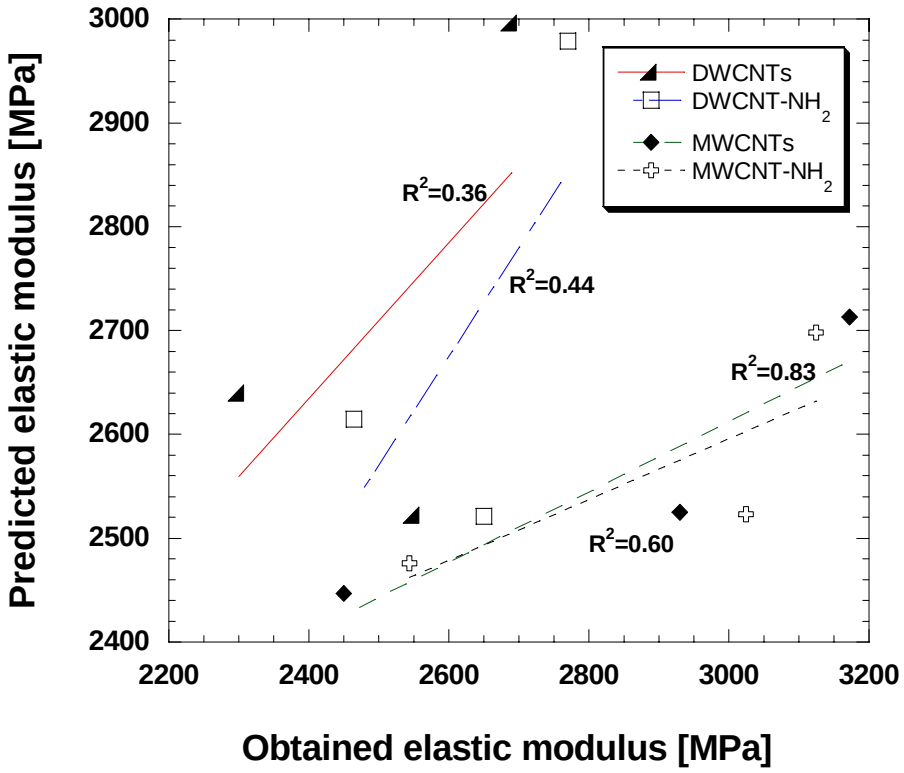

Figure 7.6. Predicted elastic modulus values as a function of experimentally obtained ones at CNT content.

Hence, hypothetically, MWCNTs and MWCNT-NH_2 turned out to exhibit better dispersion and thus stronger interfacial chemical bonding to the matrix resin as compared to DWCNTs and DWCNT-NH_2. This is also consistent with the experimental findings obtained so far. In brief, the results obtained showed that MWCNTs and MWCNT-NH_2 modified vinyl-ester polyester based nanocomposites featured better tensile mechanical properties as compared to those with DWCNTs and DWCNT-NH_2. Also, aspect ratios, surface area, volume content, and NH_2 functional groups over the surfaces of CNTs are particularly critical to final degree of polymerization and ultimate performance of the nanocomposites. The detailed work on these issues was already given in Chapter 5. We have shown that MWCNTs with and without amine functional groups affected the individual conversions of styrene and vinylester monomers in the resin system.

The fact that we achieved reduced properties in DWCNT modified nanocomposites relative to those with MWCNTs may be the evidence that the higher surface area and thus the larger agglomerates may have adverse effects on the degree of polymerization. This expression is highly proportional to the findings obtained in the

literature such that the higher the surface area, the lower degree of polymerization (Peng, et al. 2003, Zhu, et al. 2007). Note that the findings obtained so far are very consistent with those addressed in the previous chapters.

7.3.3. Fracture Toughness of Nanocomposites

Figures 7.7 and 7.8 give the fracture toughness values of the nanocomposites prepared with various types and amounts of carbon nanotubes, including MWCNTs, MWCNT-NH_2, DWCNTs and DWCNT-NH_2. At each loading rate, nanocomposites with MWCNTs and MWCNT-NH_2 exhibited higher fracture toughness values than those with DWCNTs and DWCNT-NH_2. Moreover, nanocomposites with MWCNT-NH_2 have high fracture toughness values relative to those with MWCNTs. However, addition of DWCNTs with and without amine functional groups has almost no significant influence on the fracture toughness values of the resultant nanocomposites. Incorporation of 0.3 wt. % of MWCNT-NH_2 resulted in the highest fracture toughness values, which corresponds to an improvement by 40 % as compared to that of neat hybrid resin. Table 7.1 gives the calculated fracture energy of the nanocomposites with various types of CNTs. As seen in the table, the highest energy, which is almost twice as much as that of neat hybrid polymer, was obtained from the nanocomposites with MWCNT-NH_2, while the lowest one was achieved in the nanocomposites with DWCNTs. These results are proportional to those achieved in tensile mechanical response of their corresponding nanocomposites. Nanotubes with their huge aspect ratio are supposed to show fiber-like structure behavior.

As discussed earlier, partially agglomerated morphology was in general observed for each type of CNTs, but especially for DWCNTs due to their relatively high surface area. It was concluded that large surface area leads to a more efficient improvement of fracture toughness, and that improper impregnated agglomerates act as defects in the polymer based nanocomposites (Bai 2003, Meguid and Sun 2004, Fiedler, et al.2006). Gojny et al. (2004) suggested that a combination of well dispersed nanotubes with well impregnated smaller agglomerates is the most promising state of dispersion which enhances substantially the fracture toughness of the corresponding resin system. However, this corresponding approach is not entirely valid for our case. As elucidated in the previous sections, nano-fillers with high surface area turn out to be not appropriate for free radically polymerized resins.

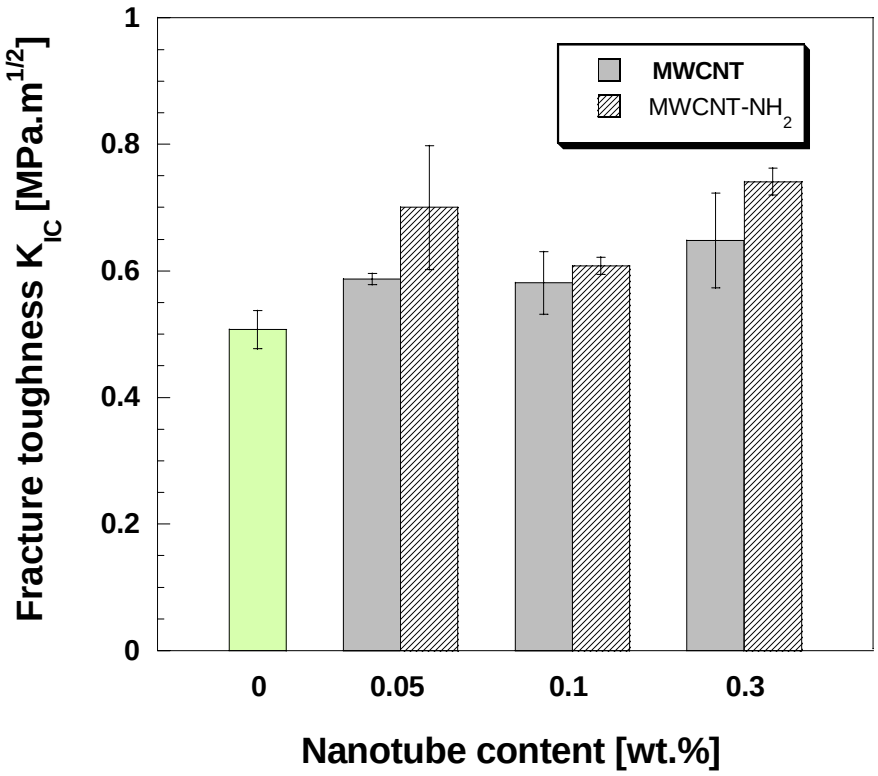

Figure 7.7. Fracture toughness values of nanocomposites with MWCNT and MWCNT-NH_2 with respect to nanotube content.

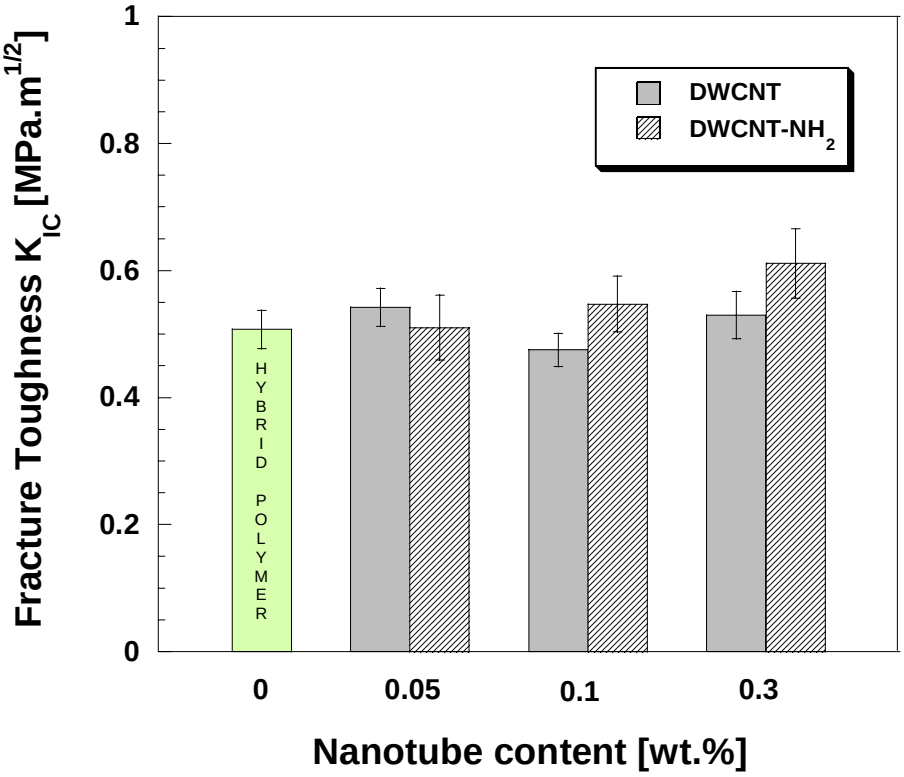

Figure 7.8. Fracture toughness values of nanocomposites with DWCNT and DWCNT-NH_2 with respect to nanotube content.

Table 7.1. Calculated fracture energy of each corresponding nanocomposite (J/m^2).

Weight %	MWCNTs	MWCNT-NH_2	DWCNTs	DWCNT-NH_2
0.05	140.5	197.6	114.3	98.15
0.1	114.8	119.1	96.3	121.3
0.3	129.1	172.5	104.1	134.3

Neat hybrid polymer = 105.7

In other words, the larger the surface area of CNTs is, the more probable it would be for free radicals to be trapped within galleries of nanotubes. This lowers the degree of polymerization while at the same time reducing the cross-linking density. As a result, the final mechanical properties of the nanocomposites are decreased. Regardless of type of CNTs or amine functional groups, anomalous fracture behavior was observed for the nanocomposites such that a conflict occurs between weight content of CNTs and the fracture toughness values of their resulting nanocomposites, as seen in the figures. This may be highly associated with the chemical interactions between the dense nanotube agglomerates and the free radicals in the resin system dependent on amine functional groups. The reason of this conflict was discussed in details together with the fracture surface of the samples under the following title.

7.3.4. Analysis of Failure Modes by SEM Examination

The fracture surfaces of the failed tensile and fracture test specimens are worth examining to relate the CNT induced fracture mechanisms and failure modes to the fracture behavior of the resultant nanocomposites. Figures 7.9 a, b, c and d are the SEM tensile fracture surfaces of the nanocomposites prepared with 0.3 wt. % of MWCNTs, MWCNT-NH_2, DWCNTs and DWCNT-NH_2, respectively. As seen in the photo (Figure 7.9 a), MWCNTs have homogenous dispersion with very few separate agglomerates in the surrounding matrix resin. However, DWCNTs (Figure 7.9 c) exhibited relatively dense large agglomerates and few individuals around them. In fact, this trend is expected because DWCNTs have relatively high surface area. Therefore, hypothetically

more energy is needed than applied for MWCNTs via 3-roll milling to disperse their agglomerates into individual ones. On the other hand, the matrix cracking passing through mid-plane of agglomerated MWCNT-NH_2 is highly visible, as indicated by a white arrow on the photo (Figure 7.9 b). Moreover, agglomerates of DWCNT-NH_2 (Figure 7.9 d) exhibited relatively weak adhesion to the matrix resin in such a way that extensive de-bonding and incurable matrix cracking that occur around the agglomerates (as indicated by white arrow) are highly noticeable.

Please note that the SEM photos showing the dense agglomerates of amino functionalized nanotubes were intentionally selected to associate the mechanical properties of the nanocomposites with curing behavior of the nanocomposites. In fact, these observations showed that amine functional groups, degree of nanotube agglomeration, size of the nanotube agglomerates and their distribution within the surrounding matrix are vastly critical to the ultimate response of the nanocomposites.

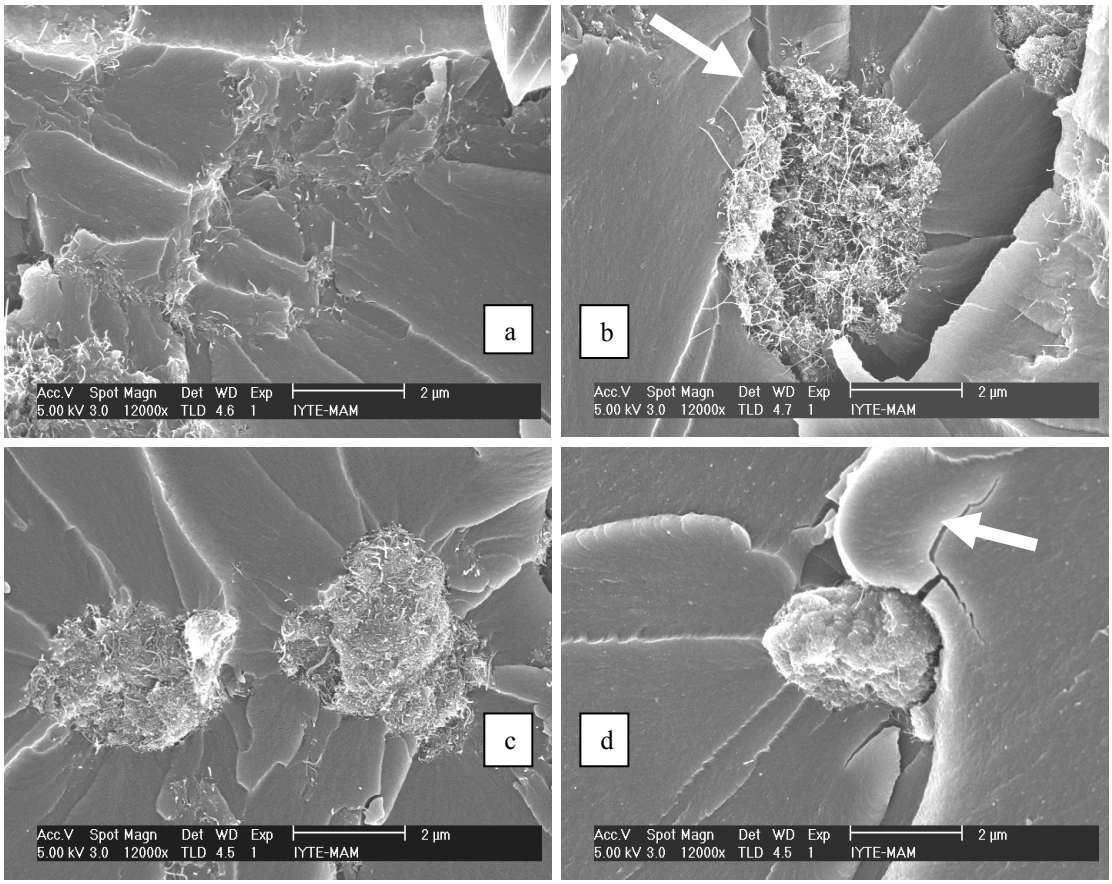

Figure 7.9. SEM image of tensile fracture surface of nanocomposites with a) MWCNT b) MWCNT-NH_2 c) DWCNT d) DWCNT-NH_2 at 0.3 wt. % CNT content.

Figures 7.10 a and c are the SEM fracture surfaces of the compact tension (CT) composite specimens prepared with 0.3 wt. % of DWCNT-NH_2 and MWCNT-NH_2, respectively. Figures 7.10 b and d show the magnified zone indicated by the arrows on Figures 7.10 a and c, respectively. The same trend as in the case of tensile fracture surfaces is observable. In terms of fracture mechanics, dense agglomerates act probably as defects, triggering void nucleation and/or micro-crack coalescences at the interface between CNTs and the surrounding matrix resin. At this stage, the characteristics of the bulk matrix may also play a crucial role in overall response of the entire nanocomposite part. In other words, one could further say that the property of the bulk matrix around the larger agglomerates may be locally different from the overall response of the entire composite dependent on the type of CNTs and amine functional groups.

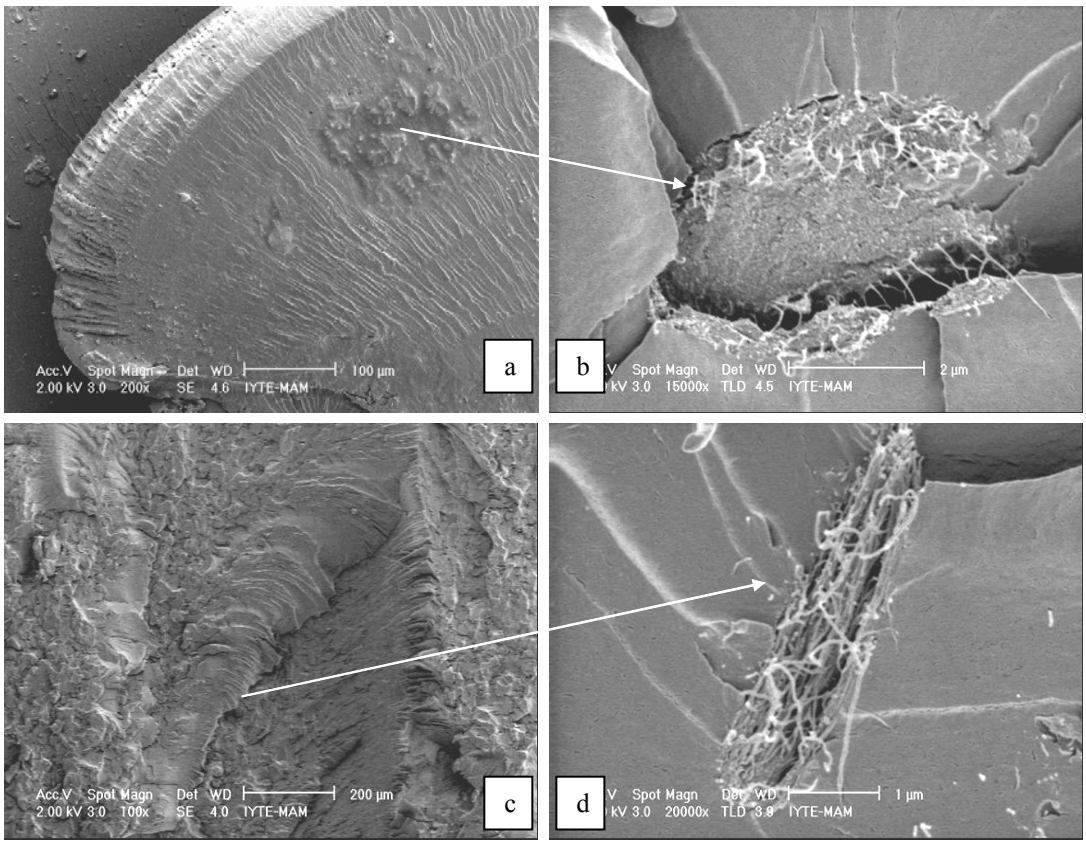

Figure 7.10. SEM photos of compact tension fracture surfaces of nanocomposites containing 0.3 wt. % CNT a) DWCNT-NH_2 b) the same of (a) at higher magnification c) MWCNT-NH_2 d) the same of (c) at higher magnification.

This is because the amount of free radicals trapped within galleries of CNTs is highly dependent on the physical properties of CNTs, including aspect ratio and surface area. This would alter the array of crack paths across the corresponding part prior to its failure under load. In fact, all these expressions could explain the reason of the anomalous trend observed for the fracture toughness of the nanocomposites.

7.4. Conclusions

In this chapter, the effect of various types of CNTs including MWCNTs and DWCNTs with and without NH_2 functional groups on the tensile mechanical behavior and fracture toughness of vinylester-polyester hybrid resin system was investigated. It was found that addition of CNTs has no significant effect on the tensile strength of the resulting nanonanocomposites. It was also revealed that nanonanocomposites containing MWCNTs with and without NH_2 functional groups resulted in higher tensile modulus, fracture toughness and fracture energy values in comparison to those prepared with DWCNTs or DWCNT-NH_2. Moreover, experimentally measured elastic moduli of the nanonanocomposites were fitted to Halphin-Tsai's analytical model. The predicted and the measured values of nanonanocomposites with MWCNTs and MWCNT-NH_2 were found to be in good agreement with each other. On behalf of the experimental findings achieved, we conclude that reinforcing efficiency of DWCNTs and DWCNT-NH_2 is low relative to MWCNTs and MWCNT-NH_2, when incorporated into free radically polymerized thermosetting resins such as polyester or vinylester. This is due to the fact that DWCNTs have low aspect ratio and high SSA relative to MWCNTs. This leads to DWCNTs to show greater tendency to form relatively large and dense agglomerates within the cured polymer matrix, which may trap the free radicals released by MEKP during polymerization at room temperature. Entrapment of free radicals decreased the degree of polymerization and cross-linking density. This may significantly influence the cure kinetics of the resin system by altering the chemical interactions at the interface, which are directly related to ultimate performance of the final composite parts. This subject of interest was already discussed in details in Chapter 5.

CHAPTER 8

ELECTRICAL PROPERTIES OF CNT MODIFIED NANOCOMPOSITES

8.1. Introduction

Polymer based materials are expected to dissipate static electric to avoid electrostatic charging in their various applications, such as automotive parts and some household products (Sandler, et al. 1999a, Gojny et al. 2006). In this manner, conductive fillers such as carbon black (CB) have been commonly added to polymers. However, in most cases, CB content required to attain the desired level ($\sigma=10^{-6}$ Sm^{-1}) of electrical conductivity in polymers leads to reduction in mechanical properties such as tensile strength of the final product (Şimşek, et al. 2007) On the other hand, application of highly conductive nanoparticles to an isolating polymer matrix is supposed to induce a higher electrical conductivity at relatively low filler contents, as compared to CB particles. In this respect, potential of carbon nanotubes as conducting filler in polymer nanocomposites has been successfully recognized. At very low loading rates of nanotubes, several orders of magnitude improvement in electrical conductivity was accomplished in the polymer matrices, while sustaining mechanical properties of polymers (Allaoui, et al.2003, Bai and Allaoui 2003). These conductive nanocomposites have widespread use in various types of applications such as electrostatic dissipation, electrostatic painting, and electromagnetic interference (EMI) shielding.

The electrical conductivity of nanocomposites is mainly based upon percolated pathways of conductive particles. The percolation theory is used to account for the conductivity of polymer nanocomposites (Sandler, et al. 1999a). In this theory, percolation threshold refers to onset of the electrical conductivity due to conductive pathways formed once a critical filler concentration is accomplished in the system of interest (Munson 1991). In other words**,** percolation threshold can be distinguished by a prompt significant increase in the conductivity by many orders of magnitude due to the formation of three dimensional conductive networks of fillers within the corresponding matrix resin (Prasse, et al. 2003, Sandler, et al. 1999a). Nevertheless, the percolation

theory was formerly established for spherical particles. Therefore, it shows relatively poor validity for rod-like fillers, such as chopped carbon fibers, carbon nanofibers (CNFs) and CNTs which possess huge aspect ratio (l/d>>1) and low percolation threshold relative to spherical ones (Martin, et al. 2004). An advanced percolation theory which considers also the aspect ratio of fillers was proposed to predict the critical volume fraction at which a percolated network of conductive fillers is formed (Sandler, et al. 1999a, Martin, et al. 2004). Accordingly, critical volume contents for percolation threshold of rod-like fillers with an aspect ratio of more than 100 were predicted to vary from 0.24 to 1.35 vol. %. Therefore, replacing CB micro particles, generally in spherical form, with the CNTs that have huge aspect ratio is relatively more effective to achieve a percolation threshold at very low filler contents. In the literature, reported amount of CNT loading within polymer matrices for a percolation threshold varies widely from less than 1 % to over 10 % in weight (Sandler, et al. 2003). This is because of the some dependent parameters affecting the composite conductivities, such as aspect ratio of CNTs, orientation of nanotubes in the resin system (alignment), dispersion state of nanotubes as well as processing temperature and curing conditions of their resulting nanocomposites (Martin, et al. 2005). Brying et al. (2005) studied the conductivity of epoxy nanocomposites prepared with SWCNTs having two different aspect ratios (150 and 380). They found a lower percolation threshold with higher aspect ratio nanotubes. Bai and Allaoui (2003) concluded that the threshold concentration of MWCNT within epoxy resin was 8-fold lower when the length of MWCNTs was increased from 1 to 50μm.

Process-induced negative surface charges on carbon black or carbon nanotubes may be utilized to produce initially charged stabilized dispersions, which become then capable of forming aligned networks under application of either direct current (DC) or alternating current (AC) fields (Prasse, et al. 1998, Martin, et al. 2005). Alignment of the CNTs in the polymer matrix has profound effect on the electrical conductivity and its percolation threshold. In principle, the resulting structure of the conductive filler networks is highly dependent upon the type of electric field applied during curing. Prasse et al. (2003) applied AC fields for the alignment and network formation of carbon nanofibers (CNFs) within an epoxy resin during curing. However, this attempt possessed poor results with regard to the required content for the formation of a conductive filler network (>1 wt. %). In addition, they revealed that the maximum composite conductivity achieved by CNFs is not significantly larger than that of CB

within the same epoxy matrix. It was also revealed that both AC and DC electric fields can be utilized to induce the formation of aligned CNT networks by adjusting the gap between electrodes in contact with the dispersion (Martin, et al. 2005, Martin, et al. 2004). Moreover, they also stated that more uniform and more aligned networks can be accomplished in AC field as compared to DC field. This is because DC field leads to relatively inhomogeneous and branching network structures. In other words, AC fields result in more homogeneous networks as compared to DC fields.

A number of theoretical percolation models have been proposed to identify the critical filler volume content, at which a network is formed in conductive polymer compounds. In addition, temperature variation of conductivity can also be investigated and transport mechanisms are explained by various models, including Luttinger liquid, one dimensional disordered wire, activated process, variable range hopping and fluctuation-induced tunneling through the barriers between the metallic regions model (Kymakis, et al. 2002, Astorga and Mendoza 2005, Jiang, et al. 2005, Mischenko, et al. 2001, Kymakis, et al. 2006, Bajpai, et al. 2007).

In this chapter, temperature dependency of the electrical properties of polyester based nanocomposites produced by the second approach, containing various amounts of multi walled carbon nanotubes (MWCNTs) and double walled carbon nanotubes (DWCNTs) with and without amine functional groups ($-NH_2$) were evaluated. Please note that the same results were also obtained from the vinylester-polyester nanocomposites produced by the third approach under identical processing conditions. Since the experimental data for the nanocomposites produced by the second approach was already published (Şimşek, et al. 2007), we did not find it necessary to mention about the same subject of interest for vinylester-polyester based nanocomposites in this dissertation. Moreover, the effects of amine functional groups over the surfaces of the CNTs on the electrical behavior of their final nanocomposites were also discussed in details. Some analytical models were used to be able to identify the mechanisms for electrical conductivity of the nanocomposites with respect to temperature. Furthermore, room temperature electrical conductivity of the vinylester polyester based nanocomposites (the third approach) was measured. The influence of randomly oriented and electric field induced aligned CNTs on the electrical conductivity and thermal behavior of a vinylester polyester hybrid matrix was also pinpointed. Note that room temperature electrical measurements and alignment of CNTs were carried out just on

vinylester-polyester based nanocomposites. This is because we already switched the resin system while these experiments were done.

8.2. Experimental

8.2.1. Four Point Probe Test

Temperature dependence electrical conductivity of nanocomposites was measured by conventional DC method from room temperature to 77 K. Figure 8.1 illustrates the corresponding experimental set up.

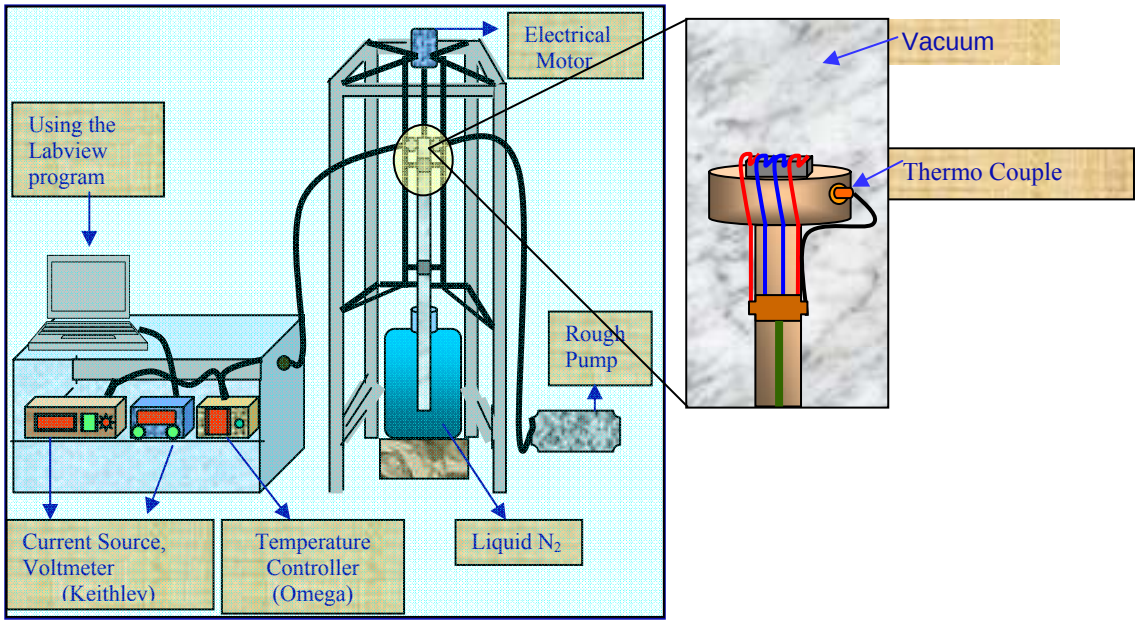

Figure 8.1. Illustration of the experimental set up for the measurement of the conductivity with respect to temperature.

The rectangular samples were sectioned from the cast samples in two different directions. Homogeneity of the samples was tested by performing measurements with contacts obtained from each face of the rectangular samples. The four-point probe was contacted on rectangular bulk samples with silver paint. Resistance versus temperature data of the nanocomposites was obtained using computer controlled data acquisition system.

8.2.2. Impedance Spectroscopy

Room temperature electrical conductivity of the CNTs modified nanocomposites cured with and without application of AC electric field was measured by dielectric spectroscopy using a HP 4284a Impedance Analyzer. Figure 8.2 shows the experimental set up. For each set, at least three specimens with a dimension of 10x10x1 mm. were tested with voltage amplitude of 1.0 V in a frequency range between 20 Hz and 1MHz. The corresponding electrical conductivity of the samples was calculated from the complex impedance $|Z^*|$ with respect to the frequency according to the equation below.

$$\sigma(v) = 1/|Z^*(v)|t/A \tag{8.1}$$

Where σ is the electrical conductivity, v is the frequency, t is the thickness of the sample, and A is the cross sectional area of the specimens.

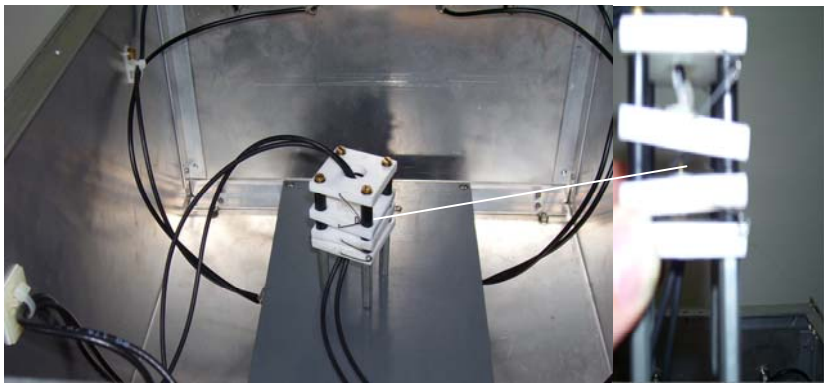

Figure 8.2. The experimental set up for the measurement of the room temperature conductivity of the samples.

8.2.3. Alignment of CNTs under AC electric field

To align the CNTs within the polymer matrix, resin suspensions with 0.005, 0.02 and 0.05 wt % of MWCNTs were exposed to sinusoidal AC electric field of 400 V/cm during curing by utilization of parallel brass plates. Typical electrode dimensions embedded in the brass plates are 9 x 18 mm^2 with a spacing of 4.5 mm. Note that

MWCNTs were selected as filler constituents to perform these corresponding experiments because their nanocomposites exhibited the highest conductivity values at each loading rate, just in the same manner as in the second approach resin system (Şimşek, et al. 2007). Figure 8.3 depicts the experimental set up. After the resin suspensions were cured with application of the AC electric field, the resulting nanocomposites were subjected to post-curing at 120^{o}C for 2 hours. The samples were subsequently cut and contacted in the directions parallel and perpendicular to the direction of the applied electric field to assess the anisotropy of electrical conductivity in the nanocomposites. Note that given field strength refers to the peak value of the AC field, which was applied at a frequency of 1 kHz throughout the experiments.

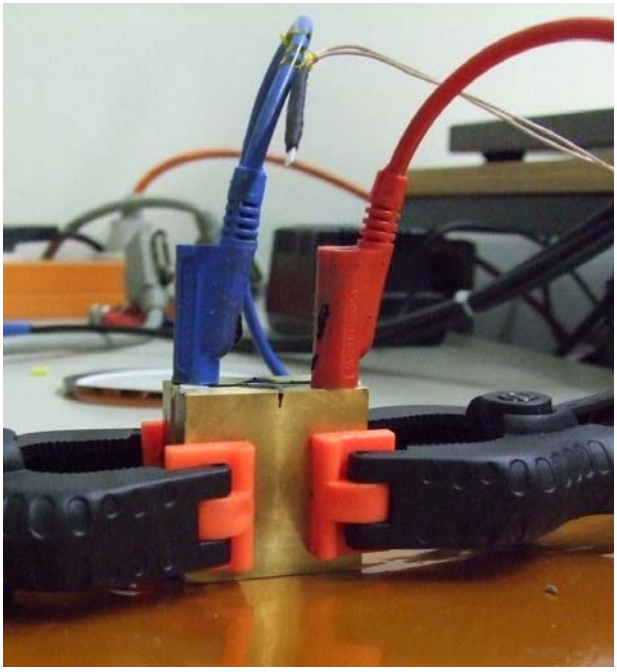

Figure 8.3. The experimental set up used to align CNTs within the hybrid matrix resin.

8.2.4. DSC measurements

DSC was utilized to investigate the T_g value of the corresponding nanocomposites cured with and without the application of AC electric field. The measurements were performed by TA Instruments Q-10 scanning calorimeter. For the measurements, a small quantity of the samples (5-10 mg) was taken from neat hybrid polymer and its nanocomposites containing 0.05 wt. % of randomly oriented and AC

electric field-induced aligned MWCNTs. Runs were carried out, using an aluminum empty pan as a reference. Each sample was first heated from room temperature up to 200°C with a constant heating rate of 5°C/min. in nitrogen atmosphere. After cooled down to room temperature, the same samples were subsequently reheated up to 200°C with a heating rate of 5°C/min. to determine their T_g values.

8.3. Results and Discussion

8.3.1. Temperature dependence of electrical conductivity in nanocomposites

Figures 8.4a and b show the measured electrical conductivity of nanocomposites at room temperature and 77 K with respect to volume content of CNTs, respectively. The volume fraction of CNTs corresponding to weight percentages is seen in Table 1.

Table 8.1. The volume fraction of CNTs corresponding to weight percentages.

Wt.%	Volume fraction % (DWCNT) (DWCNT-NH_2)	Volume fraction % (MWCNT) (MWCNT-NH_2)
0.1	0.105	0.049
0.3	0.316	0.149
0.5	0.523	0.247

Figure 8.4a indicates that the presence of very low amount of CNTs within the polyester resin blend stimulated an electrical conduction to the resulting nanocomposites. Furthermore, increasing CNT volume content gives a rise to the conductivity of the nanocomposites with MWCNTs and DWCNTs. However, regardless of type of CNTs, nanocomposites containing amino functionalized nanotubes possessed lower electrical conductivity compared to those with untreated CNTs. As an example, electrical conductivities of nanocomposites containing 0.247 and 0.149 vol. % of MWCNT-NH_2 are six and hundred times lower than those of nanocomposites with untreated CNTs. On the other hand, the conductivity of the nanocomposites containing 0.105 vol. % of DWCNT–NH_2 could not be measured because the value was not in the sensitivity range,

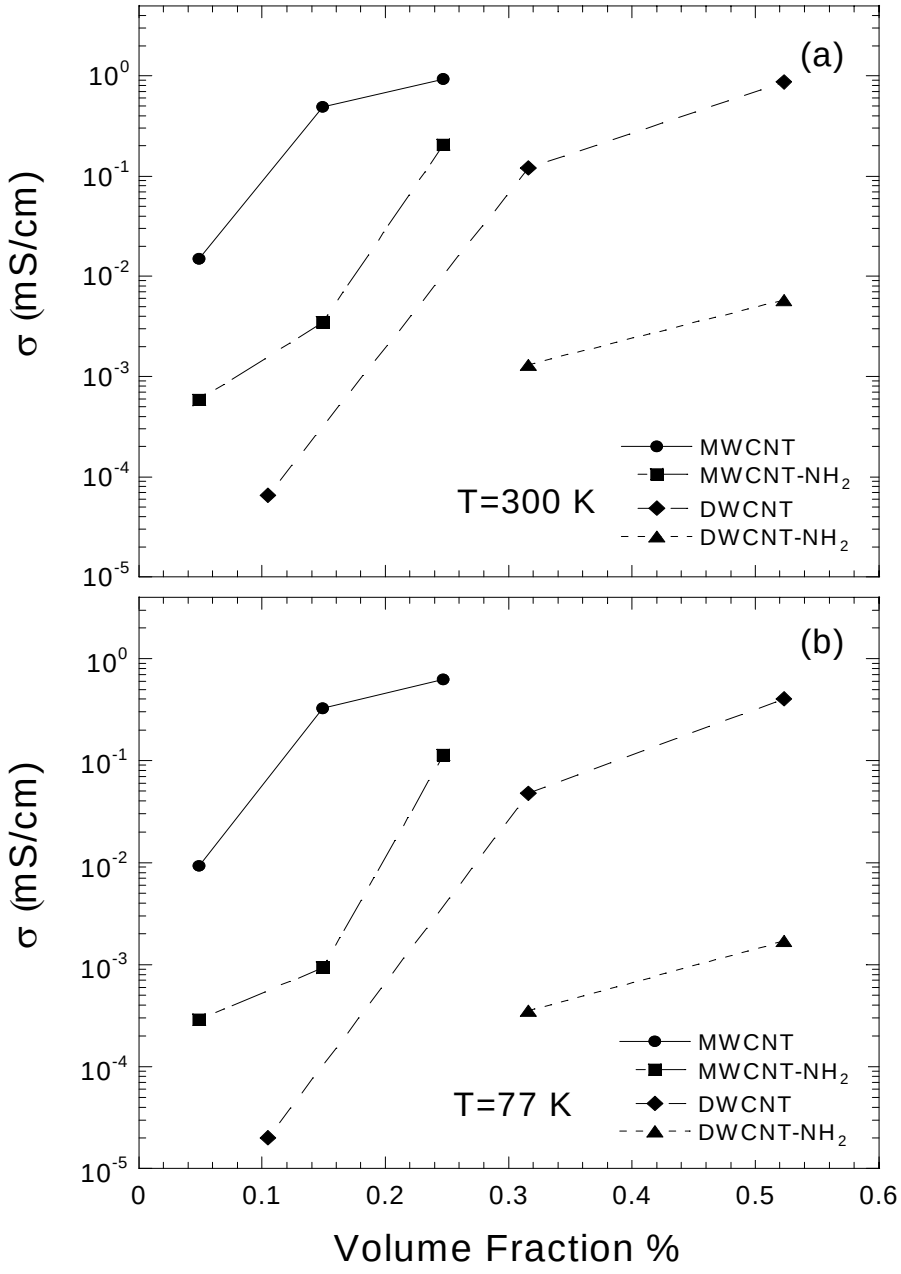

Figure 8.4.Electrical conductivity of two different types of CNT polymer nanocomposites with and without amine functional groups, including MWCNT and DWCNT with different volume content. (a) room temperature, (b) 77 K.

while those of the nanocomposites with 0.316 and 0.523 vol. % of DWCNT-NH_2 were easily obtained From theoretical point of view, depending upon volume fraction, the carbon nanotubes with relatively high densities are anticipated to possess the lowest percolation threshold, which is very proportional to our findings as well. On the other

hand, it was concluded that nanocomposites with the amino functionalized nanotubes have a higher percolation threshold than those with untreated nanotubes. These findings may be attributed to surface functionalization process. The amino groups are chemically attached onto the surfaces of CNTs via ball-milling process performed in ammonia solution by the manufacturer. During the process, the CNTs are broken in length and their aspect ratios are reduced to some extent. As a result, the percolation threshold, which is particularly interrelated to the aspect ratio and volume content of the tubes, shifted to higher filler contents for nanocomposites containing amino functionalized nanotubes. Moreover, incorporation of amine functional groups into a conjugated л-electron system as in the case of graphite structures like carbon nanotubes leads to formation of sp^3-carbons, which carry the functional groups. Thus, the consequent modifications in structure interrupt the conjugation and induce a distortion of the graphitic layer. When handled in term of electron conduction, sp^3- carbons are very likely to be considered as defects, which reduce drastically the maximum conductivity of the individual nanotube. In brief, functionalization of the CNTs is presumed detrimental for the overall conductivity of their final polymer based products. This is because a thin isolating polymer layer forms around the nanotubes as a consequence of improved interactions between CNTs and the polymer, which causes higher contact resistance to occur between CNTs. In other words, enhanced chemical interactions at the interface between CNTs and the polyester chains is very likely to occur with some chemical reactions between the polymer chains and amine groups over CNT surfaces, which raises the resistivity of the corresponding nanocomposites. However, it is a big challenge to monitor these complex reactions, including the interactions between styrene, polyester resins and amine functional groups due to complicated free radical polymerization of the corresponding resin systems. The intensive determination of these reactions and interactions were addressed in Chapter 5. However, we can safely say that amino groups over the surfaces of CNTs alter the chemical characteristics of the bulk matrix. This corresponding alteration may also play substantial role in the reduced electrical conductivity values observed for amino functionalized nanotubes.

The results obtained indicated that the variations in conductivity of nanocomposites containing DWCNTs are relatively larger than those with MWCNTs. This implies that DWCNTs need to be added into polyester resin blend at relatively high concentrations to achieve the same electrical conductivity of the nanocomposites containing MWCNTs. A relatively high tendency of DWCNTs for agglomeration

within the corresponding resin system due to their so pronounced large surface area may associate with higher resistivity of the nanocomposites with DWCNTs as compared to those with MWCNTs.

Figure 8.4b gives the conductivity values at 77 K. It was found that the conductivity of the samples at 77 K is one and half to three and half times lower than those of the samples at room temperature. Figure 8.5 shows normalized resistivity versus temperature curves of nanocomposites with MWCNT at 0.3 wt. % loadings. The data shown in the figure were taken from two different samples to evaluate the homogeneity of the nanocomposites. The samples exhibited a conductivity of 0.49 and 0.44 mS/cm at room temperature. As seen in the figure, both of the samples showed the same temperature dependence, as it is expected. A similar behavior was obtained for all the nanocomposites prepared with various CNT contents as well. So, the presented resistivity curves in this article are representative of the material properties. On the other hand, the maximum deviation of resistivity values was found to be 75% in nanocomposites containing 0.3 wt. % of DWCNT-NH_2. A relatively large deviation of the resistivity for this group of samples might be related with the reduced aspect ratios and higher agglomeration tendency of the DWCNT-NH_2 in the matrix, as discussed in detail previously. Another reason may be the altered chemistry of the resin system with presence of amine groups in the resin system.

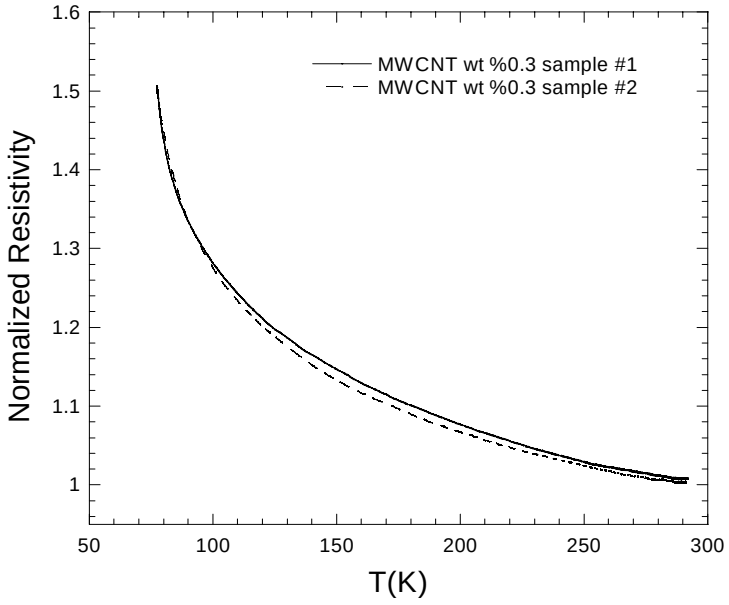

Figure 8.5. Normalized resistivity versus temperature of MWCNT 0.3 wt. % from two distinct samples.

Since DWCNTs have larger surface are than MWCNTs, it could be expected that DWCNTs may probably interact more with free radicals generated by decomposition of initiators than MWCNTs do. As a result, polymerization reaction in the system could be adversely affected, thus resulting in an inconsistency with local bulk properties across the cured system. This could explain the reason why much higher deviation of resistivity values was obtained from DWCNT-NH_2 modified nanocomposites compared to the other ones. Figure 8.6 shows the normalized resistivity versus temperature for MWCNT and DWCNT nanocomposites at various CNT contents with and without amine functional groups for comparison. The results of temperature dependence of resistivity showed that nanocomposites exhibited semiconductor like behavior regardless of the types of carbon nanotubes (MWCNT or DWCNT) or the presence of functional groups over the CNTs. On the other hand, the resistivity values exhibits very rapid increase below 100 K. A similar finding was reported in the literature that nanocomposites exhibit a valley in temperature dependence data (Sheng 1980). It was revealed that the metallic conduction is a dominant mechanism around room temperature while at low temperatures the tunneling becomes foremost in conduction mechanism. In our samples, we obtain only increasing resistivity with decreasing temperature, so tunneling is likely the dominant mechanism.

8.3.1.1 Tunneling Fit

The electrical conductivity mechanisms in CNT/polymer nanocomposites were investigated using various models in the literature; such as Luttinger liquid model (Bockrath, et al. 1999), one dimensional disordered wire model (Mischenko, et al. 2001), and fluctuation induced tunneling through the barriers between the metallic regions model (Kymakis and Amaratunga 2006, Astorga and Mendoza 2005, Jiang, et al. 2005, Mischenko, et al. 2001, Kymakis, et al. 2006). Of all these models, the fluctuation induced tunneling model (FITM) based on thermally activated voltage fluctuations across insulating gaps in disordered materials such as CNT/polymer nanocomposites was found to match best with our temperature dependent experimental data. In our nanocomposites, there are large conduction regions, i.e.; CNTs separated by small insulating barriers (polyester resin).

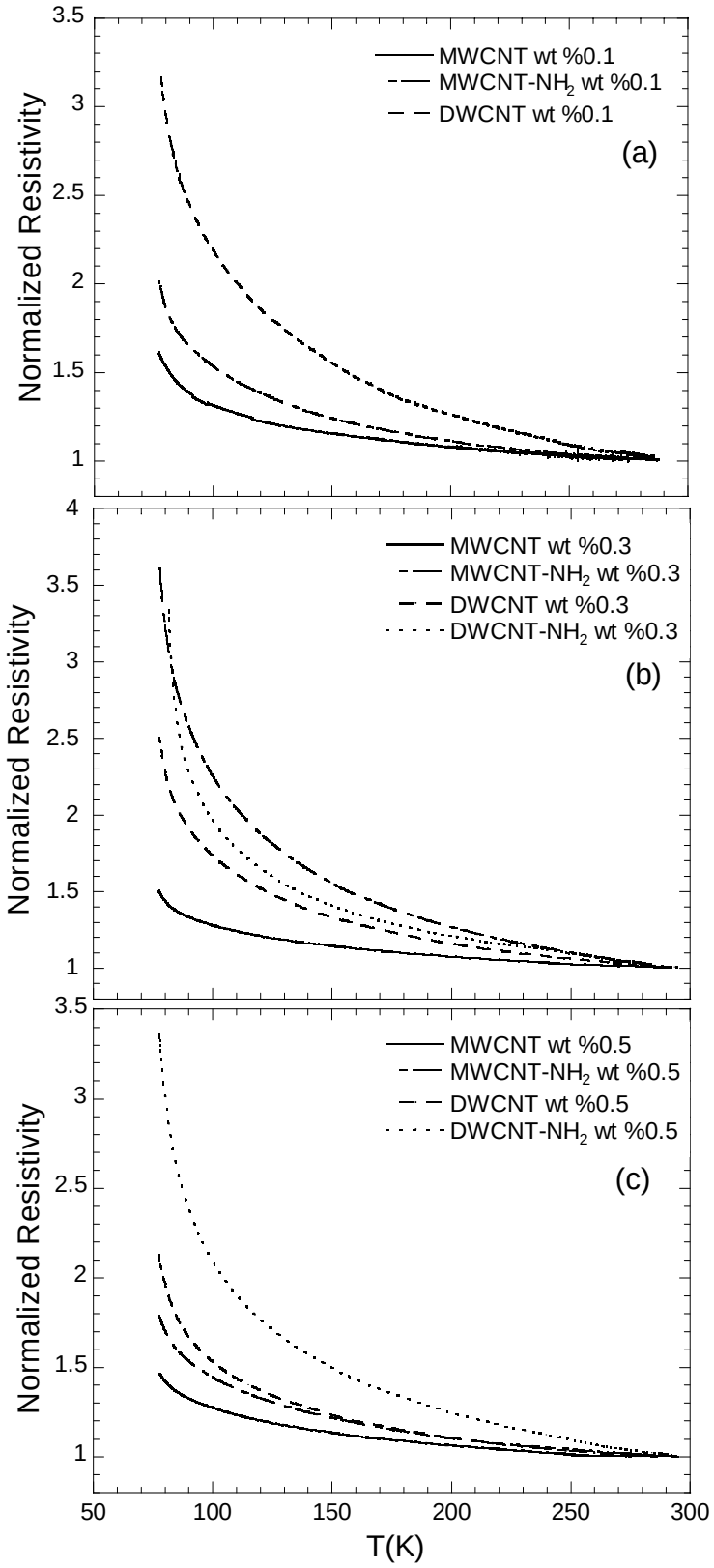

Figure 8.6. Normalized resistivity versus temperature of CNT polymer nanocomposites with various weight fractions (a) CNTs 0.1 wt% (b) CNTs 0.3 wt% (c) CNTs 0.5 wt.%.

The thickness and height of the tunneling barrier plays an important role in determining the temperature and magnetic field dependence of conductivity since electrons tunnel between insulator regions. In other words, the electron tunneling probability exponentially depends on the insulating barrier thickness changing with temperature. Also, it is known that that the degree of nonlinearity of tunneling current decreases as the temperature increases, due to narrowing of barrier by fluctuation. According to FITM the temperature dependence of electrical resistivity, ρ is given by the equation below (Sheng 1980).

$$\rho = \rho_0 \exp\left(\frac{T_t}{T_s + T}\right) \tag{8.2}$$

where ρ_o is the resistivity at $T >> T_t$ and T_s. In other words, at very high temperature resistivity is independent of temperature. In the equation, T_t is a measure of the energy required to move an electron across the insulating gap where magnitude of the thermal fluctuations become comparable to the magnitude of the tunneling barriers. T_s is a temperature much below which the resistivity reduces to temperature independent tunneling. T_t and T_s are the fitting parameters. They are predicted, using experimental data. Figures 8.7 (a) and (b) show the experimental results of temperature dependence of resistivity for nanocomposites prepared with DWCNT at 0.1 and 0.3 wt% loading rates in comparison with FITM predictions. The parameters T_t and T_s were found to be 132 and 8 K for nanocomposites with 0.1 wt% of DWCNT and 91 and 2 K for nanocomposites with 0.3 wt% of DWCNT. As seen in the figures, the FITM model fits well with the experimental data obtained at high temperatures; however, below 100 K a deviation becomes more visible from the fitting curve. A similar behavior was reported in the literature recently for single walled carbon nanotubes (SWCNTs)/polymer nanocomposites (Kymakis and Amaratunga 2006). Based on analysis of Figure 8.7 using FITM, temperature dependence of resistivity shows that above T_s=8 K thermally activated conduction over the barrier begin to occur. In addition, the change in resistivity above the temperature T_t=132 K begin to decrease because of reducing domination of charge carrier tunneling through the barrier. After this temperature, electron-electron and electron-phonon interactions begin to occur and contribute to resistivity. In general, resistivities predicted by these fit parameters correlates well with our experimental results at temperatures between 100 and 300 K.

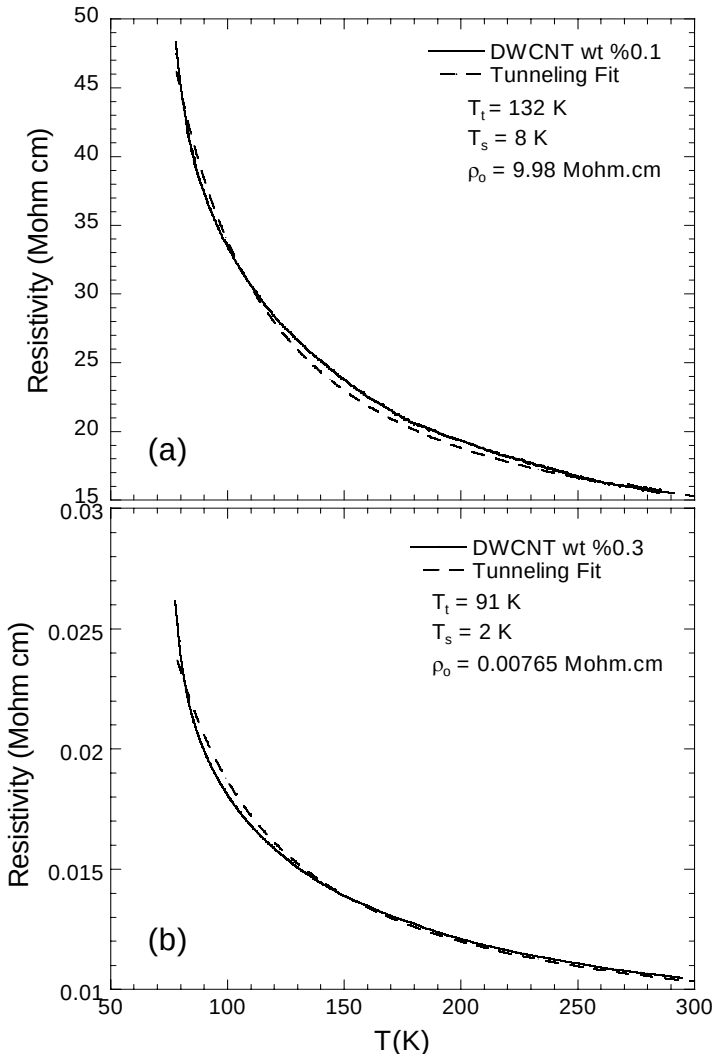

Figure 8.7. Temperature dependence of resistivity (solid lines) and FITM model fits (dashed lines) for (a) DWCNT %0.1 wt., (b) DWCNT %0.3 wt. The fits follow experimental data for high temperatures and there is a strong deviation at low temperatures.

However, they are not explicit values to form general aspect with respect to different filler content and attachment of amine functional groups over the surface.

Figures 8.8 (a) and (b) show temperature dependence of resistivity for the nanocomposites containing 0.3 wt. % of MWCNT with and without amine functional groups. The dashed lines represent FITM fits. The presence of amine functionalized nanotubes in the resin system increases T_t from 42 to 152 K, in which the tunnel barrier is increasing between the CNTs. Since CNTs with amine functional groups have higher T_t values than those without amine functional groups, the conduction is dominated by

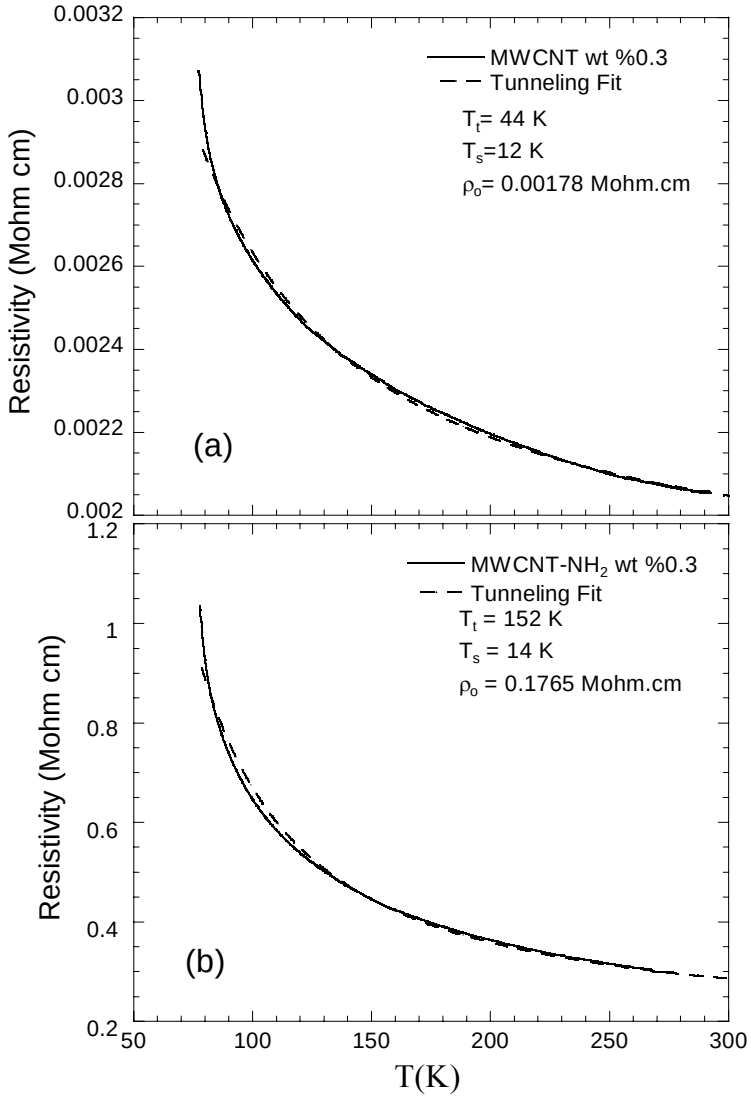

Figure 8.8. Temperature dependence of resistivity (solid lines) and FITM model fits (dashed lines) for (a) MWCNT %0.3 wt., (b) MWCNT-NH_2 %0.3 wt., T_t is considerably larger for functionalized CNT loadings.

tunneling of charge carriers for nanocomposites with amino functionalized CNTs at room temperature.

8.3.2. Room Temperature Electrical Conductivity of Nanocomposites

Figure 8.9 shows the specific conductivity of the nanocomposites containing randomly oriented CNTs as a function of weight content. Please note that vinylester - polyester resins were used as a matrix material in these measurements.

In principle, the percolation threshold, defined as the filler content to achieve a conductivity of 10^{-6} S/m, is observed to be lower for fiber-shaped fillers than for spherical ones (Sandler, et al. 2003). As seen in the figure, in general, nanocomposites with NH_2 functionalized CNTs showed lower electrical conductivity values than nanocomposites with untreated ones. In addition, the lowest percolation threshold (below 0.05 wt. %) was observed for MWCNTs. On the other hand, the percolation threshold value for DWCNTs was found to be in the range of 0.05 and 0.1 wt. %.

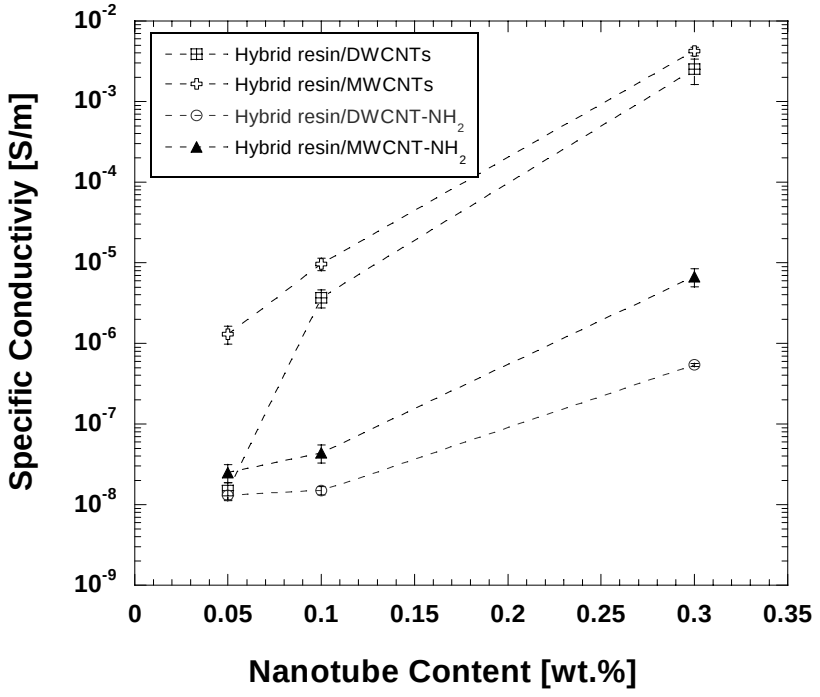

Figure 8.9. The specific conductivity of the nanocomposites containing randomly oriented CNTs as a function of weight content.

As a result, the NH_2 functionalized CNTs seemed to show percolation threshold at much higher concentrations than given in this study. This is due to the presence of amino-groups grafted onto the surfaces of CNTs. Introduction of amine functional groups disturbed the graphitic structure of CNTs and reduced the conductivity of the tubes by forming an electrically insulating layer between CNTs and the matrix resin, enhancing the compatibility in between (Simsek, et al. 2007). As a result, the percolation threshold, which is highly related to the aspect ratio, shifted to higher values

for NH_2 functionalized CNTs, as earlier discussed in details in this chapter (Prasse, et al. 2003, Martin, et al. 2004).

8.3.3. Electrical Conductivity of Nanocomposites Containing Aligned CNTs

On behalf of the results obtained from Figure 8.9, MWCNTs emerged as the most promising candidate that induced the highest electrical conductivity to the hybrid polymer matrix. Therefore, MWCNTs were used as filler constituents in the further experiments aimed to accomplish the aligned CNTs in nanocomposites with the application of AC electric field. Figure 8.10 shows the typical specific conductivity of the nanocomposites cured with application of the AC electric field with respect to frequency on a log-log scale in the directions parallel and perpendicular to the electric field.

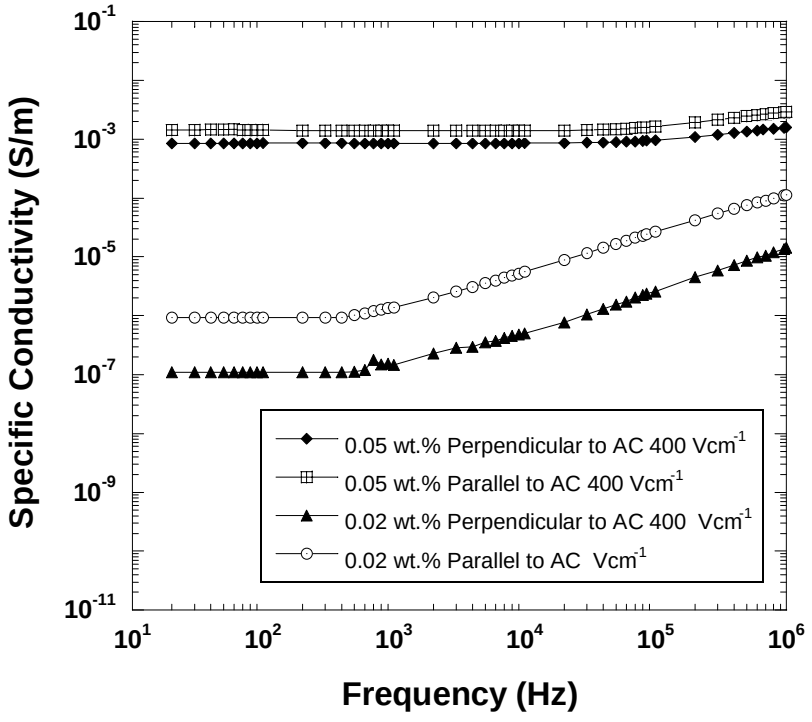

Figure 8.10. Typical specific conductivity of the nanocomposites cured with application of the AC electric field with respect to frequency on a log-log scale in the directions parallel and perpendicular to the electric field.

Note that the nanocomposites containing 0.005 wt.% of MWCNTs shows typical dielectric behavior like pure neat hybrid resin such that its electrical conductivity steadily increase on the log-log scale. The samples with 0.05 wt. % of MWCNTs, exposed to the given AC electric field, showed a frequency independent electrical conductivity. However, samples with 0.02 wt. % of MWCNTs have a similar response up to a specific knee frequency, above which a transition to dielectric behavior was observed. Furthermore, nanocomposites with 0.02 wt. % of MWCNTs were observed to exhibit almost an order of magnitude higher conductivity parallel to AC field than perpendicular to AC field. In the same manner, nanocomposites containing 0.05 wt. % of MWCNTs showed slightly higher conductivity parallel to AC field than perpendicular to AC field. These findings can be regarded as ample evidence for achievement of anisotropy in the resultant nanocomposites. Moreover, at 0.05 wt. % concentration, conductivity of the nanocomposites (10-6 S/m as seen in Figure 9) cured without application of AC electric field is about three orders of magnitude lower as compared to that (10-3 S/m as seen in Figure 10) of the nanocomposites cured with application of the AC electric field. This implies that the AC electric field applied during curing may alter the orientation, size and array of CNTs agglomerates to some extent, thus reducing percolation threshold value of the resultant nanocomposites.

Figure 8.11 a and b show the optical micrographs of thin polished film samples sectioned from composites containing 0.05 wt. % of MWCNTs, cured with and without application of the AC electric field, respectively. Note that there is a slight variation in thickness of the samples due to polishing, which leads to a change in contrast in micrographs. As seen in Figure 4 a, uniform and partially aligned CNTs were observed in the composites cured with application of the AC electric field. On the other hand, relatively large CNT agglomerates with inhomogeneous distribution are visible within the composites cured without application of the AC electric field, as depicted in Figure 4b. Martin et al. (2004) pointed out that polarization of CNTs in an electric field leads to an additional attractive interaction between individual nanotubes and existing nanotubes bundles, which is of great importance in characteristics of conductive network formed within the surrounding matrix resin. During the cutting, the tubes may have displayed an alignment along the cutting direction. Ajayan et al. (1994) showed, based on the results of TEM image analysis, that longer and thinner nanotubes were oriented, while the thicker and shorter ones were randomly dispersed within thermosetting polymer matrices.

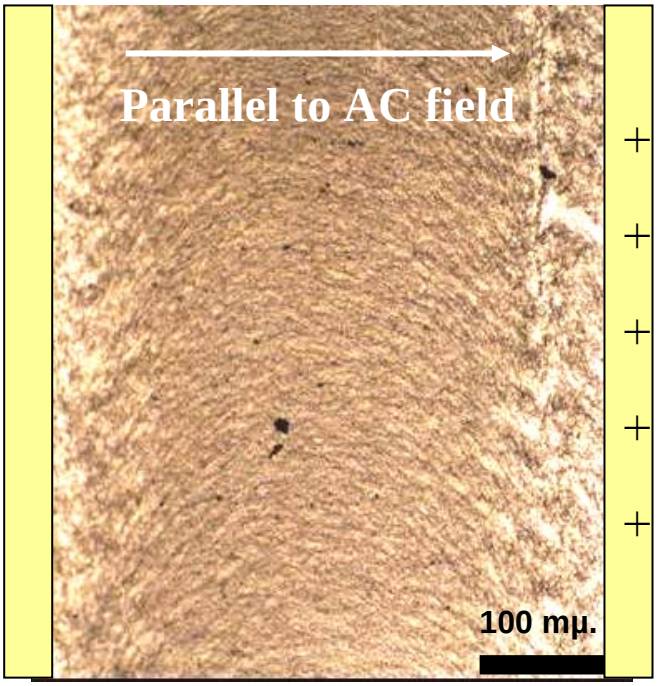

a)

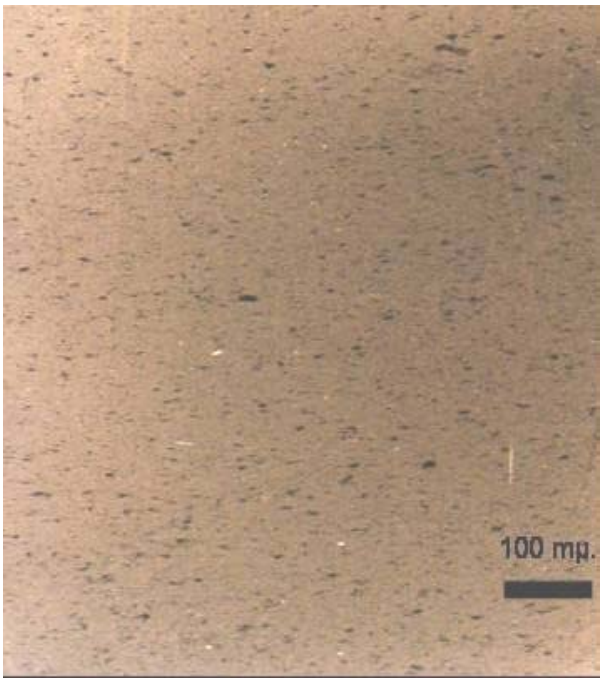

b)

Figure 8.11. The optical micrographs of thin polished film samples sectioned from composites containing 0.05 wt. % of MWCNTs, (a) cured with and (b) without application of the AC electric field.

They ascribed this behavior to the action of the directional cutting that created shear within the material such that the tubes in contact with the knife were pulled out or deformed from the matrix and showed preferred orientation.

On the other hand, aligned and polarized CNTs may have had profound effects upon entanglements of polymer chains during free radical polymerization, affecting the distribution of radicals generated by decomposition of initiators in a different manner compared to room temperature curing. Therefore, it is reasonable investigate the thermal response of the CNT modified composites cured with and without application of the AC electric field in a comparative manner. This issue will be highlighted in the following section.

8.3.3.1. DSC results

Figure 8.12 depicts the measured T_g of the neat hybrid polymer and their composites containing 0.05 wt. % of AC field induced aligned and randomly oriented MWCNTs. As a result, it was found that there was almost no significant change in the T_g values between neat polymer matrix and composites cured without application of the AC electric field. However, composites containing aligned MWCNTs were observed to exhibit relatively high T_g value (107 ^oC), which corresponds to an improvement by about 10 % as compared to neat hybrid polymer. Gryschuck et al. (2006) reported that MWCNTs, depending on their surface area and aspect ratio, may have some adverse effects on the chemical reactions during free-radical polymerization of vinylester resin. They emphasized that the amount of accelerator and initiator to be added into the resin suspensions with CNTs may need to be accordingly optimized. They additionally concluded that nanotubes with higher aspect ratio would be more beneficial to the ultimate performance of brittle polymers such as vinylester. In a similar manner, Peng, et al. (Peng, et al. 2003) showed that free radicals released by the initiator (MEKP) are partially trapped within the galleries of carbon nanotubes during room temperature curing, which impedes the polymerization reaction to some extent, thus reducing the cross-linking density of the final product. Zhu et al. (2007) concluded that, in the presence of CNTs, the type of initiators used for room temperature and elevated temperature curing may have substantial effects on the chemistry of the resulting cured

products. In fact, free radicals are charged particles and may be capable of moving across the AC electric field. From that point of view, the application of AC electric field during curing of the resin suspensions may alter free-radical polymerization to some extent.

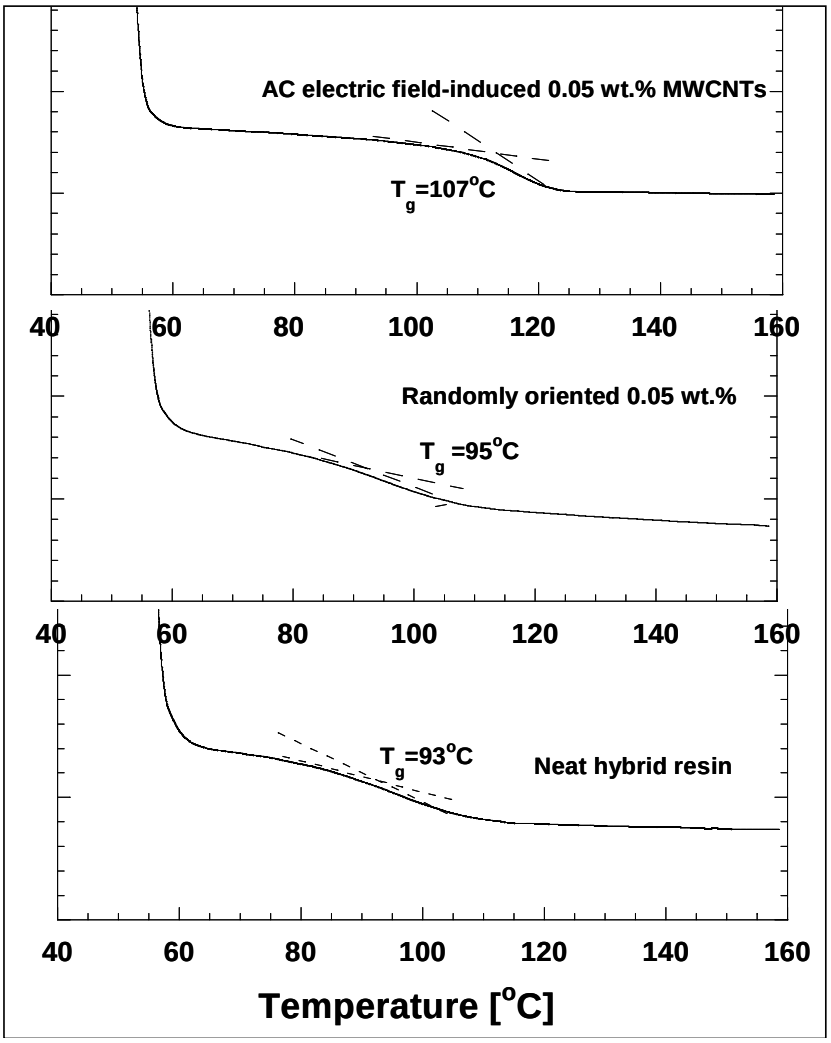

Figure 8.12. The measured T_g of the neat hybrid resin and their nanocomposites containing 0.05 wt. % of AC field induced aligned and randomly oriented MWCNTs.

In the most probable scenario, the radicals trapped within the galleries of CNTs were encouraged by AC electric field to move, recombine and terminate with another nearby radical, thus contributing to the ongoing chain polymerization. In other words, thanks to the applied AC electric field, CNTs discontinue to act as inhibitors which react with radicals and convert them to lower reactivity species that do not react any more.

In brief, it was found, based on the DSC measurements, that reorientation of larger CNT agglomerates as well as alignment of individual CNTs bring a synergy to the resultant composites. In other words, we could make an assumption that the enhancement observed for T_g values of the nanocomposites containing AC induced aligned CNTs comes from the competing effects of the heat evolved form the brass plates with application of AC electric field during curing and partially alignment of CNTs in the resin system under AC electric field. Moreover, the improved T_g values of aligned CNT modified nanocomposites support our claim that CNTs were partially aligned under AC field, as seen in Figure 8.11 a.

8.4. Conclusions

Polyester based nanocomposites (produced by the second approach) containing CNTs with amine functional groups exhibited lower electrical conductivity as compared to those with untreated ones. These findings were attributed to surface functionalization process in which the amino groups are chemically attached onto the surfaces of CNTs. During the process, the aspect ratio of the CNTs is reduced and the distortion of the graphitic structure which leads to the reduced conductivity is expected to occur. Moreover, the presence of the amine groups over the CNT surfaces may react with the polymer chains and form an electrically thin insulating layer, which may act as a barrier between the individual tubes and increases the resistivity of the nanocomposites.

Electrical conductivity of nanocomposites with MWCNT was obtained to be higher than those with DWCNTs at the same loading rate due to relatively higher tendency of DWCNTs for agglomeration within the corresponding resin system.

The results of temperature dependence of resistivity showed that nanocomposites exhibited semiconductor like behavior regardless of the types of carbon nanotubes (MWCNT or DWCNT) or the presence of functional groups over the CNTs. Also, we obtain only increasing resistivity with decreasing temperature, so tunneling is likely the dominant mechanism.

It was observed the results predicted by the fluctuation induced tunneling model were in very good agreement with those experimentally obtained temperature dependence of resistivity. The parameters T_t, T_s and ρ_0 were found for each CNT/polymer nanocomposites based on the model.

Room temperature electrical properties of the CNT modified vinylester polyester composites cured with and without application of AC electric field were also investigated by means of an impedance dielectric spectroscopy. Consequently, the composites with amino functionalized CNTs were found to exhibit lower electrical conductivity than those with untreated CNTs. At each given concentration, the highest electrical conductivities were achieved in composites prepared with untreated MWCNTs as in the case polyester based nanocomposites. MWCNTs was then selected as the most appropriate filler and resin suspensions were prepared with 0.005, 0.02 and 0.05 wt. % of MWCNTs to align the tubes within matrix resin with application of the AC electric field during curing. Based upon optical microscopy investigation and electrical conductivity measurements, it was revealed that partial alignment of CNTs within polymer matrix was achieved by AC electric field. Furthermore, T_g values of the composites cured with and without application of the AC electric field were measured via DSC to reflect the effect of the electrical inducement on the thermal properties of the composites. As a result, composites with aligned MWCNTs were found to demonstrate higher T_g value than neat hybrid polymer and composites with similar content of randomly oriented MWCNTs. The synergetic effect observed in the T_g values of the composites cured with the application of AC electric field was attributed to the interactions between the charged free radicals and the aligned CNTs within the resin system.

Overall, it can be concluded that, regardless of matrix types (polyester based or vinylester polyester hybrid resin), of all, the MWCNTs is the most appropriate nanotube to stimulate electrical conductivity to the isolating polymer matrix.

CHAPTER 9

AN APPLICATION: CNT MODIFIED GLASS FIBER REINFORCED COMPOSITES

In the previous chapters, novel processing routes to prepare CNT modified polyester and vinylester based resin suspensions were developed. In particular, CNTs were reported to possess electrically conductive polymer systems with retained mechanical properties. Of all, MWCNTs emerged as the most appropriate filler candidate. Regardless of amine functional groups, incorporation of MWCNTs enhanced the electrical, mechanical and thermal properties of the hybrid polymer. With the addition of CNTs, average toughness values of the hybrid polymer were improved by almost 30 %. MWCNTs were found to be highly capable of stimulating electrical conductivity to the non-conductive polymer system without reducing its mechanical properties. As a result, it seems to be beneficial to use a MWCNT modified resins as the matrix polymer with high performance conventional fiber reinforcements such as glass fibers. It was attempted to prepare novel electrically conductive multi-functional composites. On behalf of this purpose, in this chapter, the utilization of CNT modified hybrid resin suspensions as matrix for long glass fiber reinforcements was pinpointed. For this purpose, CNT modified composite laminates were manufactured, using Vacuum Assisted Resin Transfer Molding (VARTM) and Resin Transfer Molding (RTM) techniques. The extent of enhancement in the matrix dominated mechanical properties of VARTM processed glass fiber reinforced composite laminates with very low content (0.1 wt.%) of amino functionalized CNTs was investigated. In addition, fiber dominated properties of RTM processed laminates with relatively high content (0.3 wt. %) of CNTs were undertaken. In addition, electrical conductivity measurements were carried out on the RTM processed CNT modified laminates. Accomplishment of homogenous distribution of electrical conductivity across the composite panel promises that CNTs would be used as distributed sensors to detect onset, nature and evolution of damages that occur within the CNT modified laminates. Application of such composite materials would shed light on accurate detection of any relevant damage in the corresponding composite parts during their service life. At a first glance, composite

parts used in wind energy turbines and in aviation sector seem to be ideal candidate for such demonstration.

9.1. Introduction

Fiber reinforced polymer composites have gained substantial attention as structural engineering materials in automotive, marine and aircraft industry as well as in civil engineering applications (Tanoglu and Seyhan 2003, Gojny and Schulte 2004). This interest is due to their outstanding mechanical properties, impact resistance, high durability and flexibility in design capabilities and light weight. These composites have generally good fiber dominated in-plane properties capable of meeting the design requirements for various types of structural applications. However, Z-axis (through the thickness) properties of the composites, such as delamination resistance, have often been far below the expectations due to inadequate performance of the matrix dominated interlaminar region (Wichmann, et al. 2006, Zhu, et al. 2007) Therefore, in some special applications, these materials may exhibit lower overall structural integrity in accordance with their presumed properties. Delamination has the potential for being the major life limiting failure process. It may even occur during processing of the laminates due to contamination or regions of high void content of prepreg that leads to poor ply adhesion locally (Lee 1997, Albertsen, et al. 1995, Srivastana, et al. 1998). In general, delamination corresponds to a crack-like discontinuity between the plies and it may typically extend during application of mechanical or thermal loads or both during service life of composites (Wichmann, et al. 2006, Tanoglu and Seyhan 2003). Fracture toughness of polymer matrix and interfacial shear strength between the matrix and the fiber are of prime importance in monitoring through the thickness properties of the composites. The most common way to improve the delamination resistance of reinforced polymer composites is to incorporate some toughening agents or thermoplastic binders into the brittle matrix resins, such as epoxy, polyester or vinylester (Alveraz, et al. 2003, Tanoglu and Seyhan 2003). A treatment of fiber surface with matrix resin compatible sizing is another way to improve the interlaminar strength of the composites by enhancing the interfacial strength between the polymer matrix and the fiber. However, some of these modifications induce sometimes a compromise with other mechanical properties.

The incorporation of nano-sized fillers into polymer matrices offers the potential to accomplish nanocomposites with better mechanical properties as compared to composites containing traditional macro-scale sized fillers. In this manner, carbon nanotubes (CNTs) have gained relatively high interest as alternative filler materials for the modification of polymers, owing to their extraordinary mechanical, thermal and electrical properties, combined with their huge aspect ratio and specific surface area (SSA) (Fiedler, et al. 2006, Gojny, et al. 2005a, Simsek, et al. 2007). Gojny, et al. (Gojny, et al. 2004) found that 3-roll milling processed epoxy based nanocomposites containing 0.3 wt. % of amino functionalized double walled carbon nanotubes (DWCNT-NH_2) exhibited 42 % higher fracture toughness values as compared to neat epoxy resin, while retaining their tensile strength and modulus values. Thus, it is reasonable to merge the carbon nanotubes, which improve strength, stiffness and toughness of the polymer matrix resin, with high performance long fibers. As explained in the very beginning of this chapter, it would be a good point of view when CNT modified polymer resins are used as matrix materials to produce fabric reinforced structures. At this point, use of CNT modified matrix resin with fiber reinforcements is expected to tailor the matrix resin dominated mechanical properties (Z-direction) of the resultant glass fiber reinforced composites (Gojny 2006, Alveraz, et al. 2003, Zhu, et al. 2007).

Gojny, et al. (Gojny, et al. 2005b) showed that interlaminar shear strengths (ILSS) of glass fiber / 0.3 wt. % DWCNT-NH_2 modified epoxy matrix composites is 19 % higher than those of glass fiber / neat epoxy composites. Similar finding was also reported by Wichmann, et al. (Wichmann, et. al. 2006) such that the interlaminar strength of glass fiber reinforced composites with nano-particle modified epoxy matrix were significantly improved (16 %) with addition of only 0.3 wt. % of DWCNTs. However, they also stated that interlaminar fracture toughness values of the corresponding composites were, astonishingly, not affected in comparable manner. In brief, enhancement in fracture toughness of the matrix resin due to CNTs addition seems to be beneficial for the improvement of the matrix dominated mechanical properties such as interlaminar shear strength and fracture toughness of their associated long fiber reinforced composites. For this purpose, interlaminar fracture toughness (G_{Ic} and G_{IIc}) and the interlaminar shear strength of glass fiber non-crimp fabrics / VARTM processed CNT modified vinylester polyester based composites were investigated in conjunction with the values of the base composite laminates prepared with neat hybrid

resin. The enhancement in the tensile mechanical properties of the RTM processed glass fiber reinforced composites was also discussed with an emphasis on the distribution of CNTs within the glass fabric.

9.2. Experimental

9.2.1. Materials

Two layers of non-crimp glass fabrics (NCFs) with a $[-45^o / 90^o / +45^o / 0^o]_s$ stacking sequence from TELETEKS, Istanbul, Turkey, were employed as reinforcement to accomplish the composite laminates. Note that this stacking sequence was selected because interlaminar fracture tests are restricted in unidirectional $[0]_n$ composite laminates in which a delamination propagates between the plies all along the fiber direction appropriate to the coplanar assumption in fracture analysis (Tanoglu and Seyhan 2003, Alveraz, et al. 2003). The vinylester / polyester hybrid resin suspensions (at least 500 gr.) were prepared via 3-roll milling based on the same procedure as in the preparation of the nanocomposites.

9.2.2. Manufacturing of CNT Modified Glass Fiber Reinforced Composites

CNT modified composite laminates were produced using, two different sophisticated manufacturing methods including Vacuum Assisted Resin Transfer Molding (VARTM) and Resin Transfer Molding (RTM). In this manner, glass fiber reinforced composite laminates modified with 0.1 wt. % of MWCNT-NH_2 and 0.3 wt. % of MWCNTs were manufactured via VARTM and RTM methods, respectively.

9.2.2.1. Vacuum Assisted Resin Transfer Molding (VARTM)

Composite laminates (with about 42% fiber volume fraction) with 0.1 wt. % of MWCNT-NH_2 were manufactured using VARTM technique. In this technique, preforms were placed on a flat tool coated with a release agent in order to ease the

peeling of the composite part at the end (Tanoglu and Seyhan 2003, Seyhan, et al. 2008). Preforms were then vacuum-infiltrated with the CNT modified resin suspensions. Figure 9.1 depicts the schematic of the VARTM process and the catalyzed resin infiltrated composite parts allowed to cure at room temperature under vacuum. The cured parts were demolded and subsequently subjected to post-curing at 120°C for 2 hours. For the preparation of DCB and ENF specimens, a polyamide film was inserted in the mid-plane of the fabrics as a crack initiator prior to processing of the real composite parts.

9.2.2.2. Resin Transfer Molding (RTM)

Composite laminates with 0.3 wt. % of MWCNTs were manufactured, using RTM technique. Despite a slight increase in viscosity, composite laminates having a size of 21 x 36 cm, (with about 60 % fiber volume fraction) with and without CNT modification were successfully accomplished. Figure 9.2 gives the photos of cut fabric pre-form placed into mold prior to infusion and the set up of resin injection system. Following the placement of perform into the mold, the mold assembled of two brass plates was closed, sealed and subjected to a pressing force. Applying low pressure, the resin was forced to fill the mold through the injection ports. Once the resin injection was terminated, the infiltrated laminates were allowed to cure at room temperature under load for 2 h. The parts were then demolded and subsequently subjected to post curing at 120°C for 2h. Please note that the flow characteristic of the CNT modified resin suspensions is significantly different under VARTM and RTM processes due to the distinct flow boundaries of each process. For instance, laminates with 0.3 wt. % of MWCNTs would not be produced via VARTM technique. This is because the viscosity of the resin suspension would be too high to fill the entire glass fabric preform by means of a vacuum pump within the intended time.

As elucidated under previous section, 0.3 wt. % is a rheological threshold at which the viscosity of the resin suspensions significantly increases. This may lead to processing problems with VARTM configuration. However, in the case of RTM technique, the pressure difference applied between the source and the trap is high enough to compensate for the resistance of the resin suspensions to flow. As a result, the fibers are wet out with the CNT modified resin suspension, homogenously.

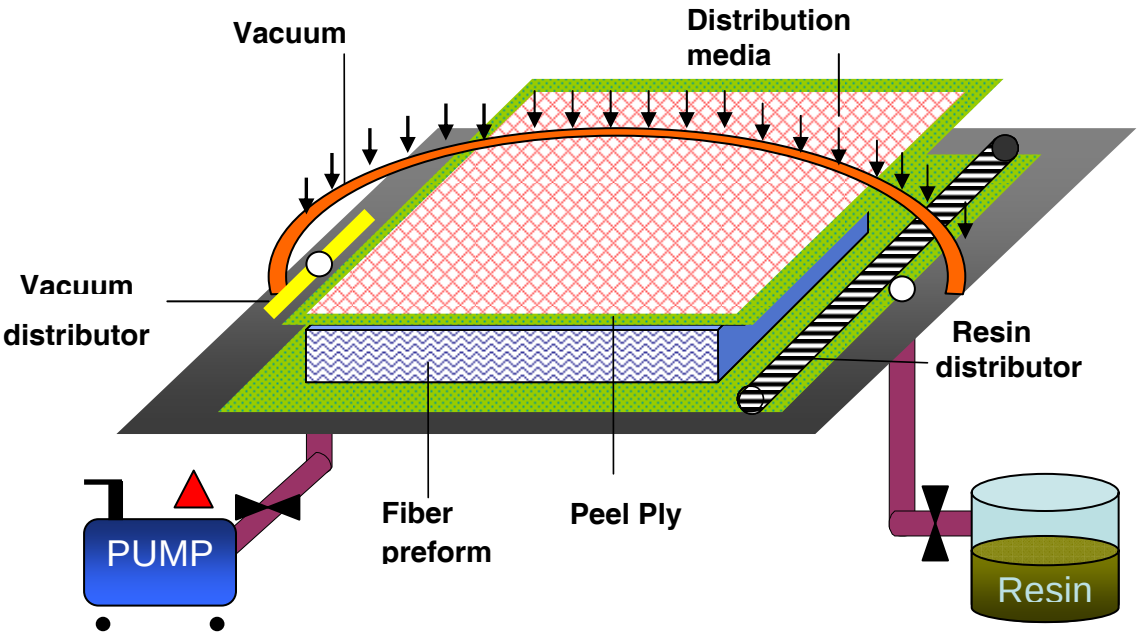

a)

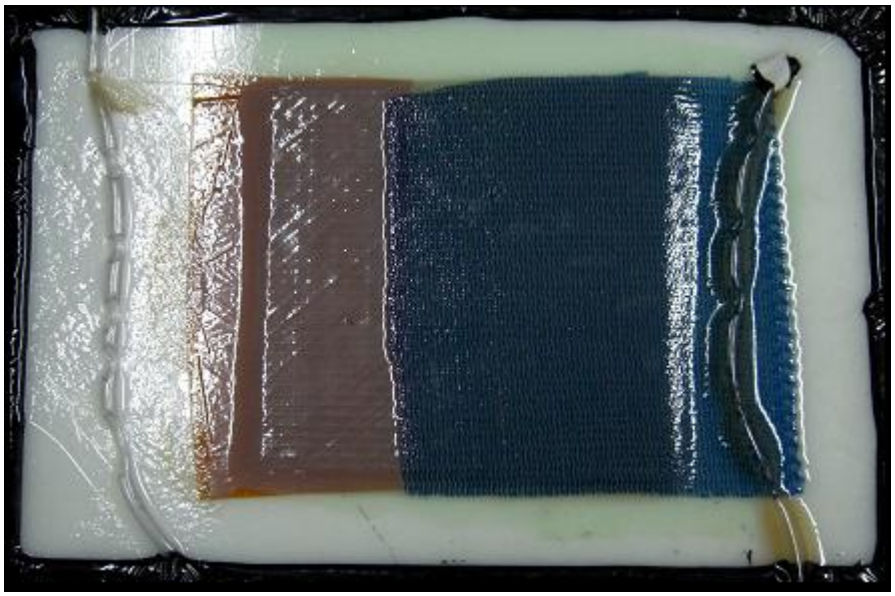

b)

Figure 9.1. a) The schematic of the VARTM process and b) the catalyzed resin infiltrated composite parts allowed to cure at room temperature under vacuum.

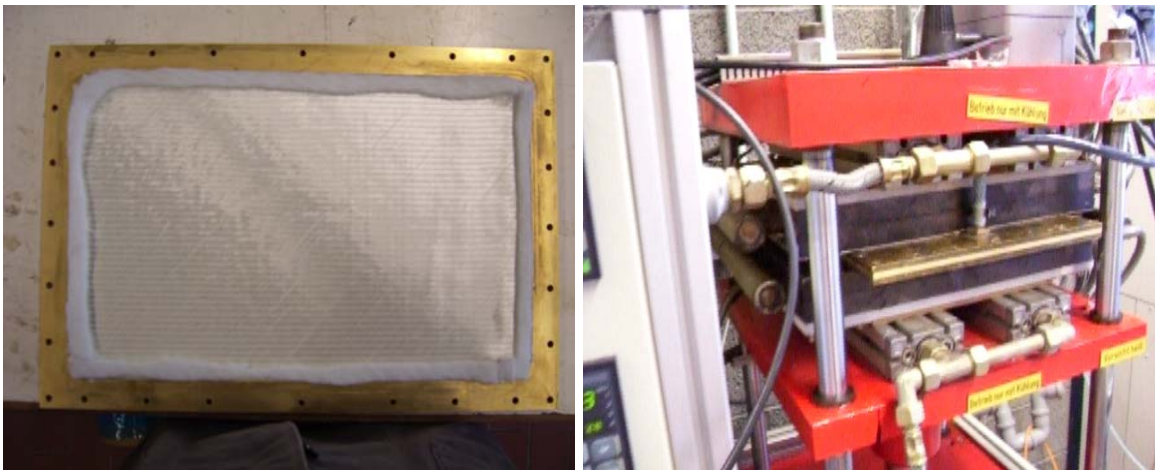

Figure 9.2. The photos of cut fabric pre-form placed into mold and the resin injection system.

9.2.3.Mechanical Characterization of CNT Modified Glass Fiber Reinforced Composites

Several different mechanical properties of VARTM and RTM processed laminates with and without CNT modification were evaluated with a particular emphasis on the effect of presence of CNTs between fiber bundles and their distribution across the part.

9.2.3.1. Double Cantilever Beam Test (DCB)

Mode I interlaminar fracture toughness (G_{Ic}) of the base and the CNT modified composite laminates was measured based on DCB test. The DCB specimens were sectioned from the VARTM processed composite laminates with the length of 180 mm and a width of 25 mm, using a diamond saw. Aluminum loading blocks were bonded to each side of the specimens such that the initial crack length, a_o, was set to 50 mm with reference to the inserted thin polyamide film. Figure 9.3 shows a typical DCB test specimen and a photo under load during testing. The DCB specimens were tested at a crosshead speed of 5 mm/min using a Schimadzu test machine with 5 kN loading cell. At least 5 specimens were tested to evaluate the interlaminar response of the composite laminates with and without CNT modification. The experimental fracture data were

recorded in the form of complete load/ displacement curve as well as load / point displacement values which correspond to crack extension length.

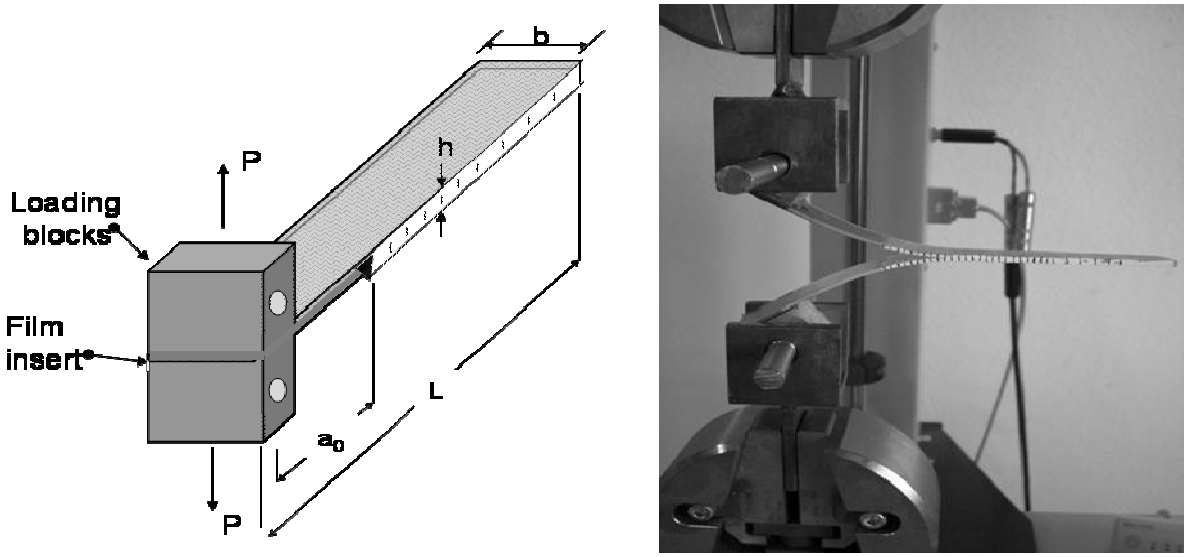

Figure 9.3. A typical DCB test specimen and a photo under load during testing.

The critical strain energy release rate *(G_c)* was computed based on the general formula from linear elastic fracture mechanics (LEFM), as follows;

$$G_c = \frac{P_c^2}{2b}\frac{\partial C}{\partial a} = \frac{P_c \delta}{2bC}\frac{\partial C}{\partial a} \tag{9.1}$$

Where P_c is the critical load at which the crack propagates, b is the width of the specimen, C is the compliance, δ is the displacement and a is the crack length.

The simple beam theory was then used to obtain the relationship between compliance and the crack length for a perfectly clamped at delamination front double cantilever beam. The equation (1) then becomes as the following (ASTM 2001a, Albertsen, et al. 1995).

$$G_{Ic} = \frac{3P\delta}{2ba} \tag{9.2}$$

In practice, this expression overshoots the G values because the relationship above is only valid for the ideal conditions assumed in the beam theory. In reality, correction is needed for large displacements, shear deformation, the stiffening effect of the end tabs, and for displacement and rotation at the delamination front (ASTM 2001a, Tanoglu and Seyhan 2003). Some of these effects can be excluded by correcting the crack length. The crack length correction, Δ for each specimen is determined by plotting the cube root of the compliance, (C) as a function of delamination length. This gives a straight line which intersects the crack length axis at - Δ. Note that the compliance, C is the ratio of load point displacement to its corresponding applied load (δ /*P*). G_{Ic} values were then calculated based on the corrected LEFM (modified beam theory) formula using the equation below (Tanoglu and Seyhan 2003, Albertsen, et al. 1995);

$$G_{Ic} = \frac{3P_c\delta}{2b(a+|\Delta|)} \tag{9.3}$$

9.2.3.2. End notched flexure test (ENF)

The purpose of the ENF test was to determine the critical strain energy release rate in pure Mode II loading (G_{IIc}) of unidirectional composites. The ENF specimens were prepared in 120 mm long and 20 to 25 mm wide. This test was performed in a three point bend fixture with a span length of 100 mm. Figure 9.4 shows the ENF specimen geometry parameters and ENF specimen under load. The specimens were placed onto supports in such a way that the crack length-to-half span ratio (a/L) is 0.5 at propagation of the crack. The load was applied with a displacement control of 1 mm/min. (Alveraz, et al. 2003, Albertsen, et al. 1995). At least 5 specimens were tested for ach type. The ENF specimen produces shear loading at the crack tip without introducing excessive friction between the crack surfaces.

However, the crack propagation is inherently unstable under displacement control. During the experiment, the load versus cross head displacement was recorded. Once the crack starts propagating, a sudden load drop was observed and the test was terminated. The ultimate load recorded and its corresponding point beam deflection measured from the cross head displacement corrected for the machine compliance were used in the data reduction.

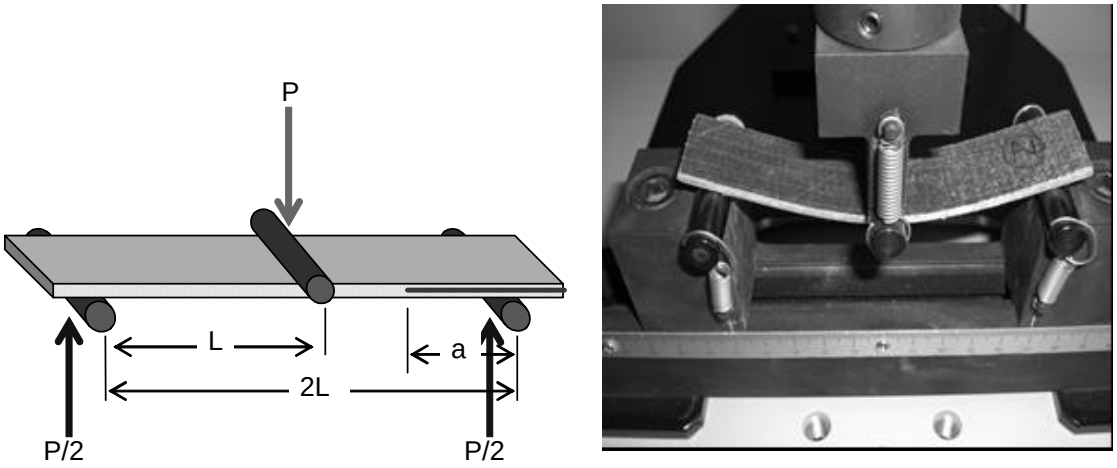

Figure 9.4. The ENF specimen geometry parameters and ENF specimen under load.

Simple beam theory allows the calculation of the compliance, C, which can be expressed for a ENF specimen as below (Albertsen, et al. 1995);

$$C = \frac{2L^3 + 3a^3}{8E_1 bh^3} \tag{9.4}$$

where E_1 is the flexural modulus and h is one half the total thickness of the beam, (in other words, the thickness of each sub-beam of the delaminated region). If C value is inserted into the Equation 1, the strain energy release rate for an ENF specimen can be obtained as follows;

$$G_{IIc} = \frac{9P_c^{\,2}a^2}{16\mathrm{E}_1 b^2 h^3} = \frac{9P_c^{\,2}Ca^2}{2b(2L^3 + 3a^3)} \tag{9.5}$$

C is also the ratio of load point displacement to its corresponding applied load (δ/P). G_{IIc} can be finally rewritten as in the equation below (Lee. 1997, Lee, et al. 2000, Albertsen, et al. 1995, Alveraz, et al. 2003).

$$G_{IIc} = \frac{9P_c \delta\, a^2}{2b(2L^3 + 3a^3)} \tag{9.6}$$

9.2.3.3. Short Beam Shear Test

The interlaminar shear strength (ILSS) of the base and CNT modified composite laminates was measured using the short beam shear (SBS) test method (ASTM 2001b). This test method involves loading a beam under three-point bending in such a way that an interlaminar failure is induced along the mid-plane rather than a tensile failure on the bottom surface of the beam. In this manner, the specimens of 21 mm in length and 10 mm in width were sectioned from the composite laminates. The length to thickness ratio and span to thickness ratio were kept constant at 7 and 5, respectively. The crosshead speed was set to 5 mm/min. At least six specimens from each set were tested using universal testing machine with 5 kN loading cell and load at break was recorded. The interlaminar shear strength (τ_{max}) was calculated based on the Equation given below.

$$\tau_{\max} = 0.75\frac{P}{bd} \tag{9.7}$$

where P is the maximum applied load, b is the width and d is the thickness of the specimens.

9.2.3.4. Tensile test

The specimens sectioned from RTM processed glass fiber reinforced composites with and without CNT modification were tested by tensile testing in 0 and 90 direction using a Schimadzu servohydraulic testing machine according to DIN EN/ ISO 527/3. In this manner, the end tabbed specimens, having dimensions of 250x25x3 mm. were fixed between the grips of the machine.

9.2.3.5. Microscopic investigation

A Nikon Optical microscopy was used to evaluate the distribution of CNTs across the composite part. Philips SEM at 3 kV voltages was also conducted to examine macro-scale fracture failure modes that occurred within the specimens under mechanical

loading. The effects of carbon nanotubes on the damage mechanisms of the composite laminates were then evaluated.

9.3. Results and Discussion

9.3.1. Distribution of nanotubes and VARTM processing

0.1 wt. % of MWCNT-NH_2 was dispersed within the resin system using a high shear mixing process called 3-roll milling technique as described above. This method was already found to be better in dispersion of CNTs within thermosetting resin systems as compared to other common methods such as sonication and mechanical stirring (Gojny, et al. 2004). Moreover, it must be emphasized that incorporation of CNTs significantly increases the viscosity of the corresponding resin blend, which causes difficulties with the VARTM processing. It was revealed, based upon rheological examinations, that transition from liquid like to pseudo-solid like behavior occurs with the resin suspensions containing 0.3 wt. % of MWCNTs and MWCNT-NH_2. It was also revealed that resin suspensions with CNT additives exhibit shear thinning behavior, regardless of type or content of nanotubes (Seyhan, et al. 2007b). On the basis of the previous findings, the content of nanotubes to be incorporated into the resin system for the present study was selected as 0.1 wt. %, which is lower than rheological threshold value of 0.3 wt. %. One reason of this selection lies in avoiding extremely high viscosity value of the resin blend during manufacture of composite laminates via VARTM process. Another one is to prevent CNT agglomerates within matrix resin due to the huge specific surface area of nanotubes that leads to enormous attractive forces to occur between the individual tubes. A comprehensive discussion with a particular emphasis on the problems regarding the dispersion of carbon nanotubes within the resin systems used in this study was already addressed in the previous sections.

Figure 9.5 shows the photos of CNTmodified hybrid resin infiltrated composite laminates cured at room temperature under vacuum and the corresponding optical micrograph of the mid-plane distribution of CNTs at the inlet, in the middle and at the vent points of the composite laminates. It seems that nanotube distribution at mid-plane of the composite laminates across its length is generally adequate. However, the specimens taken from nearby the vent region contain relatively low amount of

nanotubes. Fan et al. (2004) investigated the role of glass fabric porous media effect on the dispersion of MWCNTs during flow of MWCNT modified vinylester resin injected into the mold cavity containing glass fiber mats. They observed that the resin suspensions flow faster between the fiber tows than within the fiber tows. After some experimental trials, they concluded that the shear rate which occurs during resin flow disentangle very condensed aggregates into smaller ones due to a filtering effect, which is, however, at the same time insufficient to separate relatively tiny aggregates into individual nanotubes within the suspension. From that point of view, one could say hypothetically that uniform small sized agglomerates of CNTs within resin matrix prior to the VARTM process would be beneficial to accomplishing an overall homogeneous distribution of CNTs within the fiber tows of glass fabrics.

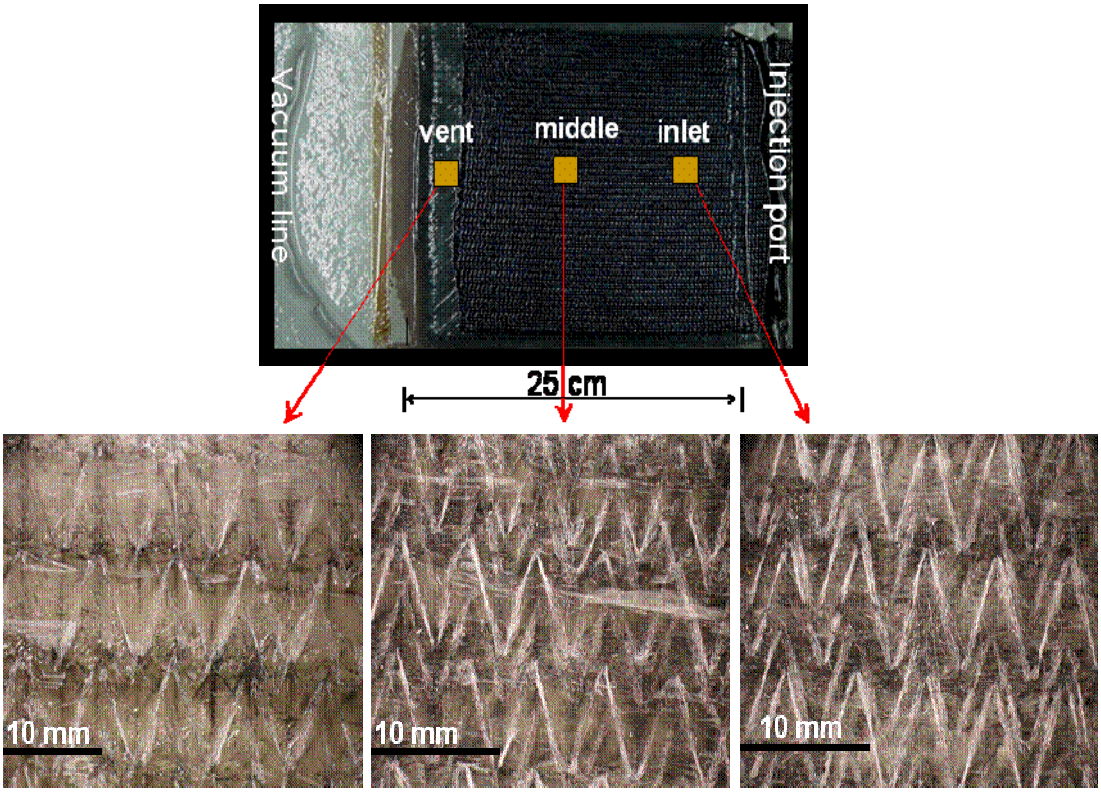

Figure 9.5. Photos of CNT modified hybrid resin infiltrated composite laminates cured at room temperature under vacuum and the corresponding optical micrograph of the mid-plane distribution of CNTs at the inlet, in the middle and at the vent points of the composite laminates.

This may explain the appearance of relatively poor nanotubes impregnated fiber bundles located at the mid-plane of the fabric closer to the vent region. Another point is that the presence of both ± 45 angle plies in the glass fabric decreased the fiber permeability, which makes it difficult for the resin to fill the part with uniform flow front.

9.3.2. Interlaminar Fracture Toughness of VARTM processed CNT Modified Glass Fiber Reinforced Composites

Figure 9.6 shows the representative load-deflection curves of the DCB specimens for the base and CNT modified laminates. As seen in the figure, both the base and CNT modified laminates show a well defined linear load-displacement relationship up to the point of crack initiation, after which they demonstrate distinct crack growth mechanism. In details, crack propagates within the base laminates by small incremental jumps without causing any sharp decrease in the load values. This indicates that the stick-slip crack growth mechanism is dominant for the base laminates across the non-linear region. However, steady crack growth mechanism within the CNTmodified laminates is visible such that no significant rise or decrease is observed for the load values with respect to displacement. In principle, at the first loading increment, the delamination starts propagating from the tip of the film insert (crack starter) without taking any influence from fiber bridging (on-set values). In other words, the onset values refer to the critical load and displacement associated with the first deviation from the linear response in the corresponding curve. As the crack further propagates, bridged fibers may crack or be pulled out from the matrix due to the progressively separated crack surfaces, which gives rise to the apparent fracture toughness (Alveraz, et al. 2003, Wichmann, et al. 2006). Once equal number of bridged fibers is achieved per unit crack area during crack propagation, steady state fracture toughness is eventually supposed to occur, which is commonly referred to as propagation fracture toughness value (Albertsen, et al. 1995, Srivistana, et al. 1998). Figure 9.7 a and b show mode I interlaminar fracture toughness (G_{IC}) values of the base and nanotubes modified composite laminates as a function of crack growth, respectively. The solid curves on the both graphs represent the general trend of the fracture toughness for the corresponding laminate as a function of crack extension.

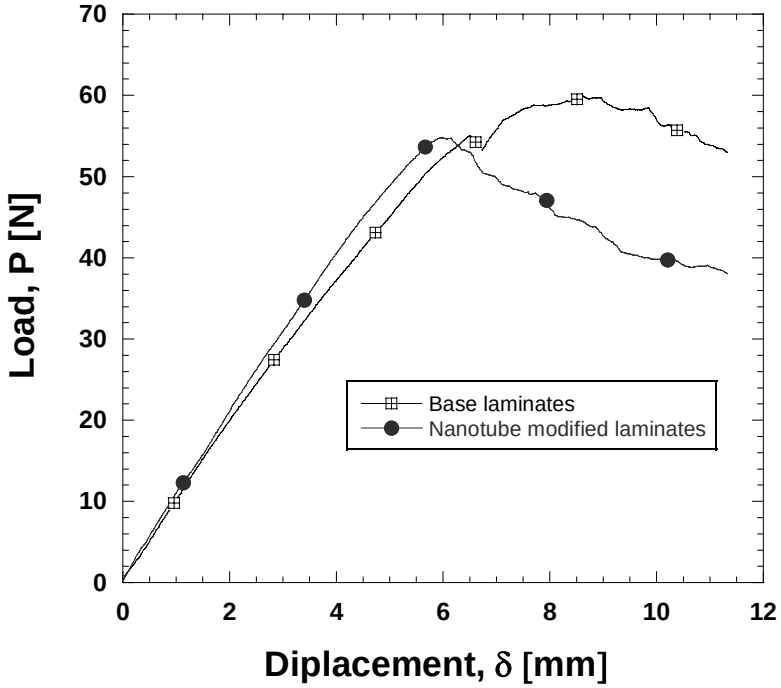

Figure 9.6. The representative load-deflection curves of the DCB specimens for the base and CNT modified laminates.

Dissimilar to behavior of the nanotube modified composite laminates within the first stage of crack extension, the G_{IC} of the base composite laminates rise sharply followed by a moderate increase for further crack extension. At about 25 mm extension, steady state fracture toughness (propagation) was observed for the base composite laminates, while this value for the CNT modified composite laminates switched to 35 mm, which shows the consistency with their load deflection curves. The presence of CNTs within the glass fiber bundles may alter the adhesion mechanism of two adjacent glass plies at the laminate mid-plane where the delamination takes place. Fiber bridging is vastly critical to the propagation toughness values of the composites because the instant increase in apparent fracture energy is highly associated with de-bonding of the larger surface area of the bridged fibers and breaking of these fibers. Fiber nesting is one major source of fiber bridging (Alveraz, et al. 2003, Tanoglu and Seyhan 2003). In our case, CNTs randomly oriented in the matrix resin would be capable of limiting fiber nesting, just diffusing into fiber tows and filling the gaps between fiber bundles by accumulating around them. This may be the reason for inconsistency in the behavior of base and the CNTmodified laminates during the extensions of crack at which the propagation of the fracture begins.

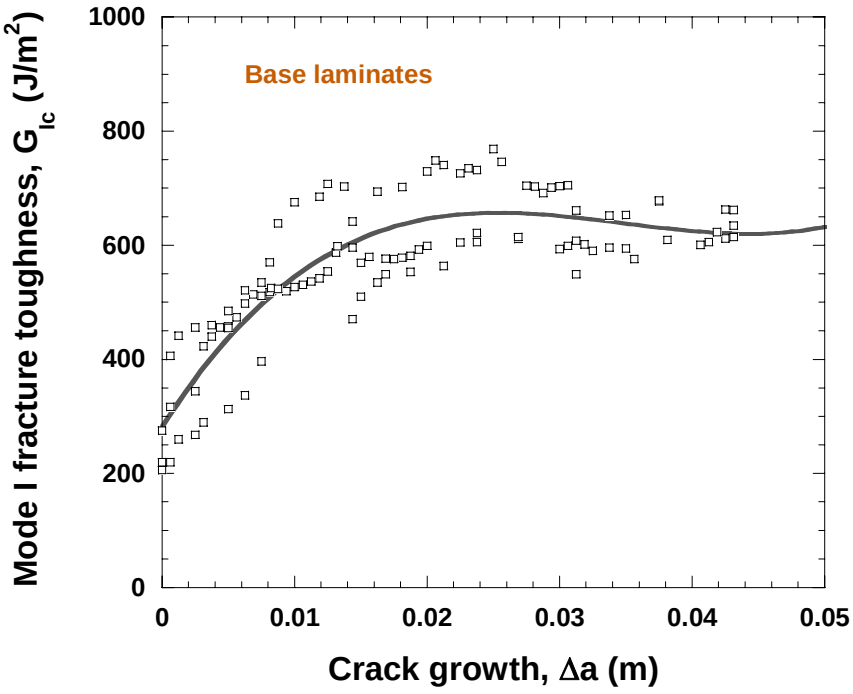

a)

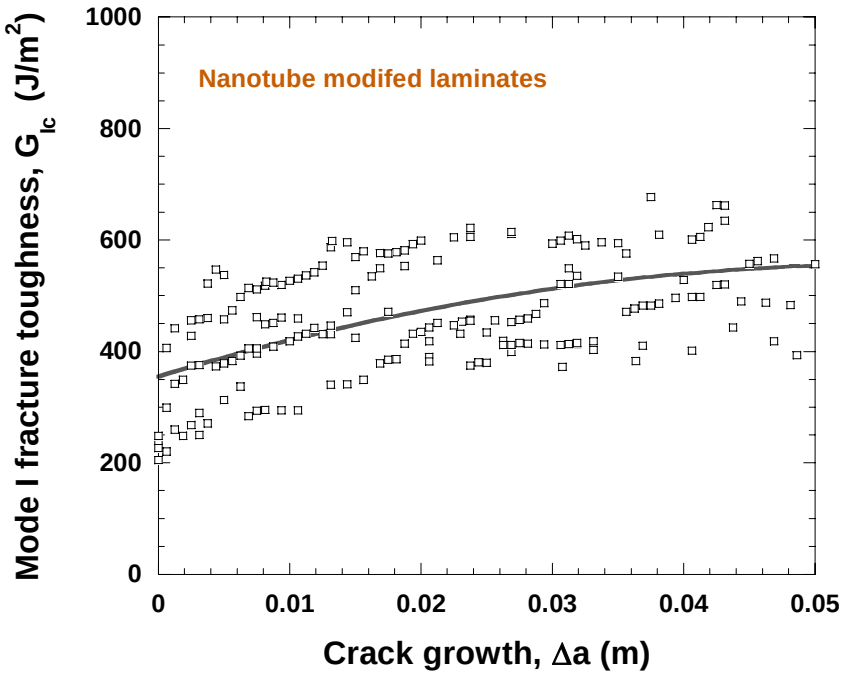

b)

Figure 9.7. Mode I interlaminar fracture toughness (G_{IC}) values of the a) base and b) nanotubes modified composite laminates as a function of crack growth.

Figure 9.8 depicts the interpreted onset and propagation fracture toughness values of the base and nanotubes modified composite laminates. As seen in the figure, there is no significant difference in the onset fracture toughness values between the base and nanotubes modified composite laminates. However, the propagation fracture value of the base composite laminates was found to be 40 % higher than that of nanotube modified composite laminates. The fact that no significant difference exists in the on-set fracture toughness values between the base and CNT laminates supports our conclusion that presence of CNTs hinders the fiber bridging effects in a considerable manner, thus reducing the degree of fiber nesting. As a result, despite the same onset toughness values obtained, the reduced propagation toughness values were obtained from CNT modified composite laminates.

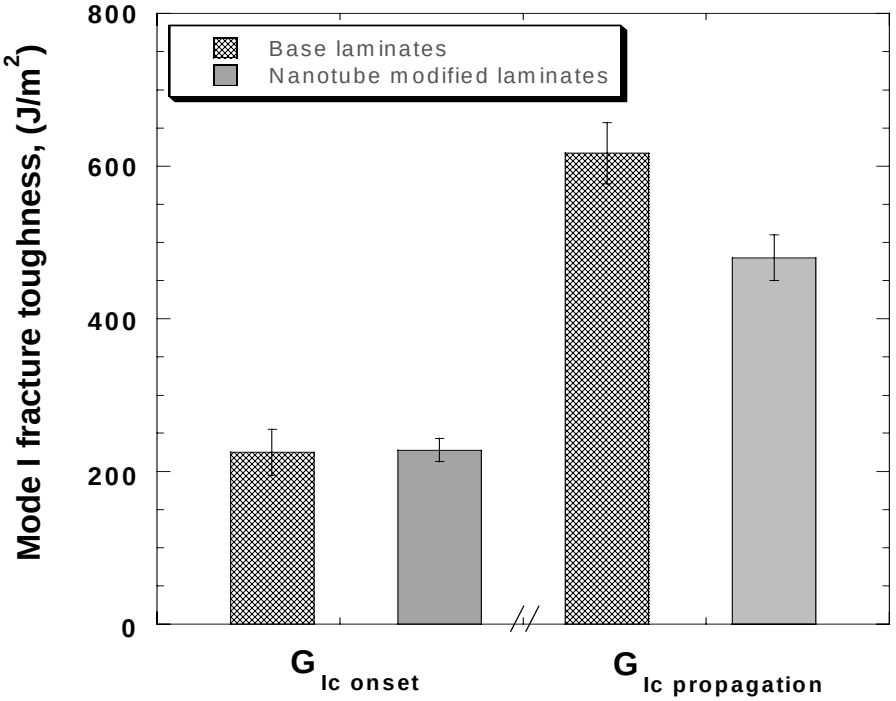

Figure 9.8. The interpreted onset and propagation fracture toughness values of the base and nanotubes modified composite laminates.

Figures 9.9 a and b are the SEM micrographs showing the mid plane fracture surfaces of the DCB specimens without and with CNT modification, respectively. Figure 9.9 c is a magnified image of a local area on Figure 9.9 b. The image shows individual glass fibers coated with CNT-rich matrix resin. As seen in the figures, the major failure mechanism is the debonding of the fiber matrix interface and matrix

fracture. It was observed that the de-bonding is more extensive for the composites with CNT modification. This implies that CNTs suppress the degree of fiber bridging to some extent, which leads to lower Gıc propagation toughness values for the composites modified with CNTs. This expression is proportional to our presumptions. Inn other words, we can roughly consider the propagation toughness values of CNT modified laminates as the fiber bridging induced effect free value of the base laminates.

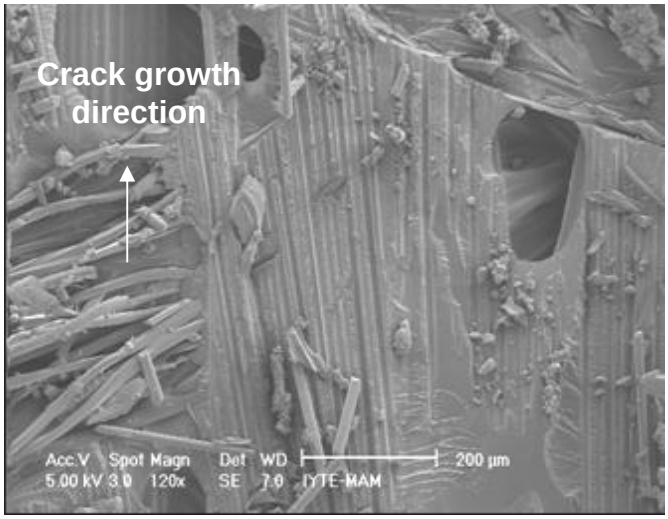

a)

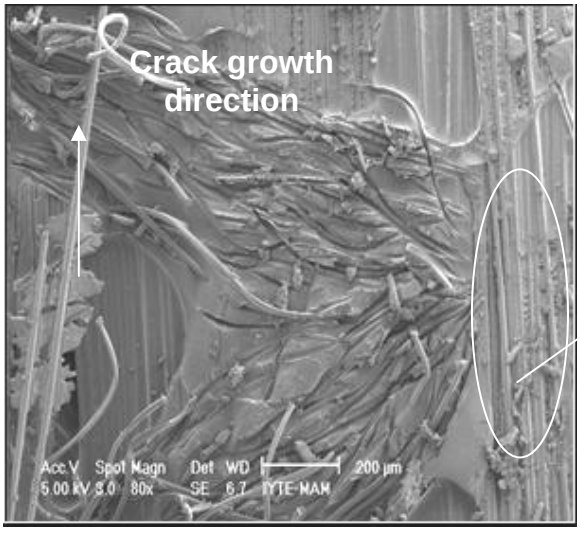

b)

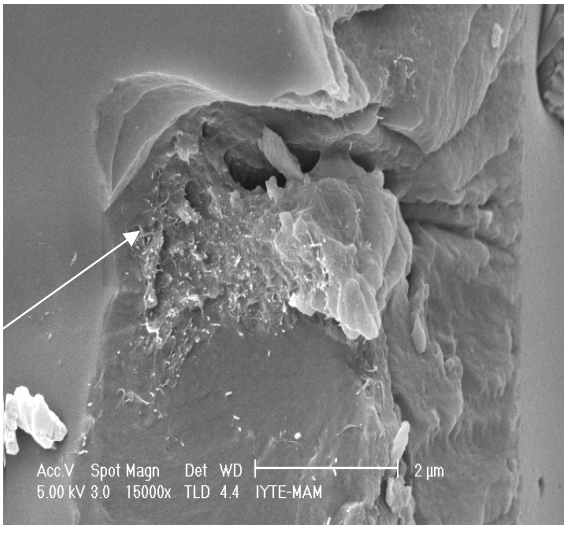

c)

Figure 9.9. SEM micrographs showing the mid plane fracture surfaces of the DCB specimens a) without and b) with CNT modification, respectively. Figure 9.9 c is a magnified image of a local area on Figure 9.9 b.

Figure 9.10 shows the representative load-deflection curves of the ENF tests for the base and nanotube modified laminates. The calculated mode II fracture toughness values of the base and nanotubes modified composite laminates were depicted in Figure 9.11.

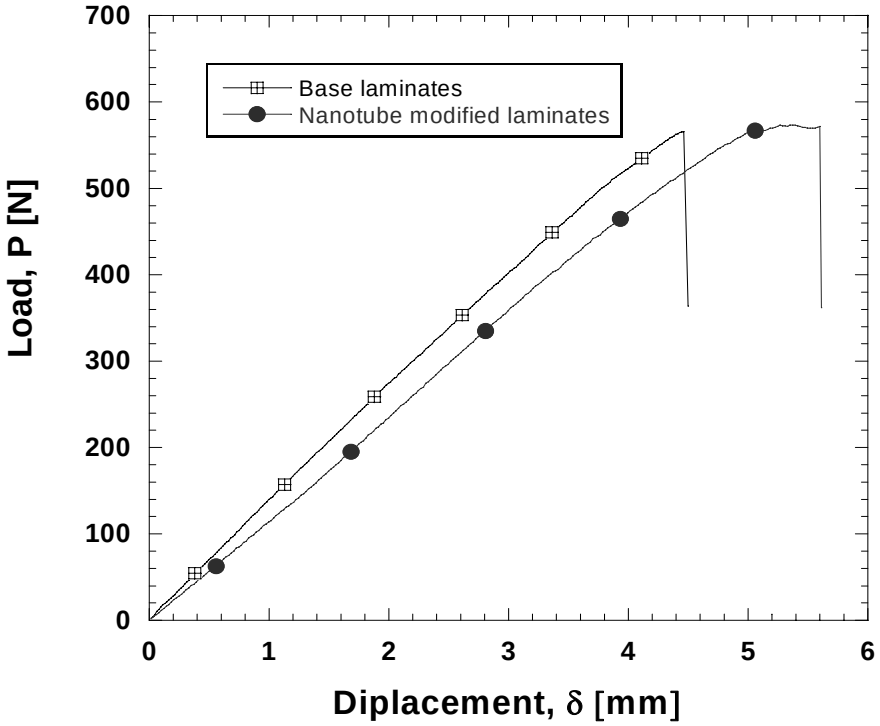

Figure 9.10. The representative load-deflection curves of the ENF tests for the base and nanotube modified laminates.

As mentioned earlier, the ENF test measures only the initiation fracture toughness. As seen in the figure, mode II fracture toughness values of the nanotube modified composite laminates are slightly higher (8 %) than those of the base composite laminates. Under mode II loading, fiber bridging does not occur. Two other important mechanisms; friction and hackles are responsible for the energy absorption. Unlike DCB specimens that exhibit continuous crack growth along the fiber /matrix interface, ENF specimens show discontinuous crack growth by micro-crack coalescence which leads to many hackles to occur at the fracture surface (Alveraz, et al. 2003). For that reason, the same CNT induced promotion observed for mode II toughness values are expected to occur as in the values of interlaminar shear strength values. This is because the both specimens failed under the same loading mode. This will be discussed in the following section. It seems that nanotube bundles act as rigid fillers which arrest the

crack, preventing or delaying the expansion of micro-cracking within the matrix rich interface area. So, it is realistic to anticipate a higher amount of hackles present at the fracture surface of the CNTmodified composite laminates as compared to that of the base composite laminates. This leads to a relatively high energy absorption by friction in nanotubes modified composite laminates. In other words, nanotubes may improve the adhesion between the interlayer and the adjacent composite layers at the same time under Mode II loading.

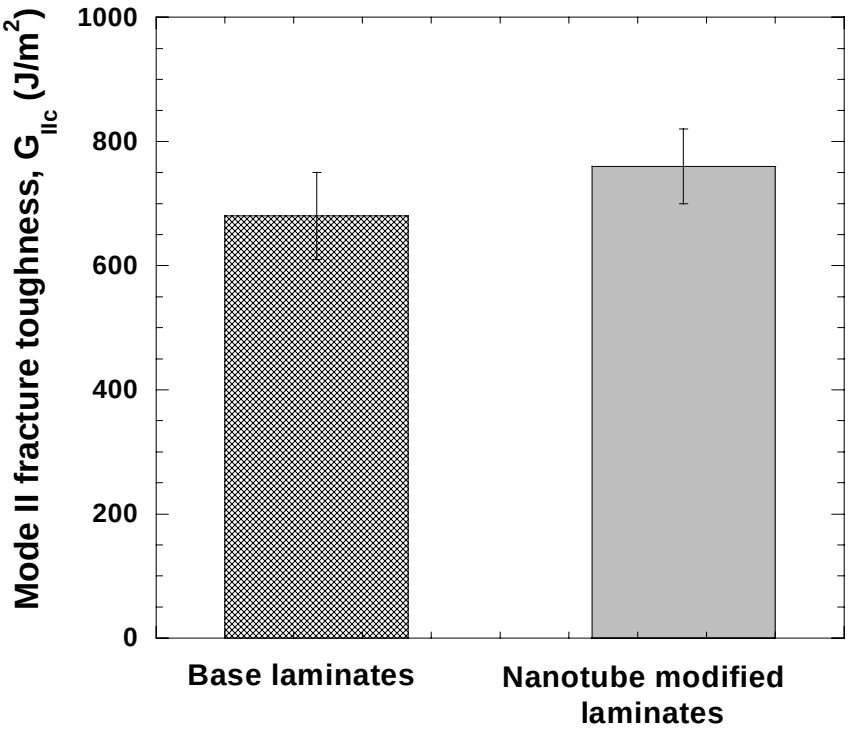

Figure 9.11. Mode II fracture toughness values of the base and nanotubes modified composite laminates.

9.3.3.Interlaminar Shear Strength of VARTM processed CNT Modified Glass Fiber Reinforced Composites

Figure 9.12 gives representative load-deflection curves of the SBS tests for the base and nanotube modified laminates. Figure 9.13 shows the ILSS of the base and nanotubes modified composite laminates together. It was found that the use of the CNT modified hybrid resin significantly increased (11 %) the interlaminar shear strength of the composite laminates.

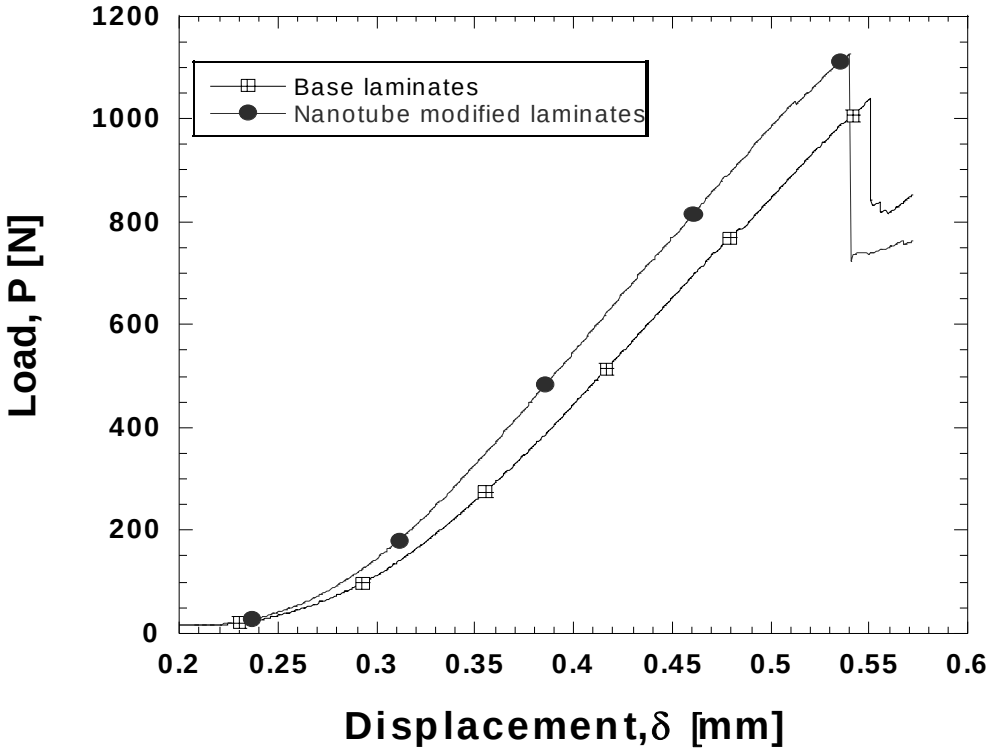

Figure 9.12. The representative load-deflection curves of the SBS tests for the base and nanotube modified laminates.

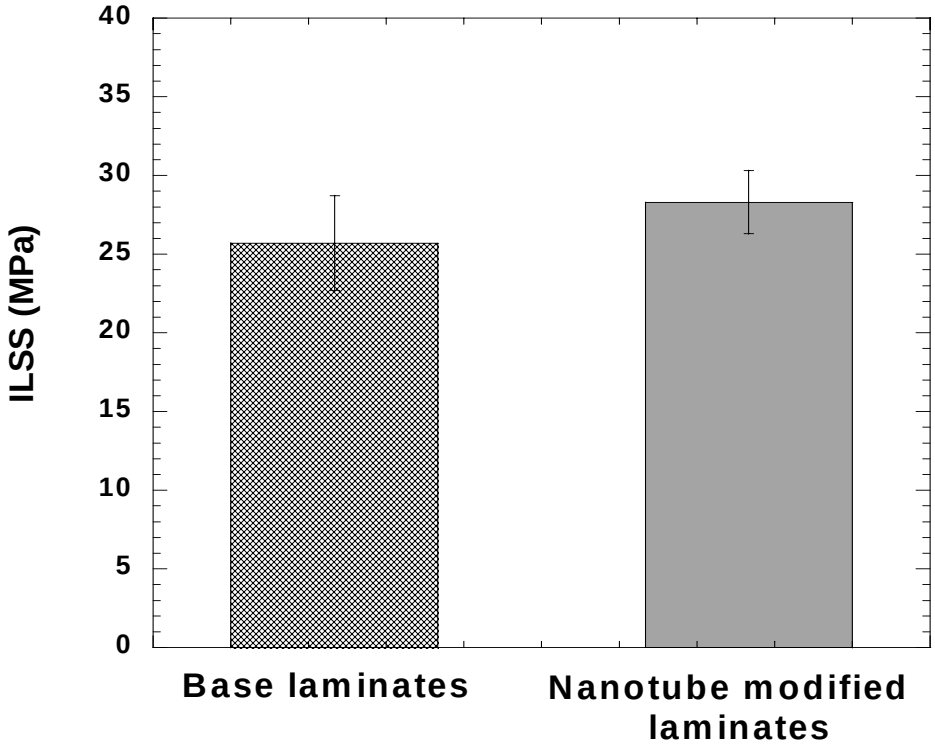

Figure 9.13. ILSS of the base and nanotubes modified composite laminates together.

The average value of the base composite laminates is 25.7 MPa, while this value increased up to 28.6 MPa for the CNT modified composite laminates. This may be attributed to larger tensile strength, modulus and fracture toughness values of a CNT modified polymer matrix as compared to those for neat hybrid resin, as addressed in details earlier. Figure 9.14 a, b, c and d show the mid-plane fracture surface of a failed short beam shear specimen taken from the CNT modified composite laminates. Note that Figure 9.14 b and d are the higher magnification of Figure 9.14 a and c, respectively.

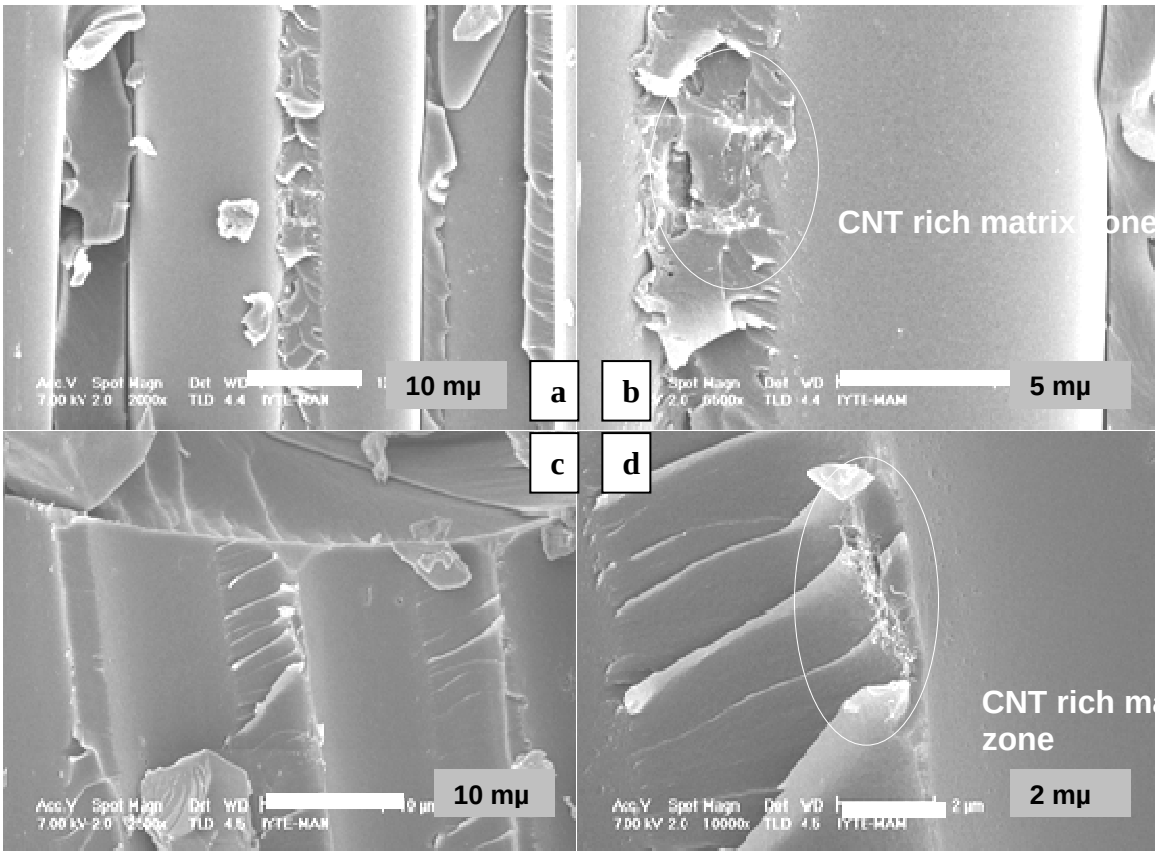

Figure 9.14. a, b, c and d show the mid-plane fracture surface of a failed short beam shear specimen taken from the CNT modified composite laminates. Note that Figure 9.14 b and d are the higher magnification of Figure 9.14 a and c, respectively.

On the other hand, CNT rich regions on the fracture surfaces are also visible on the micrographs. From that point of view, a strengthened region at interface may form

due to accumulation of nanotubes around the glass fibers. In other words, nanotube bundles and aggregates smaller than glass fiber tows may alter the interfacial strength, acting as additional reinforcement at the interlaminar region between polymer matrix and glass fiber. This leads to relatively large interlaminar shear strength values to be obtained from the nanotube modified composite laminates.

9.3.4. Distribution of CNTs and RTM processing

Figure 9.15 shows the CNT modified laminates produced by RTM. In principle, no significant filtering effect was observed for the laminates. To interpret better the distribution of CNTs around and inside the fiber tows across the entire composite panels, the samples were taken at the vent, in the middle and at the injection port of the composite laminates and their electrical conductivity values were measured using the same methods as in nanocomposites. Conductivity measurements were performed on each sample in 0^o, 90^o and Z directions, as illustrated in Figure 9.16. Note that at least 3 specimens were tested for each direction at each location. Figure 9.17 gives the measured conductivities of the samples taken from different regions across the part in the corresponding directions.

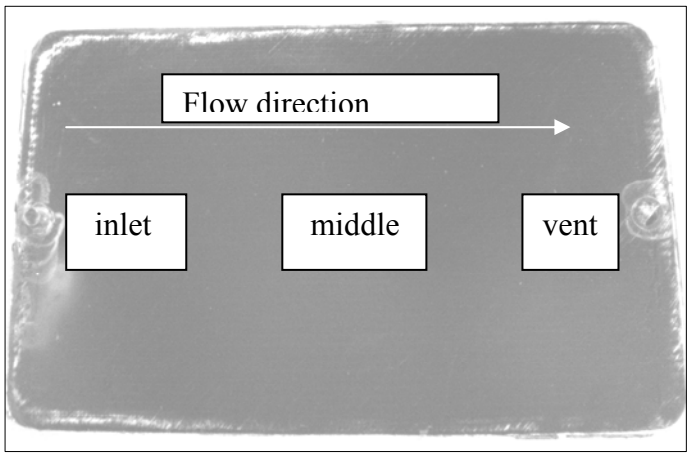

Figure 9.15. CNT modified laminates produced by RTM

In particular, the electrical properties of the composite laminates result from conductive networks formed by CNTs located in matrix channels in between and around the glass fiber tows. Regardless of location, in plane (0^o and 90^o directions) electrical

conductivity values of the composites were found to be several orders of magnitude higher than out of plane (Z direction) electrical conductivity values. This is because glass fabric layers act as barrier, which precludes the formation of conductive paths.

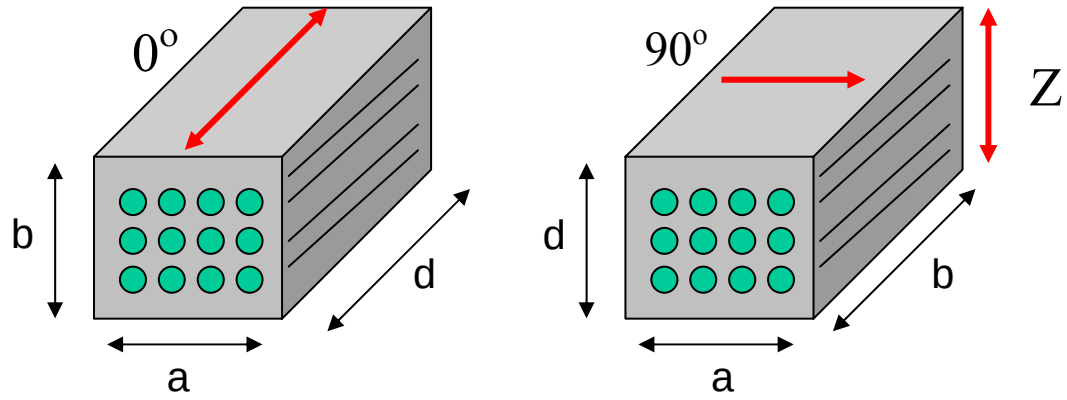

Figure 9.16. Illustration of directions in which the measurements were performed.

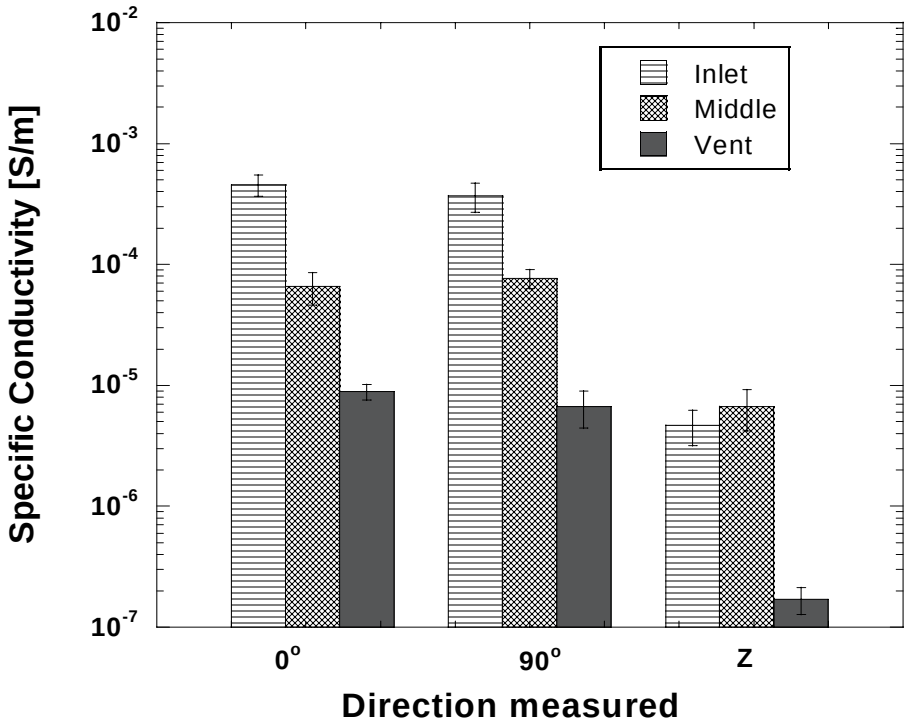

Figure 9.17. The measured conductivities in different directions for the samples taken from different regions along the part

On the other hand, the fact that in plane electrical conductivity values scattered around the same value is the evidence for almost homogenous distribution of CNTs across the entire part. Please also note that post-curing also decreases the overall

conductivity of the composite laminates because of the disrupted conductive paths during shrinkage. From that point of view, one could expect to observe slightly higher values in non-post cured samples as compared to post-cured samples.

9.3.5. Tensile properties of RTM processed CNT Modified Glass Fiber Reinforced Composites

The tensile properties of the composites were performed by tensile testing in 0^o and 90^o directions because non-crimp fabrics were used as reinforcement which exhibits different fiber volume content in different directions. Figure 9.18 and 9.19 show the measured tensile strength and modulus values for the RTM processed composite laminates with and without CNT modification, respectively. There is not any significant contribution of CNTs to the strength of the laminates. The average tensile strength of the base laminates in 0^o direction was found to be 6 % higher than that of CNT modifed composite laminates. However, there is no difference in strength values in 90^o direction between the base and CNT modified laminates. This trend is slightly different for the elastic modulus values such that, regardless of the direction, slightly higher modulus values obtained from CNT modified laminates as compared to the base laminates. The laminates showed fiber dominated behavior, as expected. In fact, this is contradictory to what is achieved in mechanical properties of VARTM processed laminates with and without modification. We can safely say that presence of CNTs within the matrix resin contributes to the out of plane properties such as enhanced resistance to delamination, rather than in-plane properties such as tensile strength that is vastly dependent on the reinforcing efficiency of the fibers.

9.4. Conclusions

In this chapter, the matrix dominated mechanical properties of long glass fiber reinforced composite laminates, including Mode I, Mode II fracture toughness and interlaminar shear strength of glass fiber / carbon nanotube (CNT) modified vinylester-polyester based composites were investigated.

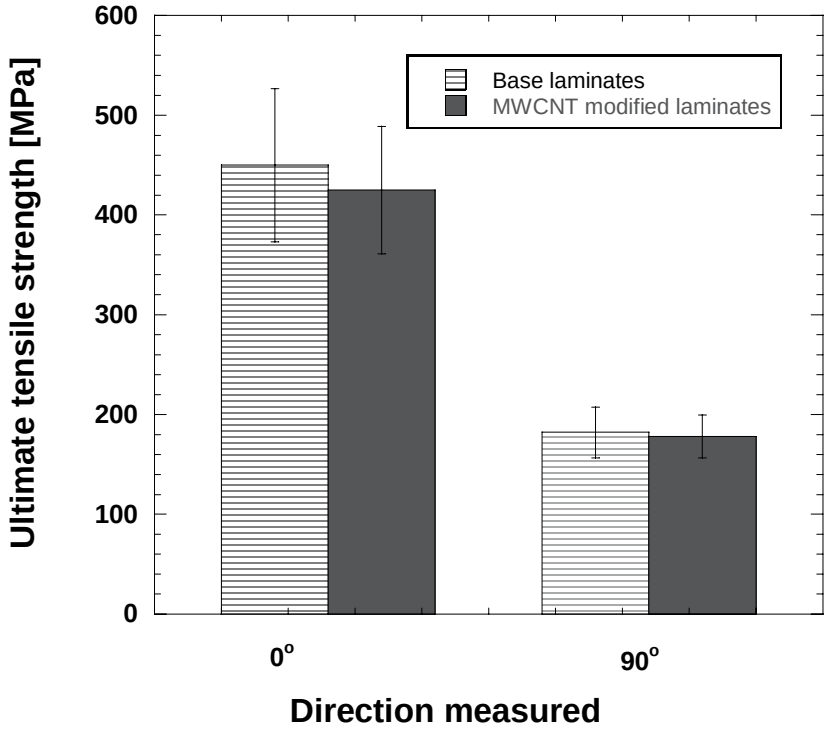

Figure 9.18. Measured tensile strength values of the base and MWCNT modified laminates in 0° and 90° directions.

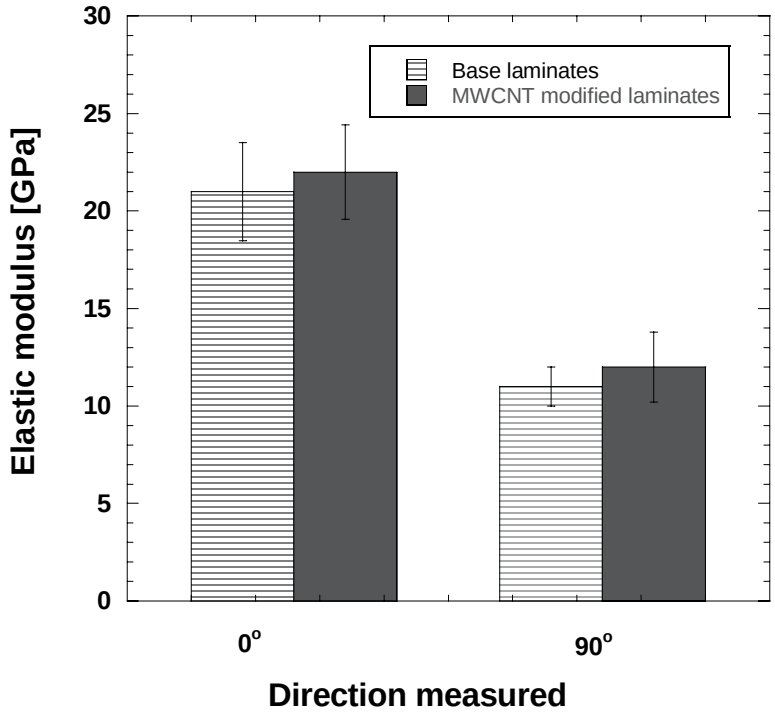

Figure 9.19. Measured elastic modulus values of the base and MWCNT modified laminates in 0° and 90° directions.

In this manner, the base and nanotubes modified composite laminates were successfully manufactured via Vacuum Assisted Resin Transfer Molding (VARTM) and Resin Transfer Molding (RTM) processes, using E-glass fiber non-crimp fabrics with a $[-45^o / 90^o / +45^o / 0^o]_s$ stacking sequence. To produce hybrid resin to be utilized as matrix material during VARTM and RTM processes, 0.1 wt. % of MWCNT-NH_2 and 0.3 wt. % of MWCNTs were first dispersed within specially synthesized styrene-free polyester resin, conducting 3-roll milling technique followed by blending the collected resin suspension with vinylester resin. In consequence, the mode I interlaminar fracture toughness value of the nanotubes modified composite laminates was found not to be significantly affected, while their mode II fracture toughness value was found to be about 8 % higher compared to the base laminate. It was also observed that the interlaminar shear strengths of the nanotubes modified composite laminates was 11 % higher than those of the base composite laminates.

Electrical measurements performed on the samples taken from different regions of the RTM processed CNT modified laminates showed that there is no significant filtration effects of glass fabrics for CNTs in the matrix resin. It was found that in plane conductivity of the laminates was more than a few orders of magnitude higher than out of plane conductivity. However, no significant differences were observed for the conductivity measured in 0^o and 90^o directions. This implies that RTM is an appropriate tool to manufacture such functional composites structures. Tensile mechanical properties of the RTM processed laminates with and without CNT modification was also pinpointed in 0^o and 90^o directions. It was found that strength values of the laminates were not adversely affected by the presence of CNTs, and that their modulus values were slightly enhanced with the presence CNTs.

As a general statement, despite a pronounced increase in the matrix toughness, it seems that it is still a big challenge to transfer the improved nanotube modified matrix properties such as fracture toughness or shear strength into conventional long fiber composites due to some difficulties with composite processing. Overall, a stronger interfacial bonding and a higher level of uniform CNT distribution within and around the glass fiber tows are the key parameters to accomplish the desired properties in their resultant composite parts. On the other hand, almost constant in plane conductivity across the RTM part could offer the potential to enable in-situ damage monitoring of the sectioned composite laminates under load.

CHAPTER 10

CONCLUSIONS AND FUTURE WORK

10.1 Conclusions

This work showed the benefits and drawbacks of CNTs as filler constituent to alter the thermal, mechanical and electrical properties of the vinylester and polyester based hybrid polymers. Dispersion of CNTs and their interfacial interactions with the surrounding polymer matrix are vastly critical to ultimate properties of the resulting nanocomposites.

3-roll milling was shown highly efficient to disperse CNTs homogenously within the matrix resin. The properties of the nanocomposites were discussed with a particular emphasis on various factors including surface area, filler content and aspect ratio of CNTs and amine functional groups over their surfaces. The micro structure property relationships were then established to interpret better the CNT induced effects on the characteristics of the final nanocomposites. It was found that at very low filler loading rates (0.05, 0.1 and 0.3) CNTs exhibit the potential to improve the mechanical, thermal but especially electrical properties of their resulting nanocomposites.

In Chapter 3, difficulties with processing of carbon nanotubes with thermosetting resins containing styrene such as polyester and vinylester was addressed. The challenges encountered during various types of processes including sonication, mechanical mixing and 3-roll milling were discussed in details. It was found that 3-roll milling technique was capable to disperse the CNTs within the matrix resin in homogenous manner. Since both commercial thermosetting resins (polyester and vinylester) contain styrene, traditional methods such as direct mixing, mechanical stirring and sonication were found to be inconvenient. It is because styrene evaporates instantly when the temperature rises due to heat induced to the resin system by rotating propeller or sonication tip. In fact, this comprises the grounds of utilizing hybrid resin system to produce nanocomposites via 3-roll milling technique. Rheological behavior and mechanical properties of the resins suspensions and their resulting nanocomposites were also given in a brief manner. It was found that mechanical strength of the

polyester based hybrid resin system was improved by 12 % with the addition of 0.3 wt. % of MWCNTs.

In Chapter 4, rheological properties of the resin suspensions were investigated. Based upon linear dynamic viscoelastic measurements, it was found that storage modulus (G') and loss modulus (G'') values of MWCNT modified resin suspensions as a function of angular frequency increased with respect to content regardless of amine functional groups. Moreover, at 0.3 wt. % loading rate, both MWCNT and MWCNT-NH_2 modified resin suspensions showed rheological threshold (pseudo-solid like behavior), especially very observable at lower frequencies. However, this trend became reverse when DWCNTs and DWCNT-NH_2 were incorporated into the same hybrid resin such that storage and loss modulus values decreased as the content of DWCNTs and DWCNT-NH_2 increased in the resin system. Moreover, no transition from liquid-like to solid-like behavior was observed in the corresponding resin suspensions. Steady shear measurements revealed that regardless of type of CNTs or amine functional groups, each suspension showed shear thinning behavior with steeper slope, while the hybrid resin was almost the Newtonian fluid. These results showed that surface area and aspect ratio of CNTs are more critical to the flow characteristics of the polymers than functional groups over their surfaces.

In Chapter 5, the cure kinetics of the hybrid resin containing 0.3 wt. % of MWCNTs and MWCNT-NH_2 were pinpointed. In this respect, various experimental techniques including DSC, FTIR, RS and TGA were systematically conducted to reveal the effects of CNTs on free radical polymerization. Non-isothermal DSC measurements at different constant heating rates revealed that the presence of CNTs within the resin system alters the polymerization reaction by increasing the heat of cure while decreasing the activation energies (Ea). In greater details, the suspension with MWCNT-NH_2 exhibits much heat of cure, besides lower activation energies as compared to neat resin blend and the suspension with MWCNTs. Autocatalytic kinetic model defines well the curing mechanism involved. Furthermore, FTIR studies were carried out to reveal the impact of CNTs on the development of the network in a polymer matrix that polymerizes via radicals. In this manner, neat vinylester resin and its suspensions with the same content of MWCNTs and MWCNT-NH_2 as the hybrid resin were employed. In consequence, very interesting results were obtained. The final conversion of styrene exceeded the final conversion of vinylester double bonds in the resin suspensions with MWCNT-NH_2, while final conversion of vinylester is higher

than that of styrene in the resin suspensions with MWCNTs. RS studies performed on the cured hybrid polymer and its nanocomposites show consistency with FTIR findings such that amine functional groups over the surfaces of CNTs altered the chemical reactions within the resin system. On the other hand, TGA measurements revealed that CNTs increased the thermal stability of the hybrid matrix resin such that E_d values of the nanocomposites prepared with MWCNTs and MWCNT-NH_2 are higher than that of the cured hybrid polymer. Moreover, at each constant heating rate, it was found that nanocomposites with MWCNT-NH_2 exhibited higher char yields as compared to neat hybrid resin and those prepared with MWCNTs. On behalf of the findings achieved, it was concluded that amine functional groups over the surfaces of CNTs enhanced the dispersibility of CNTs and influenced the relative individual fractional conversions of double bonds in the resin system at the same time. We can safely say that amine groups over the surfaces of CNTs enhance the dispersion of CNTs in the resin system while at the same time significantly affecting the individual monomer polymerization reactions. In general, it needs to be emphasized that chemical functional groups over the surfaces of CNTs are vastly crucial to the monomer conversion in free radical chain growth copolymerization.

In Chapter 6, the thermo-mechanical properties of the nanocomposites containing MWCNTs, MWCNT-NH_2, DWCNTs and DWCNT-NH_2 were investigated in association with rheological behavior of their corresponding resin suspensions. Consequently, the storage (E') and loss modulus (E'') values of the nanocomposites containing MWCNTs, MWCNT-NH_2 were found to increase with an increase in contents of CNTs. Furthermore, nanocomposites containing MWCNTs, and MWCNT-NH_2 were found to exhibit higher glass transition temperature value as compared to neat hybrid polymer. As the filler content of MWCNTs increases, higher Tg values obtained from the resultant nanocomposites. This trend is more evident for the nanocomposites containing MWCNT-NH_2. TEM studies showed that dispersion of MWCNT-NH_2 is better than that of MWCNTs in the hybrid polymer, which shows consistency with the findings obtained. However, regardless of amine functional groups, incorporation of DWCNTs was found to decrease the T_g values of the hybrid resin. This trend becomes even worse, as their concentration increases in the hybrid resin. TEM investigations performed on the cured resin samples demonstrated that the dispersion of DWCNTs, regardless of amine functional groups, within the polymer matrix was also inferior. Overall, we could say that rheological properties of the resin suspensions are highly

proportional to the thermal properties of their resulting nanocomposites independent of type of CNTs.

In Chapter 7, the effect of MWCNTs and DWCNTs with and without NH_2 functional groups on the tensile mechanical behavior and fracture toughness of vinylester-polyester hybrid resin system was investigated. It was found that addition of CNTs has insignificant influence on the tensile strength of the resulting nanocomposites. It was also revealed that nanocomposites containing MWCNTs with and without NH_2 functional groups leads to higher tensile modulus, fracture toughness and fracture energy values in comparison to those prepared with DWCNTs or DWCNT-NH_2. Moreover, experimentally measured elastic moduli of the nanocomposites were fitted to Halphin-Tsai's analytical model. The predicted and the measured values of nanocomposites with MWCNTs and MWCNT-NH_2 were found to be in good agreement with each other. On behalf of the experimental findings achieved, it was concluded that the reinforcing efficiency of DWCNTs and DWCNT-NH_2 is lower as compared to those of MWCNTs and MWCNT-NH_2, when incorporated into free radically polymerized thermosetting resins such as polyester or vinylester. Entrapment of free radicals decreased the degree of polymerization and cross-linking density. This may significantly influence the cure kinetics of the resin system by altering the chemical interactions at the interface, which are directly related to ultimate performance of the final composite parts. This subject of interest was already discussed in details in Chapter 5. The findings obtained form this chapter show consistency with those addressed in the previous chapters so far.

In Chapter 8, electrical conductivity of nanocomposites were investigated based on two different matrix resin systems including polyester based and vinylester polyester based hybrid resins. At both resin systems, nanocomposites with MWCNTs were obtained to be higher than those with DWCNTs. This result was attributed to the relatively high tendency of DWCNTs to agglomerate within the corresponding resin system. The results of temperature dependence of resistivity showed that polyester based nanocomposites exhibited semiconductor like behavior regardless of the types of carbon nanotubes (MWCNT or DWCNT) or the presence of functional groups over the CNTs. Also, increasing resistance with decreasing temperature was obtained, so tunneling was decided to be the dominant mechanism. Room temperature electrical properties of the CNT modified vinylester polyester composites cured with and without application of alternating (AC) electric field were also investigated by means of an

impedance dielectric spectroscopy. Consequently, the composites with amino functionalized CNTs were found to exhibit lower electrical conductivity than those with untreated CNTs. At each given concentration, the highest electrical conductivities were achieved in composites prepared with untreated MWCNTs. MWCNTs was then selected as the most appropriate filler and resin suspensions were prepared with 0.005, 0.02 and 0.05 wt. % of MWCNTs to align the tubes within matrix resin with application of the AC electric field during curing. Based upon optical microscopy investigation and electrical conductivity measurements, it was revealed that alignment of CNTs within polymer matrix was achieved by AC electric field. The synergetic effect observed in the T_g value of the composites cured with the application of AC electric field was attributed to the interactions between the charged free radicals and the aligned CNTs within the resin system. Therefore, location and distribution of the radicals in between CNTs is substantially important to the final performance of the resulting nanocomposites. In addition, it can be concluded that any kind of chemical treatment is unfavorable for the conductivity.

In Chapter 9, mechanical properties of VARTM and RTM processed composite laminates with and without CNT modification were highlighted. . In consequence, the mode I interlaminar fracture toughness value of the nanotubes modified composite laminates produced by VARTM was found not to be significantly affected, while their mode II fracture toughness value was found to be about 8 % higher compared to the base laminate. It was also observed that the interlaminar shear strengths of the nanotubes modified composite laminates was 11 % higher than those of the base composite laminates. On the other hand, tensile mechanical properties of RTM processed composite laminates were not improved by the use of CNT modified hybrid resin as matrix material. Moreover, anisotropic electrical conductivity was accomplished in the composite laminates such that in plane conductivity (0 and 90 directions) is several orders of magnitude higher than out of plane conductivity (z-direction). In fact, utilization of conventional fabric reinforcement together with a CNT modified matrix resin has the potential for the development of future functional nanocomposites. For example, carbon nanotubes (CNTs) embedded in polymer matrix resin can be used as in-situ sensors due to their inherent electrical properties in order to detect the onset and evolution of damage in glass fiber reinforced polymer composite (GFRP) under mechanical load.

10.2 Outlook and Future Work

CNTs have been highly promising filler constituents to tune thermal, mechanical and electrical properties of the polymers in which they are embedded. However, due to the challenging problems with processing, it is very hard to answer the question regarding the selection of appropriate type of CNTs (aspect ratio, surface area and functional groups) to realize the so pronounced properties in the resultant parts. For free radical growth copolymerization reactions, the surface area of CNTs and functional groups over their surfaces are the most substantial parameters to be considered. Free radicals generated by decomposition of initiator are too vulnerable to be trapped within the galleries of CNTs. The more radicals trapped within the galleries of CNTs, the lower degree of polymerization and cross-linking density, which leads to reduced ultimate performance in the final composite parts. Although the curing mechanism of the CNT modified resin suspensions were intensively studied in this dissertation, more information regarding the chemical interactions between CNTs and the polymer matrix resin is needed. Additional valuable information can be gathered by NMR spectroscopy in the further studies to gain an in-depth understanding of these mechanisms. In this case, more appropriate chemical functional groups rather than amine groups could be used to tailor the interface between nanotubes and matrix polymer. In addition, different types of initiators suitable for room temperature and high temperature curing could be utilized to promote the monomer conversion in the resin system. Another approach to getting a stronger interfacial bonding lies in using peroxide grafted CNTs as initiators via novel functionalization and dispersion route.

Another major point is the alignment and orientation of CNTs within the matrix resin. It was found that nanocomposites with aligned CNTs possessed higher glass transition temperature as compared to those with similar content of randomly oriented CNTs. This implies that movement of charged radicals between CNTs within polymer matrix under electrical field applied may have substantial effects on the characteristics of polymer networks formed. Therefore, new methodology and strategy can be applied to control dispersion of CNTs under electrical field. On behalf of this purpose, for example, parameters of 3-roll milling (dwell time, rotation speed and the gap between the rolls) could be optimized to prepare the resin suspensions with better dispersed CNTs.

On the other hand, in general, the nanotubes with high aspect ratio can be further utilized as filler in polymers to benefit a stronger and more lightweight composite material that could be used in several fields, including automotive, aerospace, infrastructure, and military. We already showed that RTM and VARTM techniques work well to manufacture reinforced composites with CNT modification. Especially, electrically conductive long fiber reinforced composites could promise the potential to develop the conventional aeronautical engineering structures. Since the composites become conductive, it would be possible to detect the onset, nature and progression of the damage during service life.

REFERENCES

Ago, H., K. Petritsch, M.S.P. Shaffer, A. Windle, and R.H. Friend. 1999. Composites of carbon nanotubes and conjugated polymers for photovoltaic devices, *Advanced Materials*, 11: 1281-8

Aizawa, M, and M.S.P. Shaffer. 2003. Silylation of multiwalled carbon nanotubes *Chemical Physics Letters* 368:121-124.

Ajayan, P.M. and L.S. Schandler. 2000. Single-walled carbon nanotube-polymer composites: strength and weakness, *Advanced Materials*, 12: 750–753.

Ajayan, P.M., J.C. Charlier, A.G. Rinzler. 1999. Carbon nanotubes: from macromolecules to nanotechnology, *Science* 96: 14199–14200.

Ajayan, P.M., O. Stephan, C. Colliex, and D. Trauth. 1994. Aligned carbon nanotube arrays formed by cutting a polymer resin-nanotube composite. *Science*, 26: 1212–1214.

Albertsen, H., J. Ivens, P. Peters, M. Wevers, I. Verpoest. 1995. Interlaminar fracture toughness of CFRP influenced by fiber surface treatment: Part 1 Experimental results. *Compos Science and Technology* 54:133-145

Allaoui, A., S. Bai, H. M. Cheng, J.B. Bai. 2003. Mechanical and electrical properties of MWCNT/epoxy composite. *Composites Science and Technology* 62:1993- 1998.

Alloui, A., S.Bai, H.M.Cheng, and J.B.Bai. 2002. Mechanical and electrical properties of MWNT/epoxy composites. *Composites Science and Technology* 62:1993-1998

Alveraz, V., C.R.Bernal, P.M. Fonrtini. 2003. The influence of matrix chemical structure on the mode I and II interlaminar fracture toughness of glass-fiber / epoxy composites. *Polymer Composites* 24:140-148

Amari, T, K.Uesugi, and H.Suzuki. 1997. Viscoelastic properties of carbon black suspension as flocculated percolation system. *Progress in Organic Coatings*. 31, 171-178.

Andrews, R., D. Jacques, M. Minot, and T.Rantell. 2002. Fabrication of carbon multiwall nanotube /polymer composites by shear mixing *Macromolecular Materials and Engineering* 287:395-403.

ASTM Standard D 2344-00. 2001b. *Test Method for Short Beam Strength of Polymer Matrix Composite Materials and their Laminates by Short-Beam Method,* American Society for Testing and Materials, West Conshohocken, PA.

ASTM Standard D5528-94a. 2001a. *Test Method for Mode I Interlaminar Fracture Toughness of Unidirectional Fiber-Reinforced Polymer Matrix Composites*, American Society for Testing and Materials, West Conshohocken, PA.

Astorga, R. and D. Mendoza. 2005. Electrical Conductivity of multi wall carbon nanotubes thin films *Optical Materials* 27:1228-1230.

Bae, J., J. Jang, and S.H. Yoon. 2002. Cure behaviour of the liquid-crystalline epoxy/carbon nanotube system and the effect of surface treatment of carbon fillers on cure Reaction" *Macromolecular Chemistry Physics*. 2002, 203, No. 15

Bai, J. 2003. Evidence of the reinforcement role of chemical vapour deposition multi walled carbon nanotubes in a polymer matrix. *Carbon* 41:1309-1328.

Bai, J.B. and A. Allaoui. 2003. Effect of the length and the aggregate size of MWCNTs on the improvement efficiency of the mechanical and electrical properties of nanonanocomposites-Experimental investigation, *Composites Part A* 34:689-694.

Bajpai, A. and A. K. Nigam. 2007. Fluctuation-induced tunnelling conductance and enhanced magnetoresistance in polycrystalline CrO_2 and its composites *Physics Reviews B* 75:064403-064410.

Barber, A. H., S.R. Cohen, H.D. Wagner. 2003. Measurement of carbon nanotube-polymer interfacial strength. *Applied Physics Letters* 82:4140-4142.

Batch G.L. and C.W. Macossa. 1992. Kinetic model for cross-linking free radical polymerization including diffusion limitations. *Journal of Applied Polymer Science* 44: 1711-1729.

Biercuk, M.J., M.C. Llaguno, M. Radosvljevic, J.K. Hyun and A.T. Johnson. 2002. Carbon nanotube composites for thermal management. *Applied Physics Letters* 80:15-25.

Bockrath, M., D.H. Cobden, J. Lu, A.G. Rinzler, R.E. Smalley, L. Balents, P.L. McEuen. 1999. Luttinger-liquid behaviour in carbon nanotubes *Nature* 397:598-601.

Bower, C., W. Zhu, S.H. Jin and O.Zhou. 2000. Plasma induced alignment of carbon nanotubes. *Applied Physics Letters* 77:830-832.

Brying, M.B., M.F. Islam, J.M. Kikkawa. 2005. Carbon Nanotube Aerogels. *Advanced Materials* 17:1186-1191.

Caba K.L., P.Guerrero, I.Mondragon, and J.M.Kenny. 1998. Comparative study by DSC and FTIR techniques of an Unsaturated Polyester resin cured at different temperatures. *Polymer International* 45:333-338

Calvert, P.1999. A recipe for strength. *Nature* 399:210–11.

Celzard, A., E. Mcrae, C. Deleuze, M. Dufort, G. Furdin, J.F. Mareche. 1996. Critical concentration in percolating systems containing high aspect ratio filler. *Physical Review* 53:6209-9214.

Chan, C.M., J. Wu, J.X. Li, and Y.K. Cheung. 2002. Polypropylene calcium carbonate nanocomposites *Polymer* 43:2981-2992.

Che, G., B.B. Lakshmi, C.R. Martin, E.R. Fisher, and R.S. Ruoff. 1998. Chemical vapour deposition based synthesis of carbon nanotubes and nanofibers u sing a template method. *Chemistry of Materials* 10:260-267

Coleman, J.N., S. Curran, A.B. Dalton, A.P. Davey, B. McCarthy, W.J. Blau, and R.C. Barklie. 1998. Percolation-dominated conductivity in a conjugated polymer carbon nanotube composite, *Phyical Review* B, 58: 7492–7495.

Collins, P.G., and P.Avouris. 2000. Nanotubes for electronics. *Scientific American* 283:62-69.

Cooper, C.A., R.J. Young, and M. Halsall. 2001. Investigation into the deformation of carbon nanotubes and their composites through the use of Raman spectroscopy. *Composites Part A: Applied Science and Manufacturing* 32:401-411

Curran, S., P.M. Ajaian, W.J. Blau, D.L. Carroll, J.N. Coleman, A.B. Dalton, A.P. Davey, A. Drury, B. McCarthy, S. Maier, and S. Strevens. 1998. A composite from poly (m-phenylenevinylene-co-2 and 5-dioctoxy-p- pnenylenevinylene) and carbon nanotubes: a novel material for molecular optoelectronics, *Advanced. Materials*, 10:1091–1093.

Dillon, A.C., T. Gennett, K.M. Jones, J.L. Alleman, P.A. Parilla, M.J. Heben. 1999. A simple and complete purification of single walled carbon nanotube materials, *Advanced Materials*. 11:1354–1358.

Dresselhaus, M.S., G. Dresselhaus, R. Saito, and A. Jorio. 2005. Raman spectroscopy of carbon nanotubes. *Physics Report* 409:47-99.

Dua, S., R.L. Mc Cullough, and G.R. Palmase.1999. Copolymerization kinetics of s styrene/vinyl-ester systems: Low temperature reactions. *Polymer Composites* 20:379-389.

Duesberg, G.S., M. Burghard, J. Muster, G. Philipp, and S. Roth. 1998. Separation of carbon nanotubes by size exclusion chromatography, *Chemical Communications* 11: 435-438.

Ebbesen, T.W. and P.M. Ajayan, Large scale synthesis of carbon nanotubes, *Nature*, 358, 220–22, 1992.

Ebbesen, W.T.1997.*Carbon Nanotubes Preparation and Properties*, CRC Press, Boca Raton, FL.

Fan. Z., H.T.Hsiao, S.G.Advani. 2004. Experimental investigation of dispersion during flow of multi walled carbon nanotube/ polymer suspension in fibrous porous media. *Carbon* 42:871-876.

Ferreira, J.M., O.A.Z. Errajhi, and M.O.W. Richardson. 2005. Thermogravimetric analysis of aluminized E-glass fiber reinforced unsaturated. *Polymer Testing* 25:1091-1094.

Fidelus, J.D., E. Wiesel, F.H. Gojny, K. Schulte, and H.D.Wagner. 2005. Thermo-mechanical properties of randomly oriented carbon/epoxy nanocomposites. *Composites Part A* 36:1555-1561.

Fiedler, B., F. H. Gojny, M.H.G. Wichmann, M. Nolte, and K. Schulte. 2006. Fundamental aspects of nano-reinforced composites. *Composites Science and Technology* 66:3115-3125

Frankland, S.J.V., A. Caglar, D.W. Brenner, and M. Griebe.2002. Molecular simulation of the influence of chemical cross-links on the shear strength of carbon nanotube–polymer interfaces. *Journal of Physical Chemistry B* 106:3046:3048.

Frogley, M.D., Q Zhao, and H.D. Wagner. 2002. Polarized resonance Raman spectroscopy of single walled carbon nanotubes within a polymer under strain. *Physical Review B* 65:1-4.

Gao, J. M.E. Itkis, A. Yu, E. Bekyarova, B. Zhao, and R. C. Haddon. 2005. Continuous Spinning of a Single-Walled Carbon Nanotube-Nylon Composite Fiber. *Journal of the American Chemical Society* 127:3847-3854.

Ge, M. and K. Sattler. 1994. Bundles of carbon nanotubes generated by vapour phase growth. *Applied Physics Letters* 64:710-711.

Geng, H., R.Rosen, B. Zheng, H.Shimoda, L. Fleming, J. Lui, O. Zhou. 2002. Fabrication and properties of composites of poly (ethylene oxide) and functionalized carbon nanotubes. *Advanced Materials* 14 :1387-1390.

Gojny, F.H. 2006. Evaluation of the potential of carbon nanotubes as nano-structured modification of (glass fiber reinforced) epoxy-based composites. *Technical University of Hamburg, Harburg thesis of PhD.*

Gojny, F.H. and K. Schulte. 2004. Functionalization effect on the thermo-mechanical behavior of multiwalled carbon nanotube/epoxy composites. *Composites Science and Technology* 34: 2303-2308.

Gojny, F.H., J.Nastalczyk, Z.Roslaniec, K. Schulte. 2003. Surface modified carbon nanotubes in CNT/epoxy-composites. *Chemical Physics Letters* 370:820-824.

Gojny, F.H., M.H.G Wichmann, B. Fiedler, and K. Schulte. 2005a. Influence of different carbon nanotubes on the mechanical properties of epoxy matrix composites- A comparative study. *Composites Science and Technology* 65: 2300-2313.

Gojny, F.H., M.H.G. Wichmann, B. Fiedler, I. Kinloch, W. Bauhofer, A. H. Windle, K. Schulte. 2006. Evaluation and identification of electrical and thermal conduction mechanisms in carbon nanotube/epoxy composites. *Polymer* 47:2036-2045.

Gojny, F.H., M.H.G.Wichmann, B.Fiedler, W. Bauhofer, K. Schulte. 2005b. Influence of nano-modification on the mechanical and electrical properties of conventional fiber reinforced composites - *Composites Part A* 36:1525-1535.

Gojny, F.H., M.H.G.Wichmann, U.Köpke, B.Fiedler and K.Schulte. 2004. Carbon-nanotube reinforced epoxy composites – Improved (fracture) mechanical properties at low nanotube contents. *Composites Science and Technology* 64: 2363-2371.

Gong, X., J.Liu, S. Baskaran, R.D. Voise, and J.S. Young. 2000. Surfactant assisted processing of carbon nanotube / polymer composites. *Chemistry of Materials* 12:1049-52.

Grujicic, M., Y.P. Sun, and K.L. Koudela. 2007. The effect of covalent functionalization of carbon nanotube reinforcements on the atomic-level mechanical properties of poly-vinyl-ester-epoxy. *Applied Surface Science* 253:3009:3011.

Gryschuck, O., J.K. Kocsis, R. Thomann, Z. Kanya, and I. Kiricsi. 2006. Multiwall carbon nanotube modified vinyl ester and vinyl ester- based hybrid resins. *Composites Part A* 37:1252-1261.

Gupta, S., M. Hughes, and A. H. Windle. 2004. In-situ Raman spectroelectrochemistry study of single walled carbon nanotube mat. *Diamond and Related Materials* 13: 1314-1321.

Harris, P.J.F. 2000. *Carbon nanotubes and related structures, new materials for the twenty first century.* Cambridge University Press.

Hiura, H., T.W. Ebbesen, and K.Tanigaki. 1995. Opening and purification of carbon nanotubes in high yields. *Advanced Materials* 7:275-276.

Ho, T.H., T.S. Leu, Y.M. Sun, and J.Y. Shieh. 2006. Thermal degradation kinetics and flame retardancy of phosphorus-containing dicyclopentadiene epoxy resins. *Polymer Degradation and Stability* 12:1-10.

Hsu, C.P. and L.J. Lee. 1993. Free radical cross linking copolymerization of styrene/ unsaturated polyester resins, *Polymer* 34:4506-4515.

Iijima, S.1991. Helical microtubules of graphitic carbon. *Nature* 354:56–58.

Jannesari, A,. S.R. Ghaffarian, N.Mohammadi, F.A.Taromi, and A.Molaei. 2005. Thermo analytical study of the cure characteristics of a main chain liquid crystalline oligoester: Model free approach to kinetic analysis of non- isothermal data, *Thermochima Acta* 425:91-107.

Jia, Z., Z.Wang, C.Xu, J. Liang, B. Wei, and W. Detal. 1999. Study on polymethcrylate carbon nanotube composites. *Materials Science and Engineering A* 271:395-400.

Jiang, X., Y. Bin, M. Matsuo. 2005. Fabrication and distribution of characteristics of polyurethane single-walled carbon nanotube composite with anisotropic structure. *Polymer* 46: 7418-7422.

Journet, C., and P. Bernier. 1998. Production of carbon tubes. *Applied Physics A* 67:1-9.

Kessler, M.R. and S.R White. 2002. Cure kinetics of the Ring Opening Metathesis Polymerization of Dicyclopentadiene" *Journal of polymer science Part A: Polymer Chemistry* 40:2373-2383.

Kim, B., H. Park, and W.M. Sigmund. 2005. Rheological behavior of multiwall carbon nanotubes with polyelectrolyte dispersants, *Colloids and Surfaces A* 256: 123-127.

Kim,J.A, D.G.Seong, T.J.Kang, and J.R.Youn. 2006. Effect of surface modification on rheological and mechanical properties of CNT/epoxy composites. *Carbon* 44: 1898- 1905.

Kinloch, I.A., S.A. Roberts, and A.H. Windle. 2002. A rheological study of concentrated aqueous nanotube dispersions. *Polymer* 43: 7483-7491.

Kolmorov, A.N. and V.H. Crespi. 2000. Smoothest bearings: interlayer sliding in multi walled carbon nanotubes. *Physical Review Letters* 85:4727-30.

Kosar, V. and Z. Gomzi. 2004. In depth analysis of the mathematical model of polyester thermoset curing. *European Polymer Journal* 40:2793-2802.

Kymakis, E. and G.A.J. Amaratunga. 2006. Electrical properties of single-wall carbon nanotube-polymer composite films. *Applied Physics* 99:084302-084346.

Kymakis, E., I. Alexandaou, G.A.J. Amaratunga. 2002. Single walled carbon nanotube-polymer composites: electrical, optical and structural investigation *Synthetic Metals*127:59-92

Lam, P.W. and H.P. Plaumann. 1990. An improved kinetic model for the autocatalytic curing of styrene based thermoset resins, *Journal of applied polymer science* 41:3043- 3057.

Lau, K.T. and D. Hui. 2002. The revolutionary creation of new advanced materials-carbon nanotube composites. *Composites Part: B* 33:263-77.

Lee, J.H. and J.W. Lee. 1994. Kinetic parameters estimation for cure reaction of epoxy based vinyl ester resin. *Polymer Engineering and Science* 34: 742-749.

Lee, J.J., J.O. Lim, J.S.Huh. 2000. Mode II Interlaminar fracture behavior of carbon bead- filled epoxy / glass fiber hybrid composite. *Polymer Composites* 21:343-352

Lee, SM. 1997. Mode II delamination failure mechanisms of polymer matrix composites. *Journal of Materials Science*. 32:1287-1295

Li, L., X.Sun, and L.J. Lee.1999 Low temperature cure of vinyl ester resins *Polymer Engineering and Science* 39:646-654.

Liao, Y.H., T.O. Mariaetta., Z. Liang., C. Zhang, and B. Wang. 2004. Investigation of dispersion process of SWCNTs / SC-15 epoxy resin nanocomposites. *Materials Science and Engineering A* 385:175-181.

Lordi, V. and N. Yao. 2000. Molecular mechanics of binding in carbon nanotube polymer composites. *Journal of Materials Research* 15:2770-9.

Lourie, O. and H.D. Wagner. 1999. Evidence of stress transfer and formation of fracture clusters in carbon nanotube based composites. *Composites Science and Technology* 59:975-7.

Lu, J.P. 1997. Elastic properties of single and multilayered nanotubes. *Journal of the physics and chemistry of solids* 58:1649-52.

Lu, M.G., M.J. Shim, and S.W Kim. 1998. Curing behavior of an unsaturated polyester system analyzed by Avrami equation. *Thermochimica Acta* 323:37-42.

Macan, J., H.Ivankovic, M.Ivankovic, and H.J.Mencer. 2004. Study of cure kinetics of epoxy-silica organic-inorganic hybrid materials. *Thermochimica Acta* 414:219-225.

Malek, J. 2000. Kinetic analysis of crystallization processes in amorphous materials. *Thermochimica Acta* 355:239-253.

Martin, C.A, J.K.W Sandler, A.H. Windle, M.K Schwarz, W. Bauhofer, K. Schulte,. M.S.P Shaffer. 2005. Electric field induced aligned multi wall carbon nanotube networks in epoxy composites. *Polymer* 46:877-886.

Martin, C.A., J.K.W. Sandler, M.S.P Shaffer, M.K Schwarz, W. Bauhofer, K. Schulte, A.H. Windle. 2004. Formation of percolating networks in multi wall carbon nanotube-epoxy composites. *Composites Science and Technology* 64:2309:2316

Mccrum, N.G., C.P. Buckley, C.P. Bucknell. 1997. *Principles of Polymer Engineering* Oxford Science Applications.

Meguid, S.A. and Y. Sun. 2004. On the tensile and shear strength of nano-reinforced composite interfaces. *Materials Design* 25:289-296.

Mischenko, E. G., A. V. Andreev, L.I. Glazman. 2001. Zero-Bias Anomaly in Disordered Wires *Physical Review Letters* 87:246801-346805

Mitchell, C.A., J.L.Bahr, S.Arepalli, and J.M.Tour. 2002. Dispersion of functionalized carbon nanotubes in polystyrene. *Macromolecules* 35:8825-8830

Miyagawa, H. L.T. Drzal. 2004. Thermo-physical and impact properties of epoxy nanocomposites reinforced by SWCNTs. *Polymer* 45:5163-5170

Moniruzzaman, M., and K.I. Winey. 2006. Polymer composites containing carbon nanotubes. *Macromolecules* 39:5194-5205.

Munson, S.H. 1991. Estimation of the critical concentration in an anisotropic percolation network. *Physics Review B* 43:3331:3336.

Nardelli, M.B., B.I. Yakobson, and J. Bernholc. 1998. Brittle and ductile behaviour in carbon nanotubes. *Physical Review Letters* 81:4656-4665.

Nikolaev, P., M.J.Bronikowski, R.K. Bradley, F. Fohmund, D.T. Colbert, K.A. Smith, and R.E. Smalley. 1999. Gas phase catalytic growth of single-walled nanotubes from carbon monoxide. *Chemical Physics Letters* 313:91-98.

Park, S.J., H.J. Joeng, C. Nah. 2004. A study of oxofluorination of multi-walled carbon nanotubes on mechanical interfacial properties of epoxy matrix nanocomposites. *Materials Science and Engineering A* 385:13-19

Peigney, A., C. Laurent, E. Flahaut, R.R. Basca, A. Rousset. 2001. Specific area of carbon nanotubes and bundles of carbon nanotubes. *Carbon* 39:507-514.

Peng, H., P. Reverdy, V.N. Khabasheku, and J.L. Margrave. 2003. Sidewall functionalization of single walled carbon nanotubes with organic peroxides. *Journal of the American Chemical Society* 125:15174-15184.

Pötschke, P., A. R. Battachyya, and A. Janke. 2004a. Melt mixing of polycarbonate with multiwalled carbon nanotubes: microscopic studies on the state of dispersion. *European Polymer Journal* 40: 137-148.

Pötschke, P., M. A. Goad, I. Alid, S. Dudkin, and D.Lellinger. 2004b. Rheological and dielectrical characterization of melt mixed polycarbonate –multiwalled carbon nanotube composites, *Polymer* 45:8863-8870.

Pötschke, P., T.D Fornes, and D.R. Paul. 2002. Rheological behavior of multiwalled carbon nanotube/polycarbonate composites. *Polymer* 43: 3247-3255.

Prasse, T., J.Y. Cavaille, W. Bauhofer. 2003. Electric anisotropy of carbon nanofibre/epoxy resin composites due to electric field induced alignment. *Composites Science and Technology* 63:1835:1842.

Prasse, T., L. Flandin, K. Schulte, W. Bauhofer. 1998. In-situ observation of electric field induced agglomeration of carbon black in epoxy resin. *Applied Physics Letters* 72:1-3.

Puglia, D., L. Valentini, and J.M Kenny. 2003. Analysis of the cure reaction of the epoxy/carbon nanotubes system with thermal analysis and Raman spectroscopy" *Journal of Applied Polymer Science* 88:452–458.

Qian, D., E.C. Dickey, R. Andrews, and T. Rantell. 2000. Load transfer and deformation mechanisms in carbon-nanotube polystyrene composites. *Applied Physics Letters* 76:2868-70.

Qin, L.C. and S. Iijima. 1997. Structure and formation of raft-like bundles of single walled helical carbon nanotubes produced by laser evaporation. *Chemical Physics Letters* 269:65-71.

Rosen, R., B. Zeng, and J. Liu. 2002. Fabrication and Properties of Composites of Polyethylne and functionalized Carbon Nanotubes. *Advanced Materials* 14:24-28.

Roşu, D., A.Mititelu, C.N. Caşcaval. 2004. Cure kinetics of a liquid crystalline epoxy resin studied by non-isothermal data. *Polymer Testing* 23:209-215.

Roşu, D., C.N. Caşcaval, F.Mustata, and C.Ciobanu. 2002. Cure kinetics of epoxy resin studied by non-isothermal DSC data. *Thermochima Acta* 383:119-127

Ru, CQ. 2000. Effect of van der Waals forces on axial buckling of a double walled carbon nanotube. *Journal of Applied Physics* 87:7227-7231.

Saito, Y., K. Nishikubo, K. Kawabata, and T. Matsumoto. 1996. Carbon nanocapsules and single layered nanotubes produced with platinum group metals by arc discharge method. *Journal of Applied Physics* 80:3062-7.

Salvetat, J.P., G.A.D. Briggs, J.M. Bonard, R.R. Bacsa, A.J. Kulik, and T. Stockli. 1999. Elastic and shear moduli of single walled carbon nanotube ropes. *Physical Review Letters* 82:644-651.

Sanchez E.M.S, C.A.C Zavaglia, and M.I Felisberti. 2000. Unsaturated polyester resins: influence of the styrene concentration on the miscibility and mechanical properties. *Polymer* 41:765-769.

Sandler, J., M.S.P. Shaffer, T. Prasse, W. Bauhofer, K. Schulte, and A.H. Windle. 1999. Development of a dispersion process for carbon nanotubes in an epoxy matrix and the resulting electrical properties, *Polymer*, 40: 5967–5971.

Sandler, J.K.W., J.E. Kirk, I.A. Kinloch, M.S.P. Shaffer, A.H. Windle. 2003. Ultra-low electrical percolation threshold in carbon nanotube-epoxy composites. *Polymer* 44:5893-5899.

Schandler, L.S., S.C. Giannaris, P.M. Ajayan. 1998. Load transfer in carbon nanotube epoxy composites. *Applied Physics Letters* 73:3842-4.

Scott, T.F., W.D. Cook, and J.S. Forshthe. 2002. Kinetics and network structure of thermally cured vinyl ester resin. *European. Polymer Journal*. 38:705-716

Seyhan A.T., F.H. Gojny, M. Tanoglu, K. Schulte. 2007b. Rheological and dynamic-mechanical behavior of carbon nanotube/vinyl ester–polyester suspensions and their nanocomposites. *European Polymer Journal* 43:2836-2847.

Seyhan, A.T., F.H. Gojny, M. Tanoglu, and K.Schulte. 2007a. Critical aspects related to processing of carbon nanotube/unsaturated thermoset polyester nanocomposites *European Polymer Journal* 43:374-379.

Shaffer, M.S.P. and A.H. Windle. 1999a. Fabrication and characterization of carbon nanotube/ poly vinyl alcohol composites. *Advanced Materials* 11:937-41.

Shaffer, M.S.P. and A.H. Windle. 1999b. Analogies between polymer solutions and carbon nanotube dispersions. *Macromolecules* 32 6864–6866.

Shaffer, M.S.P., X. Fan, and A.H. Windle. 1998. Dispersion and packing of carbon nanotubes. *Carbon* 36:1603–1612.

Sheng, P. 1980. Fluctuation induced tunnelling conduction in disordered materials *Physics Review* 21:2180-2185

Shih, Y.F. and R.J. Jeng. 2002. Carbon black containing interpenetrating polymer networks based on unsaturated polyester /epoxy II. Thermal degradation behavior and kinetic analysis. *Polymer Degradation and Stability* 77:67-76.

Shirono, H., Y. Amono, M.Kavaguchi, and T. Kato. 2001. Characteristics of alkyltrimethoxysilane-treated fumed silicas and rheological behavior of fumed silica suspensions in an Epoxy Resin, *Journal of Colloid and Interface Science* 239:555-562.

Şimşek, Y., L. Özyüzer, A.T Seyhan, M. Tanoglu, K. Schulte. 2007. Temperature dependence of electrical conductivity in double-wall and multi-wall carbon nanotube/polyester nanocomposites. *Journal of Materials Science* 32:9689-9693.

Smalley, R.E. 1997. Discovering the fullerenes. *Reviews of Modern Physics* 69: 723–729.

Song, Y.S. and J. R. Youn. 2005. Influence of dispersion sates of carbon nanotubes on physical properties of epoxy nanocomposites. *Carbon* 43:1378-1385.

Srivastana, V.K. and P.J. Hogg.1998. Moisture effects on the toughness, mode I and mode II of particles filled quasi isotropic glass fiber reinforced polyester resin composites. *Journal of Materials Science* 33:1129-1136

Stevanovic, D, A.Lowe, S. Kalyanasundaram, P.Y.B.Jar, and V.O.Alego. 2002. Chemical and mechanical properties of vinyl-ester/ABS blends. *Polymer* 43:4503-4514.

Tanoglu, M. and A.T Seyhan. 2003. Investigating the effects of a polyester performing binder on the mechanical and ballistic performance of E-glass fiber reinforced polyester composites. International *Journal of Adhesion and Adhesives* 23:1-8

Thostenson, E.T. and T.W. Chou. 2003. On the elastic properties of carbon nanotube-based nanocomposites: modeling and characterization. *Journal of Physics D: AppliedPhysics* 36:573-582.

Thostenson, E.T. and T.W. Chou. 2006. Processing-structure-multi-functional property relationship in carbon nanotube/epoxy composites. *Carbon* 44:3022-3029.

Thostenson, E.T., L. Chunyiu, and T.W. Chou. 2005. Nanocomposites in context *Composites Science and Technology* 65:491.

Thostenson, E.T., Z.F. Ren and T.W. Chou. 2001. Advances in the science and technology of carbon nanotubes and their composites: a review. *Composites Science and Technology* 61:1899-1912.

Tibbets, G.G. and J. Mchough. 1999. Mechanical properties of vapour-grown carbon fiber composites with thermoplastic matrices. *Journal of Materials Research* 14:2871-8.

Tollens, F.R. and L.J. Lee. 1993. Cure analysis of unsaturated polyester resins using electron spin resonance spectroscopy, differential scanning calorimetry and rheometry, *Polymer* 34:29-37.

Treacy, M.M.J., T.W. Ebbesen, and J.M. Gibson. 1996. Exceptionally high Young's modulus observed for individual carbon nanotubes. *Nature* 381:678-680.

Wagner, W.D., O. Lourie, Y. Feldman, R.Tenne. 1998. Stress-induced fragmentation of multi walled carbon nanotubes in a polymer matrix. *Applied Physics Letters* 72:188-90.

Weg, U.D., J.M. Benoit, and S. Lebedkin. 2002. Chemical functionalization of single walled carbon nanotubes. *Current Applied Physics* 43:497-501

Wichmann, W.H.G., J. Sumfleth, F.H. Gojny, M. Quaresimin, B. Fiedler, K. Schulte. 2006. Glass fiber reinforced composites with enhanced mechanical and electrical properties –Benefits and limitations of a nanoparticle modified matrix. *Engineering Fracture Mechanics* 73:2346-2359

Wong, E.W., P.E. Sheehan, C.M. Lieber. 1997. Nanobeam mechanics: elasticity, strength, and toughness of nanorods and nanotubes. *Science* 277:1971-1976.

Xie, H., B. Liu, and Z. Juan. 2004. Cure kinetics of carbon nanotubes/tetrafuntional epoxy nanocomposites by isothermal dynamic scanning calorimetry. *Journal of Polymer Science: Part B: Polymer Physics* 42:3701–3712.

Yang H, and L. J. Lee. 2001. A kinetic model for free radical cross linking Co-polymerization of styrene/vinyl ester resin. *Polymer composites* 22:1121-1129.

Yaping, Z., Z. Aibio, C. Quingha, Z. Jiaoxia, and N. Rongchnag. 2006. Functionalized effect on carbon nanotube/epoxy nanocomposites *Materials Science and Engineering A* 435:145-152.

Yasmin, A., L.A. Jandro, and I.M. Daniel. 2003. Processing of clay/epoxy nanocomposites by shear mixing. *Scripta Materialia* 49: 81-86.

Yu, M.F., B.S. Files, S.Arepalli, and R.S. Ruoff. 2000b. Tensile loading of ropes of single wall carbon nanotubes and their mechanical properties. *Physical Review Letters* 84:5552-5555

Yu, M.F., O.Lourie, M.J. Dyer, K. Moloni, T.F. Kelly, and R.S. Ruoff. 2000a. Strength and breaking mechanism of multi walled carbon nanotubes under tensile load. *Science* 287:687-640.

Zhang, H., X. Xue, D. Wang, Y. He, S. Peng. 1999. The effect of different kinds of inert gases and their pressures on the preparation of carbon nanotubes by carbon arc method. *Materials Chemistry and Physics* 58:1–5.

Zhang, Y. and S. Iijima. 1999. Formation of single wall carbon nanotubes by laser ablation of fullerenes at low temperatures. *Applied Physics Letters* 75:3087-9.

Zhao, Q. and H.D. Wagner. 2004. Raman spectroscopy of carbon-nanotube based composites. *Philosophical Transaction of the Royal Society London* 362:2407-2424.

Zhu, J., A. Imam, R. Crane, K. Lozano, V.N. Khabashesku, E. V. Barrera. 2007. Processing a glass fiber reinforced vinyl ester composite with nanotube enhancement of interlaminar shear strength. *Composites Science and Technology* 67:1509-1517

VITA

Abdullah Tugrul SEYHAN
(01.05.1977) Antalya

EDUCATION

- ✓ *B.Sc: (2000)* Department of Chemical Engineering, Ege University, Turkey (1+4) (in English).
- ✓ *M.Sc:(2003)* Materials Science and Engineering Programme, Izmir Institute of Technology, Turkey (in English).
- ✓ *PhD: (2008)* Department of Mechanical Engineering, Izmir Institute of Technology, Turkey (in English) in collaboration with Polymer Composites Section, Technische Universität Hamburg, Harburg (TUHH), Germany.

GRANTS

- ✓ TUBITAK - JULICH Joint Programme, researcher in the project of 'Development and characterization of CNT modified thermosetting polyester and vinyl ester based hybrid nanocomposites' (2004-2007). 14 months spent in TUHH
- ✓ MICRO AND NANOTECHNOLOGIES MNT 05, 19-23 April 2005 TU Berlin, "Nano polymer composites in MEMS applications" full accommodation and travel expenses.
- ✓ CENTER FOR COMPOSITE MATERIALS (CCM), University of Delaware Visiting Scholarship- 6 months.
- ✓ MANSION AWARD, with the poster presentation in the competition of Project Market 2008 sponsored by IYTE.

SELECTED PUBLICATIONS

- ✓ Tanoğlu, M., Seyhan, A. T., Investigating the effects of a polyester performing binder on the mechanical and ballistic performance of E-glass fiber reinforced polyester composites, International Journal of Adhesion and Adhesives, 23, 1-8 (2003).
- ✓ Seyhan, A.T., Tanoğlu M., Gojny, F. H., Schulte, K. Rheological and dynamic mechanical behaviour of carbon nanotube vinylester - polyester suspensions and their nanocomposites" European Polymer Journal, Volume 43/7 374-379, (2007).